

**Tree fine root and soil organic carbon  
dynamics under climate warming:  
insights from a long-term soil warming  
experiment in a temperate forest**

**DISSERTATION**

submitted to obtain the degree of Doctor of Natural Sciences

(Dr. rer. nat.)

at the Faculty of Biology, Chemistry and Earth Sciences

of the University of Bayreuth

**Steve Kwatcho Kengdo**

Born in Dschang (Cameroon)

Bayreuth, 2023

This doctoral thesis was prepared at the Department of Soil Ecology at the University of Bayreuth from April 2019 until February 2023 and was supervised by Prof. Dr. Werner Borken.

This is a full reprint of the thesis submitted to obtain the academic degree of Doctor of Natural Sciences (Dr. rer. nat.) and approved by the Faculty of Biology, Chemistry and Geosciences of the University of Bayreuth.

Date of submission: 24.02.2023

Date of defence: 30.05.2023

Acting dean: Prof. Dr. Benedikt Westermann

Doctoral committee:

Prof. Dr. Werner Borken (reviewer)

Prof. Dr. Nele Meyer (reviewer)

Prof. Dr. Lisa Hülsmann (chair)

Prof. Dr. Steven Higgins



## Summary

Temperate forest soils store large amounts of organic carbon and thus are crucial for the global carbon cycle. There is a concern that these soils lose carbon as the global temperature rises, causing a further increase in the concentration of carbon dioxide (CO<sub>2</sub>) in the atmosphere. The organic carbon stock of forest soils relies to some extent on the input of carbon by fine root systems, but long-term studies on the response of fine roots to increasing temperatures are scarce. The main aim of this thesis was to assess the dynamics of fine roots and soil organic carbon in response to long-term soil warming in a temperate mountain forest.

We took advantage of the existing long-term soil warming experiment at Achenkirch, Tyrol, Austria, where soil temperature was increased by + 4°C in the warmed plots (as compared to control) since 2005. We combined soil coring on two sampling occasions (2012 and 2019) and DNA extractions on ectomycorrhizal (EcM) root tips (sampled in 2019) to study the effect of warming on fine root biomass, fine root morphology, and EcM fungal community (Study I). Fine root turnover times and carbon input into the soil by fine root litter were studied by combining ingrowth cores and radiocarbon modeling (Study II). Furthermore, soil CO<sub>2</sub> efflux measured in 2006, 2010, 2015, and 2019 was used to assess the dynamics of soil organic carbon in response to warming. In addition, radiocarbon modeling was used to assess the transit time of carbon in the soil, the radiocarbon distribution of soil organic carbon, and the carbon released by soil organic carbon mineralization (Study III).

Fine root biomass increased by 13% and 17% with soil warming in 2012 and 2019, respectively. Fine root production in ingrowth cores was 128% higher in the warmed plots after one year and 35% higher after two years. In addition, fine root turnover estimated with ingrowth cores increased by 33%, and by 36 – 59% when considering modeled fine root turnover times and fine root biomass from soil coring. Fine root morphology also changed with soil warming on both occasions. Specific root length increased by 17 – 28%, specific root area by 18 – 84%, and root tip density by 28 – 66%. Soil warming did not affect EcM exploration types. However, it shaped the EcM community composition with an increase in the relative abundance of EcM of the genus *Cenococcum*, *Sebacina*, and *Boletus* in the warmed plots. Overall, changes in the fine root system were driven by low soil potassium and phosphorus availability in the warmed plots. Annual soil CO<sub>2</sub> efflux increased by 41% on average over the investigated years, while no difference between soil organic carbon stocks was observed between control and warmed plots. In addition, radiocarbon modeling showed that the

mineralization of soil organic carbon accounted for 37 and 29 % of the total annual soil CO<sub>2</sub> efflux in control and warmed plots, respectively.

Together, our findings suggest that climate warming may increase belowground carbon allocation of trees, the input of carbon into the soil by fine root litter, and the absorptive capacity of the fine root system for water and nutrient uptake. Although soil CO<sub>2</sub> efflux increased with warming, similar soil organic carbon stocks in both treatments suggest that rhizosphere respiration primarily contributes to the increase in soil CO<sub>2</sub> efflux by warming in this forest site. Further, increased root litter input can fully or partly compensate for carbon losses by enhanced soil organic carbon mineralization with increasing global temperatures.

## **Zusammenfassung**

Böden der gemäßigten Wälder speichern große Mengen an organischem Kohlenstoff und sind somit entscheidend für den globalen Kohlenstoffkreislauf. Es besteht die Sorge, dass diese Böden bei einem globalen Temperaturanstieg einen Teil des Kohlenstoffs durch erhöhte Mineralisation verlieren, was zu einem weiteren Anstieg der Kohlendioxidkonzentration (CO<sub>2</sub>) in der Atmosphäre führen würde. Der organische Kohlenstoffvorrat von Waldböden hängt zu einem gewissen Grad vom Kohlenstoffeintrag durch Feinwurzelsysteme ab, doch gibt es nur wenige Langzeitstudien zur Reaktion von Feinwurzeln auf steigende Temperaturen. Das Hauptziel dieser Arbeit war es, den Einfluss langfristiger Bodenerwärmung auf die Morphologie und den Umsatz von Feinwurzeln sowie auf die Freisetzung von organischem Bodenkohlenstoff in einem gemäßigten Bergwald zu untersuchen.

Hierzu nutzten wir das Langzeit-Bodenerwärmungsexperiment in Achenkirch, Tirol, Österreich, wo die Bodentemperatur in den erwärmten Parzellen (im Vergleich zur Kontrolle) um + 4 °C seit 2005 erhöht wurde. Durch Analyse von Wurzelparametern (2012 und 2019) und DNA-Extraktionen von mykorrhizierten Wurzelspitzen (2019) konnten die Auswirkungen der Erwärmung auf die Feinwurzelbiomasse, die Feinwurzelmorphologie und die Gemeinschaft der Ektomycorrhiza (EcM) bestimmt werden (Studie I). Feinwurzelumsatzzeiten und Kohlenstoffeintrag durch Feinwurzelstreu in den Boden wurden durch Kombination von Einwuchskernen und Modellierung auf Basis von Radiokarbonsignaturen untersucht (Studie II). Zudem wurde mit Radiokarbonsignaturen der bodenorganischen Substanz, der oberirdischen und unterirdischen Kohlenstoffeinträge und der Bodenkohlenstoffvorräte die Transitzeit und die Altersverteilung des organischen Kohlenstoffs im Boden und der jährliche Kohlenstoffaustrag durch Mineralisation der organischen Substanz aus dem Boden modelliert. Die in den Jahren 2006, 2010, 2015 und 2019 gemessenen CO<sub>2</sub>-Emissionen des Bodens wurden den modellierten Kohlenstoffausträgen gegenübergestellt, um das Potenzial von Vorratsänderungen im Boden durch Erwärmung abzuschätzen (Studie III).

Die Feinwurzelbiomasse stieg mit der Bodenerwärmung um 13 % (2012) bzw. 17 % (2019) an. Die Feinwurzelproduktion in Einwuchskernen war in den erwärmten Parzellen nach einem Jahr um 128 % höher und nach zwei Jahren um 35 % höher. Darüber hinaus stieg der mit Einwuchskernen geschätzte Feinwurzelumsatz um 33 % bzw. um 36 – 59 %, wenn die modellierten Feinwurzelumsatzzeiten und die Feinwurzelbiomasse aus dem Bodenproben berücksichtigt wurden. Auch die Feinwurzelmorphologie änderte sich in beiden Jahren mit der

Bodenerwärmung. Die Zunahme der spezifischen Wurzellänge betrug 17 – 28 %, der spezifischen Wurzelfläche 18 – 84 % und der Wurzelspitzendichte 28 – 66 %. Die Bodenerwärmung hatte keinen Einfluss auf die EcM-Explorationstypen. Sie prägte jedoch die Zusammensetzung der EcM-Gemeinschaft mit einer Zunahme der relativen Häufigkeit der Gattungen *Cenococcum*, *Sebacina* und *Boletus* in den erwärmten Parzellen. Insgesamt bestand ein Zusammenhang zwischen den Veränderungen im Feinwurzelsystem und geringer Kalium- und Phosphorgehalte im Boden der erwärmten Parzellen. Der jährliche CO<sub>2</sub>-Ausstoß aus dem Boden stieg in den untersuchten Jahren um durchschnittlich 41 %, während kein Unterschied zwischen den Vorräten an organischem Kohlenstoff im Boden zwischen Kontroll- und erwärmten Parzellen beobachtet wurde. Darüber hinaus zeigte die Radiokarbonmodellierung, dass die Mineralisierung des organischen Bodenkohlenstoffs 37 bzw. 29 % des gesamten jährlichen CO<sub>2</sub>-Ausstoßes aus dem Boden in Kontroll- und erwärmten Parzellen ausmachte.

Zusammengenommen deuten unsere Ergebnisse darauf hin, dass die Klimaerwärmung die unterirdische Kohlenstoffallokation von Bäumen, den Eintrag von Kohlenstoff in den Boden durch Feinwurzelstreu und die Absorptionskapazität des Feinwurzelsystems für die Wasser- und Nährstoffaufnahme erhöhen kann. Obwohl der CO<sub>2</sub>-Ausstoß aus dem Boden mit der Erwärmung zunahm, deuten ähnliche Vorräte an organischem Kohlenstoff im Boden in beiden Behandlungen darauf hin, dass die Rhizosphärenatmung hauptsächlich zum Anstieg des CO<sub>2</sub>-Ausstoßes aus dem Boden durch Erwärmung an diesem Waldstandort beiträgt. Erhöhte CO<sub>2</sub>-Emissionen sind kein Indikator für Kohlenstoffverluste im Boden durch Erwärmung. Ein erhöhter Streueintrag könnte Kohlenstoffverluste in temperaten Waldböden durch die Klimaerwärmung vollständig oder teilweise kompensieren.

# Table of contents

<b>Summary</b> .....	<b>i</b>
<b>Zusammenfassung</b> .....	<b>iii</b>
<b>Table of contents</b> .....	<b>v</b>
<b>1 Synopsis</b> .....	<b>1</b>
1.1 Introduction .....	2
1.1.1 Motivation.....	2
1.1.2 <i>In situ</i> climate warming experiment .....	4
1.1.3 Tree fine roots responses to soil warming .....	7
1.1.4 Soil organic carbon and climate warming .....	13
1.2 Objectives and hypotheses .....	16
1.3 Materials and methods .....	17
1.3.1 Overview.....	17
1.3.2 Description of the study site .....	18
1.3.3 <i>In situ</i> soil warming experimental setup at Achenkirch.....	18
1.3.4 Field sampling and sample processing .....	19
1.3.5 Analyses and radiocarbon modeling.....	22
1.3.6 Statistical analyses .....	24
1.4 Results and discussion of the key findings.....	27
1.4.1 Response of fine root biomass, production, and turnover to long-term soil warming.....	27
1.4.2 Changes in fine root morphology .....	32
1.4.3 EcM fungal community .....	34
1.4.4 Radiocarbon dynamics, soil respiration and implications for carbon cycling ...	38
1.5 Conclusions and outlook .....	44
1.6 References .....	45
<b>2 Manuscripts</b> .....	<b>62</b>
Study I: Long-term soil warming alters fine root dynamics and morphology, and their ectomycorrhizal fungal community in a temperate forest soil.....	63
Study II: Increase in carbon input by enhanced fine root turnover in a long-term warmed forest soil.....	132
Study III: Long-term warming increased CO <sub>2</sub> efflux but not the transit time of soil carbon in a temperate forest .....	170
<b>Contribution to the included manuscripts</b> .....	<b>203</b>

<b>Acknowledgments .....</b>	<b>204</b>
<b>Scientific contributions.....</b>	<b>206</b>
Peer-reviewed publications included in this thesis .....	206
Further publications.....	206
Further scientific contributions .....	207
Oral Presentations.....	207
Poster presentation.....	207
Awards .....	208
<b>Declaration.....</b>	<b>209</b>



# **1 Synopsis**

# SYNOPSIS

## 1.1 Introduction

### 1.1.1 Motivation

Soils are considered the largest carbon (C) reservoir in the terrestrial biosphere globally, storing up to 2400 Gt C down to 3m soil depth (Jobbágy & Jackson, 2000) and playing a critical role in the global carbon cycle and ecosystem functions. Soil carbon stocks are determined by the balance between the inputs and outputs of carbon (Davidson & Janssens, 2006). On the one hand, C enters the soil as dissolved organic carbon (DOC) but mainly as aboveground litter, fine root litter, and root exudates (Y. Wang & Hsieh, 2002). On the other hand, outputs of C are influenced by leaching and erosion processes on a longer time scale, but primarily by microbial decomposition of soil organic matter (SOM) releasing carbon dioxide (CO<sub>2</sub>). The latter strongly depends on climatic factors, mainly temperature (Davidson & Janssens, 2006; Lützow & Kögel-Knabner, 2009).

Global climate change, specifically climate warming, is one of the most critical environmental challenges of the 21<sup>st</sup> century (IPCC, 2021). Climate warming is caused by natural factors (variations in solar activity and volcanic eruptions, for example). However, it is mainly accelerated by anthropogenic activities (like burning fossil fuels, deforestation, land conversion, and increasing livestock farming), which are responsible for increasing concentrations of greenhouse gases like CO<sub>2</sub> in the atmosphere, from 278 in pre-industrial times to 417 ppm in 2022 (Friedlingstein et al., 2022). The global mean temperature had been forecast to increase by 1.4 – 4.4°C until 2100 (IPCC, 2021), and this increase will likely vary among biomes. The earth's mean surface temperature has already increased by at least 1°C since 1860 (NOAA National Centers for Environmental Information, 2022), and this increase in temperature is having and will likely continue to have dramatic impacts on natural ecosystems and human well-being (Costello et al., 2009; IPCC, 2021). To tackle climate change and its adverse effects, there have been international climate change negotiations since the Rio convention in 1992. More recently, the Paris agreement was established in 2015 to keep global climate warming below 2°C and limit the temperature increase to 1.5°C compared to pre-industrial levels. This agreement explicitly recognized the need to conserve and enhance carbon reservoirs to reduce climate warming (Paris Agreement, 2015).

How soil organic carbon (SOC) stocks will respond to long-term climate warming remains unclear. There has been a concern about the magnitude and direction of the feedback between climate warming and soil carbon (Lützow & Kögel-Knabner, 2009). Climate warming may

## SYNOPSIS

cause a decline in SOC stocks by increasing SOM decomposition, contributing to increased atmospheric CO<sub>2</sub> (positive feedback). Warming may also increase SOM accumulation and stabilization due to higher litter production and weathering of primary minerals (negative feedback) (Bellamy et al., 2005; Giardina & Ryan, 2000; Knorr et al., 2005; Liski et al., 1999; Trumbore et al., 1996). However, because soils are different and SOM stabilization mechanisms are diverse and operate simultaneously (Lützow et al., 2006), soils may respond differently to long-term climate warming.

Shallow soils of cool temperate forests in the Austrian Alps with high SOC concentrations of ca. 10 – 15% (D. Liu et al., 2017; Schneckner et al., 2016) store up to 112 – 120 t C ha<sup>-1</sup> (Jandl et al., 2021). These soils are of special interest because low temperatures limit microbial activity and hence the decomposition of SOM, therefore protecting their SOC stocks (Körner, 2003; Sjögersten et al., 2011). However, because regional climate models predict an above-global average increase in temperature for the Alpine region by up to 3.3°C until 2100 (Gobiet et al., 2014; Kunstmann et al., 2004; Pepin et al., 2015; Warscher et al., 2019), climate warming could lead to the release of C stored in these soils to the atmosphere, as already observed in some regions of the Alps (Prietzl et al., 2016).

Compared to aboveground plant production, belowground tree response to global warming has been less studied in forests (Blume-Werry, 2022; H. Liu et al., 2022). Most terrestrial ecosystem models generally use the response of aboveground vegetation to make future predictions about the whole ecosystem (Warren et al., 2015). However, a clear mismatch exists between aboveground and belowground plant responses to climate warming (H. Liu et al., 2022). Fine root production and turnover represent up to 33% of annual net primary productivity globally (Jackson et al., 1997). Understanding how climate warming will affect SOC and tree fine root dynamics is crucial in assessing SOC response and feedback to climate warming (Trumbore & Czimczik, 2008). This feedback has not been fully understood yet because observing and characterizing fine root dynamics is complex and challenging (Fahey et al., 2017; Lukac, 2012). Additionally, the few available results are mainly derived from relatively short timescale observations (Bronson et al., 2008; Y. Luo et al., 2001) and controlled laboratory experiments with tree seedlings (Allison & Treseder, 2008; Deslippe et al., 2012; Y. Li et al., 2015; Mucha et al., 2018; Wan et al., 2004). These limitations do not allow concluding the long-term consequences of increasing climate warming on SOC and tree fine roots.

## SYNOPSIS

### 1.1.2 *In situ* climate warming experiment

Researchers have been studying the effects of climate warming on above and belowground ecosystems processes using a variety of methods ranging from historical comparisons and space-for-time approaches (Blois et al., 2013; Faber et al., 2018; Likens, 1989; Zistl-Schlingmann et al., 2020), laboratory experiments (Deslippe et al., 2012; Pu et al., 2017; Rehschuh et al., 2022), natural gradients experiments (Frenne et al., 2013; Parts et al., 2019; W. Xu et al., 2019) and *in situ* climate warming experiments (Melillo et al., 2002; Schindlbacher et al., 2009; Soong et al., 2021). Those approaches aim to understand and predict how climate warming will affect ecosystem structure and functions. This subchapter will mainly focus on *in situ* climate warming experiments, which are of primary interest in this thesis.

*In situ* climate warming experiments (Table 1) have been used to simulate the effects of climate warming in various natural ecosystems while keeping other environmental variables, like precipitation, wind, and light, unaffected (Melillo et al., 2002; Nottingham et al., 2020; Schindlbacher et al., 2009; Soong et al., 2021). In such experiments, plots of usually a few square meters are established in the field, and a warming method is used to increase temperature and mimic climate warming (warming treatment). The response of ecological systems to one or more climate warming scenarios is inferred by comparing ecological parameters measured in warmed plots with those in which the warming treatment does not take place (control treatment). For example, air (and soil) temperature may be increased by using Open-Top Chambers (OTCs) or infra-red heaters suspended above the soil surface (Björk et al., 2007; Wan et al., 2004). In addition, heating cables may be buried at a specific soil depth to warm and bring soil temperature to the target level with the help of computer programs (Bronson et al., 2008; Dawes et al., 2015; Melillo et al., 2002; Nottingham et al., 2020; Schindlbacher et al., 2009; Soong et al., 2021).

Although *in situ* climate warming experiments have the merit to effectively simulate climate warming and improve our understanding of ecosystems' responses to increasing temperature (Finzi et al., 2020; Hollister & Webber, 2000; Schindlbacher et al., 2012), several problems have been associated with the use of this approach. These problems are mainly related to microclimate effects (modification of snow accumulation, light availability, soil drying), initial soil disturbance, unrealistic vertical temperature gradients by warming at a specific soil depth, as well as the limited applicability throughout the year (Bokhorst et al., 2011; Ettinger et al.,

## SYNOPSIS

2019; Frei et al., 2020; Kennedy, 1995). In addition, the high power supply demand and the maintenance required over time, especially in remote areas, have limited the applicability of this approach. This is why such *in situ* climate warming experiments are usually implemented on small surfaces and for relatively short observation periods.

# SYNOPSIS

**Table 1:** *In situ* field climate warming experiments in various ecosystems.

Experiment	Location	Start – End date	Treatment effect	Apparatus used	Ecosystem	Site management	Soil type	References
Harvard forest soil warming experiment	Massachusetts USA	1991 – present	+ 5° C soil warming	Buried heating cables	Temperate forest	Mature forest on formerly cultivated field	Canton series	Melillo et al. (2002; 2011)
Achenkirch soil warming experiment	Achenkirch Austria	2004 – present	+ 4° C soil warming	Buried heating cables	Temperate forest	Natural forest on former cow grazing field	Shallow Chromic Cambisols and Rendzic Leptosols	Schindlbacher et al. (2009; 2011)
Central redbed plains experiment	Oklahoma USA	1999 – 2001	+ 1.1° C air; + 2.0 – 2.6° C soil warming	Infra-red radiators	Grassland			Y. Luo et al. (2001)
The Boreal soil and air warming experiment	Thompson Canada	2004 – 2008	+ 5° C soil warming	Buried heating cables	Boreal forest	Managed forest		Bronson et al. (2008)
Flakaliden soil warming experiment	Flakaliden Sweden	1995 – unknown	+ 5° C soil warming	Buried heating cables	Boreal forest	Planted (1963) evergreen forest	Thin, podzolic, sandy, glacial till	Leppälammı-Kujansuu et al. (2013)
Oak Ridge national research facility	Oak Ridge USA	1996 – unknown	+ 4° C air warming	Open-Top-Chambers	Temperate forest	Planted deciduous trees	Caprina silt loam	Wan et al. (2004)
Latnjaure Field Station warming experiment	Abisko Sweden	May 1993 – unknown	+ 2 - 3° C air warming	Open-Top-Chambers	Dry tundra		Shallow pergelic Cryorthent	Björk et al. (2007)
FACE experiment	Davos Switzerland	2007 - 2012	+ 3.6° C soil warming	Buried heating cables	Temperate forest	Afforested area		Daves et al. (2015)
Blodgett Experimental Forest	Georgetown USA	2013 - present	+ 4° C soil warming	Buried heating cables	Temperate forest		Alfisols	Soong et al. (2021)
SWELTR experiment	Barro Colorado Island Panama	2016 – present	+ 4° C soil warming	Buried heating cables	Temperate forest		Inceptisols	Nottingham et al. (2020)

## SYNOPSIS

### **1.1.3 Tree fine roots responses to soil warming**

Fine roots are commonly defined as roots with a diameter of less than 2 mm (McCormack et al., 2015). They were estimated to account for less than 2% of the total tree biomass and contribute to up to 33% of the global terrestrial net primary productivity (Jackson et al., 1997). Functions of fine roots include tree anchorage, but most importantly, soil water and nutrients uptake, transport, and storage, as well as C input to soils as the results of their growth and mortality (Brunner & Godbold, 2007; McClaugherty et al., 1982; Pregitzer et al., 2002; Rasse et al., 2005). Fine roots are thus an important component of the carbon and nutrient cycles in temperate forests (Jackson et al., 1997; Matamala et al., 2003). Functions played by fine roots were separated according to their morphology (Eissenstat et al., 2000a; Ostonen et al., 2011), and the distinction between absorptive and transport roots has been made in the literature (McCormack et al., 2015). On the one hand, absorptive roots are lower-order fine roots (with high nitrogen content, fast turnover time, high respiration rates, and high mycorrhizal colonization) primarily responsible for nutrients and water uptake. Transport roots, on the other hand (with thick diameter, high tissue density, and slow turnover time), are primarily responsible for nutrients and water transport (Eissenstat et al., 2000a; McCormack et al., 2015). Fine root systems may respond within a few weeks or months to altered soil conditions as plant growth and competition relies on water and nutrient uptake by fine roots (Pregitzer et al., 2000). The response of fine roots to soil warming has been studied by looking at their functional traits defined as architectural, morphological, biochemical, physiological, structural, and dynamical characteristics, among others, that influence performance or fitness via its effects on reproduction, growth, and survival (Nock et al., 2016; Violle et al., 2007). Fine root functional traits extensively categorized by Freschet et al. (2020) may thus provide insight into how the tree root systems cope with environmental changes (Carmona et al., 2021; Freschet et al., 2021), specifically soil warming.

#### **1.1.3.1 Fine root biomass**

The vertical distribution of fine root biomass is well-studied in relation to climate warming (J. Wang et al., 2021), as it gives an idea about the spatial arrangement of the whole root system and the extent of the soil volume used for water and nutrient uptake (Freschet et al., 2021). Although a recent global metaanalysis highlighted that fine root biomass increased with warming globally (J. Wang et al., 2021), the response of fine roots in forest ecosystems has been inconsistent in the literature (Table 2). This response varied between increase (Leppälampi-Kujansuu et al., 2013), decrease (Bronson et al., 2008; Dawes et al., 2015;

## SYNOPSIS

Melillo et al., 2011; Wan et al., 2004; Zhou et al., 2011) or even without changes (Parts et al., 2019). In those studies, the warming effect on fine root biomass was mainly explained by indirect effects, i.e., warming-induced changes in nutrient availability (e.g., nitrogen) or reduced water availability in the soil (Table 2).

### 1.1.3.2 Fine root morphology

Morphological adaptations are also a mechanism through which trees cope with environmental changes (Ostonen et al., 1999). Contrary to fine root biomass, tree fine root morphological response to soil warming has been less studied (J. Wang et al., 2021). Traits like specific root length (SRL, the length of root per unit dry mass), specific root area (SRA, the ratio of fine root surface to fine root dry mass), root tip density (RTID, the number of root tips per soil volume), or root tissue density (RTD, the dry mass of roots per unit volume of fresh roots) have been the most measured among other. Changes in morphological traits have primarily been associated with changes in water and nutrient uptake strategies. For example, Parts et al. (2019), Björk et al. (2007), and Leppälampi-Kujansuu et al. (2013) associated the increase in SRL and SRA with warming as a strategy to acquire soil nutrients. A decrease in RTD was reported by Parts et al. (2019), while Björk et al. (2007) and Leppälampi-Kujansuu et al. (2013) found no change in RTD and RTID. Wan et al. (2004) reported no change in SRL due to increased soil nitrogen mineralization. However, a recent global meta-analysis highlighted that fine root morphological traits were unresponsive to global warming across a range of ecosystems (J. Wang et al., 2021). This contradicts an earlier hypothesis formulated by Pregitzer et al. (2000), suggesting that fine root morphology changes with increasing temperature, and does not allow concluding the relationship between warming and fine root morphology in forests.

**Table 2:** Summary of the effects of warming on fine root mass (FRB, fine root biomass; FRN, fine root necromass; FRP, fine root production) and morphology (SRL, specific root length; SRA, specific root area; RTD, root tissue density; and AvgD, average diameter) in the literature. The arrows in front of each trait indicate an increase (upward arrow) or a decrease (downward arrow) with warming. The absence of arrows indicates no changes.

## SYNOPSIS

References	Treatment effect	Ecosystem	Effects	Explanation
Melillo et al. (2011) Zhou et al. (2011)	+ 5° C soil warming	Temperate forest	FRB ↓ FRN ↓	Increasing N mineralization
Bronson et al. (2008)	+ 5° C soil warming	Boreal forest	FRB ↓	Thermal acclimation
Wan et al. (2004)	+ 4° C air warming and + 1.2° C soil warming		FRB ↓ FRP ↑ SRL	Increasing N mineralization
Dawes et al. (2015)	+ 4° C soil warming	Temperate forest	FRB ↓	Increasing N mineralization
Leppälampi-Kujansuu et al. (2013)	+ 5° C soil warming	Boreal forest	FRB ↑ SRL ↑ RTD; AvgD	Soil nutrients acquisition
Parts et al. (2019)	+ 4° C soil warming	Temperate forest	FRB SRL ↑ SRA ↑ RTD ↓	Thermal acclimation
Björk et al. (2007)	+ 2 - 3° C air warming	Dry tundra	SRL ↑ SRA ↑ RTD	

### 1.1.3.3 Fine root turnover

Fine root turnover is defined as the flux of C and nutrients from fine roots to the soil per unit area per unit time (Pregitzer et al., 2007). It provides information on how much and how fast C cycles in fine roots and, thus, is important for ecosystem C and nutrient cycling (Gill & Jackson, 2000). This information can be obtained by looking at dynamical fine root traits: fine root production, fine root mortality, and fine root turnover time (Freschet et al., 2021). Fine root production is defined as the dry mass of roots produced per unit of ground area and per year. In comparison, mortality refers to the dry mass of roots that died per unit of ground area and per year (Freschet et al., 2021). Fine root turnover time, traditionally calculated as the ratio of root dry mass over dry mass production, represents the time it would take to replace or renew a given pool of fine roots (Lukac, 2012). The different methods used to measure those traits have been extensively reviewed (Gaul et al., 2009; Lukac, 2012; Majdi et al., 2005). However,

## SYNOPSIS

they mainly suffer from the difficulty in observing and measuring dynamical fine root traits directly and simultaneously in the field.

The minirhizotron technique is one of the methods used to study fine root dynamics. The basic principle lies in using a camera installed in minirhizotron tubes to follow the dynamics of fine roots from appearance to disappearance (death) in soils. Several parameters like root length production, root diameter, and root length mortality can be obtained by comparing and analyzing sequential images taken at a predefined interval. However, an underestimation of the fine root turnover time may occur because of the disturbance created by minirhizotrons tubes in the soil and the small portion of the total root system observed by the camera (Lukac, 2012; Majdi et al., 2005). In addition, compared to grasses, tree fine root systems are much more complex, with different characteristics, ages, and functions (McCormack et al., 2015), which further complicate the use of minirhizotrons to identify the response of fine roots to global warming.

The ingrowth cores method is another approach used to study fine root dynamics. This approach makes use of ingrowth cores or bags inserted in the soil and filled with root-free soil to assess fine root production at two predefined intervals (usually covering the length of the growing season): a time  $t_0$  when ingrowths are inserted in the soil, until time of retrieval from the soil. The disturbance created by ingrowth cores installation and refilling with partly different soils and the growth of fine roots in the absence of competition are some of the problems associated with this method (Lukac, 2012; Majdi et al., 2005). Another approach developed during the last decades is radiocarbon modeling, which uses the radiocarbon signature of fine roots ( $\Delta^{14}\text{C}$ ) to estimate the turnover time of fine roots. This approach uses the natural level of  $\Delta^{14}\text{C}$  in the atmosphere, which peaked in the 1960s due to nuclear bomb testing (Figure 1), as a proxy to infer the time elapsed since the C fixed in the atmosphere during photosynthesis had been used for fine root production (Gaudinski et al., 2001; Gaudinski et al., 2010). This method usually yielded longer turnover times than others for several reasons (Ahrens & Reichstein, 2014; Gaudinski et al., 2001; Helmisaari et al., 2015; Solly et al., 2018). A surprising finding of the radiocarbon analysis was that portion of a tree's fine root may become very old, i.e., up to 20 years (Gaudinski et al., 2001; Solly et al., 2018), and therefore, the dynamics of old fine roots are overlooked by methods focusing on short-living fine roots.

The variation of estimates derived from the abovementioned methods has led to the general recommendation to combine two or more methods to accurately estimate carbon inputs from

## SYNOPSIS

fine roots into the soil (Lukac, 2012). Although those traits are commonly measured in ecosystems, studies that explicitly evaluate how soil warming affects the input of fine root C into the soil are lacking. The results of available studies appear confusing. While some pointed out that warming may increase fine root production and fine root turnover (Eissenstat et al., 2000a; Gill & Jackson, 2000), a global metanalysis (considering different biomes) revealed that fine root production increased, while fine root turnover was irresponsive to warming (J. Wang et al., 2021).

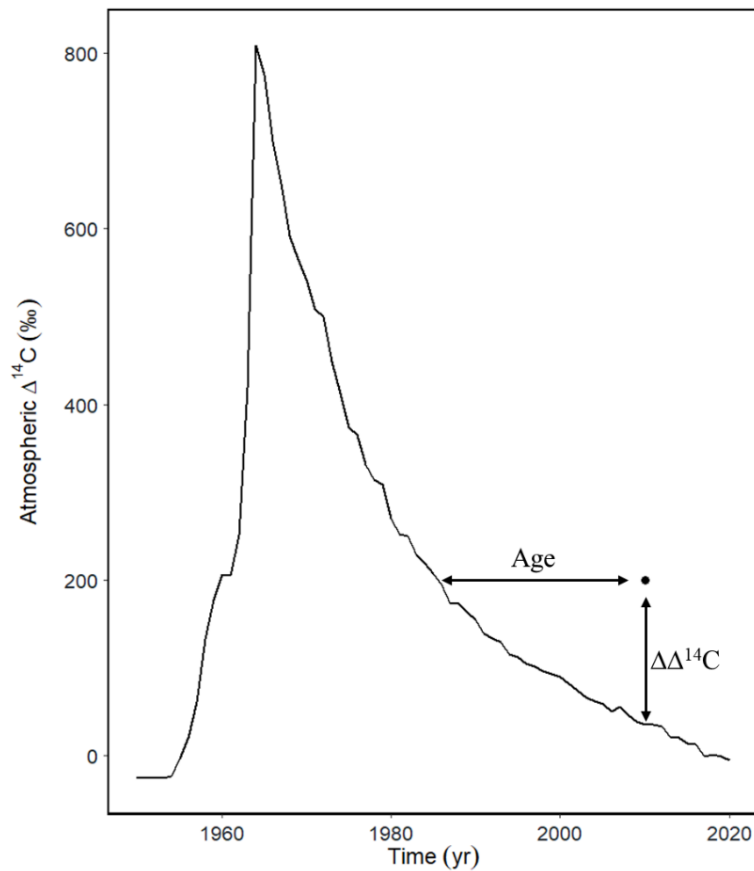


**Figure 1:** Temporal pattern of  $\Delta^{14}\text{C}$  in atmospheric  $\text{CO}_2$  constructed from the *intcal* dataset (Reimer et al., 2013) and data from the Schauinsland (1986 - 2016) and Hohenpeißenberg (2015 - 2020) stations (Hammer & Levin, 2017; Kubistin et al., 2021). The point symbol in the figure represents the  $\Delta^{14}\text{C}$  of a fine root measured in 2012. The time elapsed since the C was fixed by photosynthesis and used for fine root growth is used to infer the age of C in the fine root. The difference between the atmospheric  $\Delta^{14}\text{C}$  and the  $\Delta^{14}\text{C}$  of the sample is  $\Delta\Delta^{14}\text{C}$  (Trumbore & Gaudinski, 2003). Under steady-state (i.e., all fine roots have the same

## SYNOPSIS

probability of dying), the age of a fine root, for example, is assumed to equal the turnover time (Gaudinski et al., 2010; Rodhe, 1992).

### **1.1.3.4 Mycorrhizal symbiosis in warmed soils**

Mycorrhiza denotes the symbiotic association between plant roots and fungi, where roots provide photosynthetically fixed C, and fungi, in return, provide water and nutrients (Smith & Read, 2008). In temperate forests, most tree species are colonized by several ectomycorrhizal fungi (EcM) or arbuscular fungi. In addition to providing water and nutrients to the host plants (Brundrett & Tedersoo, 2018), EcM fungi play a role in global C cycling by contributing to CO<sub>2</sub> efflux (Heinemeyer et al., 2007; Wallander et al., 2013), soil organic matter formation and stabilization, exudate production and turnover of mycorrhizal necromass (Frey, 2019; Klink et al., 2022). EcM fungi form a Hartig net of hyphae surrounding the root cortex cell and a differentiated hyphal mantle around the root tips (Brundrett & Tedersoo, 2018; Freschet et al., 2021). Contrary to arbuscular mycorrhizas, which primarily acquire inorganic nutrients mobilized by decomposers, EcM can produce enzymes that break down litter and organic matter (Averill et al., 2014; Averill & Hawkes, 2016). Further, by developing different extraradical mycelium described and classified by Agerer (2001) as exploration types, EcM may improve the competitiveness of trees for resources by increasing the absorptive surface of fine roots.

Soil warming may influence EcM fungi directly or indirectly through changes in resource needs, carbon allocation, and soil chemistry (Mohan et al., 2014). Although EcM fungi have a high-temperature tolerance (Bennett & Classen, 2020), the direct effect of warming may result from increased metabolic activity due to temperature dependency on enzymatic activity (Staddon et al., 2002). Indirectly, warming may change EcM community composition as a result of alteration in the host-plant nutrition and shift in host-tree carbon allocation to EcM fungi (Lilleskov & Bruns, 2001; Treseder, 2004), changes in plant performance (Fernandez et al., 2017; Rygiewicz et al., 2000) or changes in soil nutrient availability (Solly et al., 2017).

The question of how EcM fungi respond to soil warming in temperate forests has received little attention in scientific work. Most available studies have been conducted in high-latitude ecosystems (Allison & Treseder, 2008; Leppälammı-Kujansuu et al., 2013; Treseder et al., 2016). The few warming studies in temperate forests mainly focused on changes in EcM community composition (Fernandez et al., 2017; Parts et al., 2019). However, other traits like EcM exploration types that connect fine root morphology and differentiation of EcM hyphae

## SYNOPSIS

to nutrient acquisition strategies (Defrenne et al., 2019) may also play an essential role in the response of fine roots to soil warming.

### **1.1.4 Soil organic carbon and climate warming**

As noted above, SOC dynamics are influenced by biotic and abiotic factors. Biotic factors, mainly plant inputs (Koven et al., 2017; Y. Wang & Hsieh, 2002), include aboveground litter, root exudation, and fine root litter. They may either increase SOC stocks by inputting plant detritus and microbial necromass C derived from the decomposition and transformation of plants residues and root exudates; or decrease SOC through the litter-induced priming effect (Kuzyakov, 2010; Lavallee et al., 2020). Abiotic factors, like temperature, are important drivers of SOC dynamics in temperate forests (Davidson & Janssens, 2006). The dynamics of SOC to warming have been extensively studied. However, most studies were short in time and mainly focused on soil respiration, mass loss by litter decomposition, or other components of the C cycle. Findings from long-term, decadal warming experiments with respect to SOC turnover and SOC stocks in forests are hardly available.

#### **1.1.4.1 Soil respiration**

Soil respiration is the CO<sub>2</sub> produced by the biological activity of all soil organisms and represents one of the most important fluxes in the global C cycle (Raich & Schlesinger, 1992). It primarily integrates root and rhizosphere respiration (autotrophic respiration) and the decomposition of SOM (heterotrophic respiration) (Ryan & Law, 2005). As an important component of the C cycle determining SOC stocks, the increase in soil respiration as a response to warming and hence the release of CO<sub>2</sub> from the soil to the atmosphere could further exert positive feedback in the global climate (Davidson & Janssens, 2006). Warming may affect soil respiration directly by increasing soil microbial and root metabolic activity (Bai et al., 2013; J. Wang et al., 2021) and the diffusion of CO<sub>2</sub> in the soil profile (Risk et al., 2002). Indirectly, warming may affect soil moisture and nutrient availability, which as a feedback loop, will affect the activity of soil microbes and CO<sub>2</sub> transport in the soil. Soil respiration under warming has been studied using field observations, but uncertainties still exist about the strength of the relationship between soil respiration and warming in forests. The effect of warming on soil respiration had been previously described as a short-term effect (Bradford et al., 2008; Y. Luo et al., 2001; Melillo et al., 2002; Melillo et al., 2017) where soil respiration and SOC loss temporarily increased but declined throughout the experiment. This was explained by the depletion of the labile C substrate, the reduction of the microbial biomass, and the acclimation

## SYNOPSIS

of the soil microbial community to warming. In other studies, the effect of warming on soil respiration has instead been described as a long-term or sustained effect because the release of CO<sub>2</sub> from the soil several years later was still as high as since the warming treatment began (Knorr et al., 2005; Melillo et al., 2017; Schindlbacher et al., 2009). Autotrophic and heterotrophic respiration may respond differently to warming, and an increase in soil CO<sub>2</sub> efflux does not necessarily result in net losses of SOC (Hicks Pries et al., 2015; M. Lu et al., 2013). As such, the effect of warming on soil respiration is one of the primary sources of uncertainties in global climate models (Carey et al., 2016; Q. Wang et al., 2019). Unraveling the long-term impact of climate warming on soil respiration remains one of the biggest challenges in climate research, a challenge further complicated by the low number of long-term observations globally (Table 1).

### 1.1.4.2 Soil organic carbon cycling under warming

The dynamics of SOC to warming have also been studied by looking at how fast C cycles in soil. Most studies assessed the effect of warming on the turnover time of SOC (Knorr et al., 2005; Z. Luo et al., 2019; J. Wang et al., 2018; Ziegler et al., 2017), which at steady-state represents the time it would take to renew all mass of C in a given SOC pool (Barrett, 2002; Z. Luo et al., 2019). The focus had been on using radiocarbon modeling as an approach to estimate SOC turnover times by taking advantage of the <sup>14</sup>C labeling of atmospheric CO<sub>2</sub> by nuclear bomb tests between 1950 and the mid-1960s (Schuur et al., 2016). Because the  $\Delta$  <sup>14</sup>C signature of the bulk soil reflects the contribution of <sup>14</sup>C inputs to the soil (via litter) and the <sup>14</sup>C decay and losses after SOM mineralization (Schuur et al., 2016), the turnover time (under steady-state) was inferred using models and the temporal variability of atmospheric <sup>14</sup>C (Ziegler et al., 2017). Early simple modeling approaches assumed that SOM is a homogenous pool of equal turnover time. As a result, SOC turnover times were derived from a *single-pool* model, which tended to underestimate SOC turnover (Trumbore, 2000). Physical or chemical fractionations were later used to identify different SOC fractions cycling at different rates. Therefore, multiple pool models were introduced and tended to consider this heterogeneity (fast- and slow-cycling, for example) and the role of litter input and the transfer of C between different SOC pools (Sierra et al., 2012, 2014).

Recently, Sierra et al. (2017) proposed adopting the concepts of *age* and *transit time* to study the dynamics of C in ecosystems. The *age* represents the time that has passed since C entered a system (hereafter, “system” refers to a set of compartments or pools, including the transfer

## SYNOPSIS

of C between them. A system is characterized by an input and output flux). In contrast, the *transit time* gives information on the C storage and flow in that system, that is, the time spent by C between his entry and exit at a specific time. This is also referred to as the age of C in the output flux (Sierra et al., 2017). Longer ages and slower transit times indicate that C has spent a relatively long time in the system and travelled relatively slowly before being released. In comparison, shorter ages and faster transit time suggest relatively young carbon in the system (Xiao et al., 2022). Studying C dynamics to warming by exploring the ages and transit time as well as the radiocarbon distribution of SOC may provide another dimension of information on C cycling in temperate forests, which to our knowledge, only one study has attempted to investigate so far (X. Lu et al., 2018).

# SYNOPSIS

## 1.2 Objectives and hypotheses

The main aim of this thesis was to assess the dynamics of tree fine roots and soil organic carbon in response to long-term soil warming (> 14 years) in a temperate mountain forest. More specifically, we studied the response of fine root biomass, production, morphology, and EcM fungal and bacterial communities to soil warming. Furthermore, we determined the effect of soil warming on fine root turnover times and carbon input from fine roots to the soil. Finally, we studied the effect of soil warming on the transit time of C in soil and soil CO<sub>2</sub> efflux.

The following hypotheses were tested in this thesis:

Soil warming

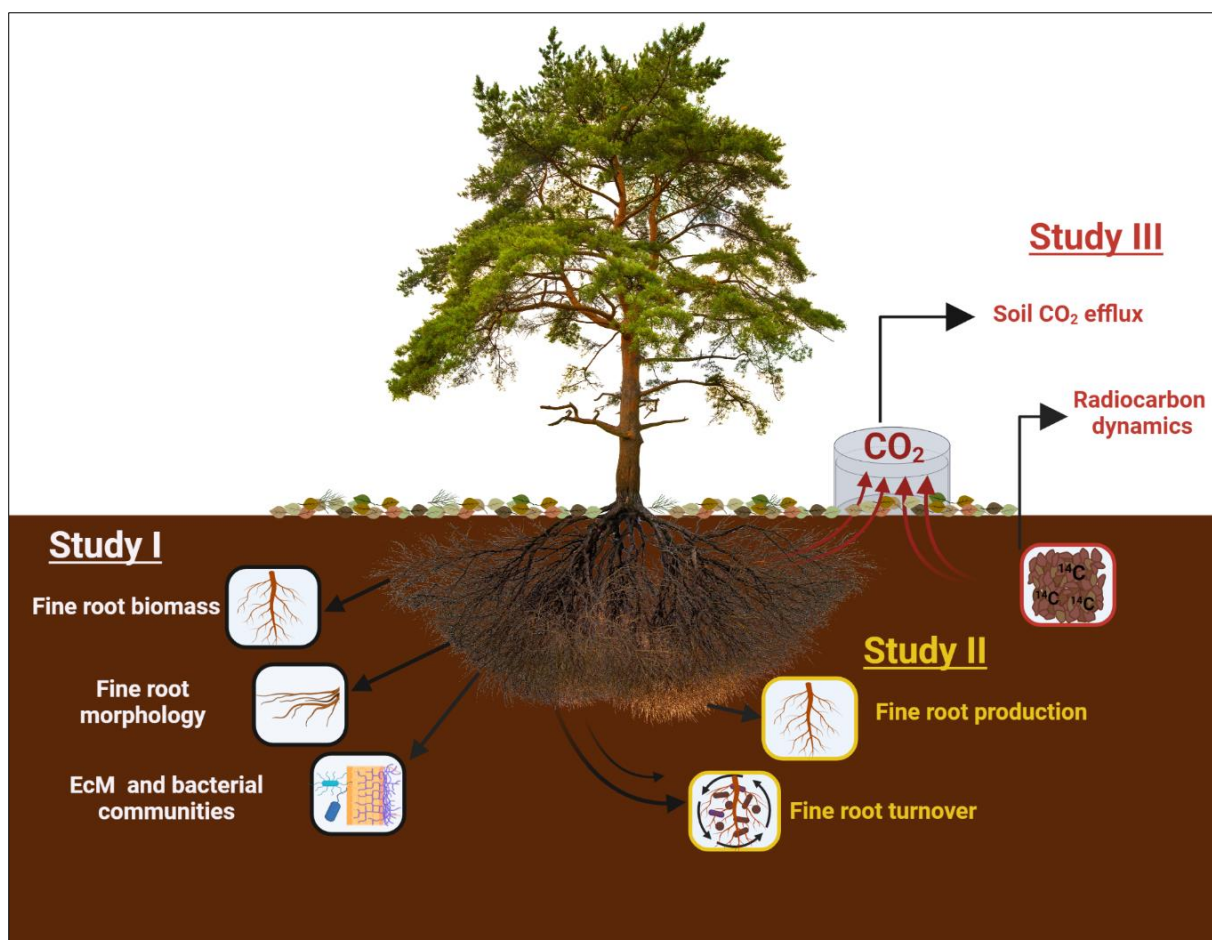
- (i) increases fine root biomass and fine root production;
- (ii) increases the input of C from fine roots to the soil via fine root mortality;
- (iii) increases specific root length, specific root area, and root tip density;
- (iv) induces a shift in the EcM exploration types but not in the EcM fungal community composition;
- (v) increases SOC loss.

# SYNOPSIS

## 1.3 Materials and methods

### 1.3.1 Overview

Tree fine roots and SOC dynamics in response to soil warming were evaluated by conducting three studies (Figure 2). First, we looked at the effects of soil warming on fine root biomass, fine root morphology, and ectomycorrhizal fungal and bacterial communities by using soil coring on two occasions (2012 and 2019) and DNA extraction on root tips sampled in 2019 (study I). Second, we studied the effects of soil warming on fine production and fine root turnover (study II) by combining several approaches (radiocarbon modeling and ingrowth cores). Third, we studied SOC dynamics to soil warming (study III) by looking at the distribution of SOC by radiocarbon signatures, the transit time of C in soil, and by analyzing a long-term record of soil respiration in both control and warming treatments over multiple years. The experimental setup and main methods used are summarized in this section, while more detailed explanations are provided in each separate study.



## SYNOPSIS

**Figure 2:** Overview of the three studies included in this thesis.

Tree image vector acquired from iStock.com/DrPAS (under the standard license agreement).  
Figure created with BioRender.com

### 1.3.2 Description of the study site

The experimental site is located at Achenkirch (Tyrol), a village in the Austrian limestone Alps ((47°34'50" N; 11°38'21" E). The site is at 910 m a.s.l, and was historically used for cow grazing. It is now a ca. 140-year-old forest and mainly comprises in its vast majority Norway Spruce (*Picea abies* L. H.Karst.) and other less abundant species like European beech (*Fagus sylvatica* L.) and Silver fir (*Abies alba* Mill.). The nitrogen deposition measured at this site was about 11 – 15 kg N ha<sup>-1</sup>yr<sup>-1</sup> between 1998 - 2000 (Herman et al., 2002). Soils storing ~ 120 t C ha<sup>-1</sup> are described as shallow Chromic Cambisols and Rendzic Leptosols. The soil profile comprises a 15 – 20 cm thick A-horizon and a C-horizon with high calcium carbonates (Schindlbacher et al., 2009; Schindlbacher et al., 2011). Mean annual air temperature and precipitation were 7°C and 1493 mm, respectively, for the period 1988 – 2017.

### 1.3.3 *In situ* soil warming experimental setup at Achenkirch

To our knowledge, the Achenkirch soil warming experiment is the world's second longest still-running soil warming experiment in a forest ecosystem. The warming experiment comprises plots of paired 2 m × 2 m subplots located adjacent to each other (Figure 3). Three plots were first installed in 2004 (three control and three warmed subplots), and another three plots were later established in 2007 (Schindlbacher et al., 2009; Schindlbacher et al., 2012). In the warmed subplots, soil temperature was increased by + 4°C using resistance heating cables (TECUTE – 0.18 Ohm m<sup>-1</sup> UV<sup>-1</sup>, Etherma, Salzburg, Austria) installed at 3cm soil depth with a spacing of 7.5cm between them. Dummy cables were also installed in control subplots to account for the disturbance created by heating cables. A computer automatically controlled the 4°C difference between control and warming treatments, and the heating system only worked during the snow-free season (April to mid-December) (Figure 4). Ancillary measurements like soil temperature, soil moisture, and DOC leaching are continually measured in each subplot. Soil temperature is measured at 5 cm soil depth using PT100 sensors (EMS, Czech Republic), while soil moisture is monitored with ECH2O-10 probes (Decagon, USA) (Schindlbacher et al., 2012).

## SYNOPSIS

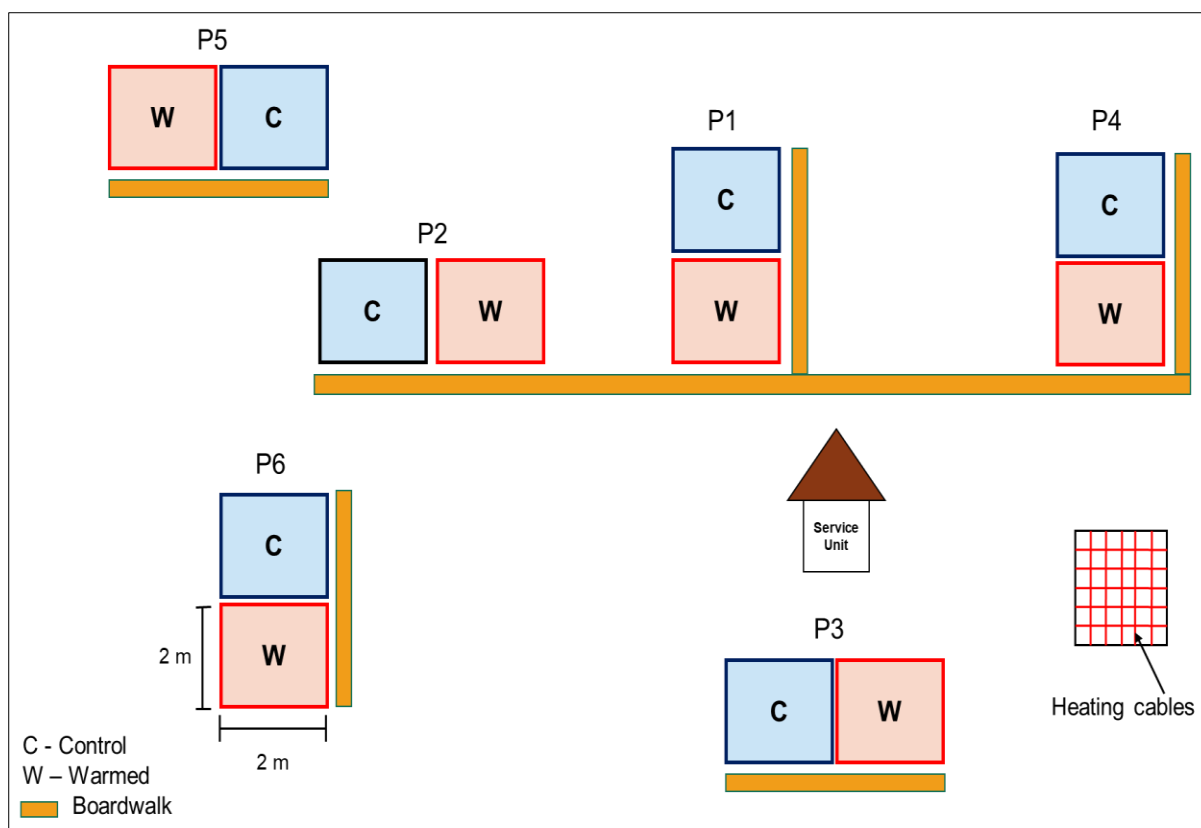


**Figure 3:** Achenkirch soil warming experimental layout with six plots. Each plot has a control (C) and warmed (W) subplot.

### 1.3.4 Field sampling and sample processing

#### 1.3.4.1 Aboveground litterfall and throughfall measurement

Aboveground litterfall was continually measured at the field site since 2007 using litter collectors (with a collecting area of  $0.5 \text{ m}^2$ ) distributed to cover the entire site. Bi-monthly litterfall was oven-dried at  $60^\circ\text{C}$ , and aboveground C input via litter was calculated assuming a C fraction of 50% dry matter. DOC input by throughfall was sampled using 15 throughfall collectors with a collecting area of  $227 \text{ cm}^2$  each from May 2020 to April 2021. DOC concentrations in biweekly throughfall samples were analyzed with a total carbon analyzer (Analytik Jena, Multi N/C 2100s). The DOC input by throughfall was estimated as the DOC concentration multiplied by the throughfall amount for each sampling occasion and cumulated for the entire sampling period.

## SYNOPSIS

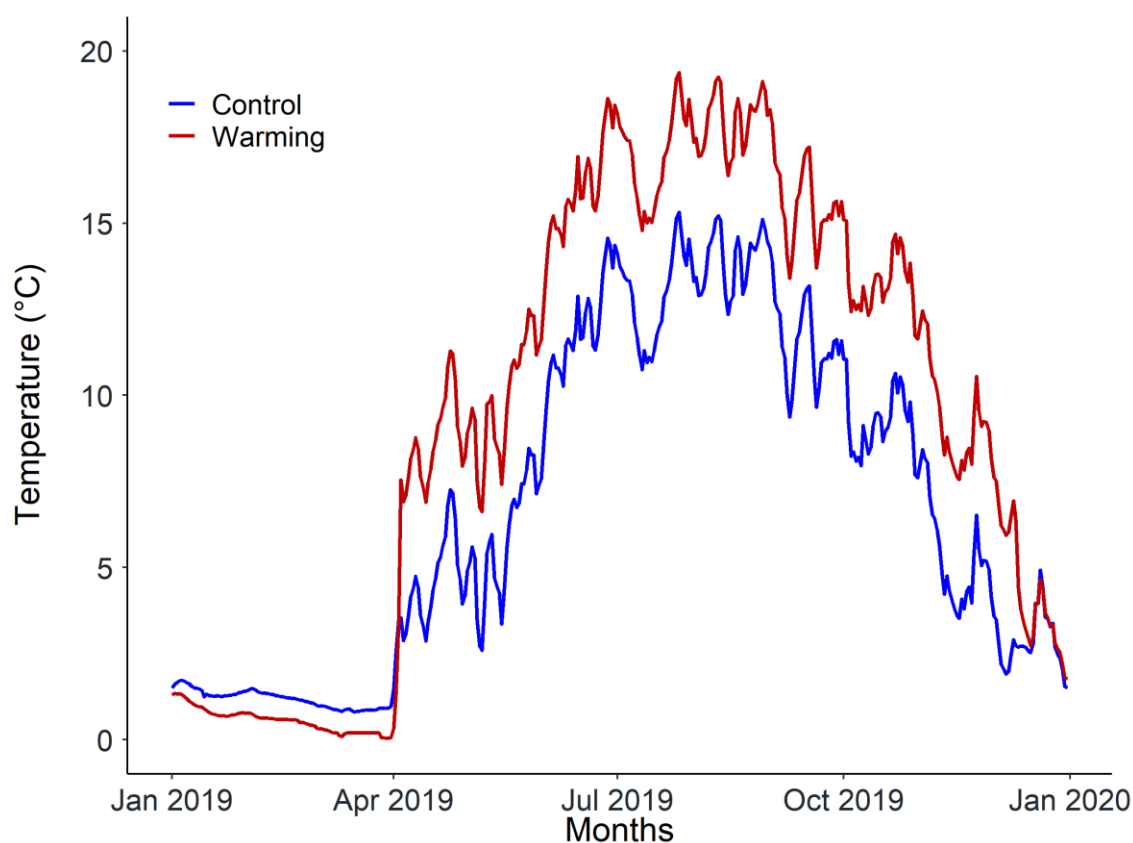


**Figure 4:** Daily soil temperature at 5 cm soil depth in control (blue line) and warming (red line) in 2019. Only the temperature of the first plot (P1 in figure 3) is shown here. The warming system was switched on in the first week of April and switched off in mid-December.

### 1.3.4.2 Soil and fine roots sampling

On two occasions, soils were sampled using a cylindrical soil corer (5cm diameter, 20 cm length). Three plots were sampled in October 2012 ( $n = 3$ ) and six in October 2019 ( $n = 6$ ). Ten soil cores were taken in each subplot at 0 – 10 cm and 10 – 20 cm soil depth. Aliquots of each soil sample per occasion were pooled per subplot and soil depth for radiocarbon analyses. Fine roots were sampled from the remaining bulk soil sampled on each occasion. Fine root processing included washing, sorting into live and dead roots (Burke & Raynal, 1994; Wu, 2000), and scanning the live root fraction with a flatbed scanner followed by image analysis with WinRhizo<sup>TM</sup> Reg 2008 (Regent Instruments Inc., Canada). Fine root biomass and necromass were estimated after drying the respective fraction at 60°C for three days.

## SYNOPSIS

Fine root production was measured with the ingrowth core method (Figure 5). In 2012, root-free sieved soil from the same site was used to refill the holes created by soil coring, while in 2019, ingrowth mesh tubes (5cm diameter, 20 cm length, mesh size 6mm × 4 mm) were inserted in the holes and filled with root-free soil from the A horizon of the study site. Ingrowth cores inserted in 2012 were sampled in June 2013 and October 2013, while those inserted in 2019 were sampled after one and two years, respectively. Newly produced fine roots were also processed similarly to fine roots sampled by soil coring and dried to determine fine root production. Table 3 below gives an overview of the fine root traits measured in this study.

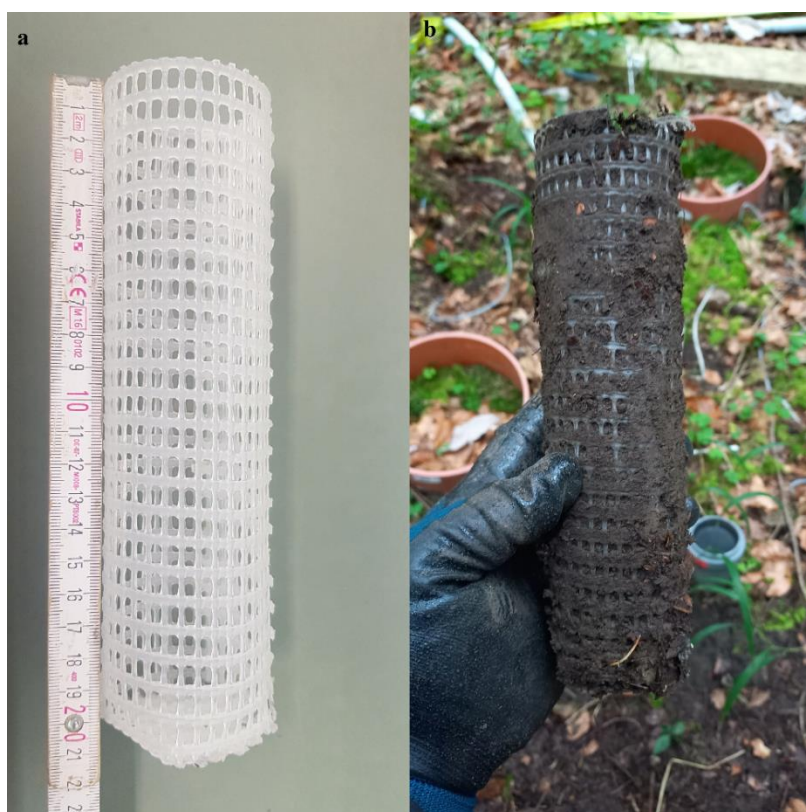


**Figure 5:** Ingrowth mesh tubes used to measure fine root production in the field in 2019 - 2021. Ingrowth mesh tubes (a) were filled with root-free soil and retrieved after one or two years (b).

### 1.3.4.3 Soil respiration measurement

Soil CO<sub>2</sub> efflux measurements have been performed at the Achenkirch site since the beginning of the warming treatment. CO<sub>2</sub> efflux was measured using the static chamber technique every two weeks (during the snow-free season) or every three weeks (during the snow season), using three permanent chambers (20 cm diameter, 10 cm height) randomly inserted in each subplot. After closure with a stainless steel lid for 300 sec, the CO<sub>2</sub> concentration in the chamber

## SYNOPSIS

headspace was measured with an infrared gas analyzer. The increase in CO<sub>2</sub> over time was used to calculate the flux. Additional details are provided in study III.

**Table 3:** Overview of the fine root traits in this study. Traits were categorized and adapted based on Freschet et al. (2021).

Category	Trait	Unit	Ecological relevance
Architecture	Fine root biomass (FRB)	$\text{g m}^{-2}$	C and nutrient cycling, uptake area
Morphology	Specific root length (SRL)	$\text{m g}^{-1}$	Soil exploration and foraging
	Specific root area (SRA)	$\text{cm}^2 \text{g}^{-1}$	Nutrients absorption
	Fine root diameter	mm	Space for mycorrhizal hyphae
	Root tissue density (RTD)	$\text{g cm}^{-3}$	Tissue density and quality
	Root area index (RAI)	$\text{m}^2 \text{m}^{-2}$	Soil exploration
	Root tip density (RTID)	$\text{tips} \times \text{cm}^{-3}$	Soil exploration
Dynamics	Fine root production (FRP)	$\text{g m}^{-2} \text{yr}^{-1}$	C and nutrient cycling, uptake area
	Fine root turnover time	yr	C and nutrient cycling
Mycorrhizal associations	Mycorrhizal colonization intensity	%	Soil exploration and nutrients absorption
	Mycorrhizal fungal community composition	n.a	Soil exploration and nutrients absorption
	Mycorrhizal exploration type	n.a	Soil exploration and nutrients absorption
Fine root Chemistry	Fine root C, N, Na, Ca, K, Mg, Fe, P, Mn	See table 2 in study I	Plant growth Nutrient cycling

### 1.3.5 Analyses and radiocarbon modeling

#### 1.3.5.1 Fine root nutrient concentrations

Fine root nutrient concentrations were determined on dried roots sampled in October 2019. Element concentrations of Na, Ca, K, Mg, Fe, P, and Mn were determined after acid digestion of fine root samples followed by analyses using ICP-OES (Optima 3200 xl; Perkin Elmer,

## SYNOPSIS

Germany) and AAS (SpectraA 220 Z; Varian, USA). TN and TC were determined using an elemental analyzer (EA1110; CE Instrument, Italy).

### **1.3.5.2 DNA extraction on EcM root tips and sequencing**

Following fine root sampling and processing in 2019, intact live roots were examined under the binocular microscope, and root tips colonized by EcM fungi were sampled. Two technical replicates per subplot and soil depth were prepared, and the ChargeSwitch® gDNA plant kit (Invitrogen™; Carlsbad, USA) was used to extract DNA from the 48 samples. The V3 and V4 regions of the 16S rRNA gene were amplified according to Illumina (2013). DNA concentration of each sample was measured using the Qubit® 2.0 fluorometer (Life Technologies). The amplicon size distribution was measured using the Bioanalyzer 2100 (Agilent Technologies GmbH & Co. KG). Sequencing was done using an Illumina MiSeq® sequencer (Illumina, Inc.) with 2 × 300 bp. Sequences were assigned to taxa using QIIME and the UNITE database v8 (Kõljalg et al., 2013).

### **1.3.5.3 Radiocarbon analysis and modeling**

#### **1.3.5.3.1 Sample pre-treatment and analysis**

For radiocarbon analyses, plant materials (fine roots and aboveground litter) were pre-treated with an acid-base-acid treatment to remove contaminants (Gaudinski et al., 2001). An internal protocol of the Keck-CCAMS Facility (Irvine, USA) was used for this purpose (<https://www.ess.uci.edu/~ams/Protocols.htm>; last accessed on February 17, 2023). Homogenized soil samples per subplot and soil depth on each sampling occasion were pre-treated with HCl to remove calcium carbonates. The C contained in fine roots, aboveground litter, and soil samples were cryogenically extracted, purified, and graphitized according to the sealed-tube zinc reduction method of X. Xu et al. (2007). Graphite samples were analyzed using an accelerator mass spectrometer (AMS, 0.5MV 1.5SDH-2 Pelletron, National Electrostatics Corporation, Middleton, Wisconsin, USA) to determine the <sup>14</sup>C content (Southon et al., 2004).

#### **1.3.5.3.2 Radiocarbon modeling**

The turnover time of fine roots was estimated using a *one-pool* model where recent photosynthates passing a storage C pool are used for fine root production. Fine roots produced enter a fine root pool which turns over at a specific rate (Figure 6). The modeling approach described in detail in study II is summarized with the model structure below:

## SYNOPSIS

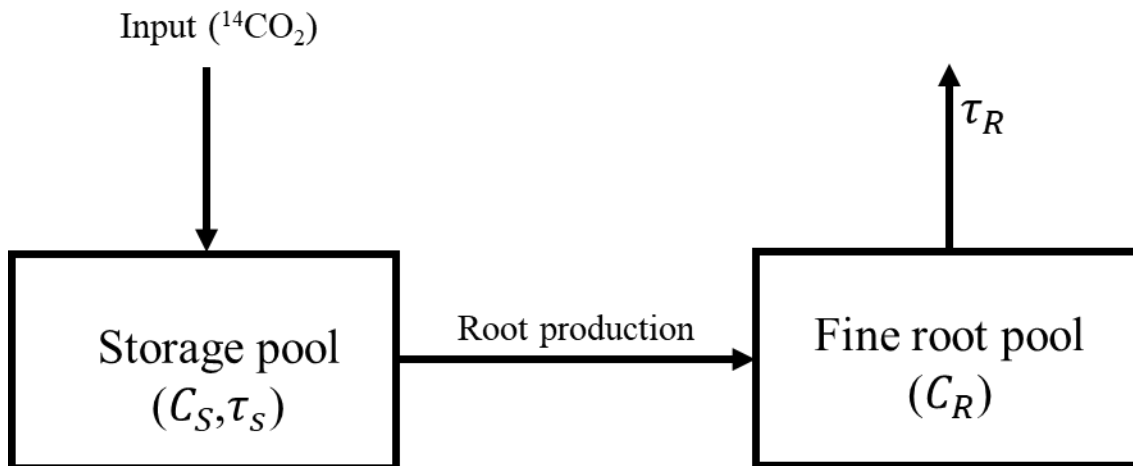


**Figure 6:** Conceptual diagram of the *one-pool* model with a storage compartment.  $^{14}\text{CO}_2$  represents recent C fixed by photosynthesis;  $C_S$  and  $C_R$  are the C in the storage and the fine root pools, respectively.  $\tau_S$  and  $\tau_R$  represent the turnover times of the storage and fine root pools, respectively.

We used a steady-state compartment model implemented in the *SoilR* package, version 1.2.105 (Sierra et al., 2014), to estimate the age and transit time distribution of SOC using the approach developed by Metzler and Sierra (2018). This second model considered a system of multiple compartments at 0 – 10 cm and 10 – 20 cm soil depths separately, assuming no C transfer between both depths (Figure 7). Using the age and transit time distribution of C, we computed the radiocarbon distribution of bulk SOC in both control and warming treatments, according to Chanca et al. (2022). Control and warming treatments were modeled separately, and radiocarbon measurements of 2012 and 2019 were aggregated per subplot and soil depth and used as a time series to better integrate the temporal dynamics of  $^{14}\text{C}$  in each pool (Baisden et al., 2013).

### 1.3.6 Statistical analyses

Statistical analyses and data visualization were conducted in R, version 4.2.1 (R Core Team, 2022), using the R package *ggplot2* (Wickham, 2016) and *gridExtra* (Auguie, 2017). Outliers in the data were identified and tested with Rosner's test using the R package *EnvStats* (Millard, 2013). The normality of the data was checked with the Shapiro-Wilk test. When necessary, data were square-root transformed before analysis to meet the normality assumption. Paired t-tests were conducted to determine the effect of soil warming on fine root functional traits (level

## SYNOPSIS

of significance  $\alpha = 0.05$ ). Principal component analysis (PCA) was carried out with the R packages *FactoMineR* (Lê et al., 2008) and *factoextra* (Kassambara, 2017) to explore the interrelation between fine root traits. Non-metric dimensional scaling (NMDS) was carried out using the R package *vegan* (Oksanen et al., 2019) to visualize the variation of the EcM community in control and warming treatments. The analysis of similarities (ANOSIM) was used to statistically test whether the EcM community composition differs (Clarke, 1993). Soil nutrients were fitted onto the NMDS ordination with the function *envfit* (based on 999 permutations) to determine factors that may drive the observed changes. More details on statistical analyses are available in each separate study.

SYNOPSIS

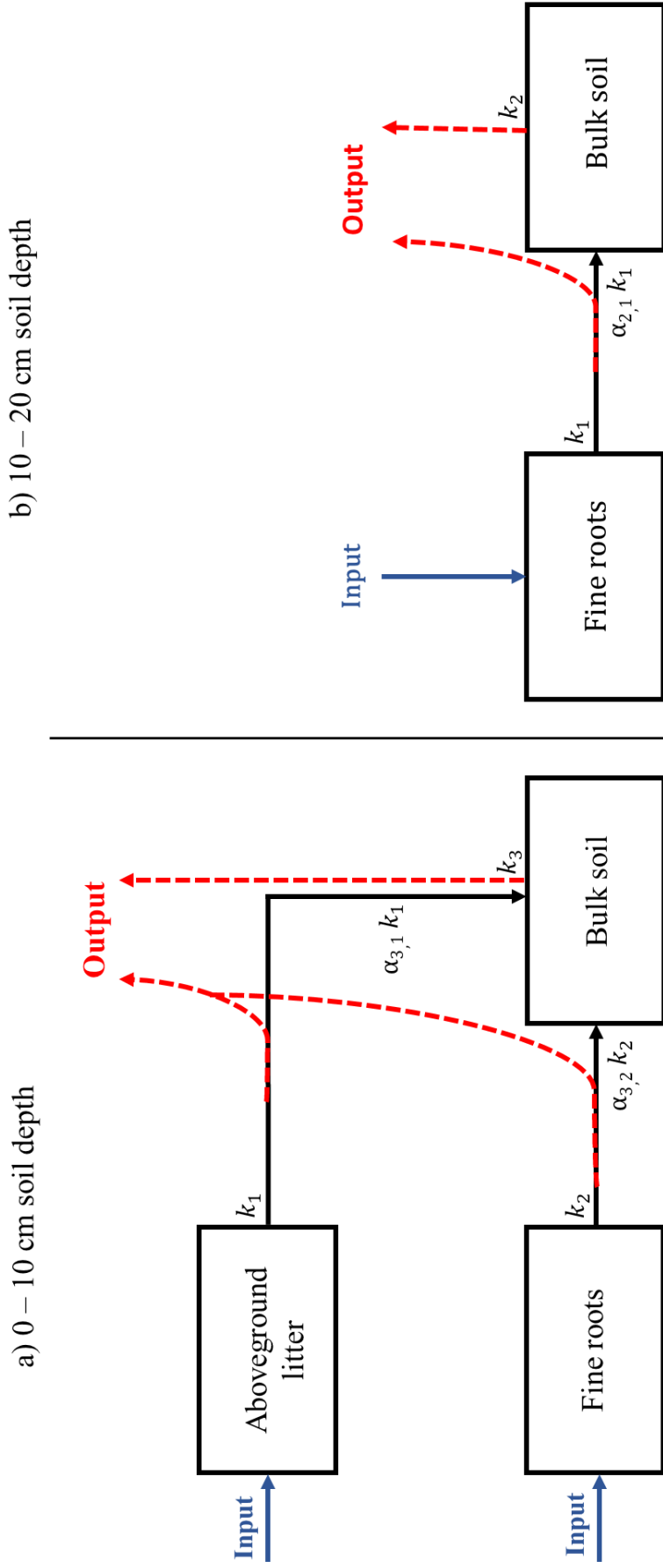


**Figure 7:** Structure of the steady-state compartment model used to estimate age, transit time, and radiocarbon distributions at (a) 0 – 10 cm and (b) 10 – 20 cm soil depths. At 0 – 10 cm,  $k_1$ ,  $k_2$  and  $k_3$  are the decay rates in aboveground litter, fine roots, and bulk SOC, respectively.  $\alpha_{3,1}$  and  $\alpha_{3,2}$  describe the proportion of C transferred from aboveground litter to bulk SOC and from fine roots to bulk SOC, respectively. At 10 – 20 cm,  $k_1$  and  $k_2$  are decay rates in fine roots and bulk SOC, respectively, and  $\alpha_{2,1}$  describes the proportion of C from fine roots to bulk soil (considering aboveground litter not relevant).

## SYNOPSIS

### 1.4 Results and discussion of the key findings

#### 1.4.1 Response of fine root biomass, production, and turnover to long-term soil warming

Fine root biomass measured with soil coring on both occasions (October 2012 and October 2019) showed the same trend at 0 – 20 cm soil depth (Figure 8). On the first occasion in 2012, fine root biomass increased by 13% with soil warming, from 513 to 582 g m<sup>-2</sup>, but the difference was not significant ( $p = 0.231$ ). During the second sampling in 2019, the biomass increased significantly by 17% with soil warming ( $p = 0.045$ ). However, the biomass was smaller, with 355 and 414 g m<sup>-2</sup> in control and warming plots, respectively (Figure 8a; see also Figure 1 in study I). Annual fine root production measured with ingrowth cores strongly increased by 128% (from 99 to 225 g m<sup>-2</sup> yr<sup>-1</sup>) with soil warming after the first year of sampling ( $p = 0.011$ ). However, when considering ingrowth cores retrieved after two years, annual fine root production increased, but not significantly, by 35% (Figure 8b). Fine root turnover measured with different approaches showed a consistent trend at 0 – 20 cm soil depth with soil warming. With the ingrowth core method, we estimated an increase in root C input into the soil by 33% with warming (from 71 to 94 g C m<sup>-2</sup> yr<sup>-1</sup>). However, estimates derived from modeled fine root turnover times and soil coring data, although showing the same trend, were variable (Figure 8c). Using modeled fine root turnover times from 2012 data, we estimated an increase in root C input from 63 to 100 g C m<sup>-2</sup> yr<sup>-1</sup>, while estimations derived from 2019 data were 41 to 49% lower in control and warming treatment, respectively (37 and 51 g C m<sup>-2</sup> yr<sup>-1</sup>). Both approaches demonstrate that litter input by fine roots responded positively to the increase in soil temperature by 4°C in different years. Although we could only identify trends in fine root turnover due to the low sample size and high variability (Fahey et al., 2017), the increase in fine root biomass and fine root production indicates that long-term soil warming increased belowground C allocation of trees and the flux of C from fine roots into the soil.

# SYNOPSIS

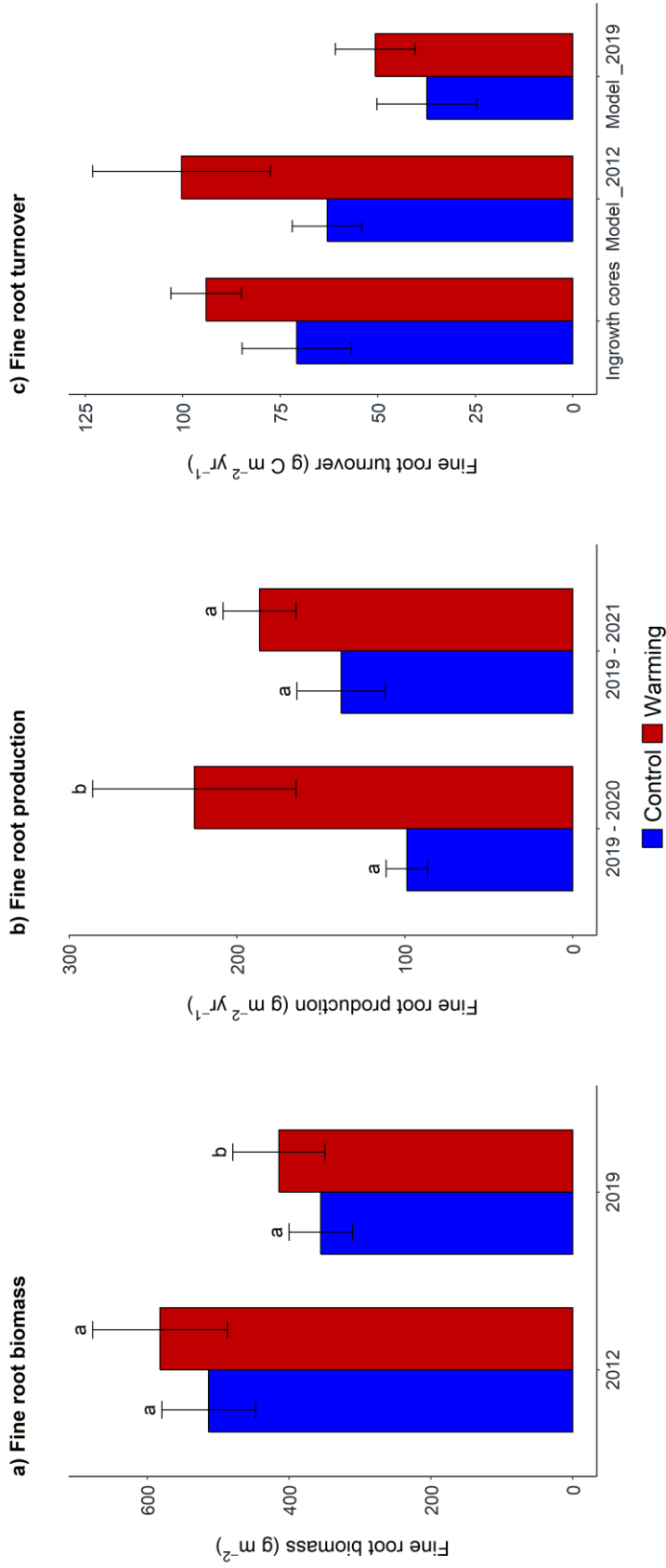


**Figure 8:** Mean fine root biomass (a), fine root production (b) and fine root turnover (c) at 0–20 cm soil depth in the control and the warming treatments. Mean fine root biomass was calculated for both sampling occasions in October 2012 (n = 3) and 2019 (n = 6). Fine root production was measured after one (2019 - 2020) and two years (2019 - 2021), respectively. Lowercase letters indicate significant differences between treatments. Error bars indicate standard errors. The absence of letters indicates that there was no significant difference.

## SYNOPSIS

With the projected change in the length of the growing season and the increase in aboveground plant productivity in the alpine region (Carlson et al., 2017; Choler et al., 2021), this trend will likely continue. Our findings align with Leppälammii-Kujansuu et al. (2013), who also found an increase in fine root biomass in their warming experiment. The observed increase in fine root biomass and fine root production also agrees with a global meta-analysis which suggested an increase of 30% and 9%, respectively (J. Wang et al., 2021). However, Parts et al. (2019), on the same site instead, found that fine root biomass did not significantly change with soil warming. This is likely due to the small sample size in their study. Compared to 2012, we found 29 to 31% lower fine root biomass in both treatments in 2019, which we attribute to interannual variability of fine root production and mortality (McCormack et al., 2014; Pregitzer et al., 2000). Fine root turnover measured in control plots in this study is in the lower range of the values reported by Brunner and Godbold (2007) for temperate forests of Central Europe. As mentioned in the introduction, the differences among studies may be partly due to the methodology. Furthermore, aboveground productivity is also important for the root system, and the cold climate and long snow period at the Achenkirch site may slow down tree growth. Better-growing conditions in the warming treatment (e.g., increase in nitrogen availability) (Pregitzer et al., 2000; J. Wang et al., 2021) or moderate soil drying (Malhotra et al., 2020) have explained the increase in fine root biomass and fine root production with warming in several studies. However, due to the high precipitation at the Achenkirch site (see description of the study site), soil moisture has shown a similar trend in control and warming treatment (Schindlbacher et al., 2009). Instead, the PCA analysis showing the relationship amongst fine root traits (Figure 9) and amongst fine root traits and soil nutrients (Figure 6 in study I) showed that the changes observed in fine root biomass and fine root production, in addition to temperature, were mainly driven by plant phosphorus (P) and potassium (K) needs. K availability is negatively affected by high Ca and Mg concentrations (much stronger sorption than K) in the dolomitic soils. In 2019, we found high Ca and Mg concentrations in fine roots and soil solutions, likely resulting from the weathering of dolomite bedrock (Table 2 in study I). In addition, there is strong evidence that K deposition and foliar K concentration in European forests declined significantly during the last three decades (Penuelas et al., 2020). Collectively, those two factors may impair the K availability for plants. In addition to K, there is also evidence of P deficiency in fine roots at Achenkirch (Table 2 in study I). This deficiency, combined with decreasing trend of P availability in European forests (Penuelas et al., 2020; Talkner et al., 2015), may further explain the observed increase in fine root biomass and

## SYNOPSIS

production. Our findings are supported by an accompanying study at the Achenkirch site which showed that 15 years of soil warming significantly reduced P availability and turnover in the soil (Tian et al., 2023). Therefore, increasing fine root biomass and production might be a tree strategy to increase P and K uptake. Because soil N availability was not affected by soil warming (Heinzle et al., 2021) and because of high N deposition in the northern Alpine region (Herman et al., 2002), we assume that soil N availability and tree N nutrition is not limited at the Achenkirch site. Together, our findings suggest that the effect of soil warming on fine root biomass and production relies on interactions between temperature, soil water, nutrient availability, and aboveground plant productivity. This may therefore result in regional or local differences in the response of fine root systems.

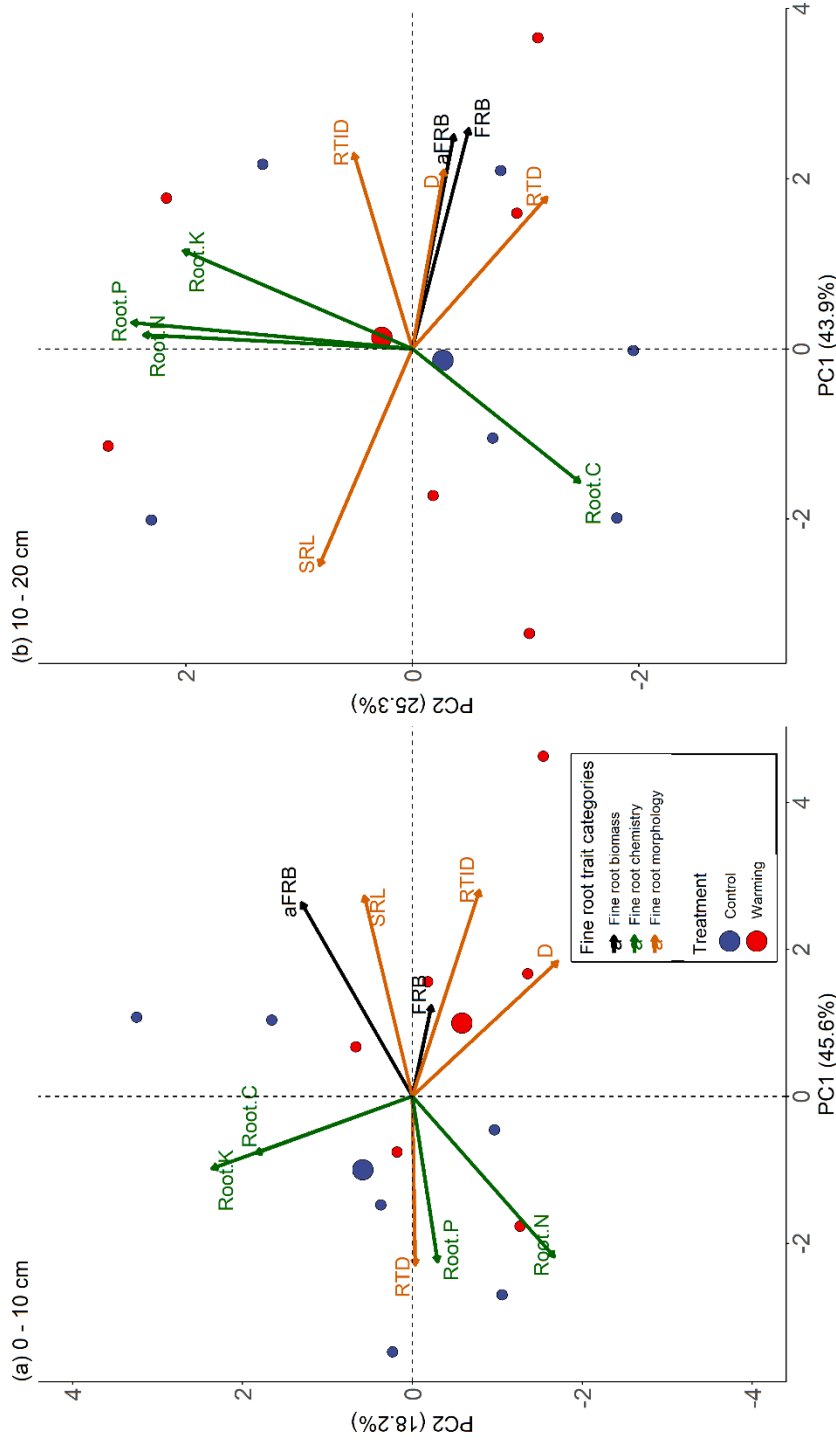


**Figure 9:** Principal component analysis (PCA) of fine root biomass, fine root chemical, and fine root morphological traits measured in 2019 at (a) 0 – 10 cm and (b) 10 – 20 cm soil depths. Principal component scores of samples in both treatments are represented by red and blues cycles, and arrows represent loadings of variables. Positively correlated variables are grouped, while negatively correlated variables are positioned on opposite sides of the plot origin. Abbreviations: FRB, fine root biomass; aFRB, absorptive fine root biomass; D, fine root diameter; RTD, root tissue density; RTID, root tip density; SRL, specific root length; Fine root chemistry (Root C; Root P; Root N and Root K).

## SYNOPSIS

### 1.4.2 Changes in fine root morphology

The morphology of the fine root system also responded to long-term soil warming at 0 – 20 cm soil depth across sampling years (Figure 10). SRL, for example, increased from 27 to 31 m g<sup>-1</sup> in 2012 and from 22 to 28 m g<sup>-1</sup> in 2019 ( $\rho = 0.008$ ) (Figure 10a). Likewise, SRA significantly increased from 185 to 339 cm<sup>2</sup> g<sup>-1</sup> in 2012 ( $\rho = 0.001$ ) and from 311 to 368 cm<sup>2</sup> g<sup>-1</sup> in 2019 ( $\rho = 0.016$ ) (Figure 10b). Root tip density showed a strong increase with warming, especially in 2019 ( $\rho < 0.001$ ). Fine root diameter, on the other hand, was not affected by the warming treatment.

Together with the changes in fine root biomass, the increase in SRL, SRA, and root tip density with soil warming across the years indicate that fine roots increased their absorptive capacity (Löhmus et al., 1989; McCormack et al., 2015; Ostonen et al., 2007). This implies that fine roots in the warming treatment adopted an acquisitive strategy for nutrients and water uptake (McCormack & Iversen, 2019). The increase in absorptive fine root biomass in the warmed plots (Table 1 in study I) and the proportion of fine root length in the 0 – 2 mm diameter class (Figure 11) which are considered highly absorptive (McCormack et al., 2015), also support this. Further, the slight increase in the percentage of EcM root tips in the warming treatment (Table 1 in study II) also indicates an increased uptake ability of fine roots in the warming treatment (see also next section).

The negative relationship between fine root morphological and chemical traits (Figure 9) and between fine root morphological traits and soil nutrients (Figure 6 in study I), especially at 0 – 10 cm soil depth, suggest that increasing SRL, SRA, and root tip density was likely a strategy to overcome the lack of soil P and K availability. With the ongoing decrease in P and K availability across European forests (Penuelas et al., 2020; Talkner et al., 2015; Talkner et al., 2019), we expect these changes in fine root morphological traits will be more pronounced under projected climate warming in temperate mountain forests. This is because more nutrients are needed under higher plant productivity, and this nutrient sink should also affect fine root morphology. Changes in fine root morphology observed in this study agree with the results of other studies (Björk et al., 2007; Leppälammil-Kujansuu et al., 2013; Parts et al., 2019). Surprisingly, a global meta-analysis suggests no warming effect on fine root morphology across various ecosystems (J. Wang et al., 2021). This discrepancy is probably because this meta-analysis considered a limited number of studies. Our findings suggest that changes in fine root morphology are linked to nutrient and water availability, and morphological adaptations

## SYNOPSIS

may only be expected in phases of transitions in the nutrient status (from well to poorly supplied, for example).

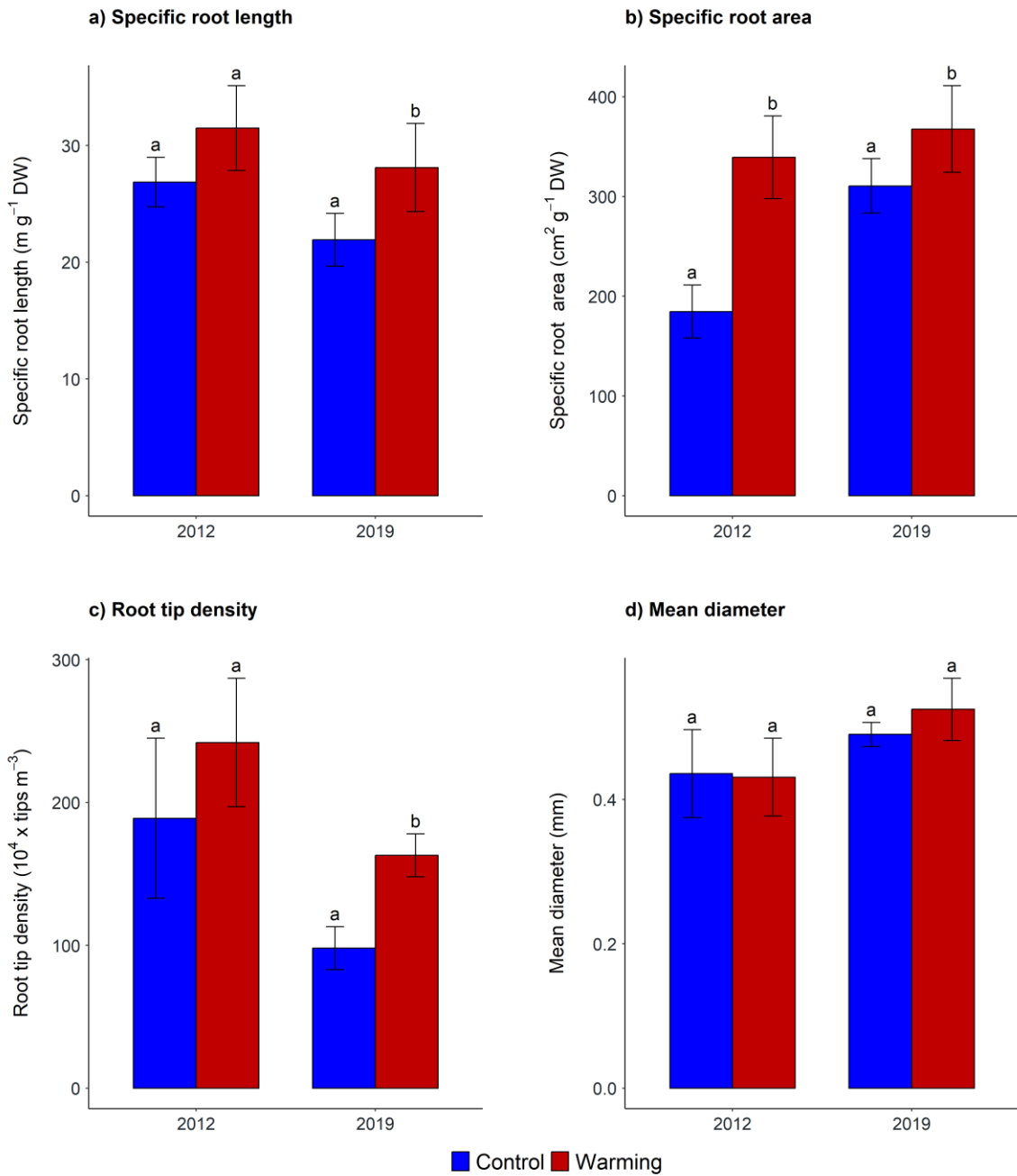


**Figure 10:** Morphological traits of fine roots in control and warmed plots in October 2012 ( $n = 3$ ) and October 2019 ( $n = 6$ ): a) specific root length, b) specific root area, c) root tip density, d) average diameter. Values are means, and error bars indicate standard errors. Different letters indicate significant differences between control and warming treatments.

## SYNOPSIS

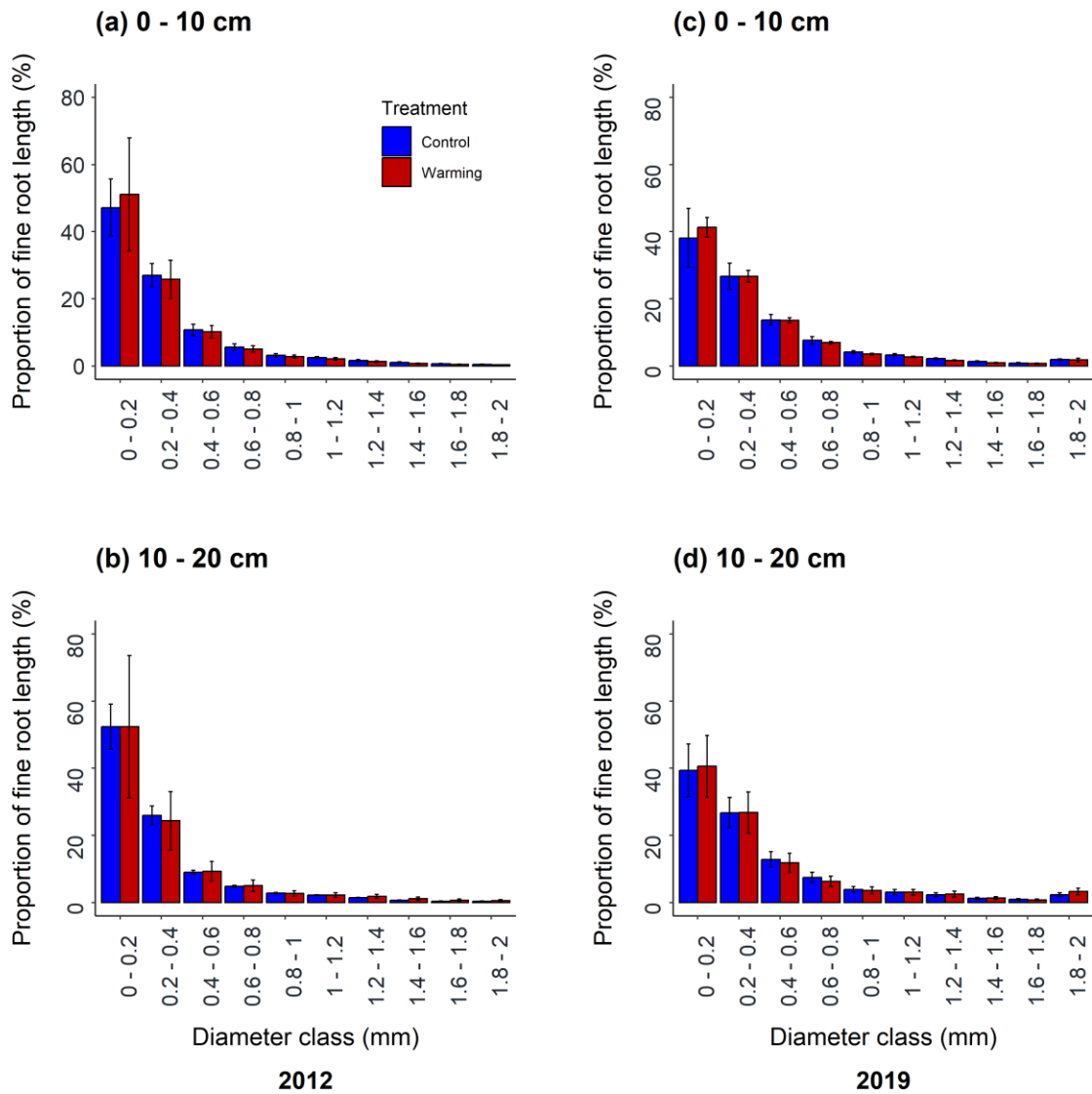


**Figure 11:** The proportion of fine root length in different diameter classes at 0 – 10 cm and 10 – 20 cm soil depth in control and warming treatments in 2012 (panels a and b) and 2019 (panels c and d). Values are means, and error bars indicate standard errors.

### 1.4.3 EcM fungal community

Along with morphological changes, EcM exploration types could also adapt to lower P and K availability. Surprisingly, long-term soil warming did not affect EcM exploration types (Figure 5 in study I), but rather, the community composition of the EcM fungal community changed with soil warming ( $p < 0.039$ ) and also soil depth ( $p < 0.002$ ) (Figure 12a, 12b and 12c). The similarity percentages breakdown (SIMPER) analysis and the classification method program

## SYNOPSIS

(CLAM) test conducted in study I (Figure 3 and 4) helped us identify which fungal genera were more abundant in the warming treatment. The most significant change observed was the increase in the relative abundance of the EcM genus *Cenococcum* by approximately 15% in the warming treatment in the upper soil depth. This genus alone explained around 8% of the dissimilarity between control and warming treatments. This short-distance EcM has demonstrated high drought tolerance (Koide et al., 2014; LoBuglio, 1999) and proteolytic abilities (Clemmensen & Michelsen, 2006; LoBuglio, 1999), which will be an advantage for the tree host under future climate warming in temperate mountain forests. At 10 – 20 cm soil depth, our results showed a strong increase in the relative abundance of EcM of the genus *Sebacina* by 44% (ca. 22% contribution to the dissimilarity). Symbiosis with *Sebacina* is often interpreted as nutrient absorption at a low C cost for the host (Defrenne et al., 2019). In addition to *Sebacina*, EcM of the genus *Boletus* also significantly increased by 26% in the warming treatment. *Boletus* is characterized by a long-distance exploration type that allows soil exploration far beyond the initial root surface (Agerer, 2006; Defrenne et al., 2021; Wallander et al., 2013) and thus might play an important role as well under warmer conditions. Our finding that the EcM community composition changed agrees well with observations from other experiments (Fernandez et al., 2017; Mucha et al., 2018; Solly et al., 2017; Treseder et al., 2016). However, the EcM community composition is very complex, as indicated by several unidentified OTUs in our study. Furthermore, some taxa occurred only in one or two subplots. High spatial and temporal variability in the EcM community requires repeated sampling to improve our understanding of changes in the EcM community structure.

In addition to indicating whether the EcM community changed, we also examined which soil nutrients (P, K) were driving the observed changes. Fitting those soil properties on the ordination space derived from the NMDS revealed that only P was significantly driving changes in the EcM community composition ( $\rho < 0.027$ ,  $R^2 = 0.28$ ). As mentioned above, due to the high N deposition at the Achenkich site, we did not expect a significant contribution of soil N in shaping the observed changes in the EcM community (Table 4). Therefore, like changes in fine root biomass and morphology, our results indicated that phosphorus needs primarily explain the changes in the EcM fungal community. This is in agreement with Treseder (2004), who found that P limitation changes the EcM community in various field studies. Our finding that soil warming did not affect EcM exploration types was also observed by Parts et al. (2019). Although we couldn't find a trend in EcM exploration types, our results indicated that long-term warming changed the EcM fungal community toward soil nutrient

## SYNOPSIS

uptake. However, the increase in nutrient uptake capacity of fine roots in the warming treatment was more visible at the level of fine root morphology than at the level of mycorrhiza associations. Therefore, repeated sampling or looking at how the EcM fungal community in the bulk soil changed may provide additional insight to complement our findings.

**Table 4:** The relationship between soil nutrient contents (soil K, P, and N) and the first (NMDS 1) and second (NMDS 2) axes of EcM community NMDS scores. The  $R^2$  values represent variance explained by the ordination.  $\rho$  values are based on 999 permutations.

Factor	NMDS1	NMDS2	$R^2$	$\rho$ value
K	0.36947	0.92924	0.0103	0.889
P	-0.30087	0.95367	0.2768	<b>0.027 *</b>
N	-0.67315	0.73950	0.0474	0.633

# SYNOPSIS

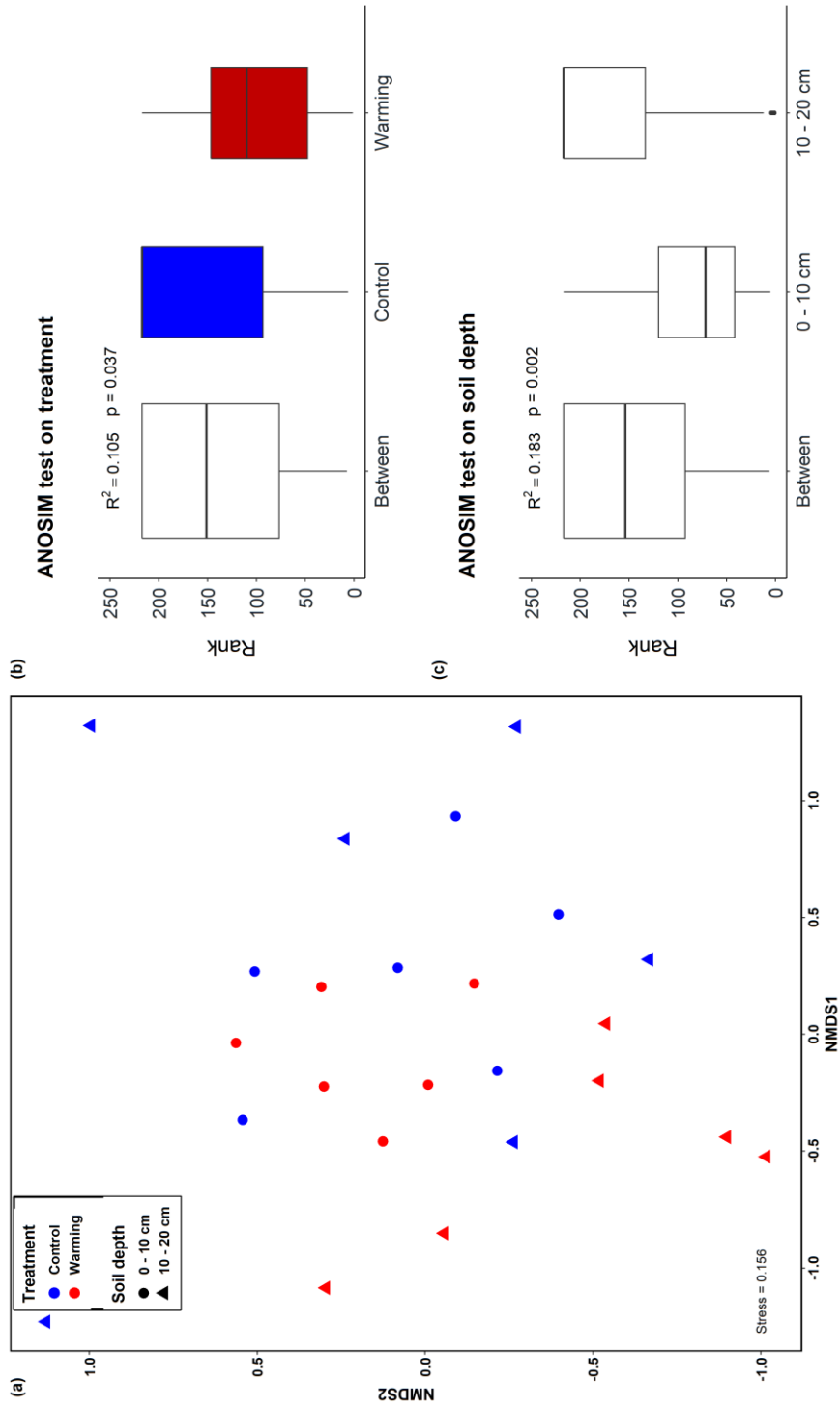


**Figure 12:** Non-metric multidimensional scaling (NMDS) ordination of the EcM community based on the relative abundance of OTUs in control and warming treatments and in both soil depths (a). Analysis of similarity (ANOSIM) test on treatment (b) and soil depth (c). According to Clarke (1993), stress:  $<0.05$  = excellent,  $<0.10$  = good,  $<0.20$  = usable. ANOSIM is based on 9999 permutations.

## SYNOPSIS

### 1.4.4 Radiocarbon dynamics, soil respiration and implications for carbon cycling

In study III, radiocarbon analyses showed no evidence that soil warming significantly affected the  $\Delta^{14}\text{C}$  signatures of bulk soil. This finding is similar to the results of Schnecker et al. (2016) at the same field site. Although we found slight changes in the distribution of SOC by radiocarbon signatures (Figure 3 in study III), the small differences in the proportional distribution do not necessarily mean changes in absolute. They do not imply whether there is more or less recent or old carbon in control or warmed soils (Chanca et al., 2022). In study III, we also evaluated the effects of soil warming on the transit time of C. The model we used showed that long-term soil warming had overall no effect on the transit time of C (Figure 2 in study III), although a slight decrease in the median transit time from 3 to 2 years was observed at 0 – 10 cm soil depth. This non-effect on the transit time of C defined above as the age of C in the output flux (Sierra et al., 2017) indicates that C may similarly “travel” in control and warming treatments.

Nevertheless, irrespective of treatment, our results showed that the transit time of C at 0 – 20 cm soil depth was relatively fast (median transit time of less than 5 and 20 years at 0 – 10 and 10 – 20 cm soil depth, respectively). This means that the C inputs may leave the soil system relatively quickly and do not contribute to long-term SOC storage in the forest studied. This is in agreement with Xiao et al. (2022), who found that younger C dominates soil C efflux at the global scale. Although preliminary data showed no change in SOC stocks between control and warming treatments (Figure 15), our analysis in study III revealed that annual  $\text{CO}_2$  efflux for the years 2006, 2010, 2015, and 2019 were high in the warming treatment.  $\text{CO}_2$  efflux increased by +40% ( $p = 0.142$ ), +37% ( $p = 0.002$ ), +39% ( $p = 0.005$ ), and +47% ( $p = 0.002$ ) in those years, respectively, compared to the control treatment (Figure 13). It should be noted that annual  $\text{CO}_2$  efflux was identical at the same soil temperature in the warmed and control plots in 2014 when the warming system was not operated (Schindlbacher, unpublished data). This, therefore, indicates that the observed differences in soil respiration can be attributed exclusively to the increase in soil temperature and not to small-scale variation among the treatments.

Taken together, our finding that soil  $\text{CO}_2$  efflux increased with soil warming even after 15 years and despite no change in SOC stocks indicates that soil respiration at the Achenkirch site has not yet acclimated to increasing soil temperature. This finding contrasts the result of the long-term soil warming experiment at the Harvard forest (ca. 30 years of +5° C soil warming),

## SYNOPSIS

where soil respiration rates in the warming plots were equal to or less than those observed in control plots after 10 years of soil warming (Melillo et al., 2017). Notably, fine root biomass decreased by 62% with soil warming at the Harvard forest (Zhou et al., 2011). The drivers of acclimation at this site were attributed to the depletion of the labile C pool (Bradford et al., 2008) and the reduction in microbial biomass (Bradford et al., 2008; Frey et al., 2008). The question remains, therefore: what is the source of the additional CO<sub>2</sub> efflux in the warming treatment at Achenkirch?

Schindlbacher et al. (2015) showed no evidence of thermal acclimation of the microbial community after 9 years of soil warming at the Achenkirch site. However, recent data showed a reduction of fungal biomass with warming (Kwatocho Kengdo, unpublished data), likely indicating a decrease in SOC decomposition (Bradford et al., 2008; Frey et al., 2008). Compared to field CO<sub>2</sub> efflux, modeled total C released (from the mineralization of soil organic matter) was small (2.4 and 2.6 t C ha<sup>-1</sup>), accounting for 37% and 29% of the measured field CO<sub>2</sub> efflux in control and warming treatments, respectively. Therefore, our finding suggests that the remaining vast majority (4.1 and 6.5 t C ha<sup>-1</sup>), accounting for 63% and 71% of the measured field CO<sub>2</sub> efflux, may primarily originate from the rhizosphere respiration. This result agrees with Boone et al. (1998), who suggested that root respiration exerted a strong response to rising temperature than the bulk soil alone in a mixed temperate forest. Our conclusion also agrees with the results of a meta-analysis suggesting that soil warming strongly increased root respiration globally (J. Wang et al., 2021). Recent findings at the Achenkirch site also revealed decreased microbial biomass and extractable C, indicating labile substrate depletion with soil warming (C. Shi et al., 2023; Tian et al., 2023). The increase in rhizosphere respiration can be explained by the respiration of fine roots as a direct metabolic response and to some extent by higher mineralization of rhizodeposits, including root exudates (Heinze et al., in review), active secretions like secondary metabolites. This also includes mucilage, cell sloughing, and senesced fine root tissues (Bowsher et al., 2018).

## SYNOPSIS

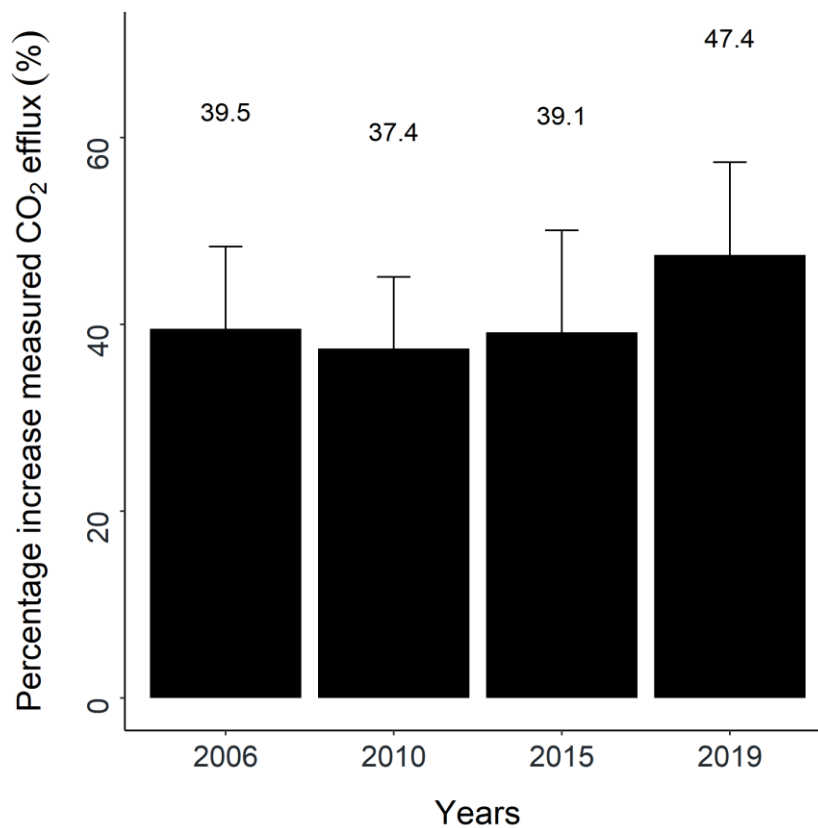


**Figure 13:** Percentage increase in measured CO<sub>2</sub> efflux in 2006, 2010, 2015, and 2019. Values are means, and error bars indicate standard errors.

In studies I and II, we found increases in fine root biomass by 13% and 17% after 9 and 15 years of soil warming, respectively. We also found an increase in absorptive fine root biomass and a change in fine root morphology with the increase in SRL, SRA, and root tip density, implying an increase in the proportion of fast metabolically active roots in the warmed plots. All these findings suggest that root respiration might be substantially important in the warming treatment as fast metabolically active roots have been shown to contribute significantly to total soil respiration (Xia et al., 2010). During the early phase of the experimental soil warming treatment at Achenkirch (2005 – 2006), Schindlbacher et al. (2009) found that autotrophic and heterotrophic respirations responded equally to soil warming. Considering the increase in fine root biomass and fine root metabolic activity with warming, we expect a high contribution of autotrophic respiration in explaining the observed difference in field CO<sub>2</sub> efflux.

## SYNOPSIS

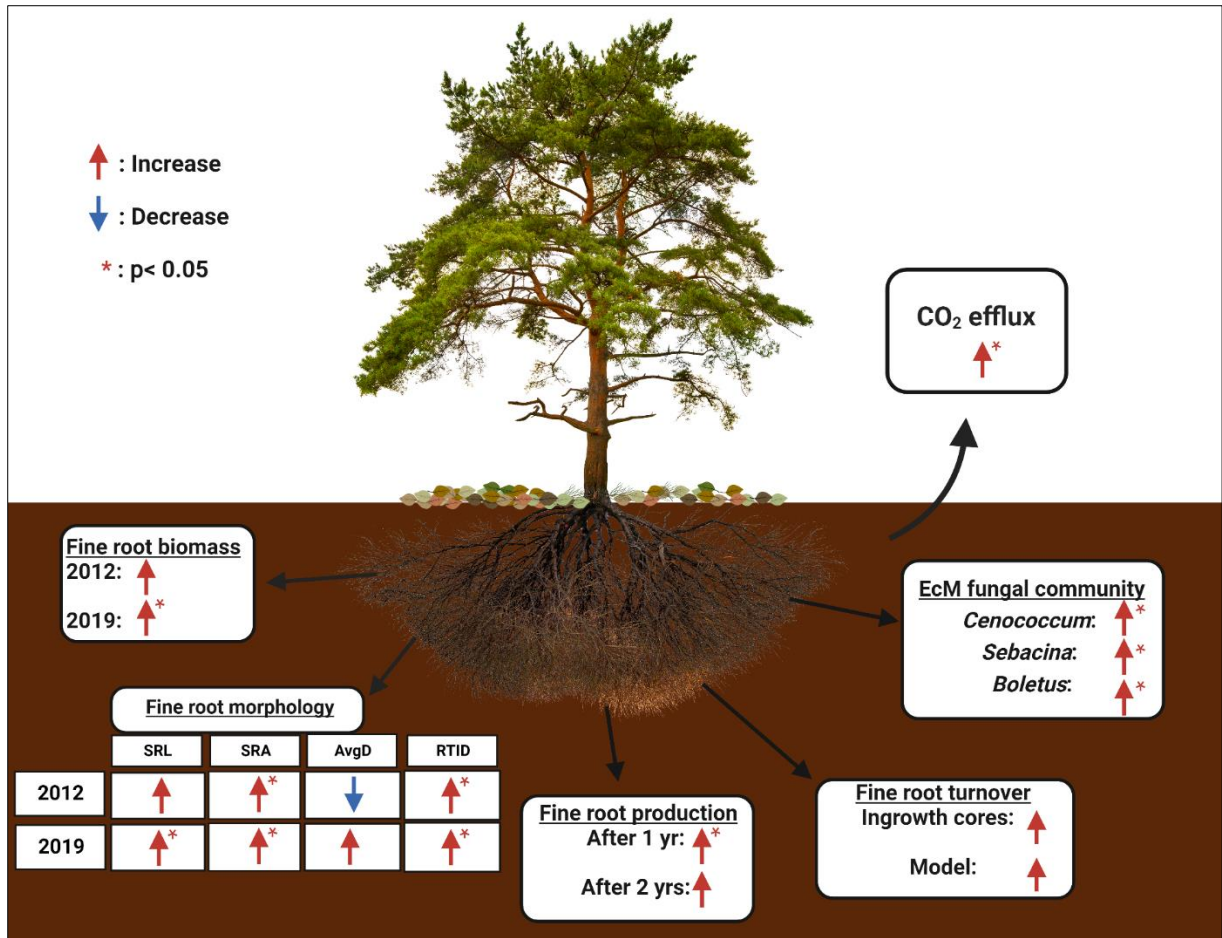


**Figure 14:** Relative change in fine root biomass, production, morphology, turnover, EcM fungal community, and soil CO<sub>2</sub> efflux with warming. Abbreviations: SRL, specific root length; SRA, specific root area; AvgD, average fine root diameter; RTID, root tip density. Tree image vector acquired from iStock.com/DrPAS (under the standard license agreement). Figure created with BioRender.com

However, considering the total C input to the soil presented in Figure 15 and in addition to methodological constraints based on the difference between modeling and CO<sub>2</sub> efflux, we assume we missed a substantial part of the C input (rhizodeposition). Therefore, an underestimation of the total C input into the soil might be possible, for example, by very fine roots or root hairs, which may be washed away or decomposed during storage and fine root processing in the laboratory (Fahey et al., 2017). If not growing to thicker fine roots, these fine roots have a very short lifetime and could be a source of CO<sub>2</sub> following microbial degradation. Because soil warming significantly changed fine root morphology toward long and thin fine roots, we assume an important C input to the soil by this fast cycling fine root fraction,

## SYNOPSIS

especially via the exudates and necromass (Keller et al., 2021; Kuzyakov, 2002). Heinzle et al. (2023) found an increase in root exudation by 30% with warming (from 0.33 to 0.43 t C ha<sup>-1</sup> yr<sup>-1</sup>) at the Achenkirch site. Fernandez et al. (2013) found *Cenococcum* to be 4 – 10 times more persistent in soil than other EcM fungi, implying that they may contribute more to C sequestration in soil. Klink et al. (2022) recently found that fungal residues were more significant plant C input to the soil than plant residues. We saw in study I an increase in the relative abundance of the EcM long-distance exploration type *Boletus* which is characterized by high mycelial biomass compared to short-distance exploration types which instead form a dense network (Agerer, 2001; Wallander et al., 2013). We assumed that the turnover of the biomass of this long-distance exploration type might contribute to soil C (Ekblad et al., 2013; Frey, 2019; Heinemeyer et al., 2007). Therefore, this unaccounted fresh C input via ectomycorrhizal roots may be rapidly respired as CO<sub>2</sub> by soil microbes (Finzi et al., 2015) without being taken into account in the present thesis.

DOC leaching presented in Figure 15 was estimated by Schindlbacher et al. (2009) using suction cups installed at 15 cm and 30 cm soil depths at each subplot. Annual DOC outflow was overall very small (0.03 and 0.02 t C ha<sup>-1</sup> in control and warming, respectively) compared to measured gaseous losses. We assume, therefore, that DOC leaching at Achenkirch does not play a big role because it represents less than 1% of the total annual soil CO<sub>2</sub> loss, irrespective of the treatment. In a lysimeter study using soil cores from the Achenkirch site, Schindlbacher et al. (2019) found that compared to DOC, dissolved inorganic carbon (DIC) leaching was more important, with ca. 0.2 t C ha<sup>-1</sup> and 0.4 t C ha<sup>-1</sup> in control and warming, respectively. This represents around 3 to 4% of the measured annual soil CO<sub>2</sub> loss in the present study.

We estimated in study III that the average difference in soil CO<sub>2</sub> efflux between control and warming treatments over the investigated years was about 2.6 t C ha<sup>-1</sup>. Whether total SOC stocks changed since the experimental treatment started remains unknown (no pre-treatment SOC stocks available). With the small SOC difference (between control and warming) measured after 15 years of soil warming, we conclude that 15 years of soil warming at Achenkirch led to high CO<sub>2</sub> efflux from the soil, but if any, the SOC losses were minimal. Climate warming is projected to increase aboveground plant productivity in the alpine region (Carlson et al., 2017; Choler et al., 2021; Rumpf et al., 2022), and this might further increase belowground C allocation and hence C input into the soil. When soil moisture is not a limiting factor, organic matter decomposition is also projected to increase with future climate warming (Davidson & Janssens, 2006). Therefore, there might be scenarios where increasing C input

## SYNOPSIS

into the soil exceed C loss by soil respiration, or even increasing C loss is compensated with increasing soil C input (M. Lu et al., 2013; Ziegler et al., 2017).

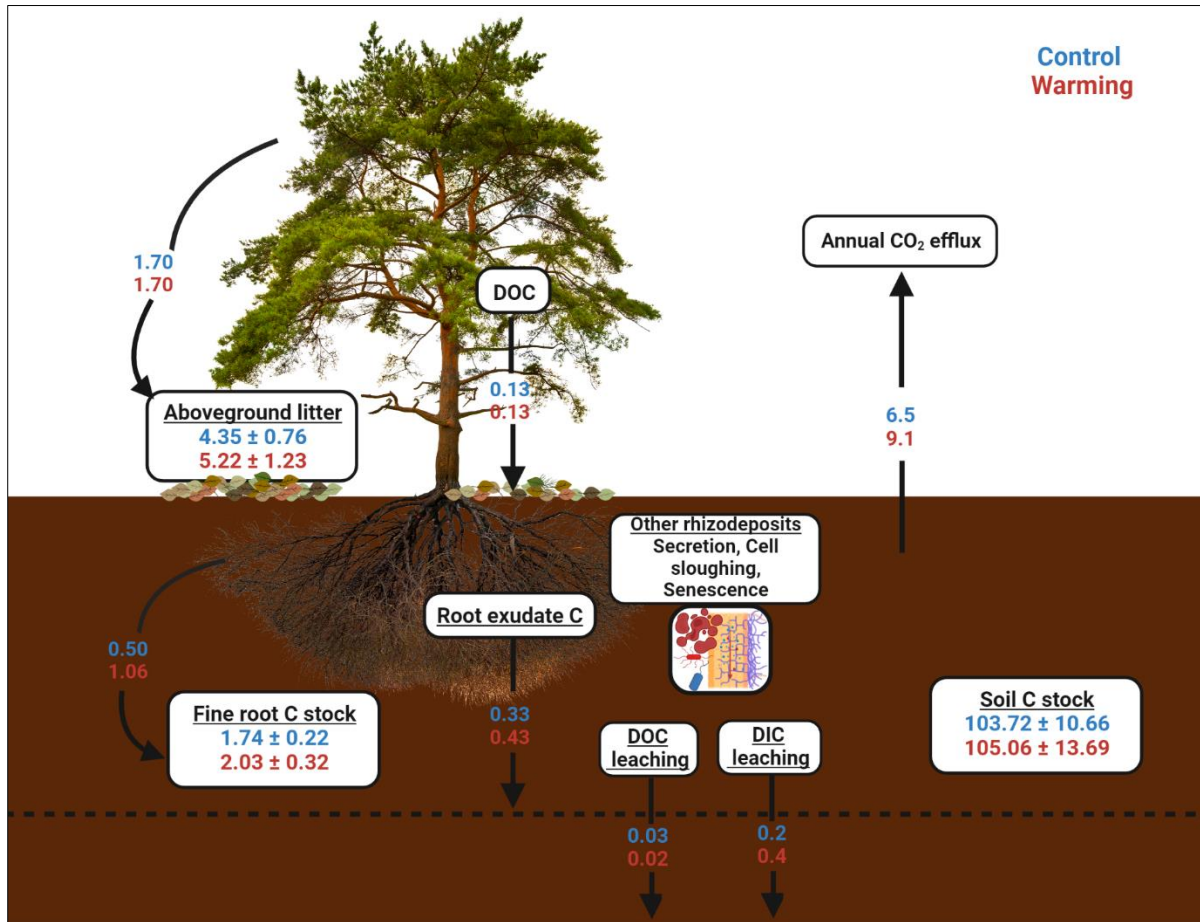


**Figure 15:** Fluxes (t ha<sup>-1</sup> yr<sup>-1</sup>) and stocks (t ha<sup>-1</sup>) of C in control and warming treatments at the Achenkirch site. Black arrows represent fluxes, and numbers in boxes represent C stocks. The aboveground litter input is the average value of the period 2008 – 2019. Root exudates were estimated by Heinzle et al. (2023). Aboveground litter, fine root, and soil C stocks were measured in 2019. The input of C by fine roots is the average value estimated from all methods in study II. Annual CO<sub>2</sub> efflux is the average value for 2006, 2010, 2015, and 2019. DOC and DIC losses were estimated by Schindlbacher et al. (2009; 2019). Other rhizodeposits were not measured in this study.

Tree image vector acquired from iStock.com/DrPAS (under the standard license agreement). Figure created with BioRender.com

## SYNOPSIS

### 1.5 Conclusions and outlook

Increases in fine root biomass, production, and turnover indicate that warming enhanced belowground C allocation of trees and the flux of C into the soil by fine root litter. Fine root morphology also strongly responded to soil warming. We found that warming changed fine root morphology toward long and thin fine roots, which are more metabolically active. This result indicates that the absorptive capacity of the fine root system increased with warming. Contrary to our expectation, soil warming did not affect EcM exploration types but changed the community composition with increased relative abundance of the genus *Cenococcum*, *Sebacina*, and *Boletus* in the warmed plots. Changes in fine root biomass, production, morphology, and EcM fungal community, in addition to temperature, were mainly driven by low soil phosphorus and potassium availability in the warmed plots. If soil phosphorus or potassium availability further decreases, ongoing soil warming could lead to higher competition between fine roots and non-root-associated microorganisms. Although soil CO<sub>2</sub> efflux in the warmed plots was 41% higher than in control, SOC stocks did not change, indicating that soil respiration was not yet acclimated to soil warming. Compared to the total annual CO<sub>2</sub> efflux, C loss by the mineralization of soil organic matter accounted for 37 and 29% in control and warmed plots, indicating that most of the CO<sub>2</sub> efflux may primarily originate from rhizosphere respiration.

Together, our findings suggest that the response of the fine root system to soil warming is likely site-specific. Similar stocks and radiocarbon distribution of SOC in both treatments suggest that climate warming has little or no effect on SOC stocks of temperate forest soils despite high and sustained soil CO<sub>2</sub> efflux with warming. However, in addition to studying the response of the whole forest ecosystem to warming, we recommend that future research should focus more on the effect of climate warming on root-soil carbon transfer, especially by looking at rhizodeposits which may play an important role in the overall response of SOC to warming.

## SYNOPSIS

### 1.6 References

- Agerer, R. (2001). Exploration types of ectomycorrhizae: A proposal to classify ectomycorrhizal mycelial systems according to their patterns of differentiation and putative ecological importance. *Mycorrhiza*, 11, 107–114. <https://doi.org/10.1007/s005720100108>
- Agerer, R. (2006). Fungal relationships and structural identity of their ectomycorrhizae. *Mycological Progress*, 5(2), 67–107. <https://doi.org/10.1007/s11557-006-0505-x>
- Ahrens, B., & Reichstein, M. (2014). Reconciling  $^{14}\text{C}$  and minirhizotron-based estimates of fine-root turnover with survival functions. *Journal of Plant Nutrition and Soil Science*, 177(2), 287–296. <https://doi.org/10.1002/jpln.201300110>
- Allison, S. D., & Treseder, K. K. (2008). Warming and drying suppress microbial activity and carbon cycling in boreal forest soils. *Global Change Biology*, 14(12), 2898–2909. <https://doi.org/10.1111/j.1365-2486.2008.01716.x>
- Auguie, B. (2017). gridExtra: Miscellaneous Functions for "Grid" Graphics. <https://CRAN.R-project.org/package=gridExtra>
- Averill, C., & Hawkes, C. V. (2016). Ectomycorrhizal fungi slow soil carbon cycling. *Ecology Letters*, 19(8), 937–947. <https://doi.org/10.1111/ele.12631>
- Averill, C., Turner, B. L., & Finzi, A. C. (2014). Mycorrhiza-mediated competition between plants and decomposers drives soil carbon storage. *Nature*, 505(7484), 543–545. <https://doi.org/10.1038/nature12901>
- Bai, E., Li, S., Xu, W., Li, W., Dai, W., & Jiang, P. (2013). A meta-analysis of experimental warming effects on terrestrial nitrogen pools and dynamics. *New Phytologist*, 199(2), 441–451. <https://doi.org/10.1111/nph.12252>
- Baisden, W. T., Parfitt, R. L., Ross, C., Schipper, L. A., & Canessa, S. (2013). Evaluating 50 years of time-series soil radiocarbon data: towards routine calculation of robust C residence times. *Biogeochemistry*, 112(1-3), 129–137. <https://doi.org/10.1007/s10533-011-9675-y>
- Barrett, D. J. (2002). Steady state turnover time of carbon in the Australian terrestrial biosphere. *Global Biogeochemical Cycles*, 16(4), 55-1-55-21. <https://doi.org/10.1029/2002GB001860>
- Bellamy, P. H., Loveland, P. J., Bradley, R. I., Lark, R. M., & Kirk, G. J. D. (2005). Carbon losses from all soils across England and Wales 1978-2003. *Nature*, 437(7056), 245–248. <https://doi.org/10.1038/nature04038>
- Bennett, A. E., & Classen, A. T. (2020). Climate change influences mycorrhizal fungal-plant interactions, but conclusions are limited by geographical study bias. *Ecology*, 101(4), e02978. <https://doi.org/10.1002/ecy.2978>
- Björk, R. G., Majdi, H., Klemedtsson, L., Lewis-Jonsson, L., & Molau, U. (2007). Long-term warming effects on root morphology, root mass distribution, and microbial activity in two dry tundra plant communities in northern Sweden. *New Phytologist*, 176(4), 862–873. <https://doi.org/10.1111/j.1469-8137.2007.02231.x>
- Blois, J. L., Williams, J. W., Fitzpatrick, M. C., Jackson, S. T., & Ferrier, S. (2013). Space can substitute for time in predicting climate-change effects on biodiversity. *Proceedings of the*

## SYNOPSIS

- National Academy of Sciences of the United States of America*, 110(23), 9374–9379. <https://doi.org/10.1073/pnas.1220228110>
- Blume-Werry, G. (2022). The belowground growing season. *Nature Climate Change*, 12(1), 11–12. <https://doi.org/10.1038/s41558-021-01243-y>
- Bokhorst, S., Huiskes, A., Convey, P., Sinclair, B. J., Lebouvier, M., van de Vijver, B., & Wall, D. H. (2011). Microclimate impacts of passive warming methods in Antarctica: implications for climate change studies. *Polar Biology*, 34(10), 1421–1435. <https://doi.org/10.1007/s00300-011-0997-y>
- Boone, R. D., Nadelhoffer, K. J., Canary, J. D., & Kaye, J. P. (1998). Roots exert a strong influence on the temperature sensitivity of soil respiration. *Nature*, 396(6711), 570–572. <https://doi.org/10.1038/25119>
- Bowsher, A. W., Evans, S., Tiemann, L. K., & Friesen, M. L. (2018). Effects of soil nitrogen availability on rhizodeposition in plants: a review. *Plant and Soil*, 423(1-2), 59–85. <https://doi.org/10.1007/s11104-017-3497-1>
- Bradford, M. A., Davies, C. A., Frey, S. D., Maddox, T. R., Melillo, J. M., Mohan, J. E., Reynolds, J. F., Treseder, K. K., & Wallenstein, M. D. (2008). Thermal adaptation of soil microbial respiration to elevated temperature. *Ecology Letters*, 11(12), 1316–1327. <https://doi.org/10.1111/j.1461-0248.2008.01251.x>
- Bronson, D. R., Gower, S. T., Tanner, M., & Linder, S. & Van Herk, I. (2008). Response of soil surface CO<sub>2</sub> flux in a boreal forest to ecosystem warming. *Global Change Biology*, 14(4), 856–867. <https://doi.org/10.1111/j.1365-2486.2007.01508.x>
- Brundrett, M. C., & Tedersoo, L. (2018). Evolutionary history of mycorrhizal symbioses and global host plant diversity. *New Phytologist*, 220(4), 1108–1115. <https://doi.org/10.1111/nph.14976>
- Brunner, I., & Godbold, D. L. (2007). Tree roots in a changing world. *Journal of Forest Research*, 12(2), 78–82. <https://doi.org/10.1007/s10310-006-0261-4>
- Burke, M. K., & Raynal, D. J. (1994). Fine root growth phenology, production, and turnover in a northern hardwood forest ecosystem. *Plant and Soil*, 162(1), 135–146. <https://doi.org/10.1007/BF01416099>
- Carey, J. C., Tang, J., Templer, P. H., Kroeger, K. D., Crowther, T. W., Burton, A. J., Dukes, J. S., Emmett, B., Frey, S. D., Heskell, M. A., Jiang, L., Machmuller, M. B., Mohan, J., Panetta, A. M., Reich, P. B., Reinsch, S., Wang, X., Allison, S. D., Bamminger, C., . . . Tietema, A. (2016). Temperature response of soil respiration largely unaltered with experimental warming. *Proceedings of the National Academy of Sciences of the United States of America*, 113(48), 13797–13802. <https://doi.org/10.1073/pnas.1605365113>
- Carlson, B. Z., Corona, M. C., Dentant, C., Bonet, R., Thuiller, W., & Choler, P. (2017). Observed long-term greening of alpine vegetation—a case study in the French Alps. *Environmental Research Letters*, 12(11), 114006. <https://doi.org/10.1088/1748-9326/aa84bd>
- Carmona, C. P., Bueno, C. G., Toussaint, A., Träger, S., Díaz, S., Moora, M., Munson, A. D., Pärtel, M., Zobel, M., & Tamme, R. (2021). Fine-root traits in the global spectrum of plant

## SYNOPSIS

- form and function. *Nature*, 597(7878), 683–687. <https://doi.org/10.1038/s41586-021-03871-y>
- Chanca, I., Trumbore, S., Macario, K., & Sierra, C. A. (2022). Probability Distributions of Radiocarbon in Open Linear Compartmental Systems at Steady-State. *Journal of Geophysical Research: Biogeosciences*, 127(3). <https://doi.org/10.1029/2021JG006673>
- Choler, P., Bayle, A., Carlson, B. Z., Randin, C., Filippa, G., & Cremonese, E. (2021). The tempo of greening in the European Alps: Spatial variations on a common theme. *Global Change Biology*, 27(21), 5614–5628. <https://doi.org/10.1111/gcb.15820>
- Clarke, K. R. (1993). Non-parametric multivariate analyses of changes in community structure. *Austral Ecology*, 18(1), 117–143. <https://doi.org/10.1111/j.1442-9993.1993.tb00438.x>
- Clemmensen, K. E., & Michelsen, A. (2006). Integrated long-term responses of an arctic–alpine willow and associated ectomycorrhizal fungi to an altered environment. *Canadian Journal of Botany*, 84(5), 831–843. <https://doi.org/10.1139/b06-039>
- Costello, A., Abbas, M., Allen, A., Ball, S., Bell, S., Bellamy, R., Friel, S., Groce, N., Johnson, A., Kett, M., Lee, M., Levy, C., Maslin, M., McCoy, D., McGuire, B., Montgomery, H., Napier, D., Pagel, C., Patel, J., . . . Patterson, C. (2009). Managing the health effects of climate change. *The Lancet*, 373(9676), 1693–1733. [https://doi.org/10.1016/S0140-6736\(09\)60935-1](https://doi.org/10.1016/S0140-6736(09)60935-1)
- Davidson, E. A., & Janssens, I. A. (2006). Temperature sensitivity of soil carbon decomposition and feedbacks to climate change. *Nature*, 440(7081), 165–173. <https://doi.org/10.1038/nature04514>
- Dawes, M. A., Philipson, C. D., Fonti, P., Bebi, P., Hättenschwiler, S., Hagedorn, F., & Rixen, C. (2015). Soil warming and CO<sub>2</sub> enrichment induce biomass shifts in alpine tree line vegetation. *Global Change Biology*, 21(5), 2005–2021. <https://doi.org/10.1111/gcb.12819>
- Defrenne, C. E., Childs, J., Fernandez, C. W., Taggart, M., Nettles, W. R., Allen, M. F., Hanson, P. J., & Iversen, C. M. (2021). High-resolution minirhizotrons advance our understanding of root-fungal dynamics in an experimentally warmed peatland. *Plants, People, Planet*, 3(5), 640–652. <https://doi.org/10.1002/ppp3.10172>
- Defrenne, C. E., Philpott, T. J., Guichon, S. H. A., Roach, W. J., Pickles, B. J., & Simard, S. W. (2019). Shifts in Ectomycorrhizal Fungal Communities and Exploration Types Relate to the Environment and Fine-Root Traits Across Interior Douglas-Fir Forests of Western Canada. *Frontiers in Plant Science*, 10, 643. <https://doi.org/10.3389/fpls.2019.00643>
- Deslippe, J. R., Hartmann, M., Simard, S. W., & Mohn, W. W. (2012). Long-term warming alters the composition of Arctic soil microbial communities. *FEMS Microbiology Ecology*, 82(2), 303–315. <https://doi.org/10.1111/j.1574-6941.2012.01350.x>
- Eissenstat, D. M., Wells, C. E., Yanai, R. D., & Whitebeck, J. L. (2000). Building roots in a changing environment: implications for root longevity. *New Phytologist*, 147(1), 33–42. <https://doi.org/10.1046/j.1469-8137.2000.00686.x>
- Ekblad, A., Wallander, H., Godbold, D. L., Cruz, C., Johnson, D., Baldrian, P., Björk, R. G., Epron, D., Kieliszewska-Rokicka, B., Kjøller, R., Kraigher, H., Matzner, E., Neumann, J., & Plassard, C. (2013). The production and turnover of extramatrical mycelium of

## SYNOPSIS

- ectomycorrhizal fungi in forest soils: role in carbon cycling. *Plant and Soil*, 366(1-2), 1–27. <https://doi.org/10.1007/s11104-013-1630-3>
- Ettinger, A. K., Chuine, I., Cook, B. I., Dukes, J. S., Ellison, A. M., Johnston, M. R., Panetta, A. M., Rollinson, C. R., Vitasse, Y., & Wolkovich, E. M. (2019). How do climate change experiments alter plot-scale climate? *Ecology Letters*, 22(4), 748–763. <https://doi.org/10.1111/ele.13223>
- Faber, J., Quadros, A. F., & Zimmer, M. (2018). A Space-For-Time approach to study the effects of increasing temperature on leaf litter decomposition under natural conditions. *Soil Biology and Biochemistry*, 123, 250–256. <https://doi.org/10.1016/j.soilbio.2018.05.010>
- Fahey, T. J., Yanai, R. D., Gonzales, K. E., & Lombardi, J. A. (2017). Sampling and processing roots from rocky forest soils. *Ecosphere*, 8(6), e01863. <https://doi.org/10.1002/ecs2.1863>
- Fernandez, C. W., McCormack, M. L., Hill, J. M., Pritchard, S. G., & Koide, R. T. (2013). On the persistence of *Cenococcum geophilum* ectomycorrhizas and its implications for forest carbon and nutrient cycles. *Soil Biology & Biochemistry*, 65, 141–143. <https://doi.org/10.1016/j.soilbio.2013.05.022>
- Fernandez, C. W., Nguyen, N. H., Stefanski, A., Han, Y., Hobbie, S. E., Montgomery, R. A., Reich, P. B., & Kennedy, P. G. (2017). Ectomycorrhizal fungal response to warming is linked to poor host performance at the boreal-temperate ecotone. *Global Change Biology*, 23(4), 1598–1609. <https://doi.org/10.1111/gcb.13510>
- Finzi, A. C., Abramoff, R. Z., Spiller, K. S., Brzostek, E. R., Darby, B. A., Kramer, M. A., & Phillips, R. P. (2015). Rhizosphere processes are quantitatively important components of terrestrial carbon and nutrient cycles. *Global Change Biology*, 21(5), 2082–2094. <https://doi.org/10.1111/gcb.12816>
- Finzi, A. C., Giasson, M.-A., Barker Plotkin, A. A., Aber, J. D., Boose, E. R., Davidson, E. A., Dietze, M. C., Ellison, A. M., Frey, S. D., Goldman, E., Keenan, T. F., Melillo, J. M., Munger, J. W., Nadelhoffer, K. J., Ollinger, S. V., Orwig, D. A., Pederson, N., Richardson, A. D., Savage, K., . . . Foster, D. R. (2020). Carbon budget of the Harvard Forest Long-Term Ecological Research site: pattern, process, and response to global change. *Ecological Monographs*, 90(4). <https://doi.org/10.1002/ecm.1423>
- Frei, E. R., Schnell, L., Vitasse, Y., Wohlgemuth, T., & Moser, B. (2020). Assessing the Effectiveness of in-situ Active Warming Combined With Open Top Chambers to Study Plant Responses to Climate Change. *Frontiers in Plant Science*, 11, 539584. <https://doi.org/10.3389/fpls.2020.539584>
- Frenne, P. de, Graae, B. J., Rodríguez-Sánchez, F., Kolb, A., Chabrierie, O., Decocq, G., Kort, H., an Schrijver, Diekmann, M., Eriksson, O., Gruwez, R., Hermy, M., Lenoir, J., Plue, J., Coomes, D. A., & Verheyen, K. (2013). Latitudinal gradients as natural laboratories to infer species' responses to temperature. *Journal of Ecology*, 101(3), 784–795. <https://doi.org/10.1111/1365-2745.12074>
- Freschet, G. T., Pagès, L., Iversen, C., M., Comas, L. H., Rewald, B., Roumet, C., Klimešová, J., Zadworny, M., Poorter, H., Postma, J. A., Adams, T. S., Bagniewska-Zadworna, A., Bengough, A. G., Blancaflor, E. B., Brunner, I., Cornelissen, J. H. C., Garnier, E., Gessler, A., Hobbie, S. E., . . . McCormack, M. L. (2021). A starting guide to root ecology:

## SYNOPSIS

- Strengthening ecological concepts and standardising root classification, sampling, processing and trait measurements. *The New Phytologist*, 232(3), 973–1122. <https://doi.org/10.1111/nph.17572>
- Freschet, G. T., Roumet, C., Comas, L. H., Weemstra, M., Bengough, A. G., Rewald, B., Bardgett, R. D., Deyn, G. B. de, Johnson, D., Klimešová, J., Lukac, M., McCormack, M. L., Meier, I. C., Pagès, L., Poorter, H., Prieto, I., Wurzburger, N., Zadworny, M., Bagniewska-Zadworna, A., . . . Stokes, A. (2020). Root traits as drivers of plant and ecosystem functioning: Current understanding, pitfalls and future research needs. *New Phytologist*. Advance online publication. <https://doi.org/10.1111/nph.17072>
- Frey, S. D. (2019). Mycorrhizal Fungi as Mediators of Soil Organic Matter Dynamics. *Annual Review of Ecology, Evolution, and Systematics*, 50(1), 237–259. <https://doi.org/10.1146/annurev-ecolsys-110617-062331>
- Frey, S. D., Drijber, R., Smith, H., & Melillo, J. (2008). Microbial biomass, functional capacity, and community structure after 12 years of soil warming. *Soil Biology and Biochemistry*, 40(11), 2904–2907. <https://doi.org/10.1016/j.soilbio.2008.07.020>
- Friedlingstein, P., O'Sullivan, M., Jones, M. W., Andrew, R. M., Gregor, L., Hauck, J., Le Quéré, C., Luijkx, I. T., Olsen, A., Peters, G. P., Peters, W., Pongratz, J., Schwingshackl, C., Sitch, S., Canadell, J. G., Ciais, P., Jackson, R. B., Alin, S. R., Alkama, R., . . . Zheng, B. (2022). Global Carbon Budget 2022. *Earth System Science Data*, 14(11), 4811–4900. <https://doi.org/10.5194/essd-14-4811-2022>
- Gaudinski, J. B., Torn, M. S., Riley, W. J., Dawson, T. E., Joslin, J. d., & Majdi, H. (2010). Measuring and modeling the spectrum of fine-root turnover times in three forests using isotopes, minirhizotrons, and the Radix model. *Global Biogeochemical Cycles*, 24(3). <https://doi.org/10.1029/2009GB003649>
- Gaudinski, J. B., Trumbore, S., Davidson, E., Cook, A., Markewitz, D., & Richter, D. (2001). The age of fine-root carbon in three forests of the eastern United States measured by radiocarbon. *Oecologia*, 129(3), 420–429. <https://doi.org/10.1007/s004420100746>
- Gaul, D., Hertel, D., & Leuschner, C. (2009). Estimating fine root longevity in a temperate Norway spruce forest using three independent methods. *Functional Plant Biology*, 36(1), 11–19. <https://doi.org/10.1071/FP08195>
- Giardina, C. P., & Ryan, M. G. (2000). Evidence that decomposition rates of organic carbon in mineral soil do not vary with temperature. *Nature*, 404(6780), 858–861. <https://doi.org/10.1038/35009076>
- Gill, R. A., & Jackson, R. B. (2000). Global patterns of root turnover for terrestrial ecosystems. *New Phytologist*, 147(1), 13–31. <https://doi.org/10.1046/j.1469-8137.2000.00681.x>
- Gobiet, A., Kotlarski, S., Beniston, M., Heinrich, G., Rajczak, J., & Stoffel, M. (2014). 21st century climate change in the European Alps--a review. *The Science of the Total Environment*, 493, 1138–1151. <https://doi.org/10.1016/j.scitotenv.2013.07.050>
- Hammer, S., & Levin, I. (2017). Monthly mean atmospheric D14CO<sub>2</sub> at Jungfraujoch and Schauinsland from 1986 to 2016. <https://doi.org/10.11588/data/10100>

## SYNOPSIS

- Heinemeyer, A., Hartley, I. P., Evans, S. P., Carreira De La Fuente, J. A., & Ineson, P. (2007). Forest soil CO<sub>2</sub> flux: uncovering the contribution and environmental responses of ectomycorrhizas. *Global Change Biology*, 13(8), 1786–1797. <https://doi.org/10.1111/j.1365-2486.2007.01383.x>
- Heinzle, J., Wanek, W., Tian, Y., Kwatcho Kengdo, S., Borken, W., Schindlbacher, A., & Inselsbacher, E. (2021). No effect of long-term soil warming on diffusive soil inorganic and organic nitrogen fluxes in a temperate forest soil. *Soil Biology and Biochemistry*, 158, 108261. <https://doi.org/10.1016/j.soilbio.2021.108261>
- Heinzle, J., Liu, X., Tian, Y., Kwatcho Kengdo, S., Heinze, B., Nirschi, A., Borken, W., Inselsbacher, E., Wanek, W., & Schindlbacher, A. (2023). Increase in fine root biomass enhances root exudation by long-term soil warming in a temperate forest. In *Front. For. Glob. Change*, 6, Article 1152142. <https://doi.org/10.3389/ffgc.2023.1152142>.
- Helmisaari, H.-S., Leppälammı-Kujansuu, J., Sah, S., Bryant, C., & Kleja, D. B. (2015). Old carbon in young fine roots in boreal forests. *Biogeochemistry*, 125(1), 37–46. <https://doi.org/10.1007/s10533-015-0110-7>
- Herman, F., Smidt, S., Englisch, M., Feichtinger, F., Gerzabek, M., Haberhauer, G., Jandl, R., Kalina, M., & Zechmeister-Boltenstern, S. (2002). Investigations of nitrogen fluxes and pools on a limestone site in the Alps. *Environmental Science and Pollution Research International*, 9(S2), 46–52. <https://doi.org/10.1007/BF02987478>
- Hicks Pries, C. E., van Logtestijn, R. S. P., Schuur, E. A. G., Natali, S. M., Cornelissen, J. H. C., Aerts, R., & Dorrepaal, E. (2015). Decadal warming causes a consistent and persistent shift from heterotrophic to autotrophic respiration in contrasting permafrost ecosystems. *Global Change Biology*, 21(12), 4508–4519. <https://doi.org/10.1111/gcb.13032>
- Hollister, R. D., & Webber, P. J. (2000). Biotic validation of small open-top chambers in a tundra ecosystem. *Global Change Biology*, 6(7), 835–842. <https://doi.org/10.1046/j.1365-2486.2000.00363.x>
- Illumina. (2013). Illumina 16S metagenomic sequencing library preparation: Preparing 16S Ribosomal RNA Gene Amplicons for the Illumina MiSeq System. [http://support.illumina.com/documents/documentation/chemistry\\_documentation/16s/16s-metagenomic-library-prep-guide-15044223-b.pdf](http://support.illumina.com/documents/documentation/chemistry_documentation/16s/16s-metagenomic-library-prep-guide-15044223-b.pdf)
- IPCC, 2021: Climate Change 2021: The Physical Science Basis. Contribution of Working Group I to the Sixth Assessment Report of the Intergovernmental Panel on Climate Change [Masson-Delmotte, V., P. Zhai, A. Pirani, S.L. Connors, C. Péan, S. Berger, N. Caud, Y. Chen, L. Goldfarb, M.I. Gomis, M. Huang, K. Leitzell, E. Lonnoy, J.B.R. Matthews, T.K. Maycock, T. Waterfield, O. Yelekçi, R. Yu, and B. Zhou (eds.)]. Cambridge University Press, Cambridge, United Kingdom and New York, NY, USA, In press, doi:10.1017/9781009157896
- Jackson, R. B., Mooney, H. A., & Schulze, E. D. (1997). A global budget for fine root biomass, surface area, and nutrient contents. *Proceedings of the National Academy of Sciences of the United States of America*, 94(14), 7362–7366. <https://doi.org/10.1073/pnas.94.14.7362>

## SYNOPSIS

- Jandl, R., Ledermann, T., Kindermann, G., & Weiss, P. (2021). Soil Organic Carbon Stocks in Mixed-Deciduous and Coniferous Forests in Austria. *Frontiers in Forests and Global Change*, 4, Article 688851. <https://doi.org/10.3389/ffgc.2021.688851>
- Jobbágy, E. G., & Jackson, R. B. (2000). The Vertical Distribution of Soil Organic Carbon and Its Relation to Climate and Vegetation. *Ecological Applications*, 10(2), 423. <https://doi.org/10.2307/2641104>
- Kassambara, A. (2017). Practical guide to principal component methods in R (Edition 1). CreateSpace Independent Publishing Platform.
- Keller, A. B., Brzostek, E. R., Craig, M. E., Fisher, J. B., & Phillips, R. P. (2021). Root-derived inputs are major contributors to soil carbon in temperate forests, but vary by mycorrhizal type. *Ecology Letters*, 24(4), 626–635. <https://doi.org/10.1111/ele.13651>
- Kennedy, A. D. (1995). Simulated climate change: are passive greenhouses a valid microcosm for testing the biological effects of environmental perturbations? *Global Change Biology*, 1(1), 29–42. <https://doi.org/10.1111/j.1365-2486.1995.tb00004.x>
- Klink, S., Keller, A. B., Wild, A. J., Baumert, V. L., Gube, M., Lehdorff, E., Meyer, N., Mueller, C. W., Phillips, R. P., & Pausch, J. (2022). Stable isotopes reveal that fungal residues contribute more to mineral-associated organic matter pools than plant residues. *Soil Biology & Biochemistry*, 168, 108634. <https://doi.org/10.1016/j.soilbio.2022.108634>
- Knorr, W., Prentice, I. C., House, J. I., & Holland, E. A. (2005). Long-term sensitivity of soil carbon turnover to warming. *Nature*, 433(7023), 298–301. <https://doi.org/10.1038/nature03226>
- Koide, R. T., Fernandez, C., & Malcolm, G. (2014). Determining place and process: Functional traits of ectomycorrhizal fungi that affect both community structure and ecosystem function. *The New Phytologist*, 201(2), 433–439. <https://doi.org/10.1111/nph.12538>
- Kõljalg, U., Nilsson, R. H., Abarenkov, K., Tedersoo, L., Taylor, A. F. S., Bahram, M., Bates, S. T., Bruns, T. D., Bengtsson-Palme, J., Callaghan, T. M., Douglas, B., Drenkhan, T., Eberhardt, U., Dueñas, M., Grebenc, T., Griffith, G. W., Hartmann, M., Kirk, P. M., Kohout, P., . . . Larsson, K.-H. (2013). Towards a unified paradigm for sequence-based identification of fungi. *Molecular Ecology*, 22(21), 5271–5277. <https://doi.org/10.1111/mec.12481>
- Körner, C. (2003). *Alpine Plant Life: Functional Plant Ecology of High Mountain Ecosystems* (2<sup>nd</sup> Edition). Springer Berlin Heidelberg. <https://doi.org/10.1007/978-3-642-18970-8>
- Koven, C., Hugelius, G., Lawrence, D., & Wieder, W. (2017). Higher climatological temperature sensitivity of soil carbon in cold than warm climates. *Nature Climate Change*, 7, 817–822. <https://doi.org/10.1038/nclimate3421>
- Kubistin, D., Plaß-Dülmer, C., Arnold, S., Lindauer, M., Müller-Williams, J., & Schumacher, M. (2021). ICOS ATC/CAL 14C Release, Hohenpeissenberg (131.0 m), 2015-09-24–2020-02-19. Atmosphere Thematic Centre. <https://hdl.handle.net/11676/sx-gduDzKEjkF3VCer06oWlv>
- Kunstmann, H., Schneider, K., Forkel, R., & Knoche, R. (2004). Impact analysis of climate change for an Alpine catchment using high resolution dynamic downscaling of ECHAM4

## SYNOPSIS

- time slices. *Hydrology and Earth System Sciences*, 8(6), 1031–1045. <https://doi.org/10.5194/hess-8-1031-2004>
- Kuzyakov, Y. (2002). Review: Factors affecting rhizosphere priming effects. *Journal of Plant Nutrition and Soil Science*, 165(4), 382–396. [https://doi.org/10.1002/1522-2624\(200208\)165:4<382::AID-JPLN382>3.0.CO;2-%23](https://doi.org/10.1002/1522-2624(200208)165:4<382::AID-JPLN382>3.0.CO;2-%23)
- Kuzyakov, Y. (2010). Priming effects: Interactions between living and dead organic matter. *Soil Biology and Biochemistry*, 42(9), 1363–1371. <https://doi.org/10.1016/j.soilbio.2010.04.003>
- Lavallee, J. M., Soong, J. L., & Cotrufo, M. F. (2020). Conceptualizing soil organic matter into particulate and mineral-associated forms to address global change in the 21st century. *Global Change Biology*, 26(1), 261–273. <https://doi.org/10.1111/gcb.14859>
- Lê, S., Josse, J., & Husson, F. (2008). FactoMineR: An R Package for Multivariate Analysis. *Journal of Statistical Software*, 25(1). <https://doi.org/10.18637/jss.v025.i01>
- Leppälammı-Kujansuu, J., Ostonen, I., Strömngren, M., Nilsson, L. O., Kleja, D. B., Sah, S. P., & Helmisaari, H.-S. (2013). Effects of long-term temperature and nutrient manipulation on Norway spruce fine roots and mycelia production. *Plant and Soil*, 366(1-2), 287–303. <https://doi.org/10.1007/s11104-012-1431-0>
- Li, Y., Sun, D., Li, D., Xu, Z., Zhao, C., Lin, H., & Liu, Q. (2015). Effects of warming on ectomycorrhizal colonization and nitrogen nutrition of *Picea asperata* seedlings grown in two contrasting forest ecosystems. *Scientific Reports*, 5, 17546. <https://doi.org/10.1038/srep17546>
- Likens, G. E. (1989). *Long-Term Studies in Ecology: Approaches and Alternatives*. Springer New York. <https://ebookcentral.proquest.com/lib/kxp/detail.action?docID=6674637>
- Lilleskov, E. A., & Bruns, T. D. (2001). Nitrogen and ectomycorrhizal fungal communities: What we know, what we need to know. *New Phytologist*, 149(2), 156–158. <https://doi.org/10.1046/j.1469-8137.2001.00042-2.x>
- Liski, J., Ilvesniemi, H., Mäkelä, A., & Westman, C. J. (1999). CO<sub>2</sub> Emissions from Soil in Response to Climatic Warming Are Overestimated: The Decomposition of Old Soil Organic Matter Is Tolerant of Temperature. *Ambio*, 28(2), 171–174.
- Liu, D., Keiblinger, K. M., Schindlbacher, A., Wegner, U., Sun, H., Fuchs, S., Lassek, C., Riedel, K., & Zechmeister-Boltenstern, S. (2017). Microbial functionality as affected by experimental warming of a temperate mountain forest soil—A metaproteomics survey. *Applied Soil Ecology*, 117-118, 196–202. <https://doi.org/10.1016/j.apsoil.2017.04.021>
- Liu, H., Wang, H., Li, N., Shao, J., Zhou, X., van Groenigen, K. J., & Thakur, M. P. (2022). Phenological mismatches between above- and belowground plant responses to climate warming. *Nature Climate Change*, 12(1), 97–102. <https://doi.org/10.1038/s41558-021-01244-x>
- LoBuglio, K. F. (1999). *Cenococcum*. In J. W. G. Cairney & S. M. Chambers (Eds.), *Ectomycorrhizal Fungi Key Genera in Profile* (pp. 287–309). Springer Berlin Heidelberg. [https://doi.org/10.1007/978-3-662-06827-4\\_12](https://doi.org/10.1007/978-3-662-06827-4_12)

## SYNOPSIS

- Löhmus, K., Oja, T., & Lasn, R. (1989). Specific root area: A soil characteristic. *Plant and Soil*, 119(2), 245–249. <https://doi.org/10.1007/BF02370415>
- Lu, M., Zhou, X., Yang, Q., Li, H., Luo, Y., Fang, C., Chen, J., Yang, X., & Li, B. (2013). Responses of ecosystem carbon cycle to experimental warming: A meta-analysis. *Ecology*, 94(3), 726–738. <https://doi.org/10.1890/12-0279.1>
- Lu, X., Wang, Y.-P., Luo, Y., & Jiang, L. (2018). Ecosystem carbon transit versus turnover times in response to climate warming and rising atmospheric CO<sub>2</sub> concentration. *Biogeosciences*, 15(21), 6559–6572. <https://doi.org/10.5194/bg-15-6559-2018>
- Lukac, M. (2012). Fine Root Turnover. In S. Mancuso (Ed.), *Measuring Roots* (pp. 363–373). Springer Berlin Heidelberg. [https://doi.org/10.1007/978-3-642-22067-8\\_18](https://doi.org/10.1007/978-3-642-22067-8_18)
- Luo, Y., Wan, S., Hui, D., & Wallace, L. L. (2001). Acclimatization of soil respiration to warming in a tall grass prairie. *Nature*, 413(6856), 622–625. <https://doi.org/10.1038/35098065>
- Luo, Z., Wang, G., & Wang, E. (2019). Global subsoil organic carbon turnover times dominantly controlled by soil properties rather than climate. *Nature Communications*, 10(1), 3688. <https://doi.org/10.1038/s41467-019-11597-9>
- Lützw, M. von, & Kögel-Knabner, I. (2009). Temperature sensitivity of soil organic matter decomposition—what do we know? *Biology and Fertility of Soils*, 46(1), 1–15. <https://doi.org/10.1007/s00374-009-0413-8>
- Lützw, M. von, Kögel-Knabner, I., Ekschmitt, K., Matzner, E., Guggenberger, G., & Marschner, B. and Flessa, H. (2006). Stabilization of organic matter in temperate soils: mechanisms and their relevance under different soil conditions – a review. *European Journal of Soil Science*, 54, 426–445. <https://doi.org/10.1111/j.1365-2389.2006.00809.x>
- Ma, H., Mo, L., Crowther, T. W., Maynard, D. S., van den Hoogen, J., Stocker, B. D., Terrer, C., & Zohner, C. M. (2021). The global distribution and environmental drivers of aboveground versus belowground plant biomass. *Nature Ecology & Evolution*, 5(8), 1110–1122. <https://doi.org/10.1038/s41559-021-01485-1>
- Majdi, H., Pregitzer, K., Morén, A.-S., Nylund, J.-E., & I. Ågren, G. (2005). Measuring Fine Root Turnover in Forest Ecosystems. *Plant and Soil*, 276(1-2), 1–8. <https://doi.org/10.1007/s11104-005-3104-8>
- Malhotra, A., Brice, D. J., Childs, J., Graham, J. D., Hobbie, E. A., Vander Stel, H., Feron, S. C., Hanson, P. J., & Iversen, C. M. (2020). Peatland warming strongly increases fine-root growth. *Proceedings of the National Academy of Sciences of the United States of America*, 117(30), 17627–17634. <https://doi.org/10.1073/pnas.2003361117>
- Matamala, R., González-Meler, M. A., Jastrow, J. D., Norby, R. J., & Schlesinger, W. H. (2003). Impacts of fine root turnover on forest NPP and soil C sequestration potential. *Science*, 302(5649), 1385–1387. <https://doi.org/10.1126/science.1089543>
- McClaugherty, C. A., Aber, J. D., & Melillo, J. M. (1982). The Role of Fine Roots in the Organic Matter and Nitrogen Budgets of Two Forested Ecosystems. *Ecology*, 63, 1481–1490. <https://www.jstor.org/stable/1938874>

## SYNOPSIS

- McCormack, M. L., Adams, T. S., Smithwick, E. A. H., & Eissenstat, D. M. (2014). Variability in root production, phenology, and turnover rate among 12 temperate tree species. *Ecology*, 95(8), 2224–2235. <https://doi.org/10.1890/13-1942.1>
- McCormack, M. L., Dickie, I. A., Eissenstat, D. M., Fahey, T. J., Fernandez, C. W., Guo, D., Helmisaari, H.-S., Hobbie, E. A., Iversen, C. M., Jackson, R. B., Leppälammı-Kujansuu, J., Norby, R. J., Phillips, R. P., Pregitzer, K. S., Pritchard, S. G., Rewald, B., & Zadworny, M. (2015). Redefining fine roots improves understanding of below-ground contributions to terrestrial biosphere processes. *The New Phytologist*, 207(3), 505–518. <https://doi.org/10.1111/nph.13363>
- McCormack, M. L., & Iversen, C. M. (2019). Physical and Functional Constraints on Viable Belowground Acquisition Strategies. *Frontiers in Plant Science*, 10, 1215. <https://doi.org/10.3389/fpls.2019.01215>
- Melillo, J. M., Butler, S., Johnson, J., Mohan, J., Steudler, P., Lux, H., Burrows, E., Bowles, F., Smith, R., Scott, L., Vario, C., Hill, T., Burton, A., Zhou, Y.-M., & Tang, J. (2011). Soil warming, carbon-nitrogen interactions, and forest carbon budgets. *Proceedings of the National Academy of Sciences of the United States of America*, 108(23), 9508–9512. <https://doi.org/10.1073/pnas.1018189108>
- Melillo, J. M., Frey, S. D., DeAngelis, K. M., Werner, W. J., Bernard, M. J., Bowles, F. P., Pold, G., Knorr, M. A., & Grandy, A. S. (2017). Long-term pattern and magnitude of soil carbon feedback to the climate system in a warming world. *Science*, 358(6359), 101–105. <https://doi.org/10.1126/science.aan2874>
- Melillo, J. M., Steudler, P. A., Aber, J. D., Newkirk, K., Lux, H., Bowles, F. P., Catricala, C., Magill, A., Ahrens, T., & Morrisseau, S. (2002). Soil warming and carbon-cycle feedbacks to the climate system. *Science*, 298(5601), 2173–2176. <https://doi.org/10.1126/science.1074153>
- Metzler, H., & Sierra, C. A. (2018). Linear Autonomous Compartmental Models as Continuous-Time Markov Chains: Transit-Time and Age Distributions. *Mathematical Geosciences*, 50(1), 1–34. <https://doi.org/10.1007/s11004-017-9690-1>
- Millard, S. P. (2013). *EnvStats: An R Package for Environmental Statistics*. Springer. <https://www.springer.com>
- Mohan, J. E., Cowden, C. C., Baas, P., Dawadi, A., Frankson, P. T., Helmick, K., Hughes, E., Khan, S., Lang, A., Machmuller, M., Taylor, M., & Witt, C. A. (2014). Mycorrhizal fungi mediation of terrestrial ecosystem responses to global change: mini-review. *Fungal Ecology*, 10, 3–19. <https://doi.org/10.1016/j.funeco.2014.01.005>
- Mucha, J., Peay, K. G., Smith, D. P., Reich, P. B., Stefański, A., & Hobbie, S. E. (2018). Effect of Simulated Climate Warming on the Ectomycorrhizal Fungal Community of Boreal and Temperate Host Species Growing Near Their Shared Ecotonal Range Limits. *Microbial Ecology*, 75(2), 348–363. <https://doi.org/10.1007/s00248-017-1044-5>
- NOAA National Centers for Environmental Information. (2022). Monthly Global Climate Report for Annual 2022. <https://www.ncei.noaa.gov/access/monitoring/monthly-report/global/202213>

## SYNOPSIS

- Nock, C. A., Vogt, R. J., & Beisner, B. E. (2016). Functional Traits. In L. John Wiley & Sons (Ed.), *Encyclopedia of life sciences* (pp. 1–8). John Wiley & Sons. <https://doi.org/10.1002/9780470015902.a0026282>
- Nottingham, A. T., Meir, P., Velasquez, E., & Turner, B. L. (2020). Soil carbon loss by experimental warming in a tropical forest. *Nature*, 584(7820), 234–237. <https://doi.org/10.1038/s41586-020-2566-4>
- Oksanen, J., Blanchet, F. G., Friendly, M., Kindt, R., Legendre, P., McGlinn, D., Minchin, P. R., O'Hara, R. B., Simpson, G. L., Solymos, P., Stevens, M. H. H., Szoecs, E., & Wagner, H. (2019). *vegan: Community Ecology Package*. <https://CRAN.R-project.org/package=vegan>
- Ostonen, I., Helmisaari, H.-S., Borken, W., Tedersoo, L., Kukumägi, M., Bahram, M., Lindroos, A.-J., Nöjd, P., Uri, V., Merilä, P., Asi, E., & Lõhmus, K. (2011). Fine root foraging strategies in Norway spruce forests across a European climate gradient. *Global Change Biology*, 17(12), 3620–3632. <https://doi.org/10.1111/j.1365-2486.2011.02501.x>
- Ostonen, I., Lõhmus, K., & Lasn, R. (1999). The role of soil conditions in fine root ecomorphology in Norway spruce (*Picea abies* (L.) Karst.). *Plant and Soil*, 208(2), 283–292. <https://doi.org/10.1023/A:1004552907597>
- Ostonen, I., Püttsepp, Ü., Biel, C., Alberton, O., Bakker, M. R., Lõhmus, K., Majdi, H., Metcalfe, D., Olsthoorn, A. F. M., Pronk, A., Vanguelova, E., Weih, M., & Brunner, I. (2007). Specific root length as an indicator of environmental change. *Plant Biosystems - an International Journal Dealing with All Aspects of Plant Biology*, 141(3), 426–442. <https://doi.org/10.1080/11263500701626069>
- Paris Agreement. (2015). Paris Agreement to the United Nations Framework Convention on Climate Change, Dec. 12, 2015, T.I.A.S. No. 16-1104.
- Parts, K., Tedersoo, L., Schindlbacher, A., Sigurdsson, B. d., Leblans, N. I. W., Oddsdóttir, E. S., Borken, W., & Ostonen, I. (2019). Acclimation of Fine Root Systems to Soil Warming: Comparison of an Experimental Setup and a Natural Soil Temperature Gradient. *Ecosystems*, 22(3), 457–472. <https://doi.org/10.1007/s10021-018-0280-y>
- Penuelas, J., Fernández-Martínez, M., Vallicrosa, H., Maspons, J., Zuccarini, P., Carnicer, J., Sanders, T. G. M., Krüger, I., Obersteiner, M., Janssens, I. A., Ciais, P., & Sardans, J. (2020). Increasing atmospheric CO<sub>2</sub> concentrations correlate with declining nutritional status of European forests. *Communications Biology*, 3(1), 125. <https://doi.org/10.1038/s42003-020-0839-y>
- Pepin, N., Bradley, R. S., Diaz, H. F., Baraer, M., Caceres, E. B., Forsythe, N., Fowler, H., Greenwood, G., Hashmi, M. Z., Liu, X. D., Miller, J. R., Ning, L., Ohmura, A., Palazzi, E., Rangwala, I., Schöner, W., Severskiy, I., Shahgedanova, M., Wang, M. B., . . . Yang, D. Q. (2015). Elevation-dependent warming in mountain regions of the world. *Nature Climate Change*, 5(5), 424–430. <https://doi.org/10.1038/nclimate2563>
- Pregitzer, K. S., DeForest, J. L., Burton, A. J., Allen, M. F., Ruess, R. W., & Hendrick, R. L. (2002). Fine Root Architecture of Nine North American Trees. *Ecological Monographs*, 72(2), 293. <https://doi.org/10.2307/3100029>

## SYNOPSIS

- Pregitzer, K. S., King, J. S., Burton, A. J., & Brown, S. E. (2000). Responses of tree fine roots to temperature. *New Phytologist*, 147(1), 105–115. <https://doi.org/10.1046/j.1469-8137.2000.00689.x>
- Pregitzer, K. S., Zak, D. R., Loya, W. M., Karberg, N. J., King, J. S., & Burton, A. J. (2007). The Contribution of Root – Rhizosphere Interactions to Biogeochemical Cycles in a Changing World. *The Rhizosphere* (pp. 155–178). Elsevier. <https://doi.org/10.1016/B978-012088775-0/50009-4>
- Prietzl, J., Zimmermann, L., Schubert, A., & Christophel, D. (2016). Organic matter losses in German Alps forest soils since the 1970s most likely caused by warming. *Nature Geoscience*, 9(7), 543–548. <https://doi.org/10.1038/ngeo2732>
- Pu, X., Yin, C., Xiao, Q., Qiao, M., & Liu, Q. (2017). Fine roots branch orders of *Abies faxoniana* respond differentially to warming in a subalpine coniferous forest ecosystem. *Agroforestry Systems*, 91(5), 955–966. <https://doi.org/10.1007/s10457-016-9970-7>
- R Core Team. (2022). R: A Language and Environment for Statistical Computing. <https://www.R-project.org/>
- Raich, J. W., & Schlesinger, W. H. (1992). The global carbon dioxide flux in soil respiration and its relationship to vegetation and climate. *Tellus B: Chemical and Physical Meteorology*, 44(2), 81. <https://doi.org/10.3402/tellusb.v44i2.15428>
- Rasse, D. P., Rumpel, C., & Dignac, M.-F. (2005). Is soil carbon mostly root carbon? Mechanisms for a specific stabilisation. *Plant and Soil*, 269(1-2), 341–356. <https://doi.org/10.1007/s11104-004-0907-y>
- Rehshuh, R., Rehshuh, S., Gast, A., Jakab, A.-L., Lehmann, M. M., Saurer, M., Gessler, A., & Ruehr, N. K. (2022). Tree allocation dynamics beyond heat and hot drought stress reveal changes in carbon storage, belowground translocation and growth. *New Phytologist*, 233(2), 687–704. <https://doi.org/10.1111/nph.17815>
- Reimer, P. J., Bard, E., Bayliss, A., Beck, J. W., Blackwell, P. G., Ramsey, C. B., Buck, C. E., Cheng, H., Edwards, R. L., Friedrich, M., Grootes, P. M., Guilderson, T. P., Haflidason, H., Hajdas, I., Hatté, C., Heaton, T. J., Hoffmann, D. L., Hogg, A. G., Hughen, K. A., . . . van der Plicht, J. (2013). IntCal13 and Marine13 Radiocarbon Age Calibration Curves 0–50,000 Years cal BP. *Radiocarbon*, 55(4), 1869–1887. [https://doi.org/10.2458/azu\\_js\\_rc.55.16947](https://doi.org/10.2458/azu_js_rc.55.16947)
- Risk, D., Kellman, L., & Beltrami, H. (2002). Carbon dioxide in soil profiles: Production and temperature dependence. *Geophysical Research Letters*, 29(6), 11-1-11-4. <https://doi.org/10.1029/2001GL014002>
- Rodhe, H. (1992). Modeling Biogeochemical Cycles. In S. S. Butcher (Ed.), *International Geophysics. Global Biogeochemical Cycles* (Vol. 50, pp. 55–72). Elsevier. [https://doi.org/10.1016/S0074-6142\(08\)62687-X](https://doi.org/10.1016/S0074-6142(08)62687-X)
- Rumpf, S., Gravey, M., Brönnimann, O., Luoto, M., Cianfrani, C., Mariethoz, G., & Guisan, A. (2022). From white to green: Snow cover loss and increased vegetation productivity in the European Alps. *Science*, 376(6597), 1119–1122. <https://doi.org/10.1126/science.abn6697>

## SYNOPSIS

- Ryan, M. G., & Law, B. E. (2005). Interpreting, measuring, and modeling soil respiration. *Biogeochemistry*, 73(1), 3–27. <https://doi.org/10.1007/s10533-004-5167-7>
- Rygiewicz, P. T., Martin, K. J., & Tuininga, A. R. (2000). Morphotype community structure of ectomycorrhizas on Douglas fir (*Pseudotsuga menziesii* Mirb. Franco) seedlings grown under elevated atmospheric CO<sub>2</sub> and temperature. *Oecologia*, 124(2), 299–308. <https://doi.org/10.1007/s004420000385>
- Schindlbacher, A., Beck, K., Holzheu, S., & Borken, W. (2019). Inorganic Carbon Leaching From a Warmed and Irrigated Carbonate Forest Soil. *Frontiers in Forests and Global Change*, 2, Article 40, 129. <https://doi.org/10.3389/ffgc.2019.00040>
- Schindlbacher, A., Rodler, A., Kuffner, M., Kitzler, B., Sessitsch, A., & Zechmeister-Boltenstern, S. (2011). Experimental warming effects on the microbial community of a temperate mountain forest soil. *Soil Biology & Biochemistry*, 43(7), 1417–1425. <https://doi.org/10.1016/j.soilbio.2011.03.005>
- Schindlbacher, A., Schnecker, J., Takriti, M., Borken, W., & Wanek, W. (2015). Microbial physiology and soil CO<sub>2</sub> efflux after 9 years of soil warming in a temperate forest - no indications for thermal adaptations. *Global Change Biology*, 21(11), 4265–4277. <https://doi.org/10.1111/gcb.12996>
- Schindlbacher, A., Wunderlich, S., Borken, W., Kitzler, B., Zechmeister-Boltenstern, S., & Jandl, R. (2012). Soil respiration under climate change: prolonged summer drought offsets soil warming effects. *Global Change Biology*, 18(7), 2270–2279. <https://doi.org/10.1111/j.1365-2486.2012.02696.x>
- Schindlbacher, A., Zechmeister-Boltenstern, S., & Jandl, R. (2009). Carbon losses due to soil warming: Do autotrophic and heterotrophic soil respiration respond equally? *Global Change Biology*, 15(4), 901–913. <https://doi.org/10.1111/j.1365-2486.2008.01757.x>
- Schnecker, J., Borken, W., Schindlbacher, A., & Wanek, W. (2016). Little effects on soil organic matter chemistry of density fractions after seven years of forest soil warming. *Soil Biology & Biochemistry*, 103, 300–307. <https://doi.org/10.1016/j.soilbio.2016.09.003>
- Schuur, E. A., Druffel, E., & Trumbore, S. E. (2016). *Radiocarbon and Climate Change*. Springer International Publishing. <https://doi.org/10.1007/978-3-319-25643-6>
- Shi, C., Urbina-Malo, C., Tian, Y., Heinzle, J., Kwatcho Kengdo, S., Inselsbacher, E., Borken, W., Schindlbacher, A., & Wanek, W. (2023). Does long-term soil warming affect microbial element limitation? A test by short-term assays of microbial growth responses to labile C, N and P additions. *Global Change Biology*. Advance online publication. <https://doi.org/10.1111/gcb.16591>
- Sierra, C. A., Müller, M., Metzler, H., Manzoni, S., & Trumbore, S. E. (2017). The muddle of ages, turnover, transit, and residence times in the carbon cycle. *Global Change Biology*, 23(5), 1763–1773. <https://doi.org/10.1111/gcb.13556>
- Sierra, C. A., Müller, M., & Trumbore, S. E. (2012). Models of soil organic matter decomposition: the SoilR package, version 1.0. *Geoscientific Model Development*, 5(4), 1045–1060. <https://doi.org/10.5194/gmd-5-1045-2012>

## SYNOPSIS

- Sierra, C. A., Müller, M., & Trumbore, S. E. (2014). Modeling radiocarbon dynamics in soils: SoilR version 1.1. *Geoscientific Model Development*, 7(5), 1919–1931. <https://doi.org/10.5194/gmd-7-1919-2014>
- Sjögersten, S., Alewell, C., Cécillon, L., Hagedorn, F., Jandl, R., Leifeld, J., Martinsen, V., Schindlbacher, A., Sebastià, M. -T., & van Miegroet, H. (2011). Mountain Soils in a Changing Climate – Vulnerability of Carbon Stocks and Ecosystem Feedbacks. In R. Jandl, M. Rodeghiero, & M. Olsson (Eds.), *Soil carbon in sensitive European ecosystems: From science to land management / by Robert Jandl, Mirco Rodeghiero, Mats Olsson* (Vol. 7, pp. 118–148). Wiley-Blackwell; Chichester: John Wiley. <https://doi.org/10.1002/9781119970255.ch6>
- Smith, S. E., & Read, D. J. (2008). *Mycorrhizal symbiosis* (3. ed.). Elsevier/Acad. Press.
- Solly, E. F., Brunner, I., Helmisaari, H.-S., Herzog, C., Leppälammı-Kujansuu, J., Schöning, I., Schruppf, M., Schweingruber, F. H., Trumbore, S. E., & Hagedorn, F. (2018). Unravelling the age of fine roots of temperate and boreal forests. *Nature Communications*, 9(1), 3006. <https://doi.org/10.1038/s41467-018-05460-6>
- Solly, E. F., Lindahl, B. D., Dawes, M. A., Peter, M., Souza, R. C., Rixen, C., & Hagedorn, F. (2017). Experimental soil warming shifts the fungal community composition at the alpine treeline. *The New Phytologist*, 215(2), 766–778. <https://doi.org/10.1111/nph.14603>
- Soong, J. L., Castanha, C., Hicks Pries, C. E., Ofiti, N., Porras, R. C., Riley, W. J., Schmidt, M. W. I., & Torn, M. S. (2021). Five years of whole-soil warming led to loss of subsoil carbon stocks and increased CO<sub>2</sub> efflux. *Science Advances*, 7(21), eabd1343. <https://doi.org/10.1126/sciadv.abd1343>
- Southon, J., Santos, G., Druffel-Rodriguez, K., Druffel, E., Trumbore, S., Xu, X., Griffin, S., Ali, S., & Mazon, M. (2004). The Keck Carbon Cycle AMS Laboratory, University of California, Irvine: Initial Operation and a Background Surprise. *Radiocarbon*, 46(1), 41–49. <https://doi.org/10.1017/S0033822200039333>
- Staddon, P. L., Heinemeyer, A., & Fitter, A. H. (2002). Mycorrhizas and global environmental change: research at different scales. *Plant and Soil*, 244(1/2), 253–261. <https://doi.org/10.1023/A:1020285309675>
- Talkner, U., Meiwes, K. J., Potočić, N., Seletković, I., Cools, N., Vos, B. de, & Rautio, P. (2015). Phosphorus nutrition of beech (*Fagus sylvatica* L.) is decreasing in Europe. *Annals of Forest Science*, 72(7), 919–928. <https://doi.org/10.1007/s13595-015-0459-8>
- Talkner, U., Riek, W., Dammann, I., Kohler, M., Göttlein, A., Mellert, K. H., & Meiwes, K. J. (2019). Nutritional Status of Major Forest Tree Species in Germany. In N. Wellbrock & A. Bölte (Eds.), *Ecological studies*, 0070-8356: volume 237. Status and dynamics of forests in Germany: Results of the National Forest Monitoring / Nicole Wellbrock, Andreas Bolte, editors (Vol. 237, pp. 261–293). Springer Open. [https://doi.org/10.1007/978-3-030-15734-0\\_9](https://doi.org/10.1007/978-3-030-15734-0_9)
- Tian, Y., Shi, C., Malo, C. U., Kwatcho Kengdo, S., Heinzle, J., Inselsbacher, E., Ottner, F., Borken, W., Michel, K., Schindlbacher, A., & Wanek, W. (2023). Long-term soil warming decreases microbial phosphorus utilization by increasing abiotic phosphorus sorption and

## SYNOPSIS

- phosphorus losses. *Nature Communications*, 14(1), 864. <https://doi.org/10.1038/s41467-023-36527-8>
- Treseder, K. K. (2004). A meta-analysis of mycorrhizal responses to nitrogen, phosphorus, and atmospheric CO<sub>2</sub> in field studies. *The New Phytologist*, 164(2), 347–355. <https://doi.org/10.1111/j.1469-8137.2004.01159.x>
- Treseder, K. K., Marusenko, Y., Romero-Olivares, A. L., & Maltz, M. R. (2016). Experimental warming alters potential function of the fungal community in boreal forest. *Global Change Biology*, 22(10), 3395–3404. <https://doi.org/10.1111/gcb.13238>
- Trumbore, S. E. (2000). Age of soil organic matter and soil respiration: radiocarbon constraints on belowground C dynamics. *Ecological Applications*, 10(2), 399–411. [https://doi.org/10.1890/1051-0761\(2000\)010\[0399:AOSOMA\]2.0.CO;2](https://doi.org/10.1890/1051-0761(2000)010[0399:AOSOMA]2.0.CO;2)
- Trumbore, S. E., Chadwick, O. A., & Amundson, R. (1996). Rapid Exchange Between Soil Carbon and Atmospheric Carbon Dioxide Driven by Temperature Change. *Science*, 272(5260), 393–396. <https://doi.org/10.1126/science.272.5260.393>
- Trumbore, S. E., & Czimczik, C. I. (2008). An Uncertain Future for Soil Carbon. *Science*, 321(5895), 1455–1456. <https://doi.org/10.1126/science.1161132>
- Trumbore, S. E., & Gaudinski, J. B. (2003). The secret lives of roots. *Science*, 302(5649), 1344–1345. <https://doi.org/10.1126/science.1091841>
- Violle, C., Navas, M.-L., Vile, D., Kazakou, E., Fortunel, C., Hummel, I., & Garnier, E. (2007). Let the concept of trait be functional! *Oikos*, 116(5), 882–892. <https://doi.org/10.1111/j.0030-1299.2007.15559.x>
- Wallander, H., Ekblad, A., Godbold, D. L., Johnson, D., Bahr, A., Baldrian, P., Björk, R. G., Kieliszewska-Rokicka, B., Kjöllér, R., Kraigher, H., Plassard, C., & Rudawska, M. (2013). Evaluation of methods to estimate production, biomass and turnover of ectomycorrhizal mycelium in forests soils – A review. *Soil Biology and Biochemistry*, 57, 1034–1047. <https://doi.org/10.1016/j.soilbio.2012.08.027>
- Wan, S., Norby, R. J., Pregitzer, K. S., Ledford, J., & O'Neill, E. G. (2004). CO<sub>2</sub> enrichment and warming of the atmosphere enhance both productivity and mortality of maple tree fine roots. *New Phytologist*, 162(2), 437–446. <https://doi.org/10.1111/j.1469-8137.2004.01034.x>
- Wang, J., Defrenne, C., McCormack, M. L., Yang, L., Tian, D., Luo, Y., Hou, E., Yan, T., Li, Z., Bu, W., Chen, Y., & Niu, S. (2021). Fine-root functional trait responses to experimental warming: A global meta-analysis. *The New Phytologist*, 230(5), 1856–1867. <https://doi.org/10.1111/nph.17279>
- Wang, J., Sun, J., Xia, J., He, N., Li, M., & Niu, S. (2018). Soil and vegetation carbon turnover times from tropical to boreal forests. *Functional Ecology*, 32(1), 71–82. <https://doi.org/10.1111/1365-2435.12914>
- Wang, Q., Zhao, X., Chen, L., Yang, Q., Chen, S., & Zhang, W. (2019). Global synthesis of temperature sensitivity of soil organic carbon decomposition: Latitudinal patterns and mechanisms. *Functional Ecology*, 33(3), 514–523. <https://doi.org/10.1111/1365-2435.13256>

## SYNOPSIS

- Wang, Y., & Hsieh, Y.-P. (2002). Uncertainties and novel prospects in the study of the soil carbon dynamics. *Chemosphere*, 49(8), 791–804. [https://doi.org/10.1016/S0045-6535\(02\)00381-8](https://doi.org/10.1016/S0045-6535(02)00381-8)
- Warren, J. M., Hanson, P. J., Iversen, C. M., Kumar, J., Walker, A. P., & Wullschleger, S. D. (2015). Root structural and functional dynamics in terrestrial biosphere models--evaluation and recommendations. *New Phytologist*, 205(1), 59–78. <https://doi.org/10.1111/nph.13034>
- Warscher, M., Wagner, S., Marke, T., Laux, P., Smiatek, G., Strasser, U., & Kunstmann, H. (2019). A 5 km Resolution Regional Climate Simulation for Central Europe: Performance in High Mountain Areas and Seasonal, Regional and Elevation-Dependent Variations. *Atmosphere*, 10(11), 682. <https://doi.org/10.3390/atmos10110682>
- Wickham, H. (2016). *ggplot2: Elegant Graphics for Data Analysis*. Springer-Verlag New York. <https://ggplot2.tidyverse.org>
- Wu, K. (2000). Fine root production and turnover and its contribution to nutrient cycling in two beech (*Fagus sylvatica* L.) forest ecosystems (A170, pp 1–130).
- Xia, M., Guo, D., & Pregitzer, K. S. (2010). Ephemeral root modules in *Fraxinus mandshurica*. *New Phytologist*, 188(4), 1065–1074. <https://doi.org/10.1111/j.1469-8137.2010.03423.x>
- Xiao, L., Wang, G., Wang, M., Zhang, S., Sierra, C. A., Guo, X., Chang, J., Shi, Z., & Luo, Z. (2022). Younger carbon dominates global soil carbon efflux. *Global Change Biology*, 28(18), 5587–5599. <https://doi.org/10.1111/gcb.16311>
- Xu, W., Yuan, W., Cui, L., Ma, M., & Zhang, F. (2019). Responses of soil organic carbon decomposition to warming depend on the natural warming gradient. *Geoderma*, 343, 10–18. <https://doi.org/10.1016/j.geoderma.2019.02.017>
- Xu, X., Trumbore, S. E., Zheng, S., Southon, J. R., McDuffee, K. E., Luttgen, M., & Liu, J. C. (2007). Modifying a sealed tube zinc reduction method for preparation of AMS graphite targets: Reducing background and attaining high precision. *Nuclear Instruments and Methods in Physics Research Section B: Beam Interactions with Materials and Atoms*, 259(1), 320–329. <https://doi.org/10.1016/j.nimb.2007.01.175>
- Zhou, Y., Tang, J., Melillo, J. M., Butler, S., & Mohan, J. E. (2011). Root standing crop and chemistry after six years of soil warming in a temperate forest. *Tree Physiology*, 31(7), 707–717. <https://doi.org/10.1093/treephys/tpr066>
- Ziegler, S. E., Benner, R., Billings, S. A., Edwards, K. A., Philben, M., Zhu, X., & Laganière, J. (2017). Climate Warming Can Accelerate Carbon Fluxes without Changing Soil Carbon Stocks. *Frontiers in Earth Science*, 5:2. <https://doi.org/10.3389/feart.2017.00002>
- Zistl-Schlingmann, M., Kwatcho Kengdo, S., Kiese, R., & Dannenmann, M. (2020). Management Intensity Controls Nitrogen-Use-Efficiency and Flows in Grasslands—A <sup>15</sup>N Tracing Experiment. *Agronomy*, 10(4), 606. <https://doi.org/10.3390/agronomy10040606>

## SYNOPSIS

## **2 Manuscripts**

## Study I

### **Long-term soil warming alters fine root dynamics and morphology, and their ectomycorrhizal fungal community in a temperate forest soil**

Steve Kwatcho Kengdo\*, Derek Peršoh, Andreas Schindlbacher, Jakob Heinzle, Ye Tian, Wolfgang Wanek, Werner Borken (2022)

Published in *Global Change Biology* 28(10): 3441–3458

DOI : <https://doi.org/10.1111/gcb.16155>

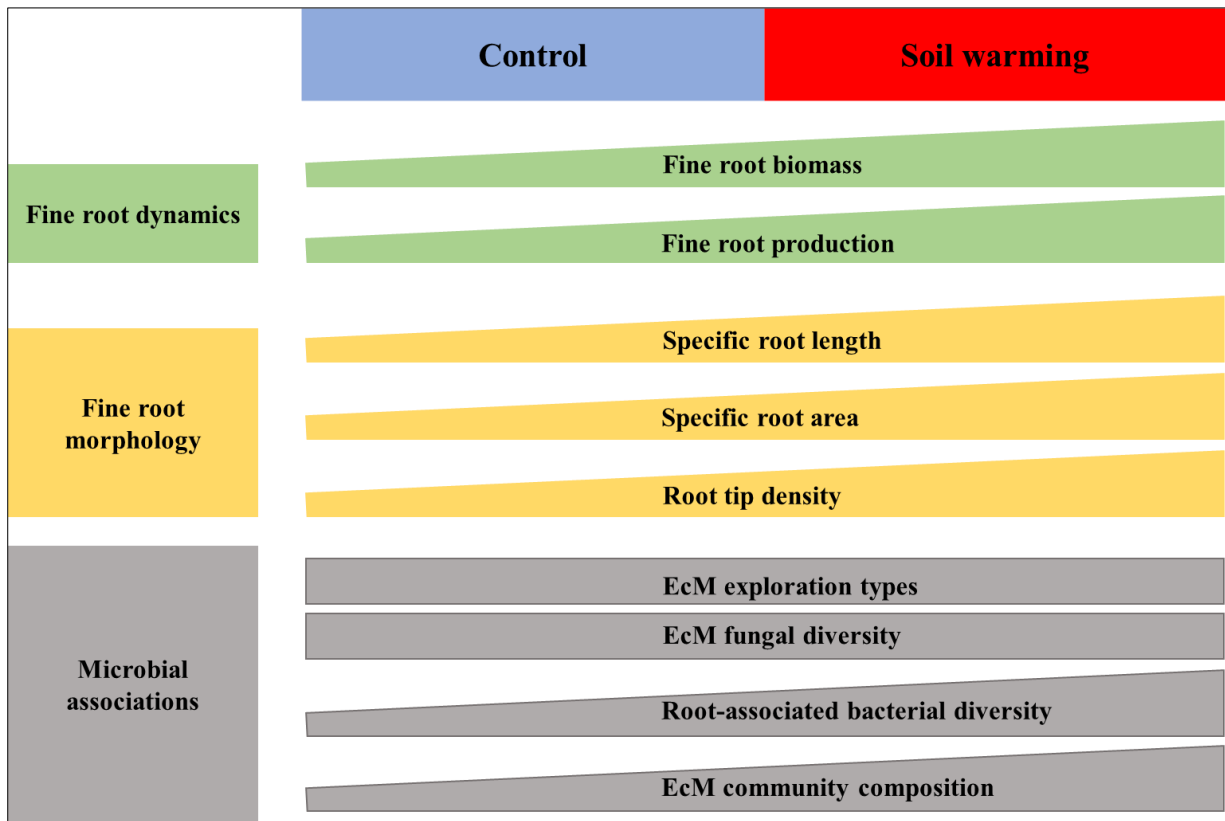
\* Corresponding author

## Abstract

Climate warming is predicted to affect temperate forests severely, but the response of fine roots, key to plant nutrition, water uptake, soil carbon and nutrient cycling is unclear. Understanding how fine roots will respond to increasing temperature is a prerequisite for predicting the functioning of forests in a warmer climate. We studied the response of fine roots and their ectomycorrhizal (EcM) fungal and root-associated bacterial communities to soil warming by 4 °C in a mixed spruce-beech forest in the Austrian Limestone Alps after 8 and 14 years of soil warming, respectively. Fine root biomass (FRB) and fine root production were 17% and 128% higher in the warmed plots, respectively, after 14 years. The increase in FRB (13%) was not significant after 8 years of treatment, whereas specific root length, specific root area, and root tip density were significantly higher in warmed plots at both sampling occasions. Soil warming did not affect EcM exploration types and diversity, but changed their community composition, with an increase in the relative abundance of *Cenococcum* at 0 – 10 cm soil depth, a drought-stress tolerant genus, and an increase in short and long-distance exploration types like *Sebacina* and *Boletus* at 10 – 20 cm soil depth. Warming increased the root-associated bacterial diversity but did not affect their community composition. Soil warming did not affect nutrient concentrations of fine roots, though we found indications of limited soil phosphorus (P) and potassium (K) availability. Our findings suggest that, in the studied ecosystem, global warming could persistently increase soil carbon inputs due to accelerated fine root growth and turnover, and could simultaneously alter fine root morphology and EcM fungal community composition towards improved nutrient foraging.

**Keywords:** climate warming, fine root biomass, fine root production, fine root morphology, ectomycorrhiza, exploration types, bacterial community, nutrients

**Graphical Abstract**



## 1 | Introduction

Tree fine roots (< 2 mm in diameter) represent less than 2% of the total biomass in forests but contribute up to 33% to the global terrestrial net primary productivity (Jackson et al., 1997; McCormack et al., 2015). Fine roots are considered a major source of plant carbon (C) input into temperate forest soils, and their biomass growth, traits, turnover, as well as their exudation of labile C are important components in soil C cycling and storage (Keller et al., 2021; Rasse et al., 2005). In temperate and boreal forests, fine roots are typically colonized by EcM mycelium (Tedersoo et al., 2012). The symbiosis of roots and EcM fungi serves as an efficient nutrient foraging strategy for trees, especially in nutrient-poor forest soils (Lõhmus et al., 2006). The mycelium of EcM fungi greatly improves access to nutrient and water resources in soils that are hardly directly accessible for fine roots (Lindahl & Tunlid, 2015; McCormack & Iversen, 2019).

Climate warming is predicted to severely affect temperate forests during the 21<sup>st</sup> century (IPCC, 2021), and thus likely also the uptake and transport of water and nutrients by fine roots. Changes in fine root functions and the diversity and functional traits of EcM fungi may alter whole ecosystem C and nutrient cycles. Developing an efficient root system through change of biomass allocation to fine roots, changes in fine root morphology and root-associated microbial communities is required to maintain plant water and nutrient uptake under changing environmental conditions (Ostonen et al., 2011). Trees can adapt their below-ground surface area by modifying root biomass and fine root morphological traits to improve soil resource uptake and plant performance (Weemstra et al., 2020). FRB is driven by the balance between root growth and mortality and depends on environmental conditions, especially soil temperature and soil moisture (Salazar et al., 2020; J. Wang et al., 2021). Soil warming has been suggested to increase FRB due to decreased soil nitrogen (N) availability (Leppälammikujansuu et al., 2013) but also to decrease FRB in temperate and boreal forests due to increased soil N availability (Dawes et al., 2015; Melillo et al., 2011; Wan et al., 2004; Zhou et al., 2011). The inconsistent findings across forest biomes illustrate the complexity of the interaction between increased soil temperature, N availability, and FRB (J. Wang et al., 2021). However, with ongoing high atmospheric N deposition in many forested regions, such as central Europe (Borken & Matzner, 2004; Talkner et al., 2019), where the current study took place, the availability of essential nutrients such as phosphorus (P) and potassium (K) may likely play a similar, or even a more important role, with regard to tree fine root responses to warming. Decreasing foliar P and K indicate poor availability of these nutrients in many European forests

in recent decades (Jonard et al., 2015; Penuelas et al., 2020; Talkner et al., 2015), though the impact of soil warming in combination with low P and K availability on fine root systems is unknown.

Morphological traits of fine roots are indicators of trees' nutrient uptake efficiency and ecosystems' responses to changes in environmental conditions (Freschet et al., 2021; Ostonen et al., 1999). Amongst those, traits like specific root length (SRL, the length of a root per unit dry mass), root tissue density (RTD, the dry mass of root per unit volume of fresh root), specific root area (SRA, the ratio of fine root surface to fine root dry mass), root area index (RAI, the surface area of roots per soil surface area), mean root diameter (D, the average of all root diameter observations of a root diameter distribution), and root tip density (RTID, the number of root tips per soil volume), are used to describe the functional characteristics of fine roots (Freschet et al., 2021; McCormack & Iversen, 2019). For example, an increase in SRL indicates morphological adaptation towards thinner and longer fine roots, which are less resistant to stress and have a shorter lifetime but are more active metabolically (McCormack et al., 2015). This is seen as a strategy to increase nutrient acquisition from the soil at low biomass production (Weemstra et al., 2020). An increase in RAI and SRA also indicates adaptation towards increased ability to explore and take up soil resources. However, only few studies have yet considered the effect of soil warming on fine root morphology in forest ecosystems (J. Wang et al., 2021). In their meta-analysis, J. Wang et al. (2021) found that SRL and fine root diameter was irresponsive to experimental warming across a wide range of terrestrial ecosystems. Of the few studies conducted in forests, Parts et al. (2019) showed that trees increased their SRL and SRA with soil warming but decreased RTD. Björk et al. (2007) reported that warming increases SRL and SRA of roots < 0.5 mm, while Leppälampi-Kujansuu et al. (2013) observed no effect on RTD and diameter of first and second-order fine roots. Hence, similar to FRB, fine root morphology can respond differently to soil warming and associated changes in nutrient availability or moisture.

Due to the interaction between fine root traits and soil biota, understanding the response of the fine root systems to soil warming also requires studying root-microbial interactions (Bennett & Classen, 2020; Weemstra et al., 2017). EcM and root-associated bacteria are particularly important because they produce extracellular enzymes that release nutrients from soil organic matter in the vicinity of fine roots (Averill et al., 2014; Averill & Hawkes, 2016). The diversity of EcM and root-associated bacteria might further increase the effectiveness of nutrient acquisition from different depths and locations in the soil (Leake, 2001). However, changes in

root-associated microbial communities have received little attention in the context of soil warming. Because of the temperature dependence of soil enzymatic activities, soil warming directly influences nutrient cycling processes (Staddon et al., 2002). This may lead to shifts in EcM community composition (Solly et al., 2017; Treseder et al., 2016) and EcM diversity. Mycorrhizal associations greatly enhance the roots' surface area and, therefore, their water and nutrient uptake capacity (Smith & Read, 2008; Weemstra, 2017). EcM fungal traits like exploration types are good predictors of ecosystem processes because they integrate species functions in functionally redundant communities (Koide et al., 2014). Exploration type is a trait that connects the morphology and differentiation of ectomycorrhizal hyphae to differences in nutrient acquisition strategies (Defrenne et al., 2019). Agerer (2001) classified EcM into exploration types and assigned specific functions to those. For example, EcM with contact, short, and medium distance exploration types (low EcM biomass) might be preferred at sites with high N availability (Hobbie & Agerer, 2010), while long-distance exploration types (high EcM biomass) might be necessary in nutrient-poor sites (Tedersoo, 2017). Thus, EcM exploration types likely are going to be affected by warming if elevated temperatures alter the availability of soil nutrients or the nutrient requirement of trees.

The effect of soil warming on fine root dynamic and root-associated bacterial-fungal communities in forests has largely remained unresolved, as most studies were short in terms of duration and differed in experimental approaches (J. Wang et al., 2021; Yuan et al., 2018). The long-term forest soil warming experiment at Achenkirch in the Austrian alps, where regional climate models predict an above-average increase in temperature (up to 3.3° C at the end of the 21<sup>st</sup> century) as compared to global average warming (Gobiet et al., 2014; Smiatek et al., 2009), offers an excellent opportunity to increase our understanding of how soil warming affects FRB, fine root production, fine root morphology, and root-associated bacterial and fungal communities in temperate forests. To achieve this, we studied fine roots in control and warmed (+ 4 °C) plots in 2012 and 2019, 8 and 14 years after starting the experimental soil warming treatment, respectively. We hypothesized that (1) soil warming increases FRB after 8 or 14 years because of the globally positive response of FRB to warming (J. Wang et al., 2021) and the potential decline in soil P and K availability in warmed soil. We also expected (2) increases in SRL, SRA and root tip density in warmed soil, which are linked to an increase in the absorptive capacity of fine roots. We did not expect significant changes in root-associated microbial community composition because previous results showed no soil warming effects on soil and root microbial community composition (Kuffner et al., 2012; Schindlbacher et al.,

2011). However, because exploration types are directly linked to fine root morphology, we expected (3) a shift in the relative abundance of EcM exploration types towards long-distance exploration types after 14 years of soil warming.

## 2 | Materials and methods

### 2 | 1 Study location and experimental design

This study was performed in the Achenkirch soil warming experiment located in a mountainous forest in the Austrian Alps (11°38'21" East; 47°34'50" North) at 910 m a.s.l (Schindlbacher et al., 2007). The 140-year-old forest is composed mainly of Norway spruce (*Picea abies* L. H.Karst.) and few other less abundant trees species, including European beech (*Fagus sylvatica* L.) and silver fir (*Abies alba* Mill.). The mean annual air temperature and mean annual precipitation from 1988 to 2017 were 7 °C and 1493 mm, respectively. The soil type was classified as a shallow Rendzic Leptosol. It consists of thin organic L and F horizons, a mineral A-horizon with about 15-20 cm thickness, with a bulk density of ~ 0.5 g cm<sup>-3</sup>, and an underlying C-horizon deriving from dolomite. The carbonic A-horizon had a pH of ~ 7, a C:N ratio between 15 and 18, and stored ~ 120 Mg ha<sup>-1</sup> of organic C. The L/F- horizons stored about 10 Mg C ha<sup>-1</sup>. Based on the 'Austrian bioindicator grid' analyses (<https://bfw.ac.at/rz/bfwcms2.web?dok=3687>), average element concentrations of live Norway spruce needles for the period 2000 – 2005 were 12.1 mg N g<sup>-1</sup>, 0.94 mg P g<sup>-1</sup> and 3.5 mg K g<sup>-1</sup>. Further site details have been published elsewhere (Herman et al., 2002; Schindlbacher et al., 2011).

The soil warming experiment comprised six blocks of paired 2 × 2 m plots (each pair consisting of one control and one warmed plot), established in 2004 (n=3) and 2007 (n=3). Six plots were warmed (hereafter termed warming treatment) using heating cables (Etherma, Salzburg, Austria) installed at 3 cm soil depth and at a distance of 7.5 cm. In the other six plots (hereafter termed control treatment), heating cables were installed, but not heated to account for the disturbance created by their installation. The heating system was controlled by a service unit that automatically kept a 4 °C difference between the control and warming treatment throughout the snow-free period (April – December). On a half-hourly interval, soil temperature was recorded at 5 and 15 cm mineral soil depth. A detailed description of the experimental setup is given in Schindlbacher et al. (2007; 2009).

## 2 | 2 Fine root sampling and processing

The sampling of fine roots (< 2 mm in diameter) took place within one day at the end of the growing season in October 2012 and October 2019 using soil corers of 5 cm diameter and 20 cm in length. Three control and three warmed plots (warmed since 2004) were sampled in October 2012 (n=3), whereas all 12 plots were sampled in October 2019 (n=6). Ten soil cores were randomly taken from 0 – 10 and 10 – 20 cm soil depth in each plot. The sampling depth was less than 20 cm depth at a few sampling points because of the shallow soil and the dolomitic bedrock. In total, 120 samples were taken in 2012 and 240 samples in 2019. Samples were immediately transferred into zip lock plastic bags, stored in cooling boxes filled with ice packs, and transported to Bayreuth, Germany, for further processing.

In the laboratory, the soil cores were stored in a + 2 °C climate chamber and processed within a maximum of three weeks. The complete processing protocol included fine root washing, sorting into live and dead roots under a microscope, and finally scanning with a flatbed scanner. Roots were separated from the soil by wet sieving. We used a 0.63 mm sieve (Retsch Technology GmbH, 42781 Haan, Germany) to process the soil cores by hand using tap water until all soil and other impurities were removed from the fine root fraction. After washing, stones were picked using tweezers, dried in small aluminum dishes, and weighed to correct soil mass. Roots were then transferred into 500 ml glass beakers filled with water and ice and washed in an ultrasonic bath to remove residual soil particles attached to the fine roots. Right after washing, fine roots were sorted into a live and dead fraction under a binocular microscope. We used the morphological characteristics described in Wu (2000) and Burke and Raynal (1994). Herbaceous roots (white, light, and succulent) were excluded during sorting. Live roots were resilient and flexible, reddish, with several lateral root tips, while dead roots were soft, dark, and easily breakable. After separation, the dead root fraction was dried in an oven at 60 °C for three days, and the dry weight on a soil area basis ( $\text{g m}^{-2}$ ) was determined.

Fine root production was measured using ingrowth cores. In October 2019, after the soil coring described above, five ingrowth polypropylene mesh tubes per plot (5 cm diameter, 20 cm long, 6mm x 4 mm mesh) were inserted into the cored soil holes. They were filled with root-free mineral sieved soil deriving from the same study site. Soil bulk density was adjusted to  $\sim 0.5 \text{ g cm}^{-3}$  (see above) by alternating filling and compaction of the soil using a funnel and a piston. After 12 months, the ingrowth cores were sampled, and roots grown within a year were processed as described above. Fine root production was calculated on a soil area basis ( $\text{g m}^{-2}$

yr<sup>-1</sup>). We also estimated absorptive fine root biomass (aFRB) by multiplying mean root tip weight (see next paragraph for detailed information) by root tip number per m<sup>2</sup> (Ostonen et al., 2017).

### 2 | 3 Fine root morphology

The live fine root fraction was scanned in 20 × 25 cm transparent trays filled with cold water using a flatbed scanner (EPSON Perfection V700, SEIKO EPSON CORP, Japan) with the following setting: scanning resolution of 400 dpi; pixel classification method based on grey level and dark root on white background. Care was taken to avoid root overlap within the tray, and images were analyzed using the software WinRhizo™ Reg 2008 (Regent Instruments Inc., Canada). Due to the many replicates, we scanned on average 80% of fine roots collected at 0 – 10 cm depth, while the complete sample collected at 10 – 20 cm depth was scanned. Images were analyzed for fine root length (cm), average diameter of the fine roots (mm), fine root volume (cm<sup>3</sup>), the number of root tips, and surface area (cm<sup>2</sup>). Based on those basic parameters, the following morphological fine root traits were calculated: specific root length, expressed as the ratio of root length to dry mass (SRL; m g<sup>-1</sup>); specific root area, expressed as the ratio of root surface to dry mass (SRA; cm<sup>2</sup> g<sup>-1</sup> d.w); root area index expressed as the ratio of root surface to soil surface (RAI; m<sup>2</sup> m<sup>-2</sup>); root branching intensity, expressed as the number of root tips per root length (RBI; tips cm<sup>-1</sup> root length) and root tip density, the number of root tips per soil volume (RTID; tips m<sup>-3</sup> soil). We recalculated root volume as the sum of all diameter class' averages (Freschet et al., 2021; Rose, 2017) and estimated RTD as the ratio of root dry mass to root volume (RTD; g cm<sup>-3</sup>). Right after scanning, root tips were excised and dried at 60 °C for two days to determine root tip weight (RTW; mg). Mycorrhizal root colonization was determined under the microscope by random examination of intact root fragments. The roots to be examined were placed in a petri dish, and using different magnification levels allowed careful examination of the presence of emanating hyphae and rhizomorphs. Roots colonized by EcM were sampled using scalpels (ca. 20 – 30 root tips per samples), transferred into 5 mL Eppendorf® tubes, and stored at – 24 °C until DNA extraction. The live fine root fraction was finally dried in an oven at 60 °C for three days to determine fine root mass. Root biomass was expressed on a soil area basis (g m<sup>-2</sup>).

## 2 | 4 Fine root chemistry

Dried fine root samples were ground using a ball mill (MM 400, Retsch Technology GmbH, 42781 Haan, Germany). Fine root chemistry was assessed on fine roots sampled in 2019. Element concentrations of P, Na, K, Ca, Mg, Fe, and Mn were determined after 65% HNO<sub>3</sub> digestion in a microwave device (Mars 5, CEM, Germany). For the digestion, 8 ml 65% HNO<sub>3</sub> was added to 100 mg dried and ground fine roots. Digests were then transferred to 50 ml volumetric flasks, diluted with deionized water, and filtered through nylon filters (0.45 µm). Element concentrations in the extracts were determined using ICP-OES (Optima 3200 xl, Perkin Elmer, Germany) and AAS (SpectraA 220 Z, Varian, USA). The organic C and total nitrogen (TN) concentrations were analyzed with an elemental analyzer (EA1110, CE Instrument, Italy).

## 2 | 5 DNA extraction and amplicon barcoding

We extracted DNA from 48 samples collected during the second fine root sampling in 2019 (two technical replicates per plot and soil depth, 10 root tips per sample) using the ChargeSwitch® gDNA plant kit (Invitrogen™, Carlsbad, USA) following the manufacturer's instructions. Amplicon libraries were prepared in two consecutive PCR runs using a liquid handling workstation (epMotion® 5075, Eppendorf, Hamburg) and a thermocycler with a high-pressure lid (peqstar 384X HPL). Amplicon libraries were prepared of the V3 and V4 regions of the 16S rRNA gene as recommended by Illumina (2013) and otherwise processed as detailed in the following for fungi. The fungal ITS2 region was first (PCR1) amplified from the DNA extracts using the primers gITS7 (Ihrmark et al., 2012) and ITS4g ("CGCTTATTGATATGCTTAAGT", as modified after Schlegel et al. (2018)). The PCR1 primers ('nGS grade', Metabion, Planegg, Germany) included the fungus-specific sequences prepended by "Tags" (barcode sequences for sample identification of 4 to 7 bp in length, Table S3) and the recommended overhang adapter sequences (<https://support-docs.illumina.com/SHARE/AdapterSeq/illumina-adapter-sequences.pdf>). The reactions were conducted in a total volume of 4 µl, including the primers (370 nM, each), 2 µl OneTaq® 2X Master Mix (NEB, Frankfurt am Main) and 0.2 µl DNA extract. The thermocycler kept the prevailing 95 °C for another 2 min after the reaction mixes were inserted. Amplification was achieved in 25 cycles of 94 °C for 20 s, 45 °C for 40 s and 68 °C for 55 s, followed by a final extension at 68 °C for 7 min. Purification of the PCR1 products was achieved by adding 3.1 µl

of a mixture of Exonuclease (3.2 U) and Shrimp Alkaline Phosphatase (0.32 U, both NEB, Frankfurt am Main) to each PCR1 product and incubating the total volume of 7.1  $\mu$ l at 37 °C for 25 min, followed by 80 °C for 15 min. Index (barcode sequences of 8 bp in length) and adapter sequences (P5 and P7, respectively) were appended to the PCR1 products in the second PCR (PCR2), utilizing the overhang adapter sequences (Table S4). The reactions were conducted in a total volume of 8  $\mu$ l, including the primers (270 nM, each), 4  $\mu$ l OneTaq® 2X Master Mix, and 2.5  $\mu$ l of purified PCR1 product. Equal volumes (1  $\mu$ l) of root-derived fungal and bacterial PCR2 products were pooled separately. The two pools were purified using CleanPCR® Nucleic acid Clean up (CleanNA, GC biotech B.V.) as recommended by the manufacturer. To discriminate against short fragments, such as primer dimers, CleanPCR® beads were applied in a volume corresponding to 70% of the volume of the pooled PCR2 products. The sequencing service of the Faculty of Biology at LMU Munich, Germany, assessed the DNA concentration (Qubit® 2.0 fluorometer, Life Technologies, Carlsbad, CA, USA) and the amplicon size distribution (Bioanalyzer 2100, Agilent Technologies GmbH & Co. KG, Waldbronn, Germany), before sequencing using an Illumina MiSeq® sequencer (Illumina, Inc., San Diego, CA, USA) with 2  $\times$  300 bp paired-end sequencing (MiSeq Reagent Kit v3 Chemistry, Illumina, Inc., San Diego, CA, USA). Sequence reads were deposited in the European Nucleotide Archive (<http://www.ebi.ac.uk/ena/data/view/PRJEB48843>).

## **2 | 6 Sequence data processing**

Sequence reads were pre-sorted by the sequencer according to the inserted dual index sequences, i.e., each combination including a unique forward and a unique reverse index. Within index combinations, reads were assigned to samples according to dual index combinations, using the open-source software QIIME version 1.9.0 (Caporaso et al., 2010). During demultiplexing, only reads with at most one ambiguity base were retained, and a quality filter (threshold phred 19) was applied: reads were truncated after nine consecutive low-quality base calls and only retained if at least 35% of the entire sequence consisted of consecutive high-quality base calls. Only the R1 reads were further processed. Reads were grouped according to the lengths of the tag-sequences and length adjusted using the FastX toolkit ([http://hannonlab.cshl.edu/fastx\\_toolkit/](http://hannonlab.cshl.edu/fastx_toolkit/)). CD-HIT-OUT (W. Li & Chang, 2017) was used for de novo clustering sequence reads to operational taxonomic units (OTUs) based on 97% sequence similarity. Sequences representing an OTU were assigned to taxa using QIIME and

the UNITE database v8 (Kõljalg et al., 2013) as a reference. Initially unassignable OTUs were assigned as detailed by Peršoh et al. (2010). A table coding the read counts per sample and OTU was generated and rarefied to 1646 reads per sample using the *rrarefy* function of the R package *vegan* (Oksanen et al., 2019). For improved comprehensibility, the OTU identification number is prepended by the assigned genus name in the following.

According to their taxonomic affiliation, fungal OTUs were assigned to functional guilds, as indicated by Agerer (2006), Cannon and Kirk (2007), and Kirk et al. (2011) and the Faces of Fungi (Jayasiri et al., 2015) and FUNGuild (Nguyen et al., 2016) databases. Taxonomic and functional assignments were verified by species-level identification or sequence comparison for abundant and discriminative OTUs, in particular for OTUs assigned to the genus *Sebacina*. Assignment and sequences of the OTUs from identified mycorrhiza taxa are provided in Table S7. Subsequent analyses were exclusively based on this (re-standardised) subset of mycorrhizal fungi. From the bacterial dataset, sequences of plant plastids were removed before normalization.

## 2 | 7 Statistical analysis

All statistical analyses and graphs were performed using R version 4.0.3 (R Core Team, 2022). The R packages *ggplot2* (Wickham, 2016) and *gridExtra* (Auguie, 2017) were used for data visualization. Potential outliers in the data set were first identified visually with boxplots and then tested with Rosner's test using the package *EnvStats* (Millard, 2013). Root traits were checked for normality using the Shapiro-Wilk test and, when needed, were square-root transformed before analysis to meet the assumption of normality. Because of the layout of our control and warmed plots in pairs, we tested the effect of warming on FRB, necromass, morphological traits, and nutrient contents with paired *t*-tests ( $\alpha = 0.05$  was used as the significance level).

We used Fisher's alpha, Shannon-Wiener, and Pielou's evenness to characterize EcM fungal and root-associated bacterial communities at the two soil depths. Fisher's alpha is a parametric diversity index that assumes that the species abundance distribution follows a log series distribution. It was calculated as  $S = a * \ln(1 + n/a)$ ; with  $S$ , the number of taxa,  $n$  is the number of individuals, and  $a$  is the Fisher's alpha. The Shannon-Wiener index considers the number of individuals as well as the number of taxa. It varies from 0 for communities with a single taxon to high values for communities with many taxa. It was calculated as  $H' =$

$-\sum [P_i \log (P_i)]$ ; where  $P$  is the proportion of the total count arising from the  $i^{\text{th}}$  species. Pielou's evenness, finally, measures the diversity along with species richness, i.e., how evenly the individuals are distributed amongst species, and was calculated as follows:  $J' = H' / \log (S)$ ; where  $S$  is the number of species and  $H'$  is the Shannon-Wiener index. It varies from 0 (no evenness) to 1 (complete evenness). A detailed description of those diversity measures is given in Clarke et al. (2014).

We used linear mixed-effects models to test the effect of treatment and soil depth on fungal and bacterial diversity using the package *lme4* (Bates et al., 2015). Treatment and soil depth were fixed factors and plot, inserted as random factor. Post-hoc pairwise comparisons amongst groups were conducted using the package *emmeans* version 1.5.4 (Lenth, 2021). To test the effect of treatment and soil depth on fungal and bacterial communities, we used permutational multivariate analysis of variance (PERMANOVA) based on Bray-Curtis dissimilarity implemented in the *adonis* function of the package *vegan*, version 2.5-6 (Oksanen et al., 2019). The contribution of individual OTUs to the dissimilarity between control and warming treatments was evaluated using the similarity percentages breakdown (SIMPER) procedure implemented in the *simper* function of the package *vegan*. We further grouped EcM fungal OTUs into different exploration types, based on Agerer (2001, 2006): contact; contact or medium-distance; short-distance; contact, short or medium-distance; medium-distance and long-distance. Because contact or medium and contact, short or medium-distance, were rare, we reclassified exploration types into short-distance (contact; short-distance) and long-distance (medium-distance and long-distance) types. Paired  $t$ -tests were performed to test for differences in exploration types between control and warming treatments.

We used the classification method program (CLAM) implemented in the package *vegan* to evaluate the preference of OTUs for either control or warming treatments. The CLAM statistical approach uses a multinomial model to classify OTUs in either generalist (i.e., well distributed between the two treatments) or specialist species (preference in one treatment) based on their relative abundance in the different treatments (Chazdon et al., 2011).

We carried out principal component analysis (PCA) to assess the interrelation between fine root traits, soil nutrients, EcM exploration types, and bacterial and fungal diversity indices using the R package *FactoMinerR* (Lê et al., 2008) and *factoextra* (Kassambara, 2017). The variation of the EcM fungal community with treatment and soil depth was visualized with non-metric dimensional scaling (NMDS) using the function *metaMDS* of the package *Vegan*.

### 3 | Results

#### 3 | 1 Fine root biomass, necromass, and fine root production

Total FRB increased by 17% (from 355 to 414 g m<sup>-2</sup>) by soil warming in 2019 (Figure 1). The effect of soil warming on FRB was stronger at 10 – 20 cm (+ 34%) than at 0 – 10 cm soil depth (+ 12%); however, the absolute increase was greater at 0 – 10 cm soil depth.

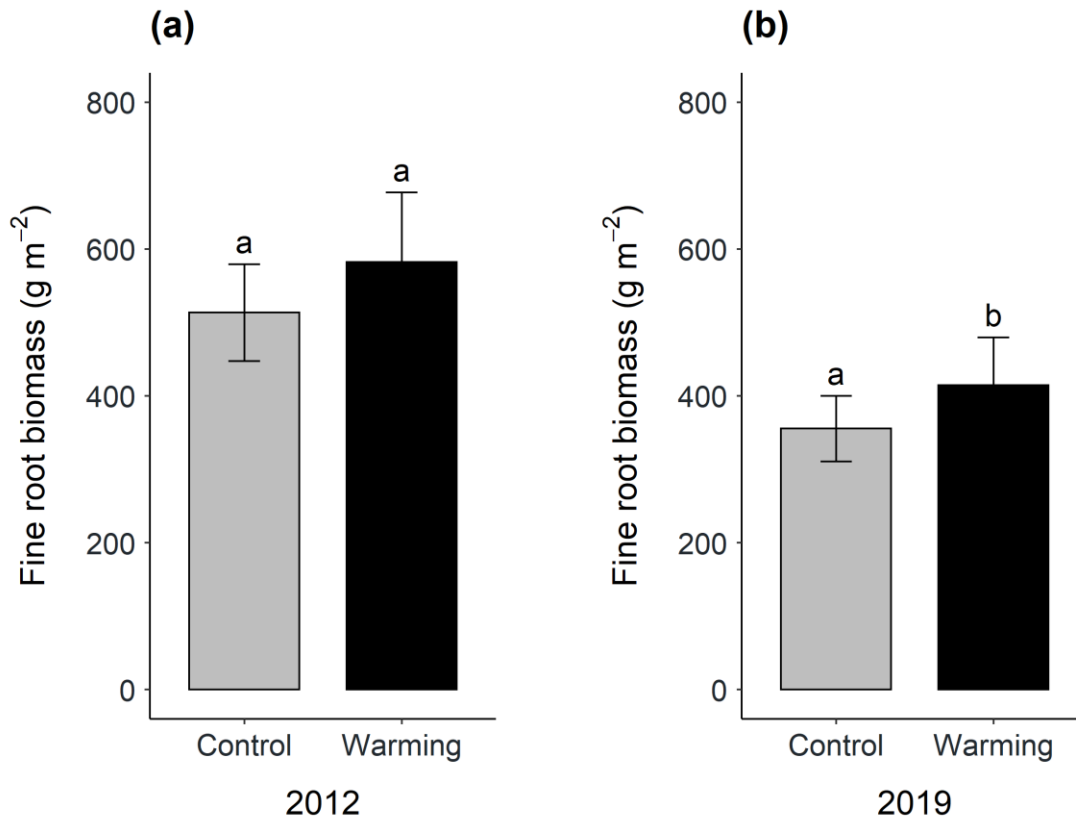


**Figure 1:** Mean ( $\pm$  SE) fine root biomass at 0 – 20 cm soil depth in the control and the warming treatments in (a) October 2012 (n=3) and (b) 2019 (n=6). Lowercase letters indicate significant differences between treatments (t-test;  $p < .05$ ).

Soil warming decreased fine root necromass by 14% in 2019 (from 85 to 74 g m<sup>-2</sup> for control and warmed plots, respectively). Absorptive fine root biomass measured in 2019 increased by 22% in warmed plots (76.6 and 93.4 g m<sup>-2</sup> in control and warming plots, respectively) and represented approximately 23% of the total FRB at 0 – 20 cm soil depth, irrespective of treatment (Table 1).

During the first sampling campaign in 2012, mean FRB amounted to 513 and 582 g m<sup>-2</sup> in control and warmed plots, respectively. Soil warming had no significant effect, although there was a trend to higher root biomass (+ 13%) in the warmed plots (Table 1). We also found that FRB decreased with soil depth on both occasions (Table 1). In comparison to 2019, soil warming did not affect fine root necromass in 2012.

In the warmed plots, fine root biomass production in ingrowth cores increased strongly, by 128% from 99 to 225 g m<sup>-2</sup> yr<sup>-1</sup> between October 2019 and October 2020 (Figure 2). While newly produced roots showed no changes in average diameter, SRL and SRA, their root tissue density and root tip density increased by 11% and 168%, respectively, in the warmed plots (Figure 2).

**Table 1:** Means  $\pm$  SE of absorptive fine root biomass, fine root necromass, and morphological traits of live roots at 0–10 and 10–20 cm soil depth in control and warmed plots in 2012 (n = 3) and 2019 (n = 6). Different letters indicate significant differences between control and warming treatments, tested separately for each soil depth (t test;  $p < .05$ ).

Fine root traits	Depth	2012		2019	
		Control	Warming	Control	Warming
aFRB (g m <sup>-2</sup> )	0–10 cm	-	-	64.2 $\pm$ 18.8 a	80.2 $\pm$ 10.6 b
	10–20 cm	-	-	12.3 $\pm$ 3.9 a	13.12 $\pm$ 3.3 a
FRN (g m <sup>-2</sup> )	0–10 cm	294 $\pm$ 13 a	293 $\pm$ 29 a	67 $\pm$ 12a	45 $\pm$ 6 b
	10–20 cm	96 $\pm$ 16 a	114 $\pm$ 58 a	18 $\pm$ 4 a	29 $\pm$ 7 b
Diameter (mm)	0–10 cm	0.46 $\pm$ 0.06 a	0.46 $\pm$ 0.07 a	0.51 $\pm$ 0.02 a	0.60 $\pm$ 0.07 b
	10–20 cm	0.44 $\pm$ 0.08 a	0.40 $\pm$ 0.02 a	0.49 $\pm$ 0.02 a	0.47 $\pm$ 0.03 a
SRL (m g <sup>-1</sup> )	0–10 cm	14 $\pm$ 1 a	16 $\pm$ 3 b	11 $\pm$ 1 a	14 $\pm$ 1 b
	10–20 cm	14 $\pm$ 1 a	17 $\pm$ 3 b	12 $\pm$ 2 a	15 $\pm$ 3 a
RTD (g cm <sup>-3</sup> )	0–10 cm	1.5 $\pm$ 0.8 a	0.9 $\pm$ 0.2 b	0.42 $\pm$ 0.04 a	0.43 $\pm$ 0.04 a
	10–20 cm	1.3 $\pm$ 0.4 a	1.5 $\pm$ 0.3 a	0.43 $\pm$ 0.04 a	0.41 $\pm$ 0.02 a
SRA (cm <sup>2</sup> g <sup>-1</sup> )	0–10 cm	124 $\pm$ 46 a	174 $\pm$ 16 b	156 $\pm$ 17 a	193 $\pm$ 21 b
	10–20 cm	68 $\pm$ 28 a	172 $\pm$ 33 b	163 $\pm$ 24 a	177 $\pm$ 27 b
RAI (m <sup>2</sup> m <sup>-2</sup> )	0–10 cm	5.2 $\pm$ 2.1 a	6.0 $\pm$ 0.7 a	3.7 $\pm$ 0.5 a	4.4 $\pm$ 0.2 b
	10–20 cm	1.2 $\pm$ 0.3 a	1.5 $\pm$ 0.6 a	1.1 $\pm$ 0.2 a	1.4 $\pm$ 0.4 b
RTID (10 <sup>5</sup> $\times$ tips m <sup>-3</sup> )	0–10 cm	154 $\pm$ 55 a	190 $\pm$ 35 b	80 $\pm$ 11 a	136 $\pm$ 18 b
	10–20 cm	39 $\pm$ 7 a	47 $\pm$ 16 b	21 $\pm$ 4 a	28 $\pm$ 7 b
RBI (Tips cm <sup>-1</sup> )	0–10 cm	3.0 $\pm$ 1.1 a	3.7 $\pm$ 0.2 b	3.3 $\pm$ 0.2 a	3.6 $\pm$ 0.1 b
	10–20 cm	3.0 $\pm$ 1.0 a	3.7 $\pm$ 0.3 b	3.0 $\pm$ 0.1 a	3.2 $\pm$ 0.3 a
RTW (mg)	0–20 cm	-	-	0.063 $\pm$ 0.009a	0.053 $\pm$ 0.005b

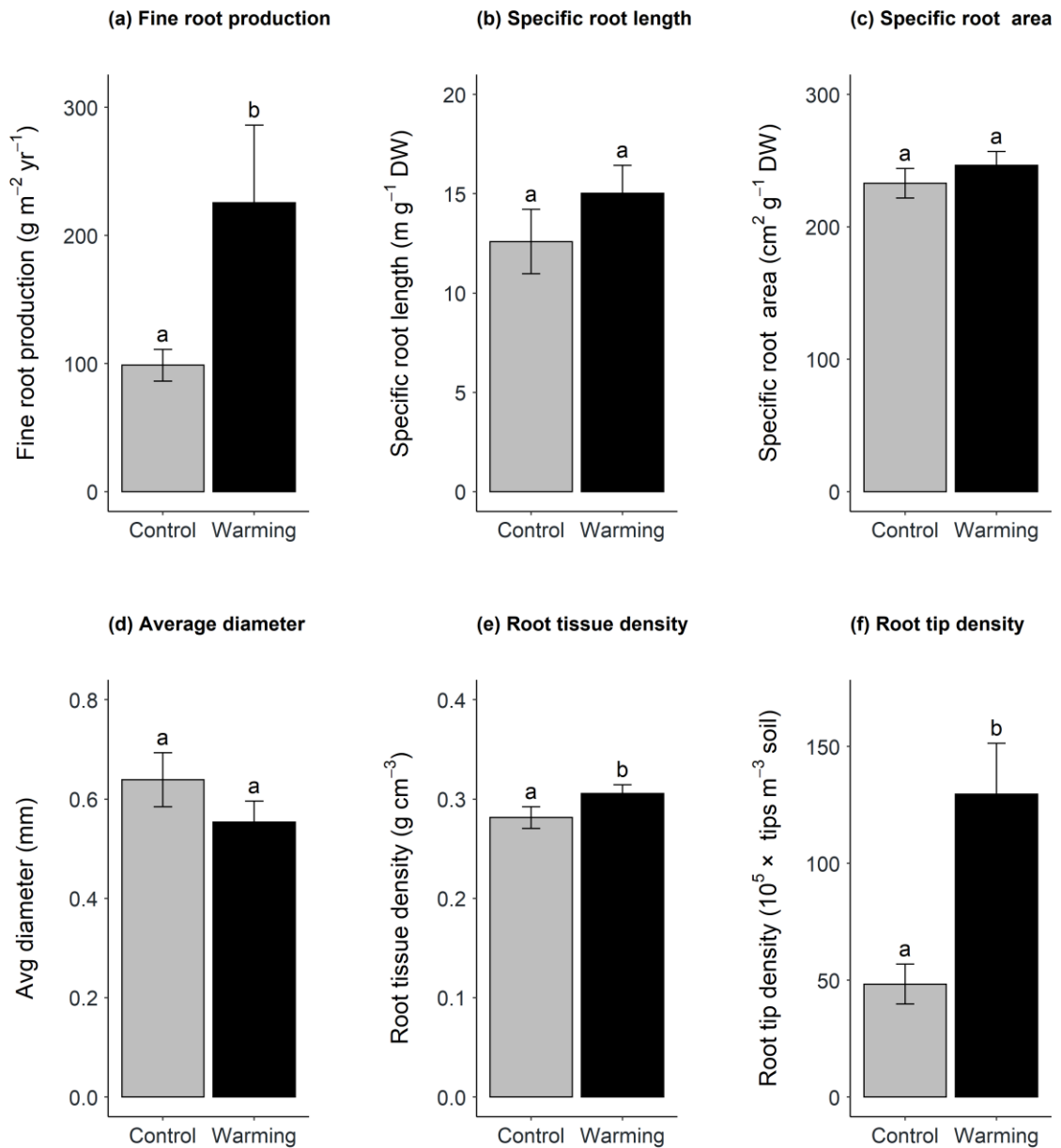


**Figure 2:** Mean ( $\pm$  SE) fine root biomass production (a) and morphological traits of fine roots from ingrowth cores in control and warmed plots between October 2019 and October 2020 ( $n = 6$ ): specific root length (b), specific root area (c), average diameter (d), root tissue density (e), and root tip density (f). Different letters indicate significant differences between control and warming treatments ( $t$  test;  $p < .05$ )

### 3 | 2 Fine root morphology

In 2019, morphological analyses of fine root samples revealed that soil warming increased SRL, SRA, RAI, RTID, and RTW. The average diameter of fine roots was also affected, especially at 0 – 10 cm (Table 1). There was an average increase in SRL by 29% under warming conditions. SRA showed a similar trend and increased in warmed plots (311 and 368 cm<sup>2</sup> g<sup>-1</sup>, under control and warming conditions, respectively, for both depths). An increase in SRA from 156 to 193 and 163 to 177 cm<sup>2</sup> g<sup>-1</sup> was observed at 0 – 10 cm and 10 – 20 cm soil depth in the control and warming treatment, respectively. Soil warming increased RAI significantly by 21% at both soil depths (from 4.7 to 5.7 m<sup>2</sup> m<sup>-2</sup>). Mean fine root diameter increased by soil warming at 0 – 10 cm depth (0.51 and 0.60 mm, in control and warmed plots, respectively), but no effect was observed at 10 – 20 cm soil depth. RBI and RTID also increased in warmed plots (Table 1). The most significant increase of the latter two was observed at 0 – 10 cm soil depth. RTD was not affected at 0 – 10 cm depth (0.42 and 0.43 g cm<sup>-3</sup>, in the control and warming treatment, respectively). Similar fine root morphological patterns were also observed in 2012. SRL, SRA, and RTID significantly increased by 11%, 43%, and 23%, respectively. On the other hand, fine root diameter and RAI were not affected by soil warming in 2012 (Table 1).

We observed an increase in the proportion of fine root length in the 0 – 0.2 mm diameter class in the warming treatment (Figure S1). We also noted a decrease in the proportion of fine root length with increasing diameter of fine roots, where warming became non-significant. Root length of the first diameter class (0 – 0.2 mm) accounted for up to 52% of the total root length, irrespective of treatment and soil depth. The first three diameter classes (0 – 0.2, 0.2 – 0.4 and 0.4 – 0.6 mm) contributed about 86% to the total fine root length in both treatments (Figure S1).

### 3 | 3 Nutrient concentrations in fine roots

The concentration of the macronutrients N, P, K, and Mg did not differ between control and warmed plots, although they showed a tendency to decrease with soil warming (Table 2). However, C and Ca concentrations significantly decreased by 5 and 28% with soil warming at 0 – 10 and 10 – 20 cm soil depth, respectively. The concentration of the micronutrients Fe and Mn were not affected by soil warming, except Na, which decreased by 40% at 10 – 20 cm soil depth.

**Table 2:** Mean  $\pm$  SE element concentrations; C:N, N:P, N:K ratios of live fine roots in control and warmed plots at 0 – 10 and 10 – 20 cm soil depth in 2019 (n=6). Different letters within each row indicate significant differences between control and warming treatments tested separately for each soil depth (t-test;  $p < .05$ ).

Parameters	Control		Warming	
	0 – 10 cm	10 – 20 cm	0 – 10 cm	10 – 20 cm
C (%)	48.5 $\pm$ 0.6 a	48.9 $\pm$ 0.8	46.1 $\pm$ 0.2 b	47.8 $\pm$ 0.5
N (%)	0.85 $\pm$ 0.05	0.73 $\pm$ 0.04	0.80 $\pm$ 0.04	0.74 $\pm$ 0.04
P (mg g <sup>-1</sup> )	0.51 $\pm$ 0.02	0.39 $\pm$ 0.04	0.50 $\pm$ 0.03	0.38 $\pm$ 0.04
K (mg g <sup>-1</sup> )	1.56 $\pm$ 0.09	1.14 $\pm$ 0.09	1.42 $\pm$ 0.05	1.20 $\pm$ 0.09
C:N	58.2 $\pm$ 3.9	68.0 $\pm$ 4.0	58.5 $\pm$ 2.3	65.4 $\pm$ 3.2
N:P	16.9 $\pm$ 0.9	19.7 $\pm$ 2.0	16.0 $\pm$ 0.7	20.4 $\pm$ 1.6
N:K	5.6 $\pm$ 0.6	6.5 $\pm$ 0.4	5.6 $\pm$ 0.3	6.3 $\pm$ 0.5
Na (mg g <sup>-1</sup> )	0.20 $\pm$ 0.04	0.24 $\pm$ 0.04 a	0.14 $\pm$ 0.01	0.15 $\pm$ 0.02 b
Mg (mg g <sup>-1</sup> )	1.27 $\pm$ 0.07	1.41 $\pm$ 0.10	1.27 $\pm$ 0.09	1.25 $\pm$ 0.15
Ca (mg g <sup>-1</sup> )	11.45 $\pm$ 1.35	14.35 $\pm$ 1.40 a	10.25 $\pm$ 0.44	10.36 $\pm$ 0.73 b
Mn (mg g <sup>-1</sup> )	0.005 $\pm$ 0.007	0.041 $\pm$ 0.004	0.067 $\pm$ 0.007	0.029 $\pm$ 0.002
Fe (mg g <sup>-1</sup> )	0.51 $\pm$ 0.08	0.45 $\pm$ 0.06	0.71 $\pm$ 0.09	0.41 $\pm$ 0.03

### 3 | 4 Response of ectomycorrhizal fungal and bacterial communities to warming

A total of 92 EcM fungal OTUs were detected across root tips of all samples. *Hysterangium*, *Sebacina*, *Tricholoma*, and *Russula* were the most abundant genera in fine roots from the upper soil layer of the control plots. *Cortinarius*, *Sebacina*, *Lactarius*, *Helvellosebacina*, *Pachyphlodes*, *Trichophaea*, and *Inocybe* were most abundant at 10 – 20 cm depth (Figure S2). Soil warming increased the relative abundance of *Sebacina*, *Amphinema*, and *Cenococcum* at 0 – 10 cm depth, while *Sebacina* and *Boletus* largely dominated at 10 – 20 cm depth. Twelve EcM fungal OTUs accounted for > 50 % (i.e., 73%) of the overall difference between fungal community composition in control and warmed plots in the upper soil layer (Figure 3). Only

six OTUs accounted for > 50 % (i.e., 60%) of the difference in fungal community composition in the deeper soil (Figure 4).

The linear mixed-effects models showed that warming, but not soil depth, significantly affected bacterial diversity. Root-associated bacterial communities were altered in warmed plots, as indicated by the Shannon-Wiener diversity index and Pielou's evenness (Table S1). For EcM fungi, not treatment but soil depth significantly affected all diversity measures (Table S2). PERMANOVA revealed a significant effect of soil depth ( $p = 0.003$ ) and warming treatment ( $p = 0.011$ ) on EcM fungal community composition (Table 3), as also indicated by the NMDS ordination (Figure S7). Soil depth and treatment explained approximately 34% of the total variation observed in the EcM community at the site. Bacterial community composition was significantly affected by depth ( $p = 0.021$ ), but not by treatment (Table 3).

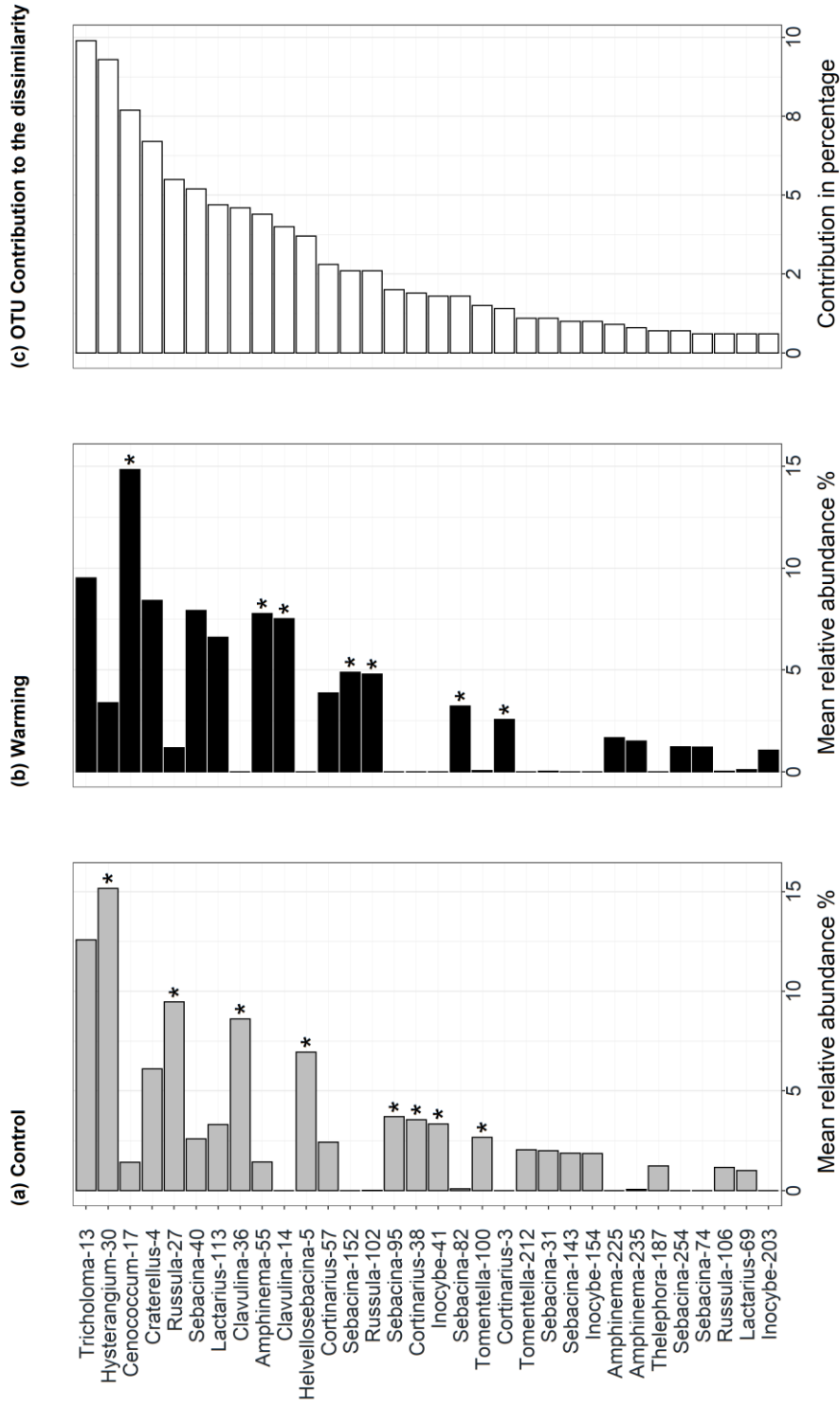


**Figure 3:** Abundance of ectomycorrhizal fungal genera with >1% relative abundance across all samples in control (a) and warmed (b) plots at 0–10 cm soil depth and their contribution to dissimilarity (c) determined by SIMPER analysis. Numbers behind genera of fungus are OTU numbers. Asterisks indicate a significantly higher abundance in either control or warmed plots.

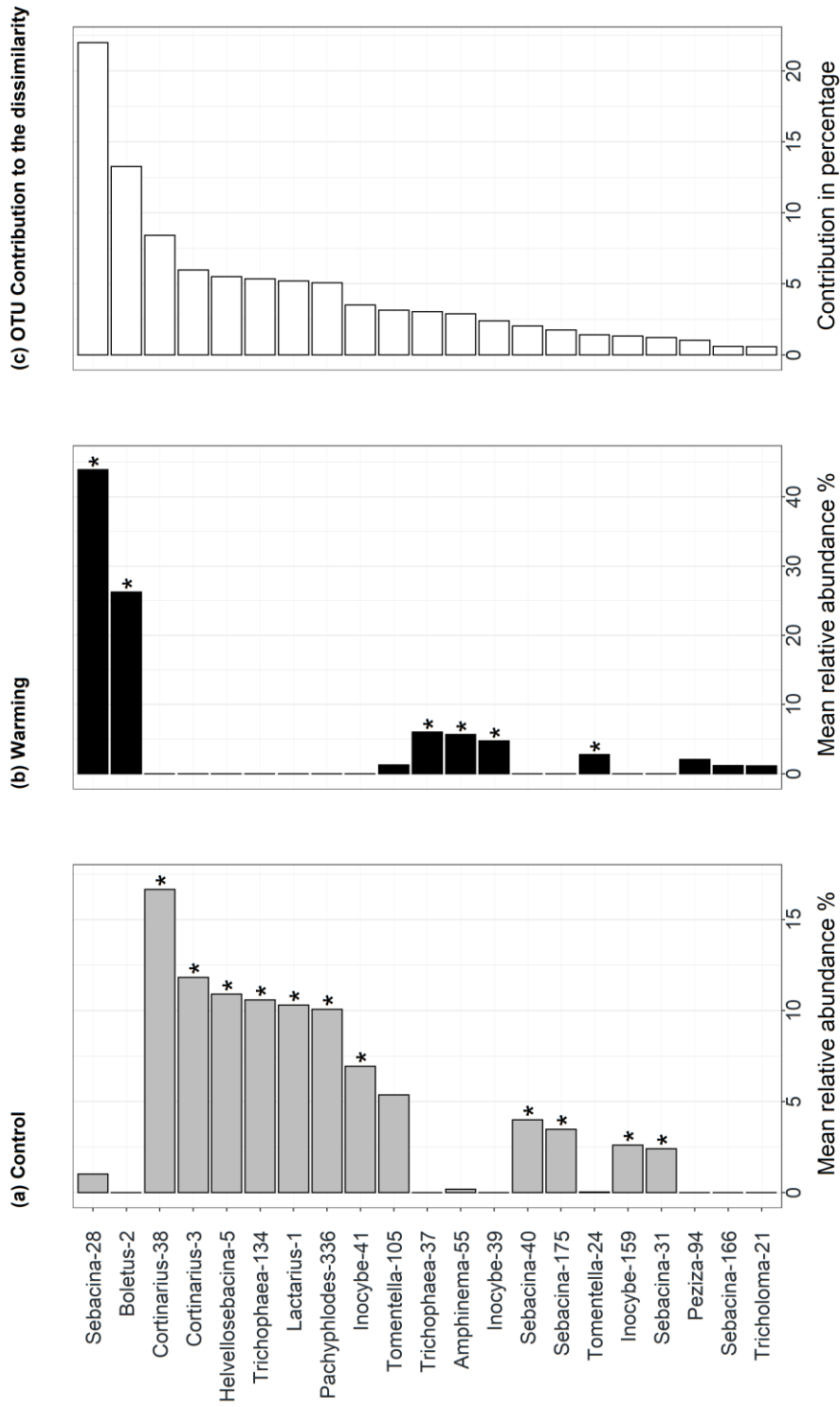


**Figure 4:** Abundance of ectomycorrhizal fungal genera with >1% relative abundance across all samples in control (a) and warmed (b) plots at 10–20 cm soil depth and their contribution to dissimilarity (c) determined by SIMPER analysis. Numbers behind genera of fungus are OTU numbers. Asterisks indicate a significantly higher abundance in either control or warmed plots.

**Table 3:** Results of PERMANOVA based on Bray–Curtis dissimilarity analysis showing the effects of treatment (T: control and warming treatments), depth (D: 0–10 and 10–20 cm soil depth) on fungal and bacterial communities.

Source	Ectomycorrhizal fungal community					Bacterial community						
	df	SS	MS	Pseudo-F	p (perm)	% Var	df	SS	MS	Pseudo-F	p (perm)	% Var
Depth	1	8107	8107	1,88	0,003**	17,8	1	4193.6	4194	2.18	0.021*	15.7
Treatment	1	7376	7376	1,71	0,011**	16	1	2435.6	2436	1.27	0.181	7.4
D x T	1	5208	5208	1,21	0,204	12,2	1	1748.8	1749	0.91	0.578	-6.2
Residual	20	86228	4311			65,7	15	28891	1926			43.9
Total	23	106840					18	37206				

According to the classification method program (CLAM), soil warming affected EcM fungal OTUs differently (Figures 3 and 4). In the upper soil layer, *Cenococcum*-17, *Clavulina*-14, *Amphinema*-55, *Sebacina*-152, *Russula*-102, *Sebacina*-82, and *Cortinarius*-3 had higher relative abundances in warmed plots, while *Hysterangium*-30, *Russula*-27, *Clavulina*-36, *Helvellosebacina*-5, *Sebacina*-95, *Cortinarius*-38, *Inocybe*-41, and *Tomentella*-100 (numbers behind genera of fungus are OTU numbers) contributed more to the overall communities in control plots (Figure 3). At 10 – 20 cm soil depth, *Cortinarius*-38, *Cortinarius*-3, *Helvellosebacina*-5, *Trichophea*-134, *Lactarius*-1, *Pachyphlodes*-336, *Inocybe*-41, *Sebacina*-40, *Sebacina*-175, *Inocybe*-159 and *Sebacina*-31 had higher relative abundances in control plots, while *Sebacina*-28, *Boletus*-2, *Trichophea*-37, *Amphinema*-55, *Inocybe*-39, and *Tomentella*-24 had higher abundances in warmed plots (Figure 4). Proportions of the different EcM exploration types were not significantly different between treatments (Figure 5).

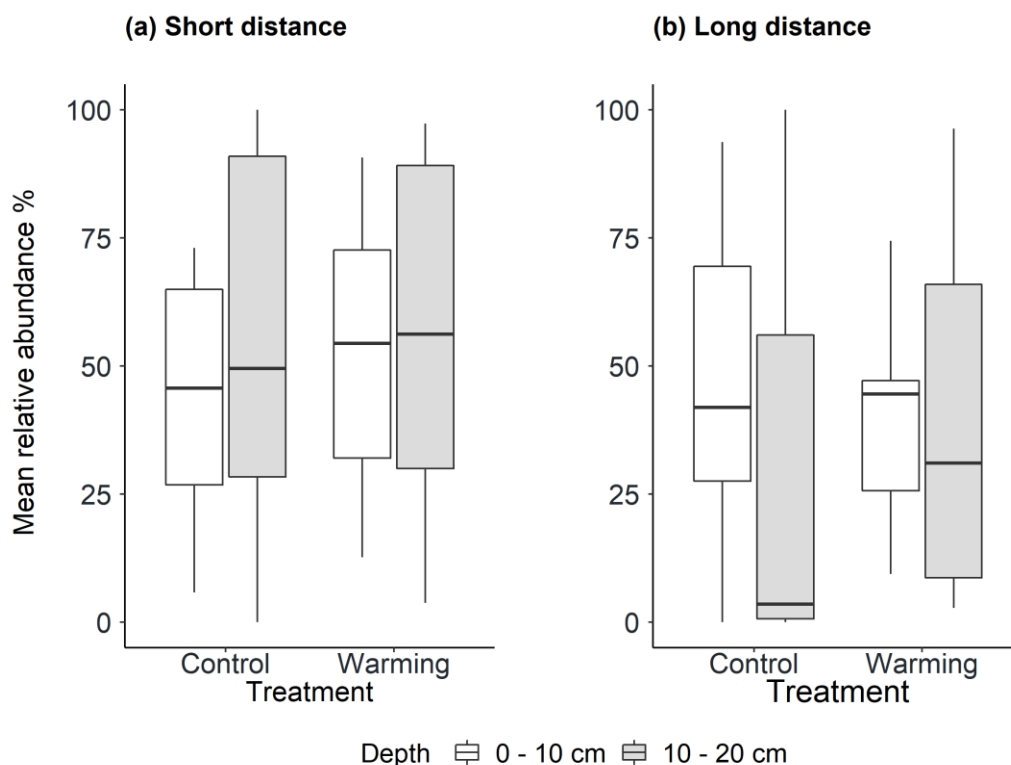


**Figure 5:** Box plots showing mean relative abundances (%) of ectomycorrhizal fungi grouped into short-distance (a) and long-distance (b) exploration types in control and warmed plots at 0–10 and 10–20 cm soil depth.

### **3 | 5 Relationship between fine root traits, soil nutrients, EcM exploration types and fungal and bacterial diversity**

At 0 – 10 cm soil depth, the first and second principal components (PC1 and PC2) explained 40% and 22% of the variance, respectively (Figure 6). PC1 was significantly correlated with SRL ( $r= 0.90$ ), RTID ( $r= 0.84$ ), aFRB ( $r= 0.82$ ), soil temperature ( $r= 0.61$ ), soil N ( $r= -0.73$ ), and RTD ( $r= -0.80$ ). PC2 was significantly correlated with EcM short-distance exploration type ( $r= 0.79$ ), EcM diversity ( $r= 0.65$ ), FRB ( $r= 0.64$ ) and EcM long-distance exploration type ( $r= -0.71$ ). At 10 – 20 cm soil depth, PC1 and PC2 explained 34% and 27% of the variance, respectively. PC1 was significantly correlated with FRB ( $r= 0.93$ ), aFRB ( $r= 0.88$ ), RTID ( $r= 0.81$ ), RTD ( $r= 0.75$ ), D ( $r= 0.62$ ), and SRL ( $r= -0.83$ ). PC2 was positively correlated with bacterial diversity ( $r= 0.72$ ) and soil temperature ( $r= 0.68$ ) and negatively associated with the long-distance exploration type ( $r= -0.60$ ), soil P ( $r= -0.65$ ), and soil N ( $r= -0.80$ ).

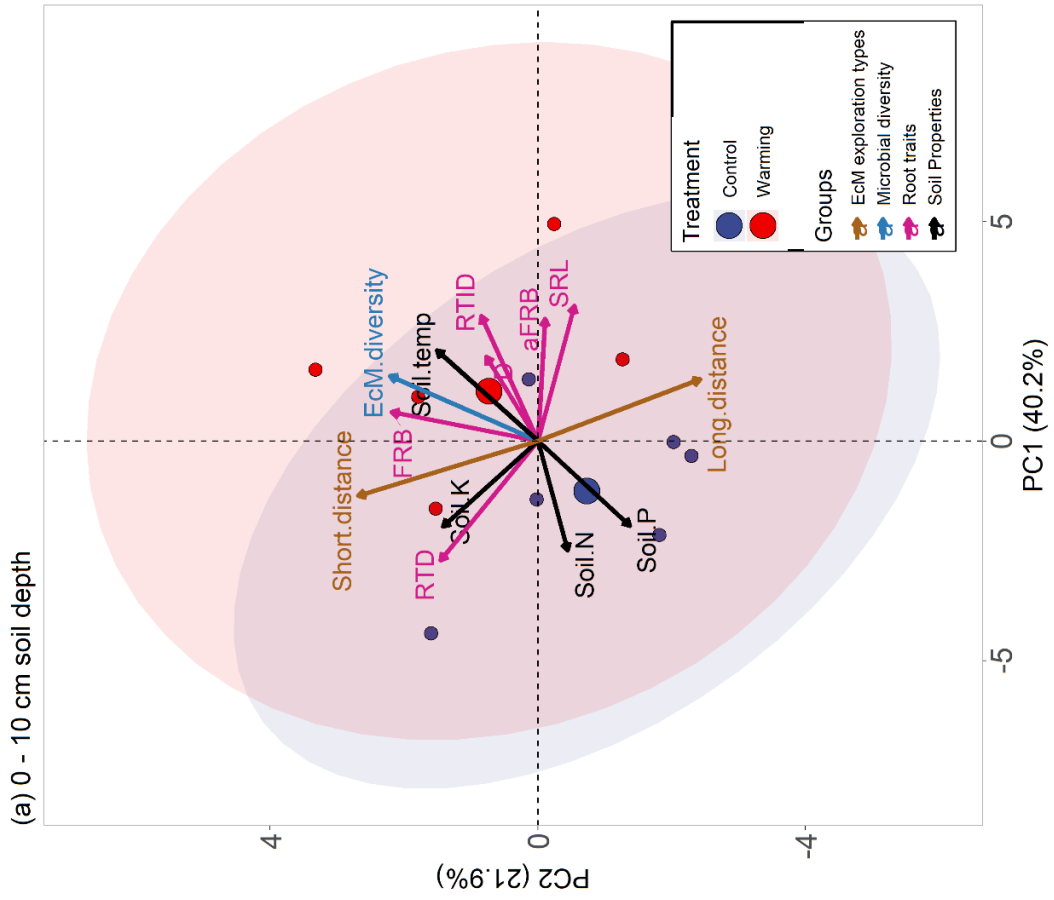
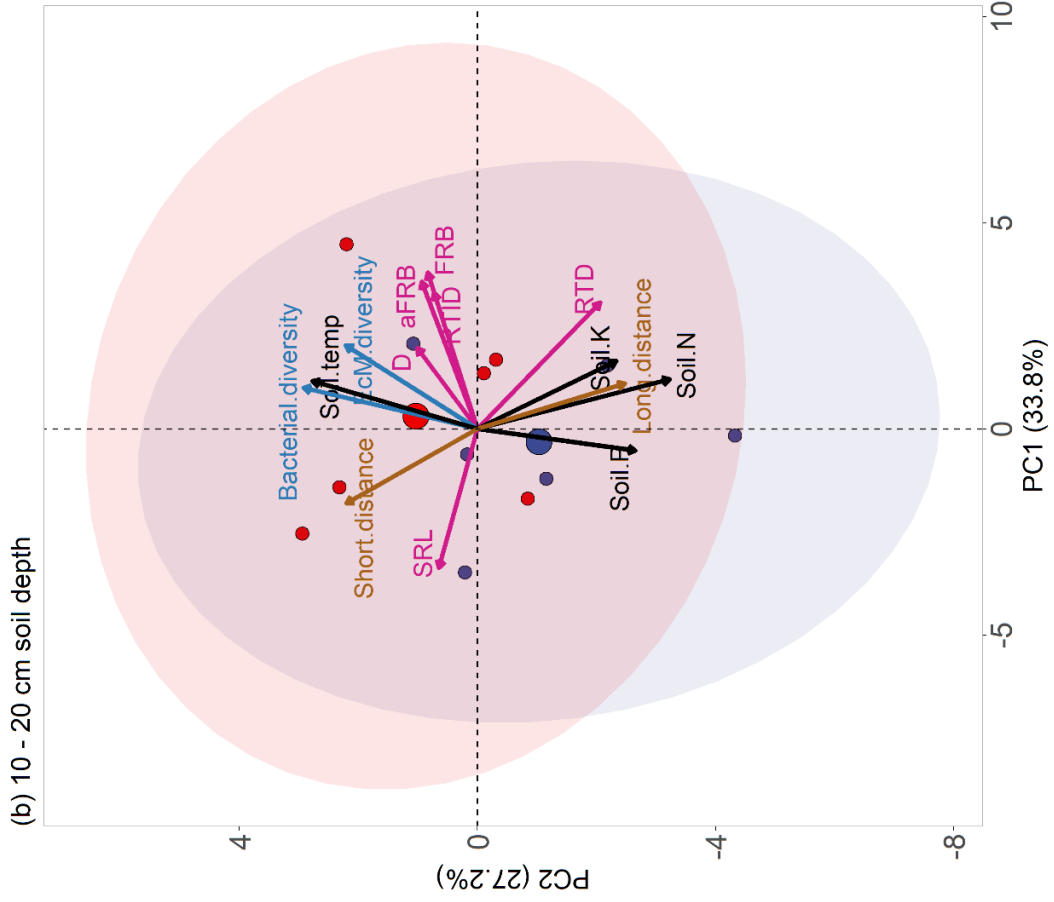


**Figure 6:** Principal component analysis (PCA) of fine root traits, EcM exploration types, bacterial and fungal diversity, and soil nutrients measured in 2019 at 0–10 cm (a) and 10–20 cm (b) soil depths. Principal component scores of samples in both treatments are represented by symbols (red and blue cycles), and arrows represent loadings of variables. Positively correlated variables are grouped together, while negatively correlated variables are positioned on opposite sides of the plot origin. The distance between variables and the plot origin measures their importance on the respective principal component. Grey arrows represent EcM exploration types (short distance and long distance); blue arrows represent root-associated microbial diversity (Fischer diversity of bacteria and EcM fungi); red arrows represent fine root traits measured (aFRB, absorptive fine root biomass; D, fine root diameter; FRB, fine root biomass; RTD, root tissue density; RTID, root tip density; SRL, specific root length) and black arrows are soil properties (Soil P, total soil phosphorus; soil N, total soil N; soil K, soil K+). Due to their strong correlation with SRL, SRA, and RAI were removed from the plots. At 0–10 cm, bacterial diversity was not important for both PCs, and therefore removed for graph visualization. 95% Ellipses are shown.

## 4 | Discussion

We explored how long-term soil warming impacts the fine root system and associated ectomycorrhizal fungi and root-associated bacterial communities in a temperate mountain forest. We found that FRB, aFRB and fine root production were consistently higher in warmed plots, indicating greater root litter input. Soil warming also changed the morphology of fine roots, including higher RAI, SRL, SRA and RTID, which increased the absorptive surface of the tree root systems for nutrient and water uptake. The community composition of ectomycorrhizal fungi was also affected by soil warming. Overall, our results suggest that the fine root system responded to warmer soil temperatures, although soil warming did not affect N availability. The low availabilities of P and K in the soil and low contents in roots and needles indicate a strong limitation of these nutrients in this temperate forest. Decreases in soil P and K availability have likely contributed to the changes of the root system in the warmed plots.

### 4 | 1 Effects of soil warming on fine root biomass

In agreement with our first hypothesis, our results showed that soil warming increased FRB, and this increase was significant after 14 years of soil warming. Absorptive fine root biomass

also increased with warming by 22%. Since there are no indications that soil warming changed soil N availability (Heinzle et al., 2021), we postulate that the increase in FRB and aFRB with soil warming in our study could be linked to the low P and K availability in the warmed plots, as explained by the optimal partitioning theory (Bloom et al., 1985). We found a tendency of increasing FRB and aFRB in warmed plots with decreasing soil P and K (Figure 6). Mean P concentration in fine roots ( $0.4 \text{ mg g}^{-1}$  in warmed plots) was below the global mean fine root P concentration ( $0.9 \text{ mg g}^{-1}$ ) (Gordon & Jackson, 2000). This P deficiency is further supported by the high N:P ratios of fine roots, indicating an imbalance between N and P in root tissues. Needle P concentration at the field site ( $0.9 \text{ mg g}^{-1}$ ) also indicated P deficiency, being below the critical P concentration of  $1.2 \text{ mg g}^{-1}$  for Norway spruce needles (Ilg et al., 2009). Average fine root K concentration ( $1.3 \text{ mg g}^{-1}$ ) was also below the global mean K concentration ( $2.8 \text{ mg g}^{-1}$ ) in fine roots (Gordon & Jackson, 2000). The few existing studies on nutrient levels in fine roots of Norway spruce ( $0.7 - 1.7 \text{ mg P g}^{-1}$  and  $2.2 - 4.4 \text{ mg K g}^{-1}$ ) (Borken et al., 2007; Brunner et al., 2002; Genenger et al., 2003) illustrate the strong P and K deficiency at the study site.

At Achenkirch, the K concentration in soil solutions was persistently below the detection limit of  $0.25 \text{ mg l}^{-1}$  in all plots during the growing season (unpublished data), suggesting that K availability is strongly limiting, and K nutrition relies on K input by atmospheric deposition and ecosystem recycling. By contrast, Ca and Mg concentrations were very high in fine roots and soil solutions, resulting from the weathering of the underlying dolomite bedrock. Phosphorus is mainly supplied through weathering, desorption, and organic matter mineralization and is immobilized by sorption, precipitation, and microbial uptake processes (Bünemann, 2015). Phosphorus limitation causes strong plant-microbe competition for labile P resources, and the low P availability suggests that P might be a key player in driving the increase in FRB and fine root biomass production, especially at 0 – 10 cm soil depth. Recent findings at our site showed that long-term soil warming decreased total P in both organic and inorganic forms (Ye Tian et al., unpublished data). One would expect that soil warming increases the availability of P and K due to the increasing mineralization of litter and soil organic matter. However, those nutrients might become depleted in the long run due to high turnover rates, increased leaching losses, or intense competition for uptake between trees and microbes (Dawes et al., 2017). The availability of these elements was low in the warmed plots, and the plant-microbe competition for these limiting nutrients therefore was likely strong. Increasing the FRB and the absorptive surface (see below) strengthens the competitiveness for nutrient uptake against other plants and non-root-associated soil microorganisms. Therefore,

increased FRB and fine root production might be a key plant strategy to efficiently take up P and K, which seems to have become more limiting for trees in warmed plots.

Our result has been confirmed globally in a meta-analysis, demonstrating that soil warming increases fine root biomass production and FRB by 30 and 9%, respectively (J. Wang et al., 2021). However, they attributed the increase in FRB to the stimulation of growth due to high photosynthetic rates and an increase in soil N mineralization. The response might, however, also be due to decreased soil moisture in the warmed plots, which is a common phenomenon in soil warming experiments (W. Xu et al., 2013), but which has not consistently been shown at the Achenkirch site, as the high site-level precipitation frequently resets any decrease in soil moisture in warmed plots, back to the levels in control soils. Therefore, while soil moisture certainly is a driver of tree fine root biomass and production, at the Achenkirch site, increased plant demands for soil P and K seems to be the major trigger of the fine root responses as observed in the warmed plots.

#### **4 | 2 Effects of soil warming on fine root morphology**

In agreement with our second hypothesis, we found significant increases in SRL, SRA, and RTID in warmed plots at both sampling occasions. This suggests a tree strategy to form long roots with a large surface area and short lifespan (Weemstra et al., 2020), which improve nutrient and water uptake as well as soil exploration in warmed plots. This aligns with an acquisitive resource plant strategy (McCormack & Iversen, 2019; Weemstra et al., 2017). There was also a tendency towards a decrease in RTD in warmed plots, indicating lower costs for production of fine roots, which then, however, are less stress-resistant, but have faster metabolic and growth rates (Birouste et al., 2014). SRL and RTID tended to be negatively correlated with soil nutrients at both soil depths. RTD and soil K were positively correlated, indicating a resource conservation strategy for soil K (Figure 6). As mentioned earlier, the low availability of soil P and K may have contributed to the above changes observed in fine root morphology. With decreasing nutrient availability, long thin roots with a high surface area might be preferred to acquire soil resources more efficiently. By enlarging the absorptive surface by 29%, fine roots improved their ability to compete with other soil organisms for limited soil nutrients. Increases in SRL and the number of root tips were also shown in warmed plots by Leppälammii-Kujansuu et al. (2013) on first and second-order roots, while Parts et al. (2019) found significant increases in SRL and SRA due to warming in fine roots < 2mm in

diameter. However, our estimates of RAI are smaller than the global estimate of  $9.8 \text{ m}^2 \text{ m}^{-2}$  for temperate deciduous forests, as reported by Jackson et al. (1997). Björk et al. (2007) reported an increase in SRL and SRA, but no effect on RTD of fine roots  $< 0.5 \text{ mm}$  in a soil warming experiment in a boreal forest in Northern Sweden. These changes in fine root morphology were also linked to increasing plant nutrient uptake efficiency. However, changes in fine root morphological traits observed in this study differ from the meta-analysis of J. Wang et al. (2021), who found no response to warming. They explained this nonresponse by the limited number of studies and the high variability of morphological traits.

At 0 – 10 cm soil depth, the mean diameter of fine roots increased in warmed plots in 2019, while no change was observed in 2012. This contradicts the assumption that SRL and fine root diameter are negatively correlated (Bergmann et al., 2020). However, the proportion of root length in the 0 – 0.2 mm diameter class tended to increase (+38% in both soil depths) in the warmed plots (Figure S1), supporting the optimization theory. Low diameter fine roots represent the most active part of the root system, which is highly relevant for plant nutrient and water uptake from soils. It is also this absorptive root size fraction that shows little secondary development, high metabolic activity, and high mycorrhizal colonization, which make them most responsive to changes in soil environmental conditions (McCormack et al., 2015). On the other hand, fine roots in the higher diameter classes were less affected, likely due to their high content of non-structural carbohydrates, making them more resistant to warming (Eissenstat et al., 2000b; McCormack et al., 2015). These changes in fine root morphology imply that warming may profoundly alter tree nutrient and water uptake.

#### **4 | 3 Effects of soil warming on root-associated fungal and bacterial communities**

Contrary to our third hypothesis, soil warming did not affect the relative abundance of EcM exploration types. With the observed changes in FRB and their morphology, one could expect a shift in the differentiation of extraradical hyphae, as fine roots are the primary source of C for EcM fungi (Koide et al., 2014). EcM fungi are usually patchily distributed in soils due to the heterogeneity in the distribution of soil nutrients (Luis et al., 2005). This micro-heterogeneity and patchiness might make it hard to detect significant responses of the EcM community at the species level. Fungal traits might contribute more clearly to shifts in ecosystem processes in the context of soil warming. For example, at 0 – 10 cm soil depth, we observed a 15% increase in the relative abundance of the EcM genus *Cenococcum* in warmed

plots (Figure 3). This wide host and habitat range (Trappe, 1962) short-distance exploration type fungus associates well with all tree species present at our study site. Its high melanin content makes it more drought stress-tolerant (Koide et al., 2014; LoBuglio, 1999) and might reduce eventual drought stress for the host tree species. *Cenococcum* mainly acquires  $\text{NH}_4^+$  as an N-source but also has well-developed proteolytic abilities (LoBuglio, 1999). However, at 10 – 20 cm soil depth, *Sebacina-28* and *Boletus-2* were most abundant in warmed plots (Figure 4). An increase in the relative abundance of *Sebacina* in warmed plots, a hydrophilic EcM genus with a short-distance exploration type, which requires low plant energy investment, might be beneficial for the host to satisfy its increased demand for water and nutrient uptake at low C investment. This fits well to changes in the fine root morphology as discussed above (increases in SRL, SRA, RAI, and RTID), because alterations in host-plant nutrition might induce a direct shift in host-tree C allocation to EcM fungi (Lilleskov & Bruns, 2001; Treseder, 2004). The increase in the relative abundance of the genus *Boletus*, a long-distance exploration EcM species, appears conflicting, but its very long and highly differentiated hydrophobic mantles and rhizomorphs, which avoid hyphal water and nutrient leakage when transported over long distances (Agerer, 2006), may indicate increasing plant demand for nutrients such as P and K. The increase in the relative abundance of long-distance EcM, like *Boletus* at 10 – 20 cm soil depth in warmed plots, was also observed in other soil warming studies (Defrenne et al., 2021), although it was mainly related to increasing water uptake from deeper soil layers.

Similar to others studies (Fernandez et al., 2017; Mucha et al., 2018; Parts et al., 2019), soil warming did not affect EcM fungal diversity. Fernandez et al. (2017) attributed the lack of a significant effect of experimental warming on fungal diversity to the high density of boreal and temperate host species in their experimental site, while Mucha et al. (2018) highlighted the dominance of generalist EcM species in their study. However, an increase in EcM fungal diversity with warming was reported in the arctic (Deslippe et al., 2011) and a boreal forest (Allison & Treseder, 2008). In our study, EcM communities were dominated by host-generalist taxa, which are known to be less sensitive to changes in environmental conditions (Mucha et al., 2018). The dominance of these host-generalist taxa might be the reason why we did not find an effect of soil warming on EcM fungal diversity. In addition, relatively high atmospheric N deposition at the site, about  $12 \text{ kg ha}^{-1} \text{ yr}^{-1}$  (Herman et al., 2002), may have potentially shifted the competitive capabilities of the EcM fungi or decreased the tree dependence on mycorrhizal N acquisition (Clemmensen et al., 2006; Lilleskov & Bruns, 2001; Treseder, 2004).

Root-associated bacterial community diversity (Pielou's evenness and Shannon-Wiener index) increased with soil warming. Greater bacterial diversity is beneficial for the ecosystem as a whole, because it promotes metabolic activities and efficient nutrient mineralization (Nautiyal & Dion, 2008). A more diverse and evenly distributed bacterial community might have greater resilience and functional stability in relation to warming (Cleland, 2011). This indicates that, in this forest ecosystem, root-associated bacterial communities may have maintained their ability to perform ecosystem multifunctionality with soil warming and fits well with the observed sustained increase in soil respiration in warmed plots since the beginning of the experimental warming manipulation at the site (Schindlbacher et al., 2011; Schindlbacher et al., 2015). Soil depth, related to a strong change in physico-chemical properties, which greatly influences soil microorganisms, affected bacterial community composition in our study. A wide range of edaphic factors such as soil nutrients, the quality and quantity of litter inputs, and root-derived C could affect the composition of soil and root-associated bacterial communities (Baldrian, 2017). Because those factors change with soil depth, a corresponding shift in the root-associated bacterial community is expected. In our study, one of the most evident changes through the soil profile was the decrease in FRB with soil depth, which may affect root exudation, a crucial C source for root-associated bacteria.

It has to be noted that the experimental warming setup had some limitations. Only a limited area of soil was warmed, whereas the above-ground parts of the tree vegetation remained unaffected and experienced ambient temperatures. Thus, we cannot exclude varying fine root responses if the whole rooting area of individual trees or the whole forest would have warmed. For instance, if soil warming increases nutrient availability, one can anticipate root (in)growth from the surrounding soil into the warmed plots. This would result in an overestimation of the warming effect on FRB growth as well as stocks. Under the preconditions in our study, such an artefact can rather be excluded since it is unlikely that trees invest into root ingrowth in warmed plots and progressively nutrient-depleted soils at the expense of ingrowth in unwarmed soil with higher nutrient availability. A general limitation of soil warming studies is that we could not predict how climate warming and the associated above-ground physiological responses will affect below-ground C allocation, fine roots and EcM dynamics. Despite these constraints, we provide important insights into long-term warming effects on tree fine root dynamics and the connected soil C and nutrient dynamics.

In conclusion, our findings suggest that soil warming profoundly changed FRB, fine root production, root morphology, and the community composition of EcM fungi, which may have

strong implications on fine root functions in temperate forests. The response of fine root systems to soil warming is linked to the availability and acquisition of soil nutrients which can differ among forests. The limited soil P and K availability align well with the observed responses in fine root biomass and morphology, though other more general physiological responses to warming, like faster growth, may have contributed to the observed changes. Compared to the strong warming response of fine roots, the effects on root-associated microbial communities seems limited, at least for the parameters measured in this study. This is surprising because the root system is seen as a continuum of roots, symbiotic fungi and bacteria (Freschet et al., 2021; Ostonen et al., 2017). More plots and seasonal replicates seem necessary to increase the statistical power of microbial community analyses and to assess their potential effects on the fine root systems. The long-term warming response of tree fine roots may have strong implications on ecosystem C dynamics. Assuming steady-state conditions between production and mortality, fine root C input to soil is around  $106 \text{ g C m}^{-2} \text{ yr}^{-1}$  in warmed plots versus  $48 \text{ g C m}^{-2} \text{ yr}^{-1}$  based on fine root production in ingrowth cores and fine root C concentration (Table 2). Because of the disturbances associated with ingrowth cores, the estimated C input only represents an approximation to the surrounding soil. Other long-term soil warming studies showed that the stimulatory effect of temperature on soil CO<sub>2</sub> efflux decreased over time (Melillo et al., 2011; Melillo et al., 2017). However, this was not yet the case at the Achenkirch site (Schindlbacher et al., 2009), indicating that the increase in FRB and fine root production increased the root system C input into the warmed soils by root exudation and fine root turnover. How mechanistically the continued increase in soil CO<sub>2</sub> efflux is linked to FRB, turnover, production, exudation, and morphological changes is currently under investigation, using field root exudation experiment and fine root radiocarbon dating methods. The consistent patterns of root responses during more than a decade of intensive soil warming indicate that changes in the fine root system are not of transient nature but likely persistently affect tree and soil C dynamics.

## **Acknowledgments**

This research was funded by the German Research Foundation (DFG, BO 1741/13-1) and the Austrian Science Fund (FWF) through the DA-Ch project I 3745. We gratefully thank Alena Hubach for fine root processing in 2012 and Renate Krauss, Uwe Hell and Karin Söllner for

technical assistance. We thank Gerhard Rambold for giving access to the mycology laboratories at the University of Bayreuth; the student helpers Humay Rahimova, Isabell Zeißig, and Grethe-Johanna Ploompou for assistance with fine root processing; and Gerasimos Makis Gkoutselis, Theresa Janssen for their help with DNA extractions. Open Access funding enabled and organized by Projekt DEAL.

### **Conflict of interest**

The authors have no conflict of interest to declare.

### **Data availability statement**

The data that support the findings of this study are openly available in Dryad at <https://doi.org/10.5061/dryad.jwstqjqbj>.

## References

- Agerer, R. (2001). Exploration types of ectomycorrhizae. A proposal to classify ectomycorrhizal mycelial systems according to their patterns of differentiation and putative ecological importance. *Mycorrhiza*, *11*, 107–114. <https://doi.org/10.1007/s005720100108>
- Agerer, R. (2006). Fungal relationships and structural identity of their ectomycorrhizae. *Mycological Progress*, *5*(2), 67–107. <https://doi.org/10.1007/s11557-006-0505-x>
- Allison, S. D., & Treseder, K. K. (2008). Warming and drying suppress microbial activity and carbon cycling in boreal forest soils. *Global Change Biology*, *14*(12), 2898–2909. <https://doi.org/10.1111/j.1365-2486.2008.01716.x>
- Auguie, B. (2017). *gridExtra: miscellaneous Functions for "Grid" Graphics*. <https://CRAN.R-project.org/package=gridExtra>
- Averill, C., & Hawkes, C. V. (2016). Ectomycorrhizal fungi slow soil carbon cycling. *Ecology Letters*, *19*(8), 937–947. <https://doi.org/10.1111/ele.12631>
- Averill, C., Turner, B. L., & Finzi, A. C. (2014). Mycorrhiza-mediated competition between plants and decomposers drives soil carbon storage. *Nature*, *505*(7484), 543–545. <https://doi.org/10.1038/nature12901>
- Bai, E., Li, S., Xu, W., Li, W., Dai, W., & Jiang, P. (2013). A meta-analysis of experimental warming effects on terrestrial nitrogen pools and dynamics. *New Phytologist*, *199*(2), 441–451. <https://doi.org/10.1111/nph.12252>
- Baldrian, P. (2017). Microbial activity and the dynamics of ecosystem processes in forest soils. *Current Opinion in Microbiology*, *37*, 128–134. <https://doi.org/10.1016/j.mib.2017.06.008>
- Bates, D., Mächler, M., Bolker, B., & Walker, S. (2015). Fitting linear mixed-effects models using lme4. *Journal of Statistical Software*, *67*(1), 1–48. <https://doi.org/10.18637/jss.v067.i01>
- Bennett, A. E., & Classen, A. T. (2020). Climate change influences mycorrhizal fungal-plant interactions, but conclusions are limited by geographical study bias. *Ecology*, *101*(4), e02978. <https://doi.org/10.1002/ecy.2978>
- Bergmann, J., Weigelt, A., van der Plas, F., Laughlin, D. C., Kuyper, T. W., Guerrero-Ramirez, N., Valverde-Barrantes, O. J., Bruelheide, H., Freschet, G. T., Iversen, C. M., Kattge, J., McCormack, M. L., Meier, I. C., Rillig, M. C., Roumet, C., Semchenko, M., Sweeney, C. J., van Ruijven, J., York, L. M., & Mommer, L. (2020). The fungal collaboration gradient dominates the root economics space in plants. *Science Advances*, *6*(27), eaba3756. <https://doi.org/10.1101/2020.01.17.908905>
- Birouste, M., Zamora-Ledezma, E., Bossard, C., Pérez-Ramos, I. M., & Roumet, C. (2014). Measurement of fine root tissue density: a comparison of three methods reveals the potential of root dry matter content. *Plant and Soil*, *374*(1-2), 299–313
- Björk, R. G., Majdi, H., Klemetsson, L., Lewis-Jonsson, L., & Molau, U. (2007). Long-term warming effects on root morphology, root mass distribution, and microbial activity in two dry tundra plant communities in northern Sweden. *New Phytologist*, *176*(4), 862–873. <https://doi.org/10.1111/j.1469-8137.2007.02231.x>

- Bloom, A. J., Chapin, F. S., & Mooney, H. A. (1985). Resource limitation in plants - An economic analogy. *Annual Review of Ecology and Systematics*, 16(1), 363–392. <https://doi.org/10.1146/annurev.es.16.110185.002051>
- Borken, W., Kossmann, G., & Matzner, E. (2007). Biomass, morphology and nutrient contents of fine roots in four Norway spruce stands. *Plant and Soil*, 292(1-2), 79–93. <https://doi.org/10.1007/s11104-007-9204-x>
- Borken, W., & Matzner, E. (2004). Nitrate leaching in forest soils: an analysis of long-term monitoring sites in Germany. *Journal of Plant Nutrition and Soil Science*, 167(3), 277–283. <https://doi.org/10.1002/jpln.200421354>
- Brunner, I., Brodbeck, S., & Walthert, L. (2002). Fine root chemistry, starch concentration, and ‘vitality’ of subalpine conifer forests in relation to soil pH. *Forest Ecology and Management*, 165(1-3), 75–84. [https://doi.org/10.1016/S0378-1127\(01\)00633-8](https://doi.org/10.1016/S0378-1127(01)00633-8)
- Bünemann, E. K. (2015). Assessment of gross and net mineralization rates of soil organic phosphorus – a review. *Soil Biology and Biochemistry*, 89, 82–98. <https://doi.org/10.1016/j.soilbio.2015.06.026>
- Burke, M. K., & Raynal, D. J. (1994). Fine root growth phenology, production, and turnover in a northern hardwood forest ecosystem. *Plant and Soil*, 162(1), 135–146. <https://doi.org/10.1007/BF01416099>
- Cannon, P. F., & Kirk, P. M. (2007). *Fungal families of the world*. Wallingford, Oxfordshire, UK: CAB International. Pp xiii, 456. ISBN 978 0 85199 827 5
- Caporaso, J. G., Kuczynski, J., Stombaugh, J., Bittinger, K., Bushman, F. D., Costello, E. K., Fierer, N., Peña, A. G., Goodrich, J. K., Gordon, J. I., Huttley, G. A., Kelley, S. T., Knights, D., Koenig, J. E., Ley, R. E., Lozupone, C. A., McDonald, D., Muegge, B. D., Pirrung, M., . . . Knight, R. (2010). Qiime allows analysis of high-throughput community sequencing data. *Nature Methods*, 7(5), 335–336. <https://doi.org/10.1038/nmeth.f.303>
- Chazdon, R. L., Chao, A., Colwell, R. K., Lin, S.-Y., Norden, N., Letcher, S. G., Clark, D. B., Finegan, B., & Arroyo, J. P. (2011). A novel statistical method for classifying habitat generalists and specialists. *Ecology*, 92(6), 1332–1343. <https://doi.org/10.1890/10-1345.1>
- Clarke, K. R., Gorley, R. N., Somerfield, P. J., & Warwick, R. M. (2014). *Change in marine communities: an approach to statistical analysis and interpretation* (3rd edition). PRIMER-E: Plymouth.
- Cleland, E. E. (2011). Biodiversity and ecosystem stability. *Nature Education Knowledge*, 3(10).
- Clemmensen, K. E., Michelsen, A., Jonasson, S., & Shaver, G. R. (2006). Increased ectomycorrhizal fungal abundance after long-term fertilization and warming of two arctic tundra ecosystems. *New Phytologist*, 171(2), 391–404. <https://doi.org/10.1111/j.1469-8137.2006.01778.x>
- Dawes, M. A., Philipson, C. D., Fonti, P., Bebi, P., Hättenschwiler, S., Hagedorn, F., & Rixen, C. (2015). Soil warming and CO<sub>2</sub> enrichment induce biomass shifts in alpine tree line vegetation. *Global Change Biology*, 21(5), 2005–2021. <https://doi.org/10.1111/gcb.12819>

- Dawes, M. A., Schleppei, P., Hättenschwiler, S., Rixen, C., & Hagedorn, F. (2017). Soil warming opens the nitrogen cycle at the alpine treeline. *Global Change Biology*, *23*(1), 421–434. <https://doi.org/10.1111/gcb.13365>
- Defrenne, C. E., Childs, J., Fernandez, C. W., Taggart, M., Nettles, W. R., Allen, M. F., Hanson, P. J., & Iversen, C. M. (2021). High-resolution minirhizotrons advance our understanding of root-fungal dynamics in an experimentally warmed peatland. *Plants, People, Planet*, *3*(5), 640–652. <https://doi.org/10.1002/ppp3.10172>
- Defrenne, C. E., Philpott, T. J., Guichon, S. H. A., Roach, W. J., Pickles, B. J., & Simard, S. W. (2019). Shifts in Ectomycorrhizal Fungal Communities and Exploration Types Relate to the Environment and Fine-Root Traits Across Interior Douglas-Fir Forests of Western Canada. *Frontiers in Plant Science*, *10*, 643. <https://doi.org/10.3389/fpls.2019.00643>
- Deslippe, J. R., Hartmann, M., Mohn, W. W., & Simard, S. W. (2011). Long-term experimental manipulation of climate alters the ectomycorrhizal community of *Betula nana* in arctic tundra. *Global Change Biology*, *17*(4), 1625–1636.
- Eissenstat, D. M., Wells, C. E., Yanai, R. D., & Whitbeck, J. L. (2000). Building roots in a changing environment: implications for root longevity. *New Phytologist*, *147*(1), 33–42.
- Fernandez, C. W., Nguyen, N. H., Stefanski, A., Han, Y., Hobbie, S. E., Montgomery, R. A., Reich, P. B., & Kennedy, P. G. (2017). Ectomycorrhizal fungal response to warming is linked to poor host performance at the boreal-temperate ecotone. *Global Change Biology*, *23*(4), 1598–1609. <https://doi.org/10.1111/gcb.13510>
- Freschet, G. T., Pagès, L., Iversen, Colleen, M., Comas, L. H., Rewald, B., Roumet, C., Klimešová, J., Zadworny, M., Poorter, H., Postma, J. A., Adams, T. S., Bagniewska-Zadworna, A., Bengough, A. G., Blancaflor, E. B., Brunner, I., Cornelissen, J. H. C., Garnier, E., Gessler, A., Hobbie, S. E., . . . McCormack, M. L. (2021). A starting guide to root ecology: Strengthening ecological concepts and standardising root classification, sampling, processing and trait measurements. *The New Phytologist*, *232*(3), 973–1122. <https://doi.org/10.1111/nph.17572>
- Genenger, M., Zimmermann, S., Hallenbarter, D., Landolt, W., Frossard, E., & Brunner, I. (2003). Fine root growth and element concentrations of Norway spruce as affected by wood ash and liquid fertilisation. *Plant and Soil*, *255*(1), 253–264. <https://doi.org/10.1023/A:1026118101339>
- Gobiet, A., Kotlarski, S., Beniston, M., Heinrich, G., Rajczak, J., & Stoffel, M. (2014). 21st century climate change in the European Alps--a review. *The Science of the Total Environment*, *493*, 1138–1151. <https://doi.org/10.1016/j.scitotenv.2013.07.050>
- Gordon, W. S., & Jackson, R. B. (2000). Nutrient Concentrations in Fine Roots. *Ecology*, *81*(1), 275. <https://doi.org/10.2307/177151>
- Heinzle, J., Wanek, W., Tian, Y., Kengdo, S. K., Borken, W., Schindlbacher, A., & Inselsbacher, E. (2021). No effect of long-term soil warming on diffusive soil inorganic and organic nitrogen fluxes in a temperate forest soil. *Soil Biology and Biochemistry*, *158*, 108261. <https://doi.org/10.1016/j.soilbio.2021.108261>

- Herman, F., Smidt, S., Englisch, M., Feichtinger, F., Gerzabek, M., Haberhauer, G., Jandl, R., Kalina, M., & Zechmeister-Boltenstern, S. (2002). Investigations of nitrogen fluxes and pools on a limestone site in the alps. *Environmental Science and Pollution Research International*, 9(S2), 46–52. <https://doi.org/10.1007/BF02987478>
- Hobbie, E. A., & Agerer, R. (2010). Nitrogen isotopes in ectomycorrhizal sporocarps correspond to below-ground exploration types. *Plant and Soil*, 327(1-2), 71–83. <https://doi.org/10.1007/s11104-009-0032-z>
- Ihrmark, K., Bödeker, I. T. M., Cruz-Martinez, K., Friberg, H., Kubartova, A., Schenck, J., Strid, Y., Stenlid, J., Brandström-Durling, M., Clemmensen, K. E., & Lindahl, B. D. (2012). New primers to amplify the fungal ITS2 region-evaluation by 454-sequencing of artificial and natural communities. *FEMS Microbiology Ecology*, 82(3), 666–677. <https://doi.org/10.1111/j.1574-6941.2012.01437.x>
- Ilg, K., Wellbrock, N., & Lux, W. (2009). Phosphorus supply and cycling at long-term forest monitoring sites in Germany. *European Journal of Forest Research*, 128(5), 483–492. <https://doi.org/10.1007/s10342-009-0297-z>
- Illumina (2013). 16S Metagenomic sequencing library preparation preparing 16S ribosomal RNA gene amplicons for the Illumina MiSeq system. Illumina, San Diego, CA. [https://support.illumina.com/documents/documentation/chemistry\\_documentation/16s/16s-metagenomic-library-prep-guide-15044223-b.pdf](https://support.illumina.com/documents/documentation/chemistry_documentation/16s/16s-metagenomic-library-prep-guide-15044223-b.pdf)
- IPCC, 2021: Climate Change 2021: The Physical Science Basis. Contribution of Working Group I to the Sixth Assessment Report of the Intergovernmental Panel on Climate Change [Masson-Delmotte, V., P. Zhai, A. Pirani, S. L. Connors, C. Péan, S. Berger, N. Caud, Y. Chen, L. Goldfarb, M. I. Gomis, M. Huang, K. Leitzell, E. Lonnoy, J. B. R. Matthews, T. K. Maycock, T. Waterfield, O. Yelekçi, R. Yu and B. Zhou (eds.)]. Cambridge University Press. In Press.
- Jackson, R. B., Mooney, H. A., & Schulze, E. D. (1997). A global budget for fine root biomass, surface area, and nutrient contents. *Proceedings of the National Academy of Sciences of the United States of America*, 94(14), 7362–7366. <https://doi.org/10.1073/pnas.94.14.7362>
- Jayasiri, S. C., Hyde, K. D., Ariyawansa, H. A., Bhat, J., Buyck, B., Cai, L., Dai, Y.-C., Abd-Elsalam, K. A., Ertz, D., Hidayat, I., Jeewon, R., Jones, E. B. G., Bahkali, A. H., Karunarathna, S. C., Liu, J.-K., Luangsa-ard, J. J., Lumbsch, H. T., Maharachchikumbura, S. S. N., McKenzie, E. H. C., . . . Promputtha, I. (2015). The Faces of Fungi database: fungal names linked with morphology, phylogeny and human impacts. *Fungal Diversity*, 74(1), 3–18. <https://doi.org/10.1007/s13225-015-0351-8>
- Jonard, M., Fürst, A., Verstraeten, A., Thimonier, A., Timmermann, V., Potočić, N., Waldner, P., Benham, S., Hansen, K., Merilä, P., Ponette, Q., La Cruz, A. C. de, Roskams, P., Nicolas, M., Croisé, L., Ingerslev, M., Matteucci, G., Decinti, B., Bascietto, M., & Rautio, P. (2015). Tree mineral nutrition is deteriorating in Europe. *Global Change Biology*, 21(1), 418–430. <https://doi.org/10.1111/gcb.12657>
- Kassambara, A. (2017). *Practical guide to principal component methods in R* (Edition 1). CreateSpace Independent Publishing Platform.

- Keller, A. B., Brzostek, E. R., Craig, M. E., Fisher, J. B., & Phillips, R. P. (2021). Root-derived inputs are major contributors to soil carbon in temperate forests, but vary by mycorrhizal type. *Ecology Letters*, 24(4), 626–635. <https://doi.org/10.1111/ele.13651>
- Kirk, P. M., Cannon, P. F., Minter, D. W., Stalpers, J. A., Ainsworth, G. C., & Bisby, G. R. (2011). *Ainsworth & Bisby's dictionary of the fungi: by P.M. Kirk... [et al.]* (10th ed. / with the assistance of T.V. Andrianova ... [et al.]). Pp xi, 771 Pages. CABI.
- Koide, R. T., Fernandez, C., & Malcolm, G. (2014). Determining place and process: functional traits of ectomycorrhizal fungi that affect both community structure and ecosystem function. *New Phytologist*, 201(2), 433–439. <https://doi.org/10.1111/nph.12538>
- Kõljalg, U., Nilsson, R. H., Abarenkov, K., Tedersoo, L., Taylor, A. F. S., Bahram, M., Bates, S. T., Bruns, T. D., Bengtsson-Palme, J., Callaghan, T. M., Douglas, B., Drenkhan, T., Eberhardt, U., Dueñas, M., Grebenc, T., Griffith, G. W., Hartmann, M., Kirk, P. M., Kohout, P., ... Larsson, K.-H. (2013). Towards a unified paradigm for sequence-based identification of fungi. *Molecular Ecology*, 22(21), 5271–5277. <https://doi.org/10.1111/mec.12481>
- Kuffner, M., Hai, B., Rattei, T., Melodelima, C., Schloter, M., Zechmeister-Boltenstern, S., Jandl, R., Schindlbacher, A., & Sessitsch, A. (2012). Effects of season and experimental warming on the bacterial community in a temperate mountain forest soil assessed by 16S rRNA gene pyrosequencing. *FEMS Microbiology Ecology*, 82(3), 551–562. <https://doi.org/10.1111/j.1574-6941.2012.01420.x>
- Lê, S., Josse, J., & Husson, F. (2008). FactoMineR: An R Package for Multivariate Analysis. *Journal of Statistical Software*, 25(1). <https://doi.org/10.18637/jss.v025.i01>
- Leake, J. R. (2001). Is diversity of ectomycorrhizal fungi important for ecosystem function? *New Phytologist*, 152(1), 1–3. <https://doi.org/10.1046/j.0028-646X.2001.00249.x>
- Lenth, R. V. (2021). *emmeans: Estimated Marginal Means, aka Least-Squares Means*. <https://CRAN.R-project.org/package=emmeans>
- Leppälammil-Kujansuu, J., Ostonen, I., Strömberg, M., Nilsson, L. O., Kleja, D. B., Sah, S. P., & Helmisaari, H.-S. (2013). Effects of long-term temperature and nutrient manipulation on Norway spruce fine roots and mycelia production. *Plant and Soil*, 366(1-2), 287–303. <https://doi.org/10.1007/s11104-012-1431-0>
- Li, W., & Chang, Y. (2017). *CD-HIT-OTU-MiSeq, an Improved Approach for Clustering and Analyzing Paired End MiSeq 16S rRNA Sequences*. <https://doi.org/10.1101/153783>
- Lilleskov, E. A., & Bruns, T. D. (2001). Nitrogen and ectomycorrhizal fungal communities: what we know, what we need to know. *New Phytologist*, 149(2), 156–158. <https://doi.org/10.1046/j.1469-8137.2001.00042-2.x>
- Lindahl, B. D., & Tunlid, A. (2015). Ectomycorrhizal fungi - potential organic matter decomposers, yet not saprotrophs. *New Phytologist*, 205(4), 1443–1447. <https://doi.org/10.1111/nph.13201>
- LoBuglio, K. F. (1999). *Cenococcum*. In J. W. G. Cairney & S. M. Chambers (Eds.), *Ectomycorrhizal fungi key genera in profile* (pp. 287–309). Springer Berlin Heidelberg. [https://doi.org/10.1007/978-3-662-06827-4\\_12](https://doi.org/10.1007/978-3-662-06827-4_12)

- Lõhmus, K., Truu, J., Truu, M., Kaar, E., Ostonen, I., Alama, S., Kuznetsova, T., Rosenvald, K., Vares, A., Uri, V., & Mander, Ü. (2006). Black alder as a promising deciduous species for the reclaiming of oil shale mining areas. In C. A. Brebbia & Ü. Mander (Eds.), *WIT transactions on ecology and the environment, Brownfield sites iii: prevention, assessment, rehabilitation and development of brownfield sites / edited by c.A. Brebbia and U. Mander* (pp. 87–97). WIT. <https://doi.org/10.2495/BF060091>
- Luis, P., Kellner, H., Zimdars, B., Langer, U., Martin, F., & Buscot, F. (2005). Patchiness and spatial distribution of laccase genes of ectomycorrhizal, saprotrophic, and unknown basidiomycetes in the upper horizons of a mixed forest Cambisol. *Microbial Ecology*, *50*(4), 570–579. <https://doi.org/10.1007/s00248-005-5047-2>
- Malhotra, A., Brice, D. J., Childs, J., Graham, J. D., Hobbie, E. A., Vander Stel, H., Feron, S. C., Hanson, P. J., & Iversen, C. M. (2020). Peatland warming strongly increases fine-root growth. *Proceedings of the National Academy of Sciences of the United States of America*, *117*(30), 17627–17634. <https://doi.org/10.1073/pnas.2003361117>
- McCormack, M. L., Dickie, I. A., Eissenstat, D. M., Fahey, T. J., Fernandez, C. W., Guo, D., Helmisaari, H.-S., Hobbie, E. A., Iversen, C. M., Jackson, R. B., Leppälammil-Kujansuu, J., Norby, R. J., Phillips, R. P., Pregitzer, K. S., Pritchard, S. G., Rewald, B., & Zadworny, M. (2015). Redefining fine roots improves understanding of below-ground contributions to terrestrial biosphere processes. *The New Phytologist*, *207*(3), 505–518. <https://doi.org/10.1111/nph.13363>
- McCormack, M. L., & Iversen, C. M. (2019). Physical and functional constraints on viable below-ground acquisition strategies. *Frontiers in Plant Science*, *10*, 1215. <https://doi.org/10.3389/fpls.2019.01215>
- Melillo, J. M., Butler, S., Johnson, J., Mohan, J., Steudler, P., Lux, H., Burrows, E., Bowles, F., Smith, R., Scott, L., Vario, C., Hill, T., Burton, A., Zhou, Y.-M., & Tang, J. (2011). Soil warming, carbon-nitrogen interactions, and forest carbon budgets. *Proceedings of the National Academy of Sciences of the United States of America*, *108*(23), 9508–9512. <https://doi.org/10.1073/pnas.1018189108>
- Melillo, J. M., Frey, S. D., DeAngelis, K. M., Werner, W. J., Bernard, M. J., Bowles, F. P., Pold, G., Knorr, M. A., & Grandy, A. S. (2017). Long-term pattern and magnitude of soil carbon feedback to the climate system in a warming world. *Science (New York, N.Y.)*, *358*(6359), 101–105. <https://doi.org/10.1126/science.aan2874>
- Millard, S. P. (2013). *EnvStats: An R Package for Environmental Statistics*. Springer. <https://www.springer.com>
- Mucha, J., Peay, K. G., Smith, D. P., Reich, P. B., Stefański, A., & Hobbie, S. E. (2018). Effect of simulated climate warming on the ectomycorrhizal fungal community of boreal and temperate host species growing near their shared ecotonal range limits. *Microbial Ecology*, *75*(2), 348–363. <https://doi.org/10.1007/s00248-017-1044-5>
- Nautiyal, C. S., & Dion, P. (2008). *Molecular mechanisms of plant and microbe coexistence. Soil biology: v. 15*. Springer. <https://doi.org/10.1007/978-3-540-75575-3>
- Nguyen, N. H., Song, Z., Bates, S. T., Branco, S., Tedersoo, L., Menke, J., Schilling, J. S., & Kennedy, P. G. (2016). FUNGuild: An open annotation tool for parsing fungal community

- datasets by ecological guild. *Fungal Ecology*, 20, 241–248. <https://doi.org/10.1016/j.funeco.2015.06.006>
- Oksanen, J., Blanchet, F. G., Friendly, M., Kindt, R., Legendre, P., McGlenn, D., Minchin, P. R., O'Hara, R. B., Simpson, G. L., Solymos, P., Stevens, M. H. H., Szoecs, E., & Wagner, H. (2019). *vegan: Community Ecology Package*. <https://CRAN.R-project.org/package=vegan>
- Ostonen, I., Lõhmus, K., & Lasn, R. (1999). The role of soil conditions in fine root ecomorphology in Norway spruce (*Picea abies* (L.) Karst.). *Plant and Soil*, 208(2), 283–292. <https://doi.org/10.1023/A:1004552907597>
- Ostonen, I., Helmisaari, H.-S., Borken, W., Tedersoo, L., Kukumägi, M., Bahram, M., Lindroos, A.-J., Nöjd, P., Uri, V., Merilä, P., Asi, E., & Lõhmus, K. (2011). Fine root foraging strategies in Norway spruce forests across a European climate gradient. *Global Change Biology*, 17(12), 3620–3632. <https://doi.org/10.1111/j.1365-2486.2011.02501.x>
- Ostonen, I., Truu, M., Helmisaari, H.-S., Lukac, M., Borken, W., Vanguelova, E., Godbold, D. L., Lõhmus, K., Zang, U., Tedersoo, L., Preem, J.-K., Rosenvald, K., Aosaar, J., Armolaitis, K., Frey, J., Kabral, N., Kukumägi, M., Leppälammi-Kujansuu, J., Lindroos, A.-J., . . . Truu, J. (2017). Adaptive root foraging strategies along a boreal-temperate forest gradient. *New Phytologist*, 215(3), 977–991. <https://doi.org/10.1111/nph.14643>
- Parts, K., Tedersoo, L., Schindlbacher, A., Sigurdsson, B. d., Leblans, N. I. W., Oddsdóttir, E. S., Borken, W., & Ostonen, I. (2019). Acclimation of fine root systems to soil warming: comparison of an experimental setup and a natural soil temperature gradient. *Ecosystems*, 22(3), 457–472. <https://doi.org/10.1007/s10021-018-0280-y>
- Penuelas, J., Fernández-Martínez, M., Vallicrosa, H., Maspons, J., Zuccarini, P., Carnicer, J., Sanders, T. G. M., Krüger, I., Obersteiner, M., Janssens, I. A., Ciais, P., & Sardans, J. (2020). Increasing atmospheric CO<sub>2</sub> concentrations correlate with declining nutritional status of European forests. *Communications Biology*, 3(1), 125. <https://doi.org/10.1038/s42003-020-0839-y>
- Peršoh, D., Melcher, M., Flessa, F., & Rambold, G. (2010). First fungal community analyses of endophytic ascomycetes associated with *Viscum album* ssp. *Austriacum* and its host *Pinus sylvestris*. *Fungal Biology*, 114(7), 585–596. <https://doi.org/10.1016/j.funbio.2010.04.009>
- Pregitzer, K. S., King, J. S., Burton, A. J., & Brown, S. E. (2000). Responses of tree fine roots to temperature. *New Phytologist*, 147(1), 105–115. <https://doi.org/10.1046/j.1469-8137.2000.00689.x>
- R Core Team. (2020). *R: A Language and Environment for Statistical Computing*. <https://www.R-project.org/>
- Rasse, D. P., Rumpel, C., & Dignac, M.-F. (2005). Is soil carbon mostly root carbon? Mechanisms for a specific stabilisation. *Plant and Soil*, 269(1-2), 341–356. <https://doi.org/10.1007/s11104-004-0907-y>

- Rose, L. (2017). Pitfalls in Root Trait Calculations: How Ignoring Diameter Heterogeneity Can Lead to Overestimation of Functional Traits. *Frontiers in Plant Science*, 8, 898. <https://doi.org/10.3389/fpls.2017.00898>
- Rustad, L., Campbell, J., Marion, G., Norby, R., Mitchell, M., Hartley, A., Cornelissen, J., & Gurevitch, J. (2001). A meta-analysis of the response of soil respiration, net nitrogen mineralization, and above-ground plant growth to experimental ecosystem warming. *Oecologia*, 126(4), 543–562. <https://doi.org/10.1007/s004420000544>
- Salazar, A., Rousk, K., Jónsdóttir, I. S., Bellenger, J.-P., & Andrésón, Ó. S. (2020). Faster nitrogen cycling and more fungal and root biomass in cold ecosystems under experimental warming: A meta-analysis. *Ecology*, 101(2), e02938. <https://doi.org/10.1002/ecy.2938>
- Schindlbacher, A., Zechmeister-Boltenstern, S., Glatzel, G., & Jandl, R. (2007). Winter soil respiration from an Austrian mountain forest. *Agricultural and Forest Meteorology*, 146(3-4), 205–215. <https://doi.org/10.1016/j.agrformet.2007.06.001>
- Schindlbacher, A., Zechmeister-Boltenstern, S., & Jandl, R. (2009). Carbon losses due to soil warming: do autotrophic and heterotrophic soil respiration respond equally? *Global Change Biology*, 15(4), 901–913. <https://doi.org/10.1111/j.1365-2486.2008.01757.x>
- Schindlbacher, A., Rodler, A., Kuffner, M., Kitzler, B., Sessitsch, A., & Zechmeister-Boltenstern, S. (2011). Experimental warming effects on the microbial community of a temperate mountain forest soil. *Soil Biology & Biochemistry*, 43(7), 1417–1425. <https://doi.org/10.1016/j.soilbio.2011.03.005>
- Schindlbacher, A., Schnecker, J., Takriti, M., Borcken, W., & Wanek, W. (2015). Microbial physiology and soil CO<sub>2</sub> efflux after 9 years of soil warming in a temperate forest - no indications for thermal adaptations. *Global Change Biology*, 21(11), 4265–4277. <https://doi.org/10.1111/gcb.12996>
- Schlegel, M., Queloz, V., & Sieber, T. N. (2018). The endophytic mycobiome of European ash and sycamore maple leaves - geographic patterns, host specificity and influence of ash dieback. *Frontiers in Microbiology*, 9, 2345. <https://doi.org/10.3389/fmicb.2018.02345>
- Smiatek, G., Kunstmann, H., Knoche, R., & Marx, A. (2009). Precipitation and temperature statistics in high-resolution regional climate models: evaluation for the European alps. *Journal of Geophysical Research*, 114(D19). <https://doi.org/10.1029/2008JD011353>
- Smith, S. E., & Read, D. J. (2008). *Mycorrhizal symbiosis* (3. ed.). Elsevier/Acad. Press.
- Solly, E. F., Lindahl, B. D., Dawes, M. A., Peter, M., Souza, R. C., Rixen, C., & Hagedorn, F. (2017). Experimental soil warming shifts the fungal community composition at the alpine treeline. *New Phytologist*, 215(2), 766–778. <https://doi.org/10.1111/nph.14603>
- Staddon, P. L., Heinemeyer, A., & Fitter, A. H. (2002). Mycorrhizas and global environmental change: Research at different scales. *Plant and Soil*, 244(1/2), 253–261. <https://doi.org/10.1023/A:1020285309675>
- Talkner, U., Meiwes, K. J., Potočić, N., Seletković, I., Cools, N., Vos, B. de, & Rautio, P. (2015). Phosphorus nutrition of beech (*Fagus sylvatica* L.) is decreasing in Europe. *Annals of Forest Science*, 72(7), 919–928. <https://doi.org/10.1007/s13595-015-0459-8>

- Talkner, U., Riek, W., Dammann, I., Kohler, M., Göttlein, A., Mellert, K. H., & Meiwes, K. J. (2019). Nutritional Status of Major Forest Tree Species in Germany. In N. Wellbrock & A. Bölte (Eds.), *Ecological studies, 0070-8356: volume 237. Status and dynamics of forests in Germany: Results of the National Forest Monitoring / Nicole Wellbrock, Andreas Bolte, editors* (Vol. 237, pp. 261–293). Springer Open. [https://doi.org/10.1007/978-3-030-15734-0\\_9](https://doi.org/10.1007/978-3-030-15734-0_9)
- Tedersoo, L. (2017). *Biogeography of Mycorrhizal Symbiosis* (Vol. 230). Springer International Publishing. <https://doi.org/10.1007/978-3-319-56363-3>
- Tedersoo, L., Bahram, M., Toots, M., Diédhiou, A. G., Henkel, T. W., Kjølner, R., Morris, M. H., Nara, K., Nouhra, E., Peay, K. G., Pölme, S., Ryberg, M., Smith, M. E., & Kõljalg, U. (2012). Towards global patterns in the diversity and community structure of ectomycorrhizal fungi. *Molecular Ecology*, *21*(17), 4160–4170. <https://doi.org/10.1111/j.1365-294X.2012.05602.x>
- Trappe, J. M. (1962). *Cenococcum graniforme-its distribution, ecology, mycorrhiza formation, and inherent variation*. University of Washington. <https://digital.lib.washington.edu/researchworks/handle/1773/5550>
- Treseder, K. K. (2004). A meta-analysis of mycorrhizal responses to nitrogen, phosphorus, and atmospheric CO<sub>2</sub> in field studies. *New Phytologist*, *164*(2), 347–355. <https://doi.org/10.1111/j.1469-8137.2004.01159.x>
- Treseder, K. K., Marusenko, Y., Romero-Olivares, A. L., & Maltz, M. R. (2016). Experimental warming alters potential function of the fungal community in boreal forest. *Global Change Biology*, *22*(10), 3395–3404. <https://doi.org/10.1111/gcb.13238>
- Wan, S., Norby, R. J., Pregitzer, K. S., Ledford, J., & O'Neill, E. G. (2004). CO<sub>2</sub> enrichment and warming of the atmosphere enhance both productivity and mortality of maple tree fine roots. *New Phytologist*, *162*(2), 437–446. <https://doi.org/10.1111/j.1469-8137.2004.01034.x>
- Wang, J., Defrenne, C., McCormack, M. L., Yang, L., Tian, D., Luo, Y., Hou, E., Yan, T., Li, Z., Bu, W., Chen, Y., & Niu, S. (2021). Fine-root functional trait responses to experimental warming: a global meta-analysis. *New Phytologist*, *230*(5), 1856–1867. <https://doi.org/10.1111/nph.17279>
- Weemstra, M. (2017). *Below-ground uptake strategies: how fine-root traits determine tree growth*. <https://doi.org/10.18174/400247>
- Weemstra, M., Sterck, F. J., Visser, E. J. W., Kuypers, T. W., Goudzwaard, L., & Mommer, L. (2017). Fine-root trait plasticity of beech (*Fagus sylvatica*) and spruce (*Picea abies*) forests on two contrasting soils. *Plant and Soil*, *415*(1-2), 175–188. <https://doi.org/10.1007/s11104-016-3148-y>
- Weemstra, M., Kiorapostolou, N., Ruijven, J., Mommer, L., Vries, J., & Sterck, F. (2020). The role of fine-root mass, specific root length and life span in tree performance: a whole-tree exploration. *Functional Ecology*, *34*(3), 575–585. <https://doi.org/10.1111/1365-2435.13520>
- Wickham, H. (2016). *ggplot2: Elegant Graphics for Data Analysis*. Springer-Verlag New York. <https://ggplot2.tidyverse.org>

- Wu, K. (2000). *Fine root production and turnover and its contribution to nutrient cycling in two beech (Fagus sylvatica.) forest ecosystems* (A170, pp 1–130).
- Xu, W., Yuan, W., Dong, W., Xia, J., Liu, D., & Chen, Y. (2013). A meta-analysis of the response of soil moisture to experimental warming. *Environmental Research Letters*, 8(4), 44027. <https://doi.org/10.1088/1748-9326/8/4/044027>
- Yang, Y., Klein, J. A., Winkler, D. E., Peng, A., Lazarus, B. E., Germino, M. J., Suding, K. N., Smith, J. G., & Kueppers, L. M. (2020). Warming of alpine tundra enhances below-ground production and shifts community towards resource acquisition traits. *Ecosphere*, 11(10). <https://doi.org/10.1002/ecs2.3270>
- Yuan, Z. Y., Shi, X. R., Jiao, F., & Han, F. P. (2018). Changes in fine root biomass of *Picea abies* forests: Predicting the potential impacts of climate change. *Journal of Plant Ecology*, 11(4), 595–603. <https://doi.org/10.1093/jpe/rtx032>
- Zhou, Y., Tang, J., Melillo, J. M., Butler, S., & Mohan, J. E. (2011). Root standing crop and chemistry after six years of soil warming in a temperate forest. *Tree Physiology*, 31(7), 707–717. <https://doi.org/10.1093/treephys/tpr066>

## Supplementary tables and figures

**Table S1:** Results of the linear mixed-effects models showing the effect of treatment and soil depth on bacterial diversity. Abbreviations: SE – standard error; p – p-values. Significance level given as \*\*\* $p < 0.001$ ; \*\* $p < 0.01$ ; \* $p < 0.05$ .

Parameter	Fisher alpha			Pielou's Evenness			Shannon-Wiener		
	Estimates	SE	p	Estimates	SE	p	Estimates	SE	p
<b>Fixed effects</b>									
Intercept	21.085	10.272	0.054*	0.703	0.073	<0.001***	2.974	0.445	<0.001***
Treatment	11.457	5.997	0.071	0.092	0.042	0.044*	0.651	0.260	0.021*
Depth	0.121	0.599	0.842	0.0003	0.0004	0.931	0.003	0.026	0.655
<b>Random effects</b>									
Variance	0.0			0.0			0.0		
Standard deviation	0.0			0.0			0.0		

**Table S2:** Results of the linear mixed-effects models showing the effect of treatment and soil depth on EcM fungal diversity. Abbreviations: SE – standard error; p – p-values. Significance level given as \*\*\* p<0.001; \*\* p<0.01; \* p<0.05.

Parameter	Fisher alpha			Pielou's Evenness			Shannon-Wiener		
	Estimates	SE	p	Estimates	SE	p	Estimates	SE	p
<b>Fixed effects</b>									
Intercept	7.034	1.096	<0.001***	0.720	0.102	<0.001***	2.520	0.386	<0.001***
Treatment	0.109	0.648	0.869	0.031	0.061	0.187	0.170	0.233	0.473
Depth	-0.215	0.065	0.004**	-0.018	0.006	0.008**	-0.075	0.023	0.003**
<b>Random effects</b>									
Variance	0.271			0.00			0.00		
Standard deviation	0.521			0.00			0.00		

**Table S3:** Identifier sequences introduced in PCR1 during library construction. Sequences (5'-3') of the PCR1 forward (FW) and reverse (RV) orientated primers targeting fungi were TCGTCGGCAGCGTCAGATGTGTATAAGAGACAG-TAG-GTGARTCATCGARTCTTTG and GTCTCGTGGGCTCGGAGATGTGTATAAGAGACAG-TAG-CGCTTATTGATATGCTTAAGT, respectively. Bacterial 16S was amplified using the TAGS listed below in the primers TCGTCGGCAGCGTCAGATGTGTATAAGAGACAG-TAG-CCTACGGGNGGCWGCAG and GTCTCGTGGGCTCGGAGATGTGTATAAGAGACAG-TAG-GACTACHVGGGTATCTAATCC, respectively, as recommended by Illumina (2013).

PCR1 TAG (FW) for fungi	PCR1 TAG (RV) for fungi	PCR1 TAG (FW) for bacteria	PCR1 TAG (RV) for bacteria
Ff11: TCGGAGA	Rf44: TGGATAG	Fb11: GAG	Rb11: CACGATTA
Ff31: CTGAC	Rf24: GCATA	Fb31: GGCCGA	Rb31: GGCCGA
Ff12: GTCGCTA	Rf43: TTGAGAT	Fb12: TCT	Rb12: AACGAGTC
Ff32: CGTCA	Rf23: GACTC	Fb32: GTCAGA	Rb32: GTACTA
Ff13: TGAGCTA	Rf42: GTGCTAG	Fb13: CTA	Rb13: CACTCTGA
Ff33: ATGCA	Rf22: TCAGC	Fb33: ACTAGC	Rb33: TGCAGC
Ff14: GTAGAGA	Rf41: TTGCGAT	Fb14: AGC	Rb14: ACAGATGA
Ff34: AGTAC	Rf21: TCCGA	Fb34: AAGCGA	Rb34: TTCCGC
Ff21: CAGCTA	Rf34: ATCTGT	Fb21: CGATT	Rb21: GAGCATA
Ff41: TCAT	Rf14: ACGC	Fb41: CATGCGGT	Rb41: ATGG
Ff22: AATCTC	Rf33: CTAGTG	Fb22: CGCTG	Rb22: TCTCATA
Ff42: GCAG	Rf13: CAGA	Fb42: ACTGCGTG	Rb42: CGGT
Ff23: ACGCTC	Rf32: AGCGGT	Fb23: GCGGT	Rb23: GCGACTA
Ff43: GAAT	Rf12: ACTA	Fb43: TTAGCTGT	Rb43: AGTT
Ff24: CATCGC	Rf31: AGATTG	Fb24: TATGG	Rb24: TATCAGC
Ff44: TACG	Rf11: AATC	Fb44: GGCGAGTT	Rb44: CTTG

**Table S4:** Identifier sequences introduced in PCR2 during library construction. Sequences (5'-3') of the PCR2 forward (FW) and reverse (RV) orientated primers were AATGATACGGCGACCACCGAGATCTACAC-index- TCGTCGGCAGCGTC, the reverse sequence CAAGCAGAAGACGGCATAACGAGAT-index- GTCTCGTGGGCTCGG, respectively.

PCR2 index (FW)	PCR2 index (RV)
N510v0: CGTCTAAT	N714v0: TCATGAGC
N511v0: TCTCTCCG	N715v0: CCTGAGAT
N513v0: TCGACTAG	N716v0: TAGCGAGT
N516v0: CCTAGAGT	N723v0: GAGCGCTA
N518v0: CTATTAAG	N724v0: CGCTCAGT
N520v0: AAGGCTAT	N727v0: ACTGATCG
N521v0: GAGCCTTA	N728v0: TAGCTGCA
N511v5: TCTCCTGC	N715v5: TCCGGATA
N513v5: GCTATCGA	N716v5: GATCAGTG
N516v5: TCCAAGTG	N723v5: GAGCCGAT
N518v5: ATCTATGA	N724v5: CGCTACTG
N520v5: GAAGTCTA	N728v5: GATCGTAC
N521v5: GAGCTCAT	N714v6: CTTAAGCG
N510v6: GCCTATTA	N715v6: CCGTGATA
N511v6: CTCTCTGC	N716v6: ATCGAGTG
N513v6: CTAGTCGA	N723v6: AGCGCGAT
N516v6: CCATAGTG	N727v6: CAGTTAGC
N518v6: TCTAATGA	N728v6: ATCGGTAC
N521v6: AGCGTCAT	N714v7: ATTCGGCA
N513v7: GTACACGT	N715v7: TCGCAATG
N516v7: TCACGGTA	N716v7: GTCAGGTA
N520v7: GAGAACTT	N723v7: GGCATGAC
N510v8: TGCCAATT	N724v7: CCTGGCTA
N511v8: TCCTCCGT	N728v7: GTCACTAG

**Table S5:** Soil properties in control and warmed plots at 0 – 10 cm and 10 – 20 cm soil depth in 2019. Values represent means (SD). Different letters within each row indicate significant differences between control and warming treatments tested separately for each soil depth (t-test;  $p < 0.05$ ).

Parameters	Control		Warming	
	0 – 10 cm	10 – 20 cm	0 – 10 cm	10 – 20 cm
pH	6.7 (0.2)	7.3 (0.2)	6.6 (0.4)	7.2 (0.2)
C (%)	14.1 (3.1)	6.9 (1.4)	11.9 (2.0)	6.1 (1.8)
N (%)	0.8 (0.2)	0.5 (0.1)	0.8 (0.2)	0.4 (0.1)
C:N	16.7 (1.8)	15.2 (0.7)	16.0 (2.1)	15.3 (0.6)
Total P ( $\mu\text{mol g}^{-1}$ )	25.6 (5.7)	20.3 (4.6)a	21.6 (6.7)	12.2 (2.2)b
$\text{K}^+$ (mmolc $\text{kg}^{-1}$ )	1.9 (0.4)	0.9 (0.3)	1.6 (0.3)	0.9 (0.3)
$\text{Na}^+$ (mmolc $\text{kg}^{-1}$ )	0.95 (0.3)	0.46 (0.2)	0.72 (0.2)	0.52 (0.2)
$\text{Ca}^{++}$ (mmolc $\text{kg}^{-1}$ )	460.1 (111)	278.4 (78)	405.4 (77)	262.5 (83)
$\text{Mg}^{++}$ (mmolc $\text{kg}^{-1}$ )	189.5 (45)	117.2 (30)	175.0 (36)	115.2 (24)
$\text{Mn}^{++}$ (mmolc $\text{kg}^{-1}$ )	0.37 (0.28)	0.04 (0.01)	0.42 (0.25)	0.08 (0.06)

**Table S6:** Plots and trees characteristics at the Achenkirch soil warming experiment. Abbreviations: N° trees – number of trees within 6m distance to the plot center; Distance – mean distance of surrounding trees to the center of the plot; Total BA – the total basal area of trees; BA - the total basal area of trees considering a 6 m radius. Only trees within 6m distance to the plot center were considered. The number of surrounding trees, their height, distance to the plot center, total basal area, and the proportion (%) of beech and spruce are given for each plot. Letters after plot codes are control (C) and warming (W) treatments.

Plots	N° trees	Height (m)	Distance (m)	Spurce BA (m2)	Beech BA (m2)	Total BA (m <sup>2</sup> )	BA (m <sup>2</sup> ha <sup>-1</sup> )	% Spuce	% Beech
P1C	8	21.4	3.9	0.5	0.1	0.7	61.9	78.7	21.3
P2C	10	18.0	4.9	0.5	0.2	0.6	53.1	71.9	28.1
P3C	5	21.0	3.5	0.3	0	0.4	35.4	87.3	12.7
P4C	4	21.3	3.9	0.3	0	0.3	26.5	100	0
P5C	10	22.8	4.0	0.7	0.2	0.9	79.6	80.4	19.6
P6C	2	23.8	3.4	0.2	0	0.2	17.7	100	0.0
P1W	4	20.0	3.9	0.2	0	0.2	17.7	81.0	19
P2W	7	17.9	3.8	0.3	0.1	0.4	35.4	73.9	26.1
P3W	5	22.5	4.8	0.5	0	0.5	44.2	100	0
P4W	9	21.2	3.8	0.6	0	0.6	53.1	100	0
P5W	8	21.6	3.6	0.5	0.2	0.7	61.9	74.4	25.6
P6W	3	24.9	4.7	0.4	0	0.4	35.4	100	0
Mean Control	6.5	21.4	3.9	0.4	0.1	0.5	45.7	86.4	13.6
Mean Warming	6.0	21.4	4.1	0.4	0.1	0.5	41.3	88.2	11.8

**Table S7:** Taxonomic assignment and sequences of the OTUs representing mycorrhizal fungi

OTU_ID and OTU name	Phylum and Class	Order and Family	Genus and Species	OTU Sequence
OTU1 Lactarius-1	Basidiomycota Agaricomycetes	Russulales Russulaceae	Lactarius Lactarius pseudosrobiculatus	ATCATCGAATCTTTGAACGCACCTTGGCCCTTGGTATTCGAGGGGCACAC CCGTTTGAGTGTGTAATAATCTCAACCTTCTCGGTTTCTGGACACCGAA GGAGCTTGGACTTTGGAGGCTTTGCTGGTGTCTCTCTCTCTGAAACCCAG CTCCTTAAATGAATTAGCGGGTCTCTTTTGCTGATCTCGACGTGTGATA AGATGTTT
OTU2 Boletus-2	Basidiomycota Agaricomycetes	Boletales Boletaceae	Boletus Boletus luridus	GTCATCGAGTCTTTGAACGCACCTTGGCTCCTTGGTATTCGAGGGGCATGC CTGTTTGAGTGTGATCGAATTTCAACCATGTCTTGATCGATTTCAAGGCCAT GGCTTGGAGTTGGGGTGTCTGGGGGACGAGCTGTGGCTCTCCTGAAAT GCATTAGCAAAGGGCAGCAAGTCTTTGACGTGCACGGCTTCGACGTGATAA TGATCGTCTGT
OTU3 Cortinarius-3	Basidiomycota Agaricomycetes	Agaricales Cortinariaceae	Cortinarius Cortinarius odorifer	ATCATCGAGTCTTTGAACGCACATTTGGCCCTTTGGTATTCGAAAGGCATGC CTGTTTGAGGCTCATATCACCCCTCAAGCCTCGTGTGGTGTGGACGGAC GGTCGAGGCTCCCCCTCGACCCCTCTAAAGACAATGACGGCGGCTGTGG CACCCCGTACACTGAGCTTCTCACCGGACCGTATCGGACAAGGGCGTCC GGACCCCGGT
OTU4 Craterellus-4	Basidiomycota Agaricomycetes	Cantharellales Cantharellaceae	Craterellus Craterellus lutescens	ATCATCGAATCTTTGAACGCACATTTGCACCTCTGTTTCGGCAGAGTATGCCTGT TTGAGAACTCTATAGTATTCATCTCCAACCTTTGGGTATTCATACCTAGGGAAG GAGAGATTTGAGGGCTCGCACTTACCCTGCGTGCCCTTAAAAACTATTGTGCT GGATACTGTCAAGTAAAGGAAAAAGTATGTGTATGGAACCTTCGGTTCCTCTAAT ACTTAGTA
OTU5 Helvelloseba cina-5	Basidiomycota Agaricomycetes	Sebacinales Sebacinaceae	Helvellosebacina unidentified	ATCATCGAGTCTTTGAACGCACATTTGGCTCCCTGGTATTCGAGGGGCATGC CTGTCGAGCGTCAATACCCCTCAAGCTCTGCTTGGTGTGGGCCCCCGCG CCCCGGGGCCCTAAAGTCAAGTGGGGTCCGCTCCGCTCCGAGCGTAGTA ATCTTCTCGCTCTGGAGGCCCGCCCGTCCCGCTAGCAACCCCCCAATTTT TTTCAGGTT
OTU13 unidentified- 13	Basidiomycota Agaricomycetes	Unidentified unidentified	Unidentified unidentified	GTCATCGAGTCTTTGAACGCACCTTGGCTCCTTGGTATTCGAGGGGCATGC CTGTTTGAGTGTGATCGAATTTCAACCATGTCTTGATCGAATTTCAAGGCCAT GGCTTGGAGTTGGGGTGTCTGGGGGACGAGCTGTGGCTCTCCTGAAAT GCATTAGCAAAGGGCAGCAAGTCTTTGACGTGCACGGCTTCGACGTGATAA TGATCGTCTGT

OTU14 Clavulina-14	Basidiomycota Agaricomycetes	Cantharellales Clavulinaceae	Clavulina unidentified	ATCATCGAGTCTTTGAACGCATCTTCGGCTCCTTGGTATTCTGAGGAGCATGC CTGTTGAGTGTCAATAAATCTCAACCACACACTGGTGGCTTGGATTTGGG TTGTTGGGCTTTTTTTTGTAGTCTGCTCCCTGAAATAAATTAGCGGTAC CTTGGTGAACCTGTCTACAGGTGTGATAAATTATCTACATCCTAGACATCTGCT GGAATGC
OTU15 Inocybe-15	Basidiomycota Agaricomycetes	Agaricales Inocybaceae	Inocybe Inocybe fraudans	GTCATCGAATCTTTGAACGCACATTTGGCCCGCCAGTATTCTGGCGGGCATGC CTGTCCGAGCGTCAATTC AACCCCTCGAACCCCTCCGGGGTCCGGCTTGGGG ATCGGCCCTTAACCGGCCGCCCCGAAATACAGTGGCGGCTCCGCCGACGC TCTCATGCGCAGTAGTTTGCACACTCGCACCCGGGAGCGCGGCCACAG CCGTAAACA
OTU17 unidentified- 17	Unidentified unidentified	Unidentified unidentified	Unidentified unidentified	ATCATCGAATCTTTGAACGCACATTTGGCTTGGCAGTATTCTGCCAGGCATGC CTGTCCGAGCGTCAATTCACCACTCAAGCTCTGCTTGGTGTGGAGGACCCCG GTTACCGCGGGCCCGAAATGCATCGGCTGTTGTATTTGCAGCTTCCCTGTG TAGTAATGCTTAGCTTACACTTTGAAACTTTATATGACATGCCGGTAAACCC TCAATTTT
OTU18 Hydnobolites -18	Ascomycota Pezizomycetes	Pezizales Pezizaceae	Hydnobolites unidentified	ATCATCGAGTCTTTGAACGCACATTTGGCCCGCCAGCAATTTCTGGCGGCATGC CTGTTGAGCGTCAATTTCAACCCCTCAGGCCCCCTCTCGGGGCTTGGCGTT GGGACCGGCCCGCCCTCGCGGGTGCGCCGCCCTAAATAACAGTGGCGG TCCTGCCGAGCCTCCTCTGCGTAGTAGCTCTTGAAACCTCGCACCCGGAGCGG GGCTCGGCC
OTU21 Tricholoma- 21	Basidiomycota Agaricomycetes	Agaricales Tricholomataceae	Tricholoma Tricholoma vaccinum	ATCATCGAGTCTTTGAACGCACATTTGGCCCTTTGGTATTCGGAAGGCATGC CTGTTGAGCGTCAATATCACCCCTCAAGCCTCGTGTCTTGGTTGGACGGAC GGTTCGAGGTCCTCCCTCGACCCCTCTAAAGACAATGACGGCGGCTGTGG CACCCCGGTACACTGAGCTTCTCACCCGAGCACGTATCGGACAAGGGCGGTCC GGACCCGGT
OTU24 Tomentella- 24	Basidiomycota Agaricomycetes	Thelephorales Tricholomataceae	Tomentella Tomentella pilosa	GTCATCGAGTCTTTGAACGCACCTTTGGCTCCTTGGTATTCGAGGAGCATGC CTGTTGAGTGTCAATAATATCAACCTTTCAGCTTTTGTGTGCGAGATGG TTGGATGTGGGGGTGTTTTGTGGCTTTTTTGGAGGTACGCTCCCTGAAAT GCATTAGCGGAACAATTTGTGACTCCGTTCAATGGTGTGATAACTATCTAAG CTAATTA
OTU27 Russula-27	Basidiomycota Agaricomycetes	Russulales Russulaceae	Russula Russula sichuanensis	ATCATCGAGTCTTTGAACGCACATTTGGCCCTTGGTATTCGAGGGGCATGC CTATTCGAGCGTCAATATCACCCCTCAAGCCTAGCTTGGTGTGAGGCCTGCT GTAAAGGCAGCTCTAAATCAGTGGCAGTGTGTGAGGCTCAAGCGGTAGT AAAATTCATCGCTATAGACACCTGGTGGACACTCGCCAGAAACCCCTCATTTT TTAATGATT
OTU28 Sebacina-28	Basidiomycota Agaricomycetes	Sebacinales Sebacinaceae	Sebacina Sebacina incrustans	GTCATCGAATCTTTGAACGCATCTTGGCTCCTTGGTATTCGAGGAGCATGC CTGTTGAGTGTCAATAAGTTCTCAACTGCACACTAGTTCTTCTGGTGCAGCTTG GATGTGGGGGTGTTTTTTTGCAGGCTTTTCAAAAGTCCGCTCCCTGAAATGCA

				TTAGTGGTCTCCTAGCAGAGAAAACCTGCTACAGGTGTGATAAATTATCTATGCGCTTAGTAC
OTU30	Basidiomycota Hysterangium m-30	Hysterangiales Hysterangiaceae	Hysterangium unidentified	GTCATCGAATCTTTGAACGCACCTTGGCTCCTTGGTATTCGGAGGAGCATGCTGTTTGAGTGTGATGTTCTCAACTTACAAGCTTTTGAATGAAGAGTTGGATTTGGAGGCTTGTGTTGGCTCGAAAGAGTTGACTCCTCTGAAAATGCATTAGTGTAGCCTTTACGGATCGCCTCCAGTGTGATAAATGTCTACCGCTGTGGTGTGAAAGTAT
OTU31	Basidiomycota Sebacina-31	Sebacinales Sebacinaceae	Sebacina unidentified	ATCATCGAATCTTTGAACGCACATTTGCACTCTGTTTCGGCAGAGTATGCCTGTITGAGAATCTATAGTATTCATCTCCAACCTTGGGTATTCATACCTAGGGAAGGAGATTTGAGCGTTCGCACTTACCCTGCGTGCCTTTTAAAACTAATTTGCTGCTGGATCTGCAAGTAAACGGAAAAGTATGTGATGGAACCTTCGGTTTCTCTAATACTTAGTAA
OTU36	Basidiomycota Clavulina-36	Cantharellales Clavulinaceae	Clavulina Clavulina reae	GTCATCGAATCTTTGAACGCACATTTGGCCCCCGGCTTCCCGGGGGGCATGCTGTCCGAGCGTCAITGGCCATCCCCTCAAAGCTTTGCTTGGCTTGTGGGCCAGCGTCCGCTGCGGCTCCTGTGCGGGGGACGGGCCCGAAAAGGCAGTGGCGGCTCCTGGAGACTTGGTCCITTTGGGCGGTGATGCATGGGTCTCTTCATCCACCGTCCCGTGG
OTU37	Ascomycota Trichophaea-37	Pezizales Pyrenomataceae	Trichophaea unidentified	GTCATCGAGTCTTTGAACGCACATTTGGCCCCCTTGGTATTCGGAGGGGCATGCTGTTGAGCGTCAITACAACCCTCAAAGCATTTGCTTGGTCTTGGGCTCCGCTGCTTCCCAGCGGGCTTAAAAATCAATGGCGGTGCCGTGGGCCCTTGAGCGGTAATAATCTTCTCGCTACAGGGTGTGATGGACGCTGGCCATCAACCCCCCACTCTCTAAGTT
OTU38	Basidiomycota Cortinarius-38	Agaricales Cortinariaceae	Cortinarius Cortinarius nucicolor	GTCATCGAGTCTTTGAACGCACATTTGGCCCCCTTGGTATTCGGAAAGGCATGCTGTCCGAGCGTCAITTAACACTCTCAAGCCCTGCTTGGTATTTGGGTGCGGGTCCGGCAGGACCCCTCCCGTAACTCGTTGGCGGAACCCCGGCTTCAAGCGTAAAGATTTTCCCTCGCTTGGGAGCTCTGGTGGTGCCTGCCAGGGAAAGCACACTTAAAGTT
OTU39	Basidiomycota Inocybe-39	Agaricales Inocybaceae	Inocybe Inocybe umbrinella	ATCATCGAATCTTTGAACGCATCTTGGCTCCTTGGTATTCGGAGGAGCATGCTGTTTGAGTGTCAATAATTTCTCAACTACACTGATTTTTTTTTTGGTGTAGATTGGATTTGGGGTGTATTTTTTGGGGCTTTTGTAAAAATGAAATCGGCTCCCCTGAAATTGATTAGTGGTACCTTAGTAGAACCATCTACAGGTGTGATAATTTATCTACTCC
OTU40	Basidiomycota Sebacina-40	Sebacinales Sebacinaceae	Sebacina Sebacina flagelliformis	ATCATCGAATCTTTGAACGCATCTTGGCTCCTTGGTATTCGGAGGAGCATGCTGTTTGAGTGTCAITTAATAATTTCAAAACCACTTGACAGTGGCTTTGGATGTGGGGCTCAITTTGCAAGGCTTTCTTCTCAAAGCCTGCTCCCCTGAAAATGCATTAGTGGTATCTGGAGCGGAAAACCGCTAGGTGTGATAAATTAATCGTCTACGCGCTTTGGTATGC

OTU41 Inocybe-41	Basidiomycota Agaricomycetes	Agaricales Inocybaceae	Inocybe Inocybe cervicolor	ATCATCGAGTCTTTGAACGCACATTGCGCTCCCTGGTATCCGGGGAGCATGC CTGTCCGAGCGTCATTACAACCCTCAAGCTCTGCTTTGGTTGGCCCCGCGG CCCCGGGGCCCTAAAGTCAGTGGGGTCCGCTCCGGCTCCGAGCGTAGTA ATCTTCTCGCTCTGGAGGCCCGCGCTGCCGCTAGCAACCCCCCAATTTT TTTCAGGT
OTU43 Clavulina-43	Basidiomycota Agaricomycetes	Cantharellales Clavulinaceae	Clavulina Clavulina cinerea	ATCATCGAGTCTTTGAACGCAGGCCCGCCCTTGCCATATCATTCGTGTTATCGC AAGGCATCTACGTATGAGTGTAGCCCAATATCCTTTTGGTTAATGGTAATA TTATGTAATTTGAATCCATATGCGAGTATCTTTTTGATACACGCGTTTAAAC AAAAGAATATGTGTCTGCGCTCATATGTGGAAGGTTACCCCGCTGGACTTAAAG ATATCAAT
OTU55 Amphinema-55	Basidiomycota Agaricomycetes	Atheliales Atheliaceae	Amphinema unidentified	ATCATCGAATCTTTGAACGCACATTGCGCCTTCTGGTATTCGGGAGGCACGT CTGTTTGAGCGTCAGCTAAACCCTTCCGGCCCTGGCTTTTGTCTGGGGCA CGGCGTGTGGCGTCAAGGGACTGAGGCCCGCCGCTCCGGCGCGGGTACAG GTCTCCCCCGCTTAAACCCTGTGGAAGCTAGCGGGCATGGTCCCCGATCTTGC GAAACAATC
OTU57 Cortinarius-57	Basidiomycota Agaricomycetes	Agaricales Cortinariaceae	Cortinarius Cortinarius acidophilus	ATCATCGAATCTTTGAACGCACATTGCGCCCGCCAGCATCTGCGGGCATGC CTGTTGAGCGTCATTTCTCTCAAAATCTTCGGATTTGGTTTTGAGTGATACT CCTCGAAGCCCCGAAACACAGCGCGGTCCCGTCCCGCACCGAGCGTAGT AGCACATCTCGTATGGCGGTTCCGGCGGTGGCCTGCCGGAACCCCTTATT TTCGTGGTT
OTU61 Sebacina-61	Basidiomycota Agaricomycetes	Sebacinales Sebacinaceae	Sebacina unidentified	GTCATCGAGTCTTTGAACGCACATTGCGCCCTTTGGTATTCCAAAGGGCATGC CTGTTGAGCGTCATTTCTCTCAAAATCTTCGGATTTGGTTTTGAGTGATACT CTTAGTCAGACTAAGCGTTTGGTTGAAATGTAATGGCATGAGTGGTACTAGAT AGTGTGAACCTGTTTCAAATGTAATAGGTTTATCCAACTCGTTGACCAGTAAAG TATTTGT
OTU68 Hygrophorus-68	Basidiomycota Agaricomycetes	Agaricales Hygrophoraceae	Hygrophorus Hygrophorus discoideus	GTCATCGAGTCTTTGAACGCACATTGCGCCCTTTGGTATTCCAAAGGGCATGC CTGTTGAGCGTCATTTCTCTCAAAATCTTCGGATTTGGTTTTGAGTGATACT CTTAGTCAGACTAAGCGTTTGGTTGAAATGTAATGGCATGAGTGGTACTAGAT AGTGTGAACCTGTTTCAAATGTAATAGGTTTATCCAACTCGTTGACCAGTAAAG TATTTGT
OTU69 Lactarius-69	Basidiomycota Agaricomycetes	Russulales Russulaceae	Lactarius Lactarius pallidus	GTCATCGAGTCTTTGAACGCACATTGCGCCCTTTGGTATTCCAAAGGGCATGC CTGTTGAGCGTCATTTCTCTCAAAATCTTCGGATTTGGTTTTGAGTGATACT CTTAGTCAGACTAAGCGTTTGGTTGAAATGTAATGGCATGAGTGGTACTAGAT AGTGTGAACCTGTTTCAAATGTAATAGGTTTATCCAACTCGTTGACCAGTAAAG TATTTGT
OTU74 Sebacina-74	Basidiomycota Agaricomycetes	Sebacinales Sebacinaceae	Sebacina unidentified	GTCATCGAGTCTTTGAACGCACATTGCGCCCTTTGGTATTCCAAAGGGCATGC CTGTTGAGCGTCATTTCTCTCAAAATCTTCGGATTTGGTTTTGAGTGATACT CTTAGTCAGACTAAGCGTTTGGTTGAAATGTAATGGCATGAGTGGTACTAGAT AGTGTGAACCTGTTTCAAATGTAATAGGTTTATCCAACTCGTTGACCAGTAAAG TATTTGT

OTU78	Basidiomycota	Sebacinales	Sebacina	AGTGTGAACCTGTTTCAATGTAATTAGGTTTATCCAACTCGTTGACCAGTAAAG TATTTGT
Sebacina-78	Agaricomycetes	Sebacinaceae	Sebacina unidentified	GTCATCGAGTCTTTGAACGCACATTTGGCCCTTTGGTATTCCAAAAGGGCATGC CTGTTTGAGCGTCATTTCTCTCAAAATCTTCGGATTTGGTATTGAGTGATACT CTTAGTCAGACTAAGCGTTTGTCTTGAATGTAATGGCATGAGTGGTACTAGAT AGTGTGAACCTGTTTCAATGTAATTAGGTTTATCCAACTCGTTGACCAGTAAAG TATTTGT
OTU82	Basidiomycota	Sebacinales	Sebacina	GTCATCGAGTCTTTGAACGCACATTTGGCCCTTTGGTATTCCAAAAGGGCATGC CTGTTTGAGCGTCATTTCTCTCAAAATCTTCGGATTTGGTATTGAGTGATACT CTTAGTCAGACTAAGCGTTTGTCTTGAATGTAATGGCATGAGTGGTACTAGAT AGTGTGAACCTGTTTCAATGTAATTAGGTTTATCCAACTCGTTGACCAGTAAAG TATTTGT
Sebacina-82	Agaricomycetes	Sebacinaceae	Sebacina dimithica	GTCATCGAGTCTTTGAACGCACATTTGGCCCTTTGGTATTCCAAAAGGGCATGC CTGTTTGAGCGTCATTTCTCTCAAAATCTTCGGATTTGGTATTGAGTGATACT CTTAGTCAGACTAAGCGTTTGTCTTGAATGTAATGGCATGAGTGGTACTAGAT AGTGTGAACCTGTTTCAATGTAATTAGGTTTATCCAACTCGTTGACCAGTAAAG TATTTGT
OTU87	Basidiomycota	Thelephorales	Pseudotomentella	GTCATCGAGTCTTTGAACGCACATTTGGCCCTTTGGTATTCCAAAAGGGCATGC CTGTTTGAGCGTCATTTCTCTCAAAATCTTCGGATTTGGTATTGAGTGATACT CTTAGTCAGACTAAGCGTTTGTCTTGAATGTAATGGCATGAGTGGTACTAGAT AGTGTGAACCTGTTTCAATGTAATTAGGTTTATCCAACTCGTTGACCAGTAAAG TATTTGT
Pseudotomen tella-87	Agaricomycetes	Thelephoraceae	Pseudotomentella alobata	GTCATCGAGTCTTTGAACGCACATTTGGCCCTTTGGTATTCCAAAAGGGCATGC CTGTTTGAGCGTCATTTCTCTCAAAATCTTCGGATTTGGTATTGAGTGATACT CTTAGTCAGACTAAGCGTTTGTCTTGAATGTAATGGCATGAGTGGTACTAGAT AGTGTGAACCTGTTTCAATGTAATTAGGTTTATCCAACTCGTTGACCAGTAAAG TATTTGT
OTU94	Ascomycota	Pezizales	Peziza	GTCATCGAGTCTTTGAACGCACATTTGGCCCTTTGGTATTCCAAAAGGGCATGC CTGTTTGAGCGTCATTTCTCTCAAAATCTTCGGATTTGGTATTGAGTGATACT CTTAGTCAGACTAAGCGTTTGTCTTGAATGTAATGGCATGAGTGGTACTAGAT AGTGTGAACCTGTTTCAATGTAATTAGGTTTATCCAACTCGTTGACCAGTAAAG TATTTGT
Peziza-94	Pezizomycetes	Pezizaceae	unidentified	GTCATCGAGTCTTTGAACGCACATTTGGCCCTTTGGTATTCCAAAAGGGCATGC CTGTTTGAGCGTCATTTCTCTCAAAATCTTCGGATTTGGTATTGAGTGATACT CTTAGTCAGACTAAGCGTTTGTCTTGAATGTAATGGCATGAGTGGTACTAGAT AGTGTGAACCTGTTTCAATGTAATTAGGTTTATCCAACTCGTTGACCAGTAAAG TATTTGT
OTU95	Basidiomycota	Sebacinales	Sebacina	GTCATCGAGTCTTTGAACGCACATTTGGCCCTTTGGTATTCCAAAAGGGCATGC CTGTTTGAGCGTCATTTCTCTCAAAATCTTCGGATTTGGTATTGAGTGATACT CTTAGTCAGACTAAGCGTTTGTCTTGAATGTAATGGCATGAGTGGTACTAGAT AGTGTGAACCTGTTTCAATGTAATTAGGTTTATCCAACTCGTTGACCAGTAAAG TATTTGT
Sebacina-95	Agaricomycetes	Sebacinaceae	unidentified	GTCATCGAGTCTTTGAACGCACATTTGGCCCTTTGGTATTCCAAAAGGGCATGC CTGTTTGAGCGTCATTTCTCTCAAAATCTTCGGATTTGGTATTGAGTGATACT CTTAGTCAGACTAAGCGTTTGTCTTGAATGTAATGGCATGAGTGGTACTAGAT AGTGTGAACCTGTTTCAATGTAATTAGGTTTATCCAACTCGTTGACCAGTAAAG TATTTGT
OTU100	Basidiomycota	Thelephorales	Tomentella	GTCATCGAGTCTTTGAACGCACATTTGGCCCTTTGGTATTCCAAAAGGGCATGC CTGTTTGAGCGTCATTTCTCTCAAAATCTTCGGATTTGGTATTGAGTGATACT CTTAGTCAGACTAAGCGTTTGTCTTGAATGTAATGGCATGAGTGGTACTAGAT AGTGTGAACCTGTTTCAATGTAATTAGGTTTATCCAACTCGTTGACCAGTAAAG TATTTGT
Tomentella- 100	Agaricomycetes	Thelephoraceae	Tomentella asperula	GTCATCGAGTCTTTGAACGCACATTTGGCCCTTTGGTATTCCAAAAGGGCATGC CTGTTTGAGCGTCATTTCTCTCAAAATCTTCGGATTTGGTATTGAGTGATACT CTTAGTCAGACTAAGCGTTTGTCTTGAATGTAATGGCATGAGTGGTACTAGAT AGTGTGAACCTGTTTCAATGTAATTAGGTTTATCCAACTCGTTGACCAGTAAAG TATTTGT
OTU102	Basidiomycota	Russulales	Russula	GTCATCGAGTCTTTGAACGCACATTTGGCCCTTTGGTATTCCAAAAGGGCATGC CTGTTTGAGTGTCATCGAATTTCAACCATGCTTGTGATCGAATTTCAAGGCCAT GGCTTGGAGTTGGGGTTGCTGGCGGACGAGCTGTCGGCTCTCCTGAAAT GCATTAACAAAAGGGCAGCAAGTCTTTGACGTGCACGGCCCTTCGACCGTGATAA TGATCGTCTGT
Russula-102	Agaricomycetes	Russulaceae	Russula Russula griseascens	GTCATCGAGTCTTTGAACGCACATTTGGCCCTTTGGTATTCCAAAAGGGCATGC CTGTTTGAGTGTCATCGAATTTCAACCATGCTTGTGATCGAATTTCAAGGCCAT GGCTTGGAGTTGGGGTTGCTGGCGGACGAGCTGTCGGCTCTCCTGAAAT GCATTAACAAAAGGGCAGCAAGTCTTTGACGTGCACGGCCCTTCGACCGTGATAA TGATCGTCTGT

OTU105	Basidiomycota	Thelephorales	Tomentella	GTCATCGAGTCTTTGAAACGCACCTTGGCTCCTTGGTATTCGGAGGAGCATGC CTGTTGAGTGTCAATCGAATTCACACCAATGCTTTGATCGATTTCAAGGCCAT GGCTTGGAGTTGGGGTTGCTGGCGGACGAGCTGTGGCTCTCCTGAAAT GCATTAGCAAAAGGGCAGCAAGTCTTTGACGTGCACGGCCTTCGACGTGATAA TGATCGTCTGT
OTU106	Basidiomycota	Russulales	Russula	GTCATCGAGTCTTTGAAACGCACCTTGGCTCCTTGGTATTCGGAGGAGCATGC CTGTTGAGTGTCAATCGAATTCACACCAATGCTTTGATCGATTTCAAGGCCAT GGCTTGGAGTTGGGGTTGCTGGCGGACGAGCTGTGGCTCTCCTGAAAT GCATTAGCAAAAGGGCAGCAAGTCTTTGACGTGCACGGCCTTCGACGTGATAA TGATCGTCTGT
Russula-106	Agaricomycetes	Russulaceae	Russula queletii	GTCATCGAGTCTTTGAAACGCACCTTGGCTCCTTGGTATTCGGAGGAGCATGC CTGTTGAGTGTCAATCGAATTCACACCAATGCTTTGATCGATTTCAAGGCCAT GGCTTGGAGTTGGGGTTGCTGGCGGACGAGCTGTGGCTCTCCTGAAAT GCATTAGCAAAAGGGCAGCAAGTCTTTGACGTGCACGGCCTTCGACGTGATAA TGATCGTCTGT
OTU113	Basidiomycota	Russulales	Lactarius	GTCATCGAGTCTTTGAAACGCACCTTGGCTCCTTGGTATTCGGAGGAGCATGC CTGTTGAGTGTCAATCGAATTCACACCAATGCTTTGATCGATTTCAAGGCCAT GGCTTGGAGTTGGGGTTGCTGGCGGACGAGCTGTGGCTCTCCTGAAAT GCATTAGCAAAAGGGCAGCAAGTCTTTGACGTGCACGGCCTTCGACGTGATAA TGATCGTCTGT
Lactarius-113	Agaricomycetes	Russulaceae	Lactarius hengduanensis	GTCATCGAGTCTTTGAAACGCACCTTGGCTCCTTGGTATTCGGAGGAGCATGC CTGTTGAGTGTCAATCGAATTCACACCAATGCTTTGATCGATTTCAAGGCCAT GGCTTGGAGTTGGGGTTGCTGGCGGACGAGCTGTGGCTCTCCTGAAAT GCATTAGCAAAAGGGCAGCAAGTCTTTGACGTGCACGGCCTTCGACGTGATAA TGATCGTCTGT
OTU115	Basidiomycota	Sebacinales	Sebacina	GTCATCGAGTCTTTGAAACGCACCTTGGCTCCTTGGTATTCGGAGGAGCATGC CTGTTGAGTGTCAATCGAATTCACACCAATGCTTTGATCGATTTCAAGGCCAT GGCTTGGAGTTGGGGTTGCTGGCGGACGAGCTGTGGCTCTCCTGAAAT GCATTAGCAAAAGGGCAGCAAGTCTTTGACGTGCACGGCCTTCGACGTGATAA TGATCGTCTGT
Sebacina-115	Agaricomycetes	Sebacinaceae	Sebacina sp	GTCATCGAGTCTTTGAAACGCACCTTGGCTCCTTGGTATTCGGAGGAGCATGC CTGTTGAGTGTCAATCGAATTCACACCAATGCTTTGATCGATTTCAAGGCCAT GGCTTGGAGTTGGGGTTGCTGGCGGACGAGCTGTGGCTCTCCTGAAAT GCATTAGCAAAAGGGCAGCAAGTCTTTGACGTGCACGGCCTTCGACGTGATAA TGATCGTCTGT
OTU119	Basidiomycota	Sebacinales	Sebacina	GTCATCGAGTCTTTGAAACGCACCTTGGCTCCTTGGTATTCGGAGGAGCATGC CTGTTGAGTGTCAATCGAATTCACACCAATGCTTTGATCGATTTCAAGGCCAT GGCTTGGAGTTGGGGTTGCTGGCGGACGAGCTGTGGCTCTCCTGAAAT GCATTAGCAAAAGGGCAGCAAGTCTTTGACGTGCACGGCCTTCGACGTGATAA TGATCGTCTGT
Sebacina-119	Agaricomycetes	Sebacinaceae	unidentified	GTCATCGAGTCTTTGAAACGCACCTTGGCTCCTTGGTATTCGGAGGAGCATGC CTGTTGAGTGTCAATCGAATTCACACCAATGCTTTGATCGATTTCAAGGCCAT GGCTTGGAGTTGGGGTTGCTGGCGGACGAGCTGTGGCTCTCCTGAAAT GCATTAGCAAAAGGGCAGCAAGTCTTTGACGTGCACGGCCTTCGACGTGATAA TGATCGTCTGT
OTU126	Basidiomycota	Agaricales	Inocybe	GTCATCGAGTCTTTGAAACGCACCTTGGCTCCTTGGTATTCGGAGGAGCATGC CTGTTGAGTGTCAATCGAATTCACACCAATGCTTTGATCGATTTCAAGGCCAT GGCTTGGAGTTGGGGTTGCTGGCGGACGAGCTGTGGCTCTCCTGAAAT GCATTAGCAAAAGGGCAGCAAGTCTTTGACGTGCACGGCCTTCGACGTGATAA TGATCGTCTGT
Inocybe-126	Agaricomycetes	Inocybaceae	Inocybe quietiodor	GTCATCGAGTCTTTGAAACGCACCTTGGCTCCTTGGTATTCGGAGGAGCATGC CTGTTGAGTGTCAATCGAATTCACACCAATGCTTTGATCGATTTCAAGGCCAT GGCTTGGAGTTGGGGTTGCTGGCGGACGAGCTGTGGCTCTCCTGAAAT GCATTAGCAAAAGGGCAGCAAGTCTTTGACGTGCACGGCCTTCGACGTGATAA TGATCGTCTGT
OTU130	Basidiomycota	Agaricales	Inocybe	ATCATCGAGTCTTTGAAACGCACCTTGGCTCCTTGGTATTCGGAGGAGCATGC CTGTTGAGTGTCAATCGAATTCACACCAATGCTTTGATCGATTTCAAGGCCAT TTGTTGTTGGGCTTTTTTTTTTTGTTAGTCTCCCTGAAATTAATTAGCGGTAC CTTGGTGGAACTGTCTACAGGTGTGATAAATTATCTACATCTTAGACATCTGCT GGAATGC
Inocybe-130	Agaricomycetes	Inocybaceae	unidentified	ATCATCGAGTCTTTGAAACGCACCTTGGCTCCTTGGTATTCGGAGGAGCATGC CTGTTGAGTGTCAATCGAATTCACACCAATGCTTTGATCGATTTCAAGGCCAT TTGTTGTTGGGCTTTTTTTTTTTGTTAGTCTCCCTGAAATTAATTAGCGGTAC CTTGGTGGAACTGTCTACAGGTGTGATAAATTATCTACATCTTAGACATCTGCT GGAATGC
OTU134	Ascomycota	Pezizales	Trichophaea	ATCATCGAGTCTTTGAAACGCACCTTGGCTCCTTGGTATTCGGAGGAGCATGC CTGTTGAGTGTCAATCGAATTCACACCAATGCTTTGATCGATTTCAAGGCCAT AGAGAGTACATTTGTAATAAAGGCCAGTGTGCATTTCTCTCTTTGAAATATAI
	Pezizomycetes	Pyronemataceae	unidentified	ATCATCGAGTCTTTGAAACGCACCTTGGCTCCTTGGTATTCGGAGGAGCATGC CTGTTGAGTGTCAATCGAATTCACACCAATGCTTTGATCGATTTCAAGGCCAT AGAGAGTACATTTGTAATAAAGGCCAGTGTGCATTTCTCTCTTTGAAATATAI

Trichophaea-134					TAGTAGATGTAAAAAGTTGTGAATTACATACACAGTTTTTGACCTAATAATAGTCA TTAATGGC
OTU139	Basidiomycota	Agaricales	Unidentified	Unidentified	GTCATCGAATCTTTGAACGCACCTTGGCTCCTTGGTATTTCCGAGGAGCATGC CTGTTGAGTGTCAATTAATCTCAACCTTATAGCTTTTGGTATAAATGGTTT GGATGTGGGGTTCTCTTTTGTGGCTTCTTTGACAGAGTCACTCCCTCGA AATGCATTAGCTGGTGCCCGGCTGGACTGTCTAATTTGGTGTGATAATTATCA ACGCCGT
OTU143	Basidiomycota	Sebacinales	Sebacina	Sebacina	ATCATCGAATCTTTGAACGCACCTTGCACCCCTTTGGCATTTCTGAAGGGTATGC TCGTTTGGAGTGTCAATGTACTCTCACACTCCCGATCTTTGATTTGGAGTGGTG GACTTGGGTTTGTGCTTCCCGGCTTACCTCAAATACGGTAGTGCAACT CTTGGTTGGACATAATACGGCGTGATAAGTGGTCTTCGCCGGTGCCTCGCAA AGAGGGT
OTU144	Basidiomycota	Sebacinales	Sebacina	Sebacina	ATCATCGAGTCTTTGAACGCACCTTGCACCCCTTTGGCATTTCCGAAGGGTATGC TCGTTTGGAGTGTCAATGTACTCTCACACTCCCGATCTTTGATTTGGAGCGGT GGACTTGGGTTGCTGCTTACCGTGGCTCACCTCAAATGGATTCGTGCATCT CTTGGTTGGACATAGTACGGCGTGATAAGTATCTTCGCCGGCGCCTCACCTCG AGGGTGGC
OTU149	Basidiomycota	Sebacinales	Sebacina	Sebacina	GTCATCGAATCTTTGAACGCACCTTGCACCCCTTTGGCATTTCCGAAGGGTATGC TCGTTTGGAGTGTCAATGTACTCTCACACTCCCGTCTTTGGATTTGGAGGTGG ACTTGGGTTGCTGCTTACCGTGGCTCACCTCAAATGGATTCGTGCAACTCT TGGTTGGACATAAGTACGGCGTAAATAAGTGTTCGCCGGCACCTCACTAGAGG GTGGCTGAT
OTU151	Ascomycota	Pezizales	Pachyphloides	Pachyphloides	ATCATCGAATCTTTGAACGCACATTTGGCCCCAATGGTATTTCCATTTGGGCATAC CTGTTTGGAGTATCAGAATCCTTTTAATTAACAACCTTTTATGTATAGAGATGTA TGTAAGATGTTTGGATATAAATTTGAGAAAAGTAGGTATTTTATAAATACT ACTTCTTAAAAACCAGAAAATATTATGTTTTGATTTTTCTTCAAATCTCAATTTG TATATT
OTU152	Basidiomycota	Sebacinales	Sebacina	Sebacina	GTCATCGAGTCTTTGAACGCACCTTGCACCCCTTTGGTATTTCCGAAGGGTATGC TCGTTTGGAGTGTCAATGTACTCTCACACTCTCTAATGCTTGCATTAGGAGCGGT GGACTTGGGTTGCTGCTTACCGTGGCTCACCTGAAATGCAATAGTGCACC TCCTGGTTGGACATAGTACGGCGTGATAAGTGTCTTCGCCGGCGCCTCGAAAAG AGGGTGG
OTU154	Basidiomycota	Agaricales	Inocybe	Inocybe	ATCATCGAATCTTTGAACGCATCTTGGCTCCTTGGTATTTCCGAGGAGCATGC CTGTTTGGAGTGTCAATCAAAATCTCAACCACACAGATTTGTTTCTGATGTGGC TTGGATGTGGGGTTGTAATTTGCAGGCTTTAGAAAATTTGAAGTCCGGCTCCC CTGAAATGCATTAGTGGTATCTGAGCAGAAAAAAGACTACTACAGGTGTGAT TAAATTTTA
Sebacina-143	Agaricomycetes	Sebacinaceae	Sebacina sp	Sebacina sp	
Sebacina-144	Agaricomycetes	Sebacinaceae	unidentified	unidentified	
Sebacina-149	Agaricomycetes	Sebacinaceae	unidentified	unidentified	
Pachyphloides-151	Pezizomycetes	Pezizaceae	Pachyphloides citrina	Pachyphloides citrina	
Sebacina-152	Agaricomycetes	Sebacinaceae	Sebacina sp	Sebacina sp	
Inocybe-154	Agaricomycetes	Inocybaceae	Inocybe leptocystis	Inocybe leptocystis	

OTU159	Basidiomycota	Agaricales	Inocybe	ATCATCGAATCTTTGAAACCGCATCTTGGCGTCTTGGTATTCGAGGGAGCATGC CTGTTGAGTGTCAATCAAGTTTCTCAACCACATCGATAATAAATTTGGTGTGGC TTGGAACATTTGGGGGTGTGCAGGCTTCTGTAGGAGTCTGCTCCCTGAAATGC ATTAGTGGTACTGTTAGCCAAACCCACAGGTGTGTGATAAAAATATCTATGCCT TTGGTATG
OTU162	Basidiomycota	Sebacinales	Sebacina	ATCATCGAGTCTTTGAAACCGCACCTTGCACCCCTTGGTATTCGAAAGGGTATGC TCGTTTGAAGTGTCAATGTAAATCTCACACTTCTGATCCTTTGGATCGGGAGTGGT GGACTTGGGIGTGTCTGTGACGGTGGCTCACCTCAAATGCAATAGTGCAAC TCCAGTTGGACATAGTACGGCGTGATAAGTATCTTCGCCGGCACCTCACCCAG AGGGTGG
OTU166	Basidiomycota	Sebacinales	Sebacina	GTCATCGAGTCTTTGAAACCGCACCTTGCACCCCTTGGCATTCGAAAGGGTATGC TCGTTTGAAGTGTCAATGTAAATCTCACACTTCCAAATCTATGGATTTGGAGCGG TGGACTTGGCGCTGTCTTACTGTGGCTCACCTCAAATGCAATAGTGCAA CCCTTGGTTAGACATAGTACGGCGTGATAAGTGTCTTCGCTGGCGCCTCACTT AGAGGGTG
OTU169	Basidiomycota	Russulales	Lactarius	GTCATCGAATCTTTGAAACCGCACCTTGGCCCTTGGTATTCGAGGGGCACAC CCGTTTGAAGTGTGCGTGAACACCTCAACCTCCTGGTTCTTCTGGAGACCCAAA GCAGGCTTGGACTTTGGAGGCTTGTGTGGCTCTCTCTTTTGAAGGCCAG CTCCTCTTAAACAAAATTAGCAGGGTCTCTTTGCCGATCCTCGACGTGTGATA AGATGTTT
Lactarius-169	Agaricomycetes	Russulaceae	Lactarius badiusanguineus	GTCATCGAATCTTTGAAACCGCACCTTGCACCCCTTGGCATTCGAAAGGGTATGC TCGTTTGAAGTGTCAATGTAAATCTCACACTCCCGATCGTTCGATTTGGAGCGGT GGACTTGGGIGTGTCTGTGACGGTGGCTCACCTCAAATGCAATAGTGCACT CTTGGTTGGACATAGTACGGCGTGATAAGTGTCTTCGCCGGCACCTCAGTAGA GGTGGCC
OTU175	Basidiomycota	Sebacinales	Sebacina	GTCATCGAATCTTTGAAACCGCACCTTGCACCCCTTGGCATTCGAAAGGGTATGC TCGTTTGAAGTGTCAATGTAAATCTCACACTCCCGATCGTTCGATTTGGAGCGGT GGACTTGGGIGTGTCTGTGACGGTGGCTCACCTCAAATGCAATAGTGCACT CTTGGTTGGACATAGTACGGCGTGATAAGTGTCTTCGCCGGCACCTCAGTAGA GGTGGCC
OTU183	Ascomycota	Pezizales	Genea	GTCATCGAATCTTTGAAACCGCACATTTGGCCCTCCTGTATTTGGGGGGCATGC CTGTTGAGAGTCAATTAACAACAATTCGAATCCTCTTCCCTTCCAGTTGTG TTGGGGGGGTGTGAATCGGTTTGGTGGAGGAGAAAAGGGGGGAGACTCC CTCTCCCAACCAAAATTCATAGGCAGTCTGTGTTTTTTGTAACCCCTTGGATAT GTTTATGG
Genea-183	Pezizomycetes	Pyronemataceae	Genea dentata	GTCATCGAATCTTTGAAACCGCACCTTGCACCCCTTGGCATTCGAGGGGGCATG CCTGTTTGAAGTATCAATGAACACCTCAACTCTCACGGTTTGCCTGGTGGAGCTT GGATTTGGGGGTTTTGTGGCTGTGGTGGCTCTCAAATGAATCAGCT TTCCAGTGTTTGGTGGCGTCAACGGGTGTGATAACTATCTACGCTCACGACCCGT CCGCCAGG
OTU187	Basidiomycota	Thelephorales	Thelephora	GTCATCGAATCTTTGAAACCGCACCTTGCACCCCTTGGCATTCGAGGGGGCATG CCTGTTTGAAGTATCAATGAACACCTCAACTCTCACGGTTTGCCTGGTGGAGCTT GGATTTGGGGGTTTTGTGGCTGTGGTGGCTCTCAAATGAATCAGCT TTCCAGTGTTTGGTGGCGTCAACGGGTGTGATAACTATCTACGCTCACGACCCGT CCGCCAGG
Thelephora-187	Agaricomycetes	Thelephoraceae	unidentified	GTCATCGAATCTTTGAAACCGCACCTTGCACCCCTTGGCATTCGAGGGGGCATG TCGTTTGAAGTGTCAATGTAAATCTCACACTCAAATGAATTTGGAGAAAGTGGAC TTGGGTTGTGCTTGTGGTGGCTCATCTTAAATAATGCTAGTGCAACTCATG
OTU196	Basidiomycota	Sebacinales	Sebacina	GTCATCGAATCTTTGAAACCGCACCTTGCACCCCTTGGCATTCGAGGGGGCATG TCGTTTGAAGTGTCAATGTAAATCTCACACTCAAATGAATTTGGAGAAAGTGGAC TTGGGTTGTGCTTGTGGTGGCTCATCTTAAATAATGCTAGTGCAACTCATG
Sebacina-196	Agaricomycetes	Sebacinaceae	unidentified	GTCATCGAATCTTTGAAACCGCACCTTGCACCCCTTGGCATTCGAGGGGGCATG TCGTTTGAAGTGTCAATGTAAATCTCACACTCAAATGAATTTGGAGAAAGTGGAC TTGGGTTGTGCTTGTGGTGGCTCATCTTAAATAATGCTAGTGCAACTCATG

				GTTGGATATAGTACAGCGTGATAAGTATCCTCGCTGGCGCCTCATGAAGAGG GTGTCCGA
OTU203	Basidiomycota	Agaricales	Inocybe	GTCATCGAGTCTTTGAACGCATCTTGGCTCCTTGGTATTTCCGAGGAGCATGC CTGTTTGAGTGCATTTCAATGTTCTCAACCTCACTCATCTTTGATGTGGCTTGGAT GGTGGAGGTTTGCAGGCTGGCTCGTCTGCTCCTCTGAAAAGCATTAGCGGTG TCGTCTCGTACTGCAGGTGTGATAAATAATCTATGCTATGGTCTGCGGTG TGGCTG
OTU212	Basidiomycota	Thelephorales	Toментella	GTCATCGAATCTTTGAACGCACCTTGGCCCTTTGGCTATTTCCGAAAGGGCATG CCTGTTGAGTATCATGAACACCTCAACTCATGTTGGTTTCCCATGATGAGCTT GGACTTTGGGGTCTTGTGGCTACGGTCAAGTCAAGTCTCTTAAATGAATCAGCT TGCCAGTGTGGTGGCATCGCAGGTGTGATAAATACTACGCTTGTGGTTTT CCATCAAG
OTU216	Basidiomycota	Sebacinales	Sebacina	ATCATCGAATCTTTGAACGCACCTTGCACCCCTTTGGCAATTCGAAAGGGTATGC TCGTTTGAAGTGCATTTGACTCTCACACTTCTGATCGTTTGGATTTGGAGCGGT GGATTTGGGTGTGGCGCTTACTGAGGCTCACTTGAATGCAATAGTGCAAC TCTTGGTTGGACATAGTACGGCGTGATAAGTCTTCCGCCGGCACCTCACCAGAG GGTGGCT
OTU220	Ascomycota	Pezizales	Hydnobolites	GTCATCGAATCTTTGAACGCACATTTGGCCCTCATGGCATTTCCGTGAGGCGATGC CCATCTCAGCGTTAGAAAATATCTCAAAATTTAGTTTTGTGCTAAAATTTGG ATCATGTCAAGGAAGTACTACTATATTTGATCGCTCTTTGGAAAATTAATA GGTCTTGAAGTTACTACTATAGAACGTGATGAATCTTTCTTCGTTCTATTGTA GTTCACT
Amphinema-225	Basidiomycota	Atheliales	Amphinema	ATCATCGAATCTTTGAACGCACCTTGGCTCCTTTGGTATTTCCGAGGAGCATGC CTGTTTGAAGTGCATTTAAATTTCAACCCACCGAATTTGTTTTGGGGGATTG GACTTGGAGTGTGTGGCGAAGGTGGCTCCTCTTAAATGCATCAGTGGAG AGAAACTTGGCCCCAGTGTGATAATCCTGTGTGTGTGGTGGGTGAAAAGTCTG CTTTCAACT
OTU228	Basidiomycota	Sebacinales	Sebacina	ATCATCGAATCTTTGAACGCACCTTGCACCCCTTTGGCAATTCGAAAGGGTATGC TCGTTTGAAGTGCATTTGACTCTCACACTTCTGATCTTTTGGTCCGGAGCGGT GGACTTGGGTGTGTGCTTTACTGTGGCTCACTCAAAATGCAATAGTGC AAC TCTTGGTTGGACATAGTACGGCGTGATAAGTATCTTCCGCCGGCACCTCGCAAG AGGTGG
OTU230	Basidiomycota	Agaricales	Cortinarius	GTCATCGAGTCTTTGAACGCACCTTGGCTCCTTTGGTATTTCCGAGGAGCATGC CTGTTTGAAGTGCATTTAAATATCAACCTCTTCAAGCTTTTGTTCGAGATGG TTGGATGTGGGGGTGTTTTGTGGCTTTTTTGGAGTCAAGTCCCTGAAAT GCATTAGCGGAACAATTTGTGCGACTCCGTTCAATTTGGTGTGATAACTATCTACG CTATTGA
Cortinarius-230	Agaricomycetes	Cortinariaceae	Cortinarius venetus	

OTU235 Amphinema-235	Basidiomycota Agaricomycetes	Atheliales Atheliaceae	Amphinema unidentified	ATCATCGAATCTTTGAACGCACCTTTGGCTCCTTGGTATTCGAGGAGCATGC CTGTTGAGTGTCAATAATCCTCAACCCACCGAATTTGCTTCGGGGGATTG GACTTGGAGCGTGTGGCGAAGGTGGCTCCTCTTTAAATGCATCAGCGGAG AAGAAAGCTCGTCCAGTGTGATAAATCCTGTTCGGCTGTGGTGGGTGAAAA TTCCGCTTTC
OTU238 Sebacina-238	Basidiomycota Agaricomycetes	Sebacinales Sebacinaceae	Sebacina Sebacina incrustans	GTCATCGAATCTTTGAACGCACCTTTGCACCCCTTTGGCATTCGGAAGGTATGC TCGTTTGAGTGTCAATTAATCCTCACACTCCCAATCCCTTTGGATTGGGAGCGG TGGACTTGGGTGTTCGGCTTACTGACTGAGGCTCACCTGAAATATGTTAGTGCAT CTCTGATTGGACATAGTACGGCGTGATAAGTGTCTTCGCCGGCTCCTCGCAA GAGGGTGG
OTU242 Sebacina-242	Basidiomycota Agaricomycetes	Sebacinales Sebacinaceae	Sebacina unidentified	ATCATCGAATCTTTGAACGCACCTTTGCACCCCTTTGGCATTCGGAAGGTATGC TCGTTTGAGTGTCAATTAATCCTCACACTCCCAATCCCTTTGGATTGGGAGCGGT GGACTTGGGTGTTCGGCTTACTGACTGAGGCTCACCTCAAAATGGAGTAGTCAAC TCTCGGTTGGACATAGTACGGCGTGATAAGTATCTTCGCCGGCGCCTCACTCG AGGGTGG
OTU249 Inocybe-249	Basidiomycota Agaricomycetes	Agaricales Inocybaceae	Inocybe Inocybe geraniodora	GTCATCGAATCTTTGAACGCACCTTTGGCTCCTTGGTATTTCTGAGGAGCATGC CTGTTTGAGTGTCAATAATCCTCAACCCACAAATTCATTTTATTTGGCATGTGG CTTGGACGTGGAGGAATGTGACGGCTTAAACCTTTGAAAGTCTGCTCCTCTAAA AAATATAAGTGTACCTATATTGGAACCTTTGGCTAGGTGTGATAAATAATCTGC ATCTAAT
OTU254 Sebacina-254	Basidiomycota Agaricomycetes	Sebacinales Sebacinaceae	Sebacina Sebacina incrustans	GTCATCGAGTCTTTGAACGCACCTTTGCACCCCTTTGGCATTCGGAAGGTATGC TCGTTTGAGTGTCAATTAATCCTCACACTCCCAATCCCTTTGGATTGGGAGCGGTG GACTTGGGTGTTCGGCTTACTGACTGAGGCTCACCTCAAAATGTTAGTCAACTC TTGGTTGGACATAGTACGGCGTGATAAGTATCTTCGCCGGTGCCTCGCAATTG CGAGGGTG
OTU262 Inocybe-262	Basidiomycota Agaricomycetes	Agaricales Inocybaceae	Inocybe unidentified	GTCATCGAATCTTTGAACGCACCTTTGGCTCCTTGGTATTCGGAAGGTATGC CTGTTTGAGTGTCAATAATCCTCAAAACCATAATGATCGTCTTTGATGTGGC TTTTGGATGTGGGGGTTTTGCAGGCTTGTATCAAGTCAAGTCAAGTCAAGTCAAGT GCATTAAGTATCTGAGCAGAGAAACTACCACAGGTGTGATAAATAATTAATCT ATGCCTTG
OTU264 Inocybe-264	Basidiomycota Agaricomycetes	Agaricales Inocybaceae	Inocybe Inocybe agordina	ATCATCGAATCTTTGAACGCACCTTTGGCTCCTTGGTATTCGGAAGGTATGC CTGTTTGAGTGTCAATAAGTTCACACCATACTAATTTTATCTATTGGTGTGGC TTGGTTATGGGGATAATTTTTGCAGGCCCTAAAAGAAAGGTCTGCTCCCTGA AATGCATTAGTGTATCTGAGCAGAGACAACTAATTTGGTGTGATAACTATCTA TGCCTTT
OTU269	Basidiomycota Agaricomycetes	Cantharellales Clavulinaceae	Clavulina Clavulina rugosa	GTCATCGAGTCTTTGAACGCACCTTTGGCTCCTTGGTATTCGGAAGGTATGC CTGTTTGAGTGTCAATAATCCTCAAGCTTGGATGGCAATTTTGTCTGTCTT AGTTTGGTGTGGGCTTTTGGCGGTGTCCTTCACTTTGGGACGGCTGGCCCTTAA

Clavulina-269				AAAACATTAGTGTCTCCTCGTGTGGAACCTGGTTCTACTCAGCGTGATAACAGTCTGATCGC
OTU307	Basidiomycota	Agaricales	Cortinarius	GTCATCGAGTCTTTGAACGCACCTTGGCGTCTTGGTATTCCGAGGAGCATGCTGTTTGAAGTGCATTAATAATCAACCTCTTCAGCTTTGCTTGTGAGTGTGGATGTGGGGGTATCTTTTGTGCTGGTCTCTTTTCTGAGTTCAGCTCCCTAAATAATAAGCGGGACAATTTGTTGACCGTTCATTTGGTGTGATAACTATCTACGCTTTGTGGATTCCTTTG
OTU332	Basidiomycota	Thelephorales	Tomentella	GTCATCGAATCTTTGAACGCACCTTGGCGCTTGGCTATTCCGAAAGGGCATACTGTTTGAAGTATCATGAACACCTCAACTCTCATGGTTTTTCCATGATGAGCTTGGACTTTGGGGTCTTGTGCTGGCCATGGTCAGCTCCTCTTAAATGAATCAGCTTGCCAGTGTGGTGGCATCGCAGGTGTGATAACTATCTACGCTTTGTGGATTTCCGTCAA
OTU335	Basidiomycota	Agaricales	Tricholoma	ATCATCGAATCTTTGAACGCACCTTGGCGTCTTGGTATTCCGAGGAGCATGCTGTTTGAAGTGCATGAATAATCTCAACCTTTTCAACTTTTCAAAAAGTTGGATAAGCTTGGATAGTGGGAGTGTCTGGGGCTTCTCAGAAAGTCTGCTCTCCTTAAATGTATTAGCAGGATCCTTGTATTGCTTTTGGTGTGATAAATTATCTACGCCATAACATGA
OTU336	Ascomycota	Pezizales	Pachyphloides	GTCATCGAATCTTTGAACGCACATTTGGCCCAATGGTATTCCGTTGGGCATACCTGTTTGAAGTATCAGATCCTTTCAATATCAAACTTTTATATATAGAGATGTATGTAAGATGTTTGGAAATAAAGTTGAGAAAAGTAGTATTAATAATCTCTTTCTTAAAAACCAGAAATATTATGTTTGTGATTTTCTTCCACCCTCAITTTTGTATGAAA
OTU347	Basidiomycota	Agaricales	Inocybe	TTTAACA ATCATCGAATCTTTGAACGCATCTTGGCGTCTTGGTATTCCGAGGAGCATGCTGTTTGAAGTGCATTTAAATTTCAAAACCCTTGACAGTGGCTTTGGATGTGGGGCTTGCAGGCTTTCTTCTCAAGTCTGCTCCCTGAAATGCATTAGTGGTATCTGGAGCGGAAACCGCTAGGTGTGATAAATTAATCGTCTACGCCCTTTGGTATGCCGCAIG
Inocybe-347	Agaricomycetes	Inocybaceae	unidentified	GTCATCGAATCTTTGAACGCACATTTGGCCCTTGGTATTCCGAGGAGCATGCTGTTTGAAGTGCATTTCAACCTCAAGCCTAGCTTGGTGTGGCGACGTCCCTTTGGGACCGCTCGAAAACGCTCGGGCGGTGGCACCGGCTTTAAAGCGTAGCAGAAATCTTTCGCTTCAAAAAGTCCGGGCCCTGCTGCCGGAAGACCTACTCGCAAAGTT
OTU364	Ascomycota	Mytilimidales	Cenococcum	ATCATCGAATCTTTGAACGCACATTTGGCCCTTGGTATTCCGAGGAGCATGCTGTTCCGAGCATTTCAACCTCAAGCCTAGCTTGGTGTGGCGACGTCCCTTTGGGACCGCTCGAAAACGCTCGGGCGGTGGCACCGGCTTTAAAGCGTAGCAGAAATCTTTCGCTTCAAAAAGTCCGGGCCCTGCTGCCGGAAGACCTACTCGCAAAGTT
Cenococcum-364	Dothideomycetes	Gloniaceae	Cenococcum geophilum	ATCATCGAATCTTTGAACGCACATTTGGCCCTTGGTATTCCGAGGAGCATGCTGTTCCGAGCATTTAAACACATTTCAAGCTTTTAAATTTCTAGCTTGGTCTTGAGGGATGAGCGAGACAGAAATCGAACITTTTAAACATTTCTTGTCTAGAAATTT
OTU366	Ascomycota	Pezizales	Unidentified	CAGTGGCGGATTTAAGCACAGATTTGGCCCCGGTGTGATACAGTTTTTTCATGTCAATCGTCCAG
unidentified-366	Pezizomycetes	Pyrenomataceae	unidentified	

OTU367 Sebacina-367	Basidiomycota Agaricomycetes	Sebacinales Sebacinaceae	Sebacina unidentified	GTCATCGAGTCTTTGAACGCACCTTGCACCCCTTTGGTATTCCGAAGGGTATGC TCGTTTGAAGTGTCAATGTACTCACACTCTGTGATCCCTTTGGATTCAAGGAGT GGTGGACTTGGGTGTTTGTCTGCTTTCCGGTGGCTCACCTCAAATGCGTTAGTG CACCTCTTGGTTGGACATAGTACGGCGTGATAAGTATCTTCGCCCGGCACCTCG CAAGAGG
OTU389 Tomentella-389	Basidiomycota Agaricomycetes	Thelephorales Thelephoraceae	Tomentella Tomentella cinereoumbrina	GTCATCGAGTCTTTGAACGCACCTTGGCCCCCTTGGCTATTCCGAAGGGCATG CCTGTTGAGLATCATGAACACCTCAAACCTCTCGTGGTTTGGCCATGATGAGCT TGGACTTTGGGGTCTTGTCTGGCCTGTGTTGGCTCCTCTCAAATGAATCAGC TTGCCAGTGTTTGGTGGCATCACAGGTGTGATAACTAICTACGCTTGTGGTTT TCTACCAG
OTU393 Sebacina-393	Basidiomycota Agaricomycetes	Sebacinales Sebacinaceae	Sebacina unidentified	ATCATCGAGTCTTTGAACGCACCTTGCACCCCTTTGGTATTCCGAAGGGTATGC TCGTTTGAAGTGTCAATGTACTCACACTCTGTGATCCCTTTGGATTCAAGGAG CGTGGACTTGGGTGTTTGTCTGCTTCCCTTGTGGCTCACCTCAAATGCGTCAAG TGCATCTCTTGGTTGGACATAGTACGGCGTGATAAGTATCTTCGCCCGGCACCT CGCAAGA
OTU401 Russula-401	Basidiomycota Agaricomycetes	Russulales Russulaceae	Russula Russula rubroalba	ATCATCGAATCTTTGAACGCACCTTGGCCCCCTTGGCAATCCGAGGGGCACAC CCGTTGAGTGTGTAATCATCAAACCTTTCTTTGATCCCTTTTGGTTCGAG AAAGGATTTTGGACTTGGAGGATCAATGCTCACTCACCTTTTGGAAAGTGA GCTCTCTCAAATAAATAGTGGGGTGTGCTTCGCCGATCCCTTGACGTGATA AGTCGTT
OTU408 Tomentella-408	Basidiomycota Agaricomycetes	Thelephorales Thelephoraceae	Tomentella unidentified	ATCATCGAGTCTTTGAACGCACCTTGGCCCCCTTTGGCTATTCCGAAGGGCATG CCTGTTGAGTATCATGAACACCTCAAACCTCTCATGGTTCGCCGTGGTGAAGCTT GGACTTTGGGGTCTTGTCTGGCCTGGGTGGCTCCCTTCAAATGAATCAGCT TTCCAGTGTTTGGTGGCATCACGGGTGTGATAAATACTACGCTTGTGGTTTC CGCCAGGT
OTU414 Craterellus-414	Basidiomycota Agaricomycetes	Cantharellales Cantharellaceae	Craterellus Craterellus lutescens	ATCATCGAGTCTTTGAATGCAATGTGCCCTCTTGGTCCGCTTCCAAATGGGGG TTGACTATAGGGGTACATCTAATTTGAGGGTCAATTTGAATCTCTCAAAGGGT TGGTTAATCTGTCTTTGGATTTTGGGTCTTGTGTGAAAATTCATCTCAGCTT ACCTTGAAGCATTAGCAAGCTGTTCACAGGTCTTTTCTTGATGAGGGCAATCT AACTGGT
OTU426 Cortinarius-426	Basidiomycota Agaricomycetes	Agaricales Cortinariaceae	Cortinarius Cortinarius salor	GTCATCGAGTCTTTGAACGCACCTTGGGCTCCCTTGGTATTCCGAGGAGCATGC CTGTTTGAAGTGTCAATAATAATCAACCTCTTCAGCTTTTGTGTAGAGTGTG GATGTGGGGTGTGTGGCTTCTAAAGGTGAGCTCCCTCAAATAATGCAATTA GCGGAACAAATCTGTTGACTGTTTCATAGTGTGATAAATATCTACATTATTGAA CTGTGAG

OTU429	Basidiomycota	Agaricales	Inocybe	GTCATCGAGTCTTTGAACGCATCTTGGCTCCTTGGTATTTCCGAGGAGCATGCC TGTTGAGTGTCACTAAATTTCAAAACCACATTTGAATTTCTTCAGTGTGGCTT GGAAAGTGGGGTTTATTTTGCAGGCTGGTTTTACATAAAAATGAAGTCTGCTC CCCTGAAATGCAATAGTGTATCTGAGCAGCGGGAACTACTACAGGTGTGATA ATTTA
Inocybe-429	Agaricomycetes	Inocybaceae	Inocybe glabripes	
OTU430	Basidiomycota	Thelephorales	Tomentella	ATCATCGAATCTTTGAACGCACCTTGGCCCTTCTGGCTATTTCCAGAGGGCATGC CTGTTGAGTATCATGAACACCTCAACTCTCATGGTTTTGCCGTGATGAGCTTG GATTTGGAGGTCTTGTGGCCCGTGGTCAGCTCCTCTCAAACGAATCAGCTTG CCAGTGTTTGGTGGCATCACAGGTGTGATAACTATCTACGGCTTGTGGCTTCCAC CAGG
Tomentella-430	Agaricomycetes	Thelephoraceae	Tomentella subclavigera	
OTU449	Basidiomycota	Agaricales	Cortinarius	GTCATCGAGTCTTTGAACGCACCTTGGCTCCTTGGTATTTCCGAGGAGCATGCC TGTTGAGTGTCAITTAATATAATCAACCTTCTCTTTTTGAGTGGTTGGATGTGG GGGTTTGTGGCCTTGAAAGGGTTTCAGCTCCCTGAAATGCAATAGCAGAAC AACCTGTTCATTTGGTGTGATAACTATCTACGGTATTGAATGTAAAGGGGCAG TTCAGC
Cortinarius-449	Agaricomycetes	Cortinariaceae	Cortinarius lucandii	
OTU476	Basidiomycota	Thelephorales	Tomentella	GTCATCGAGTCTTTGAACGCACCTTGGCCCTTGGCTATTTCCGAAAGGGCATGC CTGTTGAGCATATAAACATCAACTCTCATGGTTTCCCGTGTAGAGATTGG ACTTTGGGGTCTTGTGGCTTGTGTTGAGTCCCTCAAAATCTATCAGCTTCC CAGTGTTTGGCGGCTCACAGGTGTGATAAATAATCTACGGCTTGTGGTTCTTTGC CAGG
Tomentella-476	Agaricomycetes	Thelephoraceae	Tomentella ellisii	
OTU501	Basidiomycota	Thelephorales	Tomentella	GTCATCGAATCTTTGAACGCACCTTGGCCCTTGGCCATTTCCGAAAGGGCATGC CTGTTGAGTATCATGAACACCTCAACTCTCATGGTTTCCGTGATGAGCTTG GACTCTGGGGTCTTGTGGCCTGGTGGTCCCTCTCAAATGAATCAGCTTG CCGGTGTTTGGTGGGCATCACAGGTGTGATAAATACTACGGCTTGTGGTTTTCC ACCA
Tomentella-501	Agaricomycetes	Thelephoraceae	unidentified	
OTU507	Basidiomycota	Thelephorales	Tomentella	ATCATCGAGTCTTTGAACGCACCTTGGCCCTTGGCCATTTCCGAAAGGGCATGC CTGTTGAGTATCATGAACACCTCAACTCTCATGGTTCCGCATGATGAGCTTGG ACTTTGGGGCTTGTGGCCTACGGTCCCTCTCAAATGAATCAGCTTGC CAGTGTTTGGTGGCATCACAGGTGTGATAAATACTACGGCTTGGGATTTGCCAC CAGG
Tomentella-507	Agaricomycetes	Thelephoraceae	unidentified	
OTU525	Ascomycota	Pezizales	Hydnobolites	ATCATCGAATCTTTGAACGCACATTTGGCCCTCAATGGCATCTTTCCAGTATGCC CATCTCAGCGTTAGAAAATATTTCAAAATTTAGTTTTGTGCTAAAAATTTGGAT CATGTCAAGGAAGCTATTTCTATTTATTTGATCGCTCTTTGGAAATTAATAGGT CTTTGAGTTACTACTCATAGAATAATTAATACTTTCTTCGTTCCGATTTTAGTTT ACT
Hydnobolites-525	Pezizomycetes	Pezizaceae	unidentified	
OTU574	Ascomycota	Pezizales	Genea	GTCATCGAGTCTTTGAACGCACATTTGGCCCTCTCGTATTTCTGGGGGCATGCCGTTCG AGAGTCATTTACAACAATTTGAAATCCCCCCACCTTCAGTTTGTGTGGGGTGAATCG GTTTGGTTGAGGAGAGACTAACTACTCTCCCTCCCCACCAAAATTCATAGGCAGTC TGTGTTTTGTAAACCTTGGATAATGTTATTGGCGTGTAAA
Genea-574	Pezizomycetes	Pyronemataceae	Genea darii	

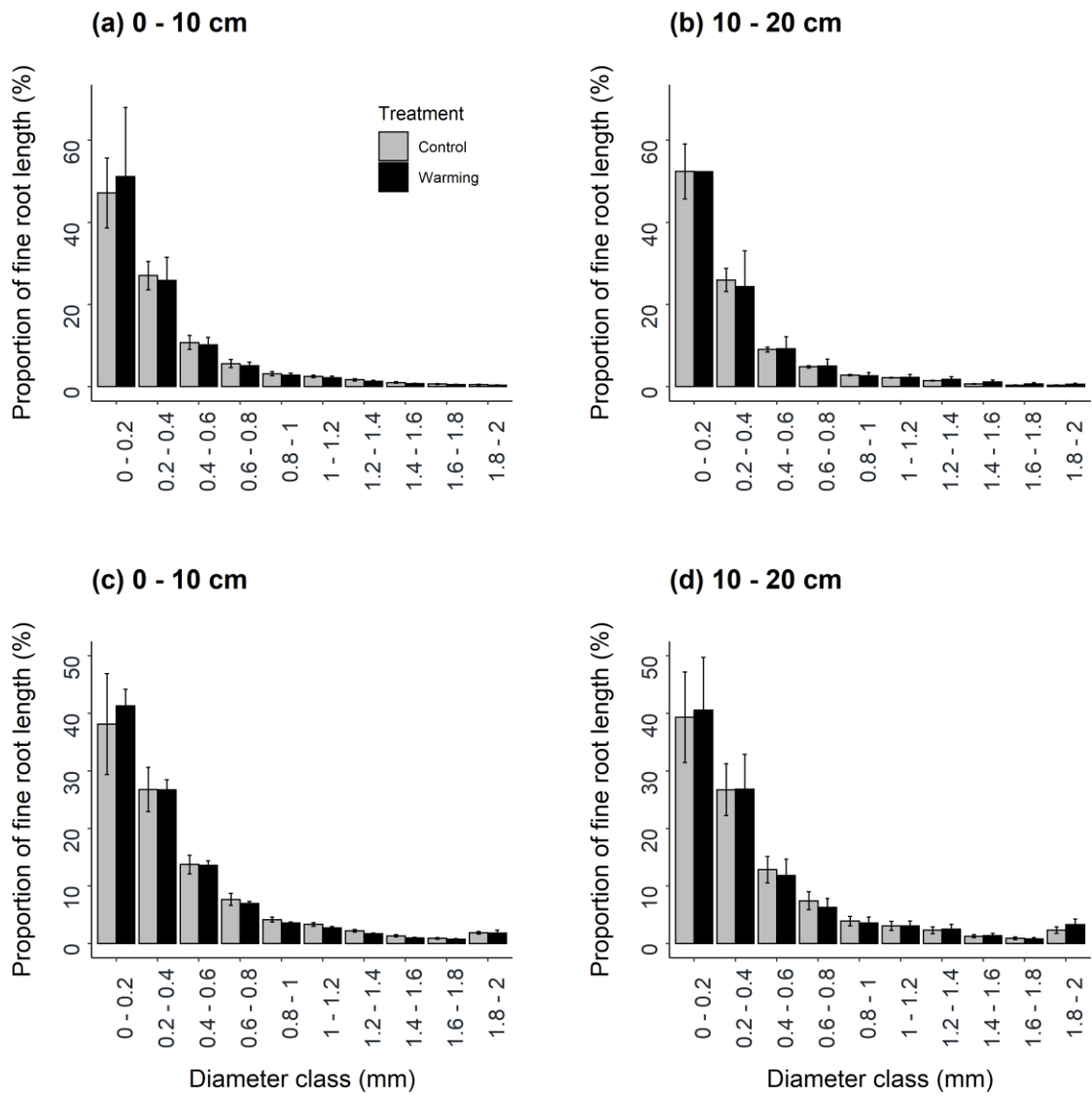


**Figure S1:** Proportion (means  $\pm$  SE) of fine root length per diameter class at 0 – 10 and 10 – 20 cm soil depth in control and warmed plots in 2012 (panels a and b) and 2019 (panels c and d).

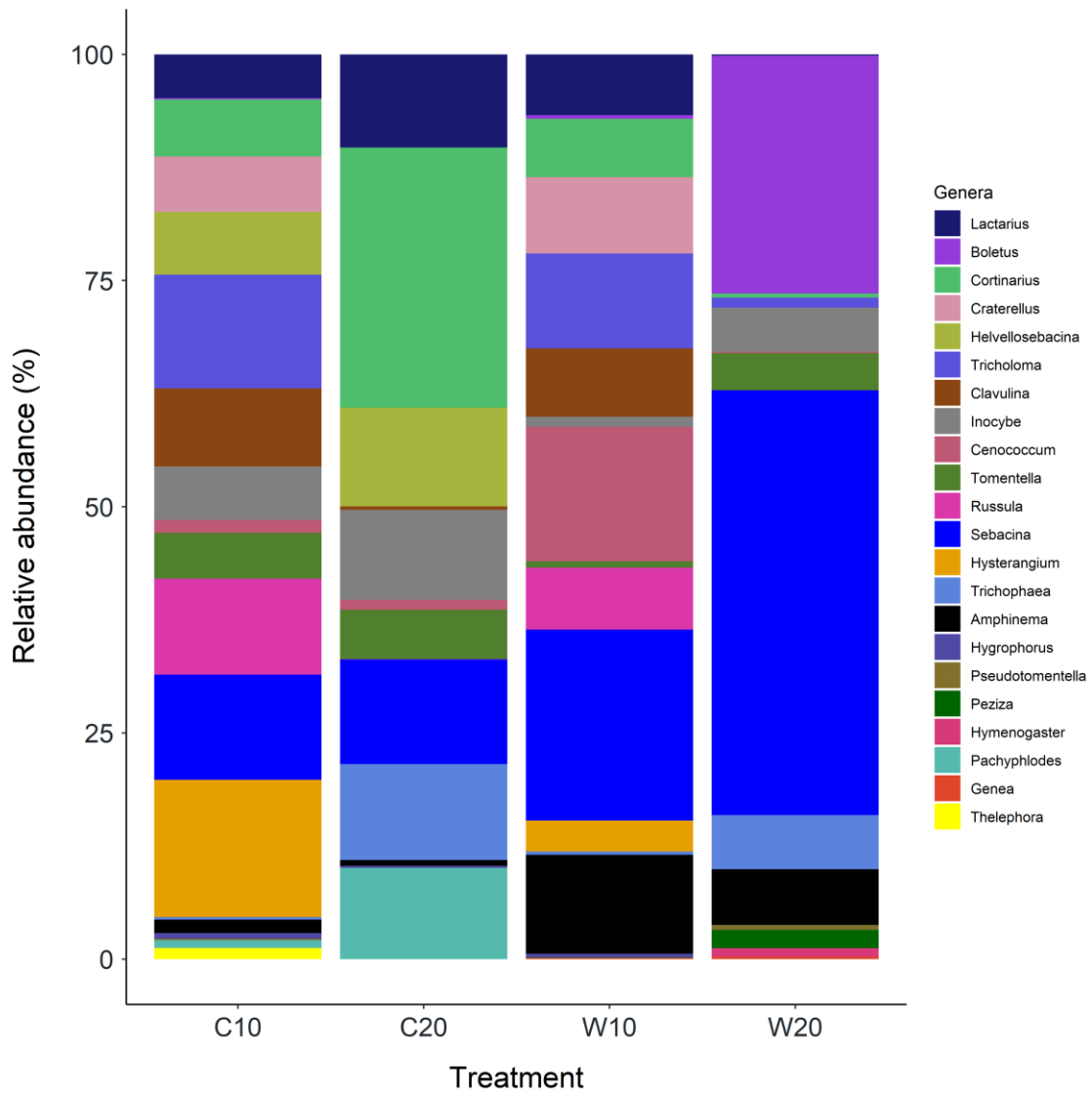


**Figure S2:** Relative abundance of ectomycorrhizal fungal genera across all samples. Abbreviations: C10 – control at 0 – 10 cm soil depth; C20 – control at 10 – 20 cm soil depth; W10 – warming at 0 – 10 cm soil depth; W20 – warming at 10 – 20 cm soil depth.

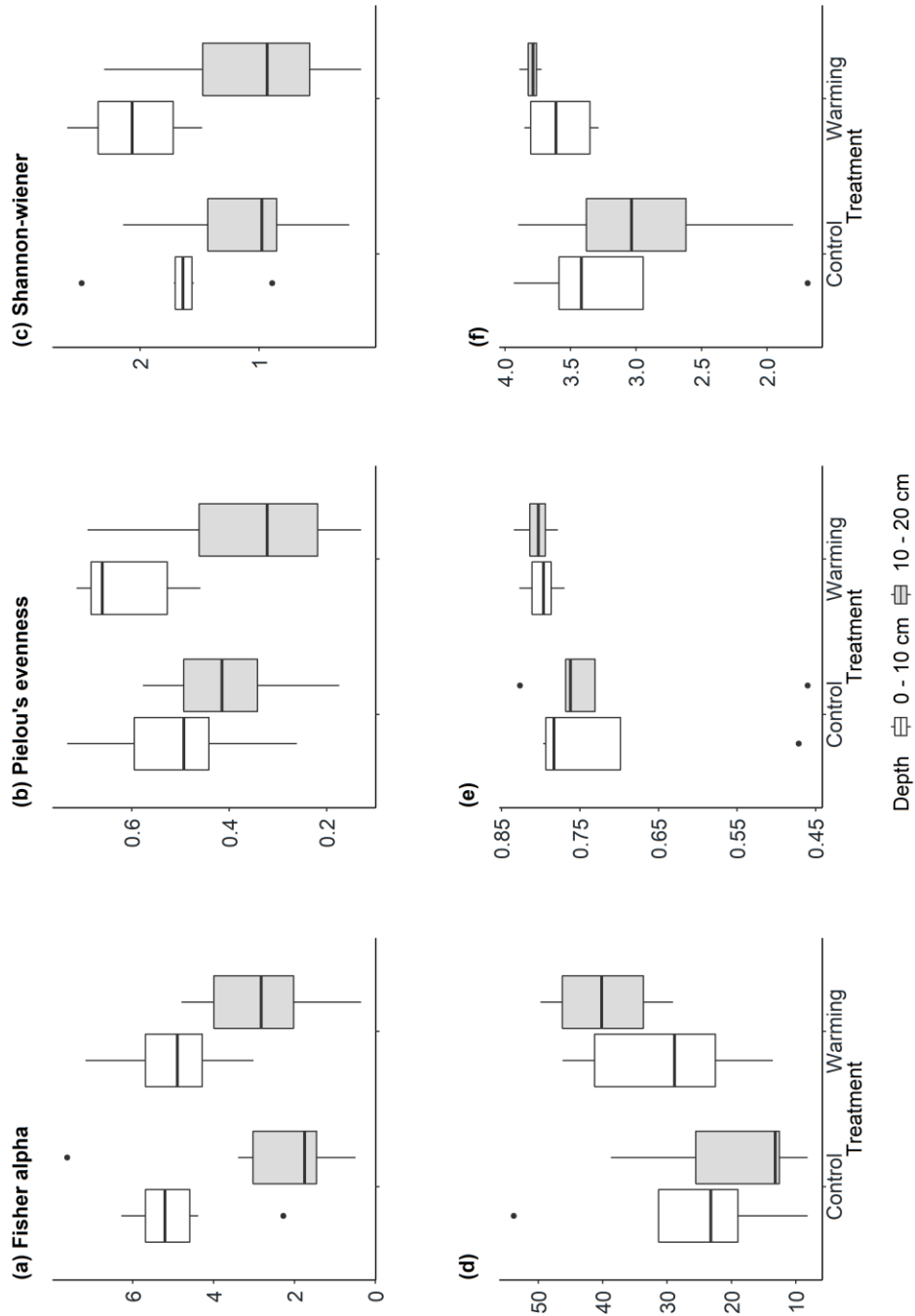


**Figure S3:** Boxplots showing genus-level fungal and bacterial diversity indices in control and warmed plots at 0 – 10 and 10 – 20 cm soil depth. Fungal diversity indices are displayed in panels a, b, c, and bacterial diversity indices in panels d, e, f, respectively.

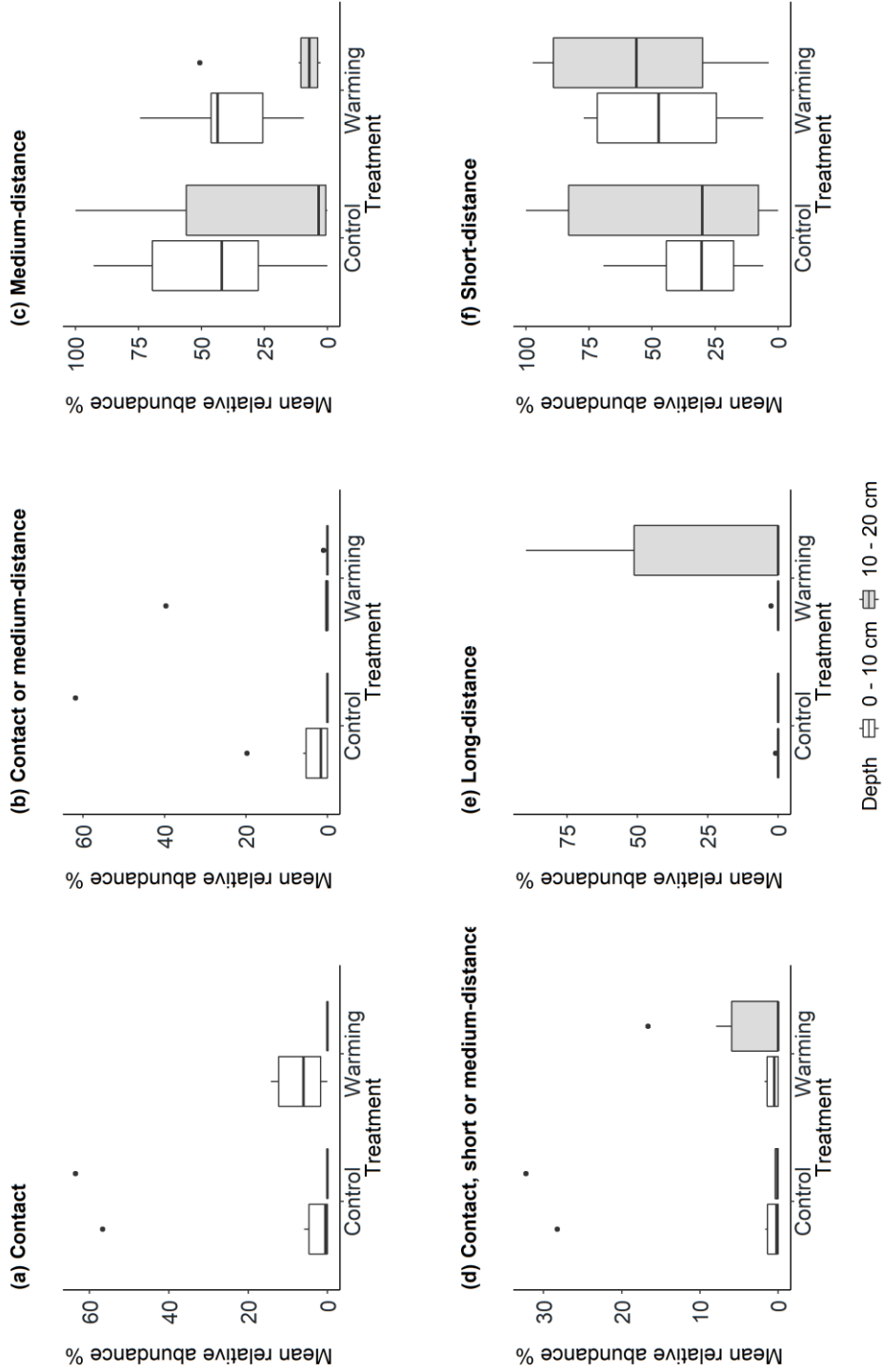


**Figure S4:** Box plots showing mean relative abundances (%) of ectomycorrhizal fungi grouped by different exploration types in control and warmed plots at 0 – 10 and 10 – 20 cm soil depth.

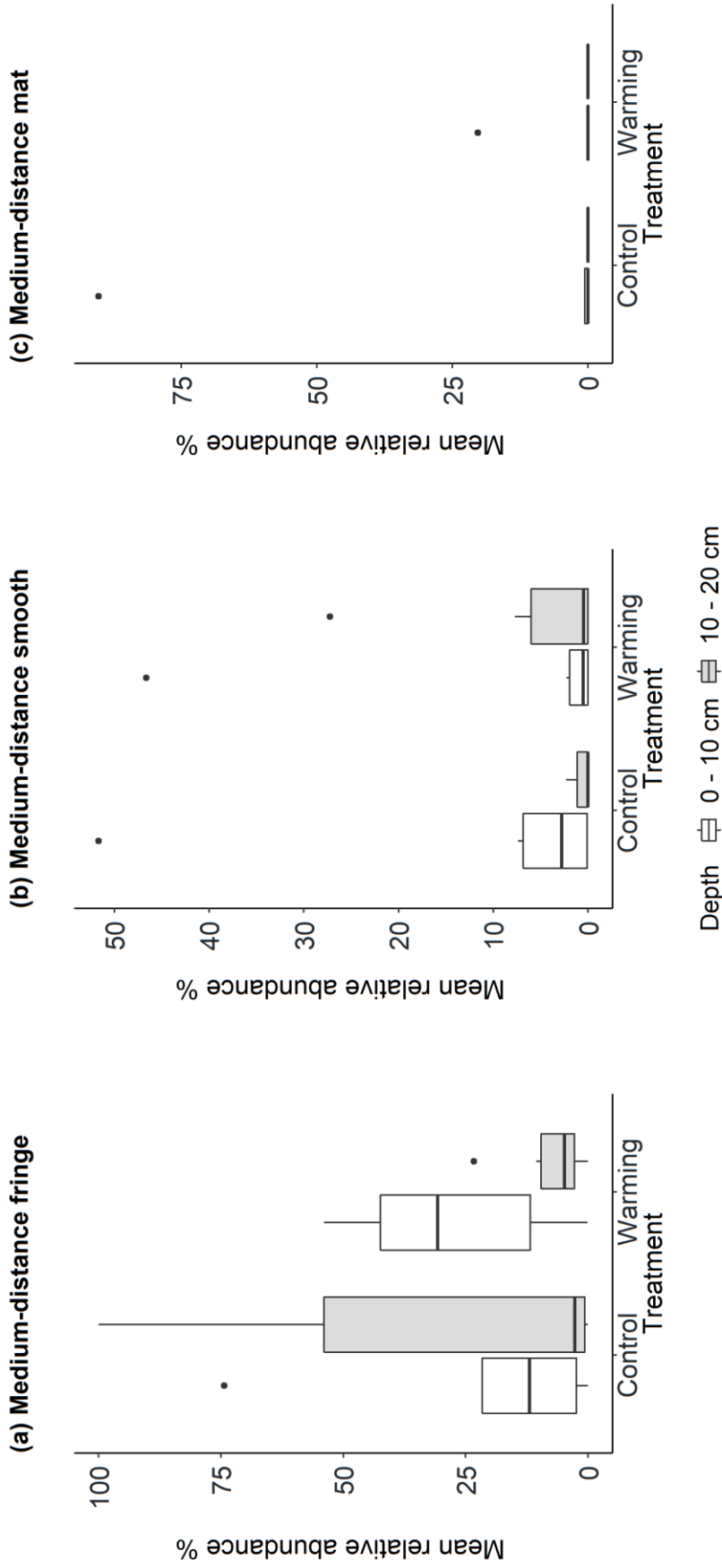


**Figure S5:** Box plots showing mean relative abundances (%) of the medium-distance exploration type grouped into (a) medium-distance fringe, (b) medium-distance smooth and (c) medium-distance mat, in control and warmed plots at 0 – 10 and 10 – 20 cm soil depth.

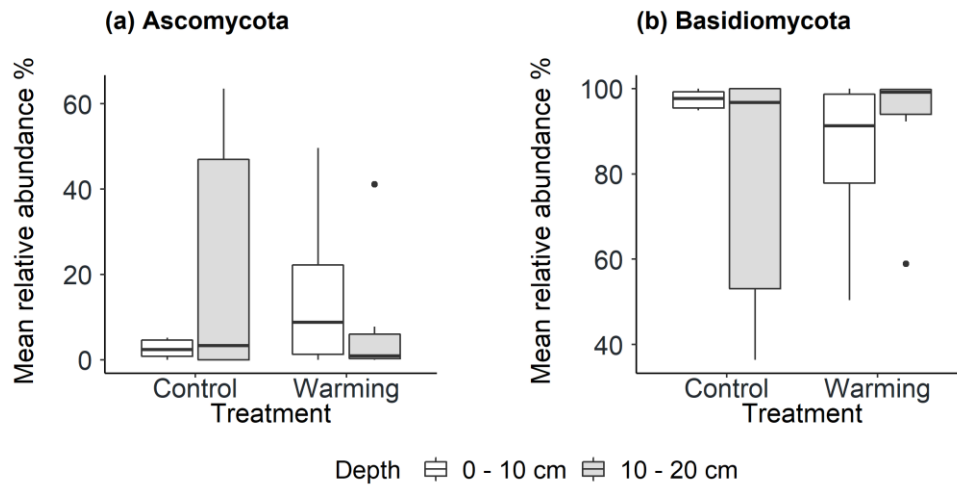


**Figure S6:** Box plots showing mean relative abundances (%) of ectomycorrhizal fungi grouped by phylum in control and warmed plots at 0 – 10 and 10 – 20 cm soil depth.

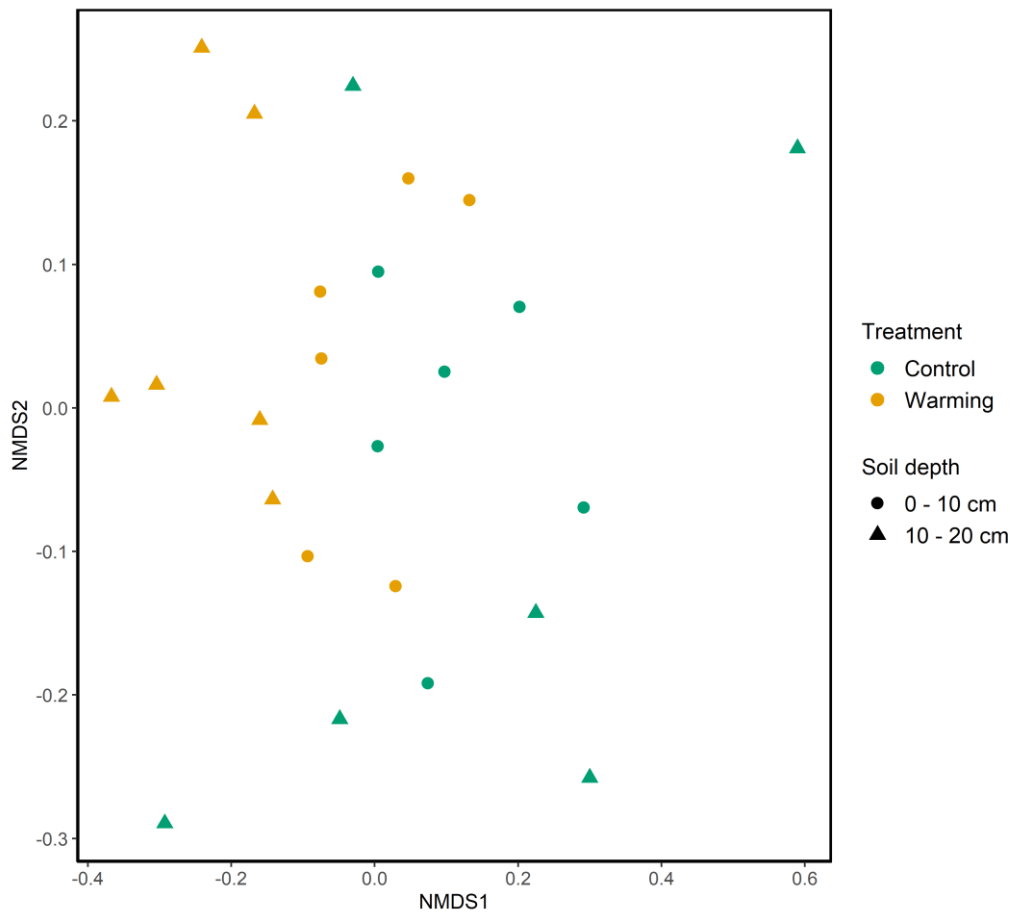


**Figure S7:** Non-metric multidimensional scaling (NMDS) plot of the ectomycorrhizal fungal communities. Points in ordination space represent individual plots based on Bray-Curtis dissimilarity indices.

## **Study II**

### **Increase in carbon input by enhanced fine root turnover in a long-term warmed forest soil**

Steve Kwatcho Kengdo\*, Bernhard Ahrens, Ye Tian, Jakob Heinzle, Wolfgang Wanek, Andreas Schindlbacher, Werner Borken (2023)

Published in *Science of The Total Environment* 855: 158800

DOI : <https://doi.org/10.1016/j.scitotenv.2022.158800>

\* Corresponding author

**ABSTRACT**

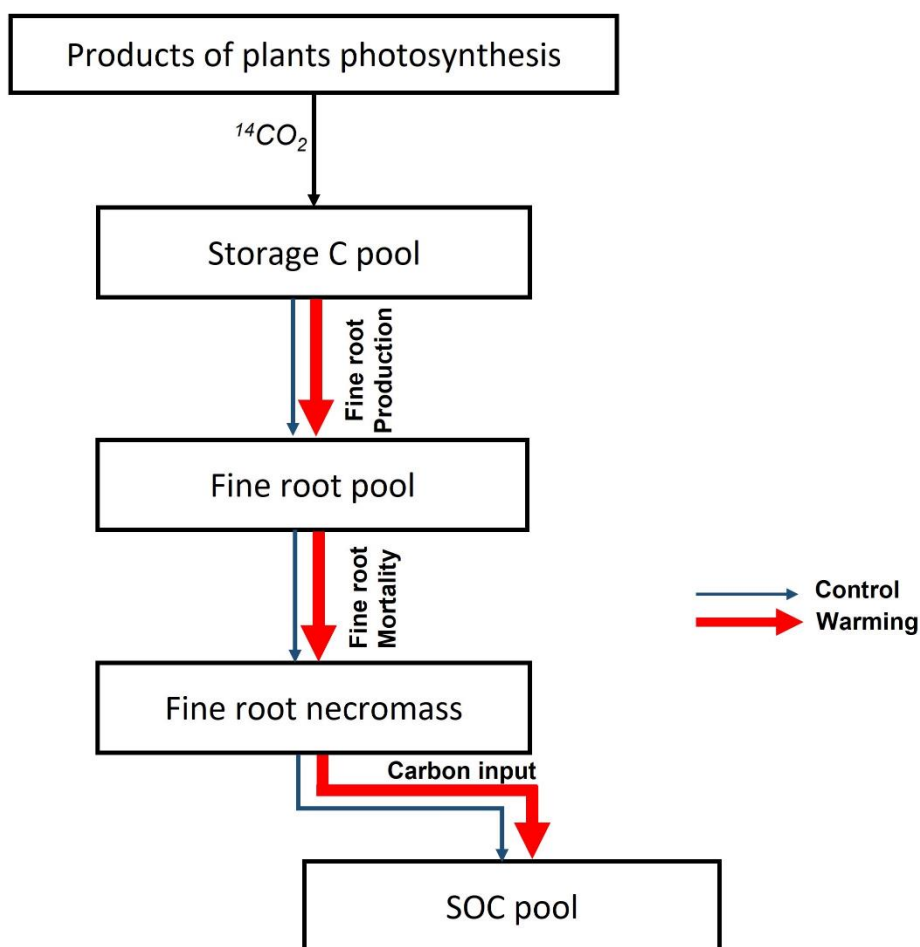
Fine root litter represents an important carbon input to soils, but the effect of global warming on fine root turnover (FRT) is hardly explored in forest ecosystems. Understanding tree fine roots' response to warming is crucial for predicting soil carbon dynamics and the functioning of forests as a sink for atmospheric carbon dioxide (CO<sub>2</sub>). We studied fine root production (FRP) with ingrowth cores and used radiocarbon signatures of first-order, second- to third-order, and bulk fine roots to estimate fine root turnover times after 8 and 14 years of soil warming (+4°C) in a temperate forest. Fine root turnover times of the individual root fractions were estimated with a *one-pool* model. Soil warming strongly increased fine root production by up to 128% within one year, but after two years, the production was less pronounced (+35%). The first-year production was likely very high due to the rapid exploitation of the root-free ingrowth cores. The radiocarbon signatures of fine roots were overall variable amongst treatments and plots. Soil warming tended to decrease fine root turnover times of all the measured root fractions after 8 and 14 years of warming, and there was a tendency for trees to use more old carbon reserves for fine root production in warmed plots. Furthermore, soil warming increased fine root turnover from 50 to 106 g C m<sup>-2</sup> yr<sup>-1</sup> (based on two different approaches). Our findings suggest that future climate warming may increase carbon input into soils by enhancing fine root turnover. If this increase may partly offset carbon losses by increased mineralization of soil organic matter in temperate forest soils is still unclear and should guide future research.

**Keywords:** climate warming; fine root production; ingrowth cores; radiocarbon signatures; soil organic matter; carbon dioxide.

**HIGHLIGHTS**

- The effects of soil warming on fine root production and turnover were studied in a temperate forest.
- Ingrowth cores, soil coring, and radiocarbon methods were combined in this study.
- Soil warming increased fine root production; fine roots tended to turn over faster with warming.
- Increased root litter input into the soil may compensate for the carbon losses by soil respiration.

**GRAPHICAL ABSTRACT**



## 1. Introduction

A large proportion of the carbon (C) fixed during photosynthesis in forests is allocated to the production of fine roots (< 2 mm in diameter), which represent the primary pathway for plant water and nutrient uptake from the soil (Jackson et al., 1997). When they die, root C accumulates in the soil or is mineralized by heterotrophic soil organisms and released back to the atmosphere as carbon dioxide (CO<sub>2</sub>) (Figure 1). Through this process, fine root production (FRP) and fine root turnover (FRT) are key components of C and nutrient cycling in forest ecosystems (Gill & Jackson, 2000).

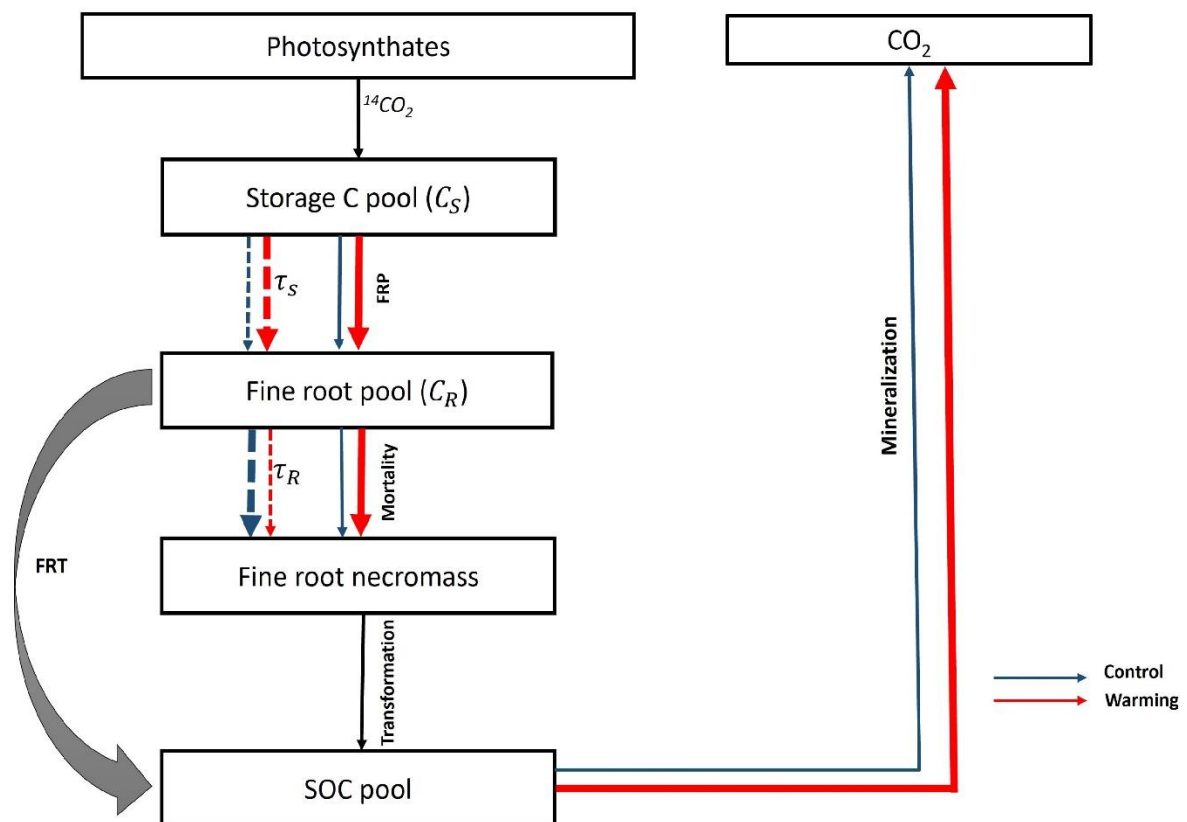


**Figure 1:** Conceptual relationship between storage C, FRP, and FRT. Black arrows represent processes we did not measure in this study. Blue and red (solid and dashed) arrows represent the magnitude of the respective processes in control and warmed plots. They reflect the hypotheses of the study or observations based on literature. In this flow chart, recent photosynthates (<sup>14</sup>CO<sub>2</sub>) can be stored in the storage C pool for an extended period and used later for FRP (FRP refers to the mass of new fine root produced per unit area per unit time; g

$\text{m}^{-2} \text{ year}^{-1}$ ). Following fine root dieback, root detritus are decomposed by soil microorganisms, and root C either accumulates in the soil organic carbon pool (SOC) (not measured in this study) or is released back to the atmosphere as respired  $\text{CO}_2$  (size of the arrows based on Schindlbacher et al. (2009) ). The storage C pool is a well-mixed carbohydrate pool of equal turnover time in one or more locations on the tree (Riley et al., 2009). This includes C stored in leaves, needles, stems, and roots. However, in this study, we will limit our understanding of the storage pool as a pool of stored C in fine roots, as we do not have data on storage C in other tree locations. The turnover time (unit in years) refers to the time it would take to renew all mass in a pool. This is represented by two parameters:  $\tau_S$  and  $\tau_R$  which are the steady-state turnover time of the storage pool ( $C_S$ ), and the fine root pool ( $C_R$ ), respectively. FRT refers to the flux of C from fine roots into soil per unit area per unit time;  $\text{g m}^{-2} \text{ year}^{-1}$  (Pregitzer et al., 2007).

Projected climate warming (IPCC, 2021) may change FRP and FRT, therefore strongly impacting forest C dynamics (Lukac, 2012). However, the contribution of fine roots to soil C in temperate forests remains poorly quantified (Brunner et al., 2013; Lynch et al., 2013; Rasse et al., 2005), especially in the context of global warming. This is mainly due to the variability of fine root turnover times and methods used to measure FRP and turnover, owing to the difficulties of measuring those processes accurately (Lukac, 2012). Our recent findings showed that soil warming increased fine root biomass (FRB) and changed fine root morphology towards thinner and longer roots with a greater absorptive surface (Kwatocho Kengdo et al., 2022). In addition, soil warming persistently increased soil  $\text{CO}_2$  efflux by ca. 40%, with roots contributing 35 - 40% of the total  $\text{CO}_2$  efflux (Schindlbacher et al., 2009; Schindlbacher et al., 2012). Taken collectively, those findings suggest that FRP may increase, and fine roots may turn over faster in warmed soils. However, the magnitude of the response may vary between forest ecosystems and the duration of warming experiments.

Other studies have pointed out that FRP and FRT may increase with warming (Eissenstat et al., 2000a; Finér et al., 2011; Gill & Jackson, 2000). This is because warming increases root maintenance respiration (Pregitzer et al., 2000) and soil nutrient availability (Melillo et al., 2002; Melillo et al., 2011). However, a recent global meta-analysis revealed that FRP increased while FRT was unresponsive to warming across a range of terrestrial ecosystems, accompanied by an increase in root respiration (J. Wang et al., 2021). This was mainly explained by the low number of available studies and the increase in FRB, which slightly balanced FRP. The relationship between FRP and FRT in the context of climate warming is primarily related to

the increase in C input and C storage in soil. This is because increased FRP and fine root litter input with warming may enhance soil organic matter stabilization (Lützow et al., 2006) and partially offset soil C losses by increased mineralization (M. Lu et al., 2013). However, to date, very few studies have looked at the effect of soil warming on FRP and FRT in temperate forests, though this information is crucial for understanding the whole-plant C allocation and predicting how terrestrial C cycling will respond to global climate warming (J. Wang et al., 2021).

The ingrowth method has been commonly used to estimate FRP in forests (Lukac, 2012). This method uses ingrowth cores with suitable mesh sizes and filled with root-free soil to measure FRP at two-time points, the start and the end of the incubation period of the cores in the field. Ingrowth cores are usually inserted into the soil and left for a short period (usually one to two years), sampled, and new roots in the cores are washed free of soil (Ostonen et al., 2005). However, the physical disturbance of the soil in ingrowth cores versus the undisturbed surrounding soil is one of the drawbacks of this method.

FRT has initially been measured with various approaches (Gaul et al., 2008; Lukac, 2012; Majdi et al., 2005). Among those, the radiocarbon ( $^{14}\text{C}$ ) method estimates fine root turnover times by comparing the  $^{14}\text{C}$  content of fine roots with the recorded atmospheric  $^{14}\text{CO}_2$  value of their year of sampling (Gaudinski et al., 2001). This interesting approach not commonly applied in root dynamics studies uses the natural level of atmospheric  $^{14}\text{CO}_2$ , a radioactive isotope of C that accounts for a small fraction of atmospheric C. The atmospheric  $^{14}\text{C}$  peaked in the 1960s due to nuclear bomb testing. This "bomb-peak" can be used to estimate the mean age of fine root C, representing the time elapsed since the C fixed from the atmosphere by photosynthesis was used to produce new roots (Schuur et al., 2016). This approach has revealed that fine roots may live longer than the 10-month average turnover time determined by Gill and Jackson (2000) in their meta-analysis. Gaudinski et al. (2001) and Helmisaari et al. (2015) used bomb  $^{14}\text{C}$  and estimated fine root turnover times between 3 and 18 years in a temperate forest and up to 14 years in a boreal forest, respectively, while Solly et al. (2018) reported fine root turnover times of 3 – 20 years in temperate beech forests.

The C used to produce new fine roots was thought to originate from current photosynthates during the year of their growth (Gill & Jackson, 2000). However, recent evidence showed that newly produced fine roots contained cellulose with radiocarbon signatures higher than that of the atmosphere, highlighting the importance of a storage pool containing relatively old C in the tree (Helmisaari et al., 2015). Therefore, the radiocarbon signature of fine roots is determined

by the mixture of recently fixed photosynthates and stored C. As a result, an attempt to estimate fine root turnover times should account for this bias (Ahrens et al., 2014; Gaudinski et al., 2009; Yiqi Luo, 2003; Yiqi Luo et al., 2004).

Because of the complexity of the fine root system in terms of functions (McCormack et al., 2015), branching patterns (Baddeley & Watson, 2005; Guo et al., 2008), tissue substrate chemistry (Guo et al., 2004; Xia et al., 2010), there is a need to accurately estimate fine root turnover times according to different fine root fractions (Joslin et al., 2006; Lynch et al., 2013). This is because the individual fine roots of the fine root system may cycle at a different rate, translating into different turnover patterns (Gill & Jackson, 2000; Guo et al., 2008). First-order fine roots differ in cellulose and nutrient contents, mycorrhizal colonization, respiration, and nutrient absorption rates relative to higher-order roots (Eissenstat et al., 2000a; McCormack et al., 2015). Another factor that might strongly influence FRT is soil depth, which directly affects soil physico-chemical properties, litter quality and quantity, and the composition of soil and root-associated microbial communities. In this regard, recent findings at the study site revealed that soil depth affected ectomycorrhizal and root-associated bacterial community composition (Kwatocho Kengdo et al., 2022). Although Gaudinski et al. (2001) suggested that fine root turnover times tended to increase with increasing soil depth, studies linking fine root turnover times and soil depth in soil warming experiments are missing.

We took advantage of a long-term (15 years) forest soil warming experiment at Achenkirch, Tyrol, Austria, to examine the effect of soil warming on FRP and fine root turnover times of different fine root fractions (first-order, second- to third-order, and bulk fine roots) collected in 2012/13 and 2019/20/21. We combined different fine root sampling methods with the aim of improving our understanding of fine root dynamics over time in a long-term warmed temperate forest. We hypothesized that (1) experimental soil warming increases FRP because of the observed positive response of FRP to warming globally (J. Wang et al., 2021). This is because root activity and nutrient turnover increase with warming. Furthermore, we expected (2) a decrease in fine root turnover times with soil warming because of increased root activity and higher fine root maintenance costs in warmed plots (Eissenstat & Yanai, 1997; McCormack & Guo, 2014). The higher root activity decreases the turnover time, and this is associated with higher costs to maintain the fine root system.

## 2. Materials and methods

### 2.1 Site description

The study site belongs to the long-term soil warming experiment at Achenkirch, Tyrol, in the Austrian Limestone Alps (47°34'50" N; 11°38'21" E). The vegetation is a 140-year-old mountain forest dominated by Norway spruce (*Picea abies* L. H.Karst.), interspersed by European beech (*Fagus sylvatica* L.) and silver fir (*Abies alba* Mill.) (Schindlbacher et al., 2007). The mean annual air temperature and precipitation were 7 °C and 1493 mm (1988 - 2017), respectively. The soils are a mosaic of shallow Chromic Cambisols and Rendzic Leptosols, with high carbonates and a near-neutral pH of 6.9 – 7.0. The mineral A-horizon has a thickness of about 15 – 20 cm. The C-horizon is derived from dolomite. The A-horizon had a C:N ratio between 15 and 18 and stored approximately 120 Mg C ha<sup>-1</sup>. The L/F- horizons stored about 10 Mg C ha<sup>-1</sup> (Schindlbacher et al., 2011).

### 2.2 Soil warming experimental setup

The Achenkirch soil warming setup comprised six blocks of paired 2 × 2 m plots (each pair consisted of one control and one warmed plot), established in 2004 (n=3) and 2007 (n=3). Six plots were warmed (hereafter called warming treatment) using resistance heating cables (Etherma, Salzburg, Austria) buried at 3 cm mineral soil depth, with a spacing between cable lines of ~ 7.5 cm. In the remaining six plots (hereafter called control treatment), dummy cables were installed but not heated to account for the disturbance created by their installation. The warming system was controlled by a service unit that automatically kept a +4 °C difference between the control and warming plots throughout the snow-free seasons (from April to December) (Schindlbacher et al., 2007; Schindlbacher et al., 2009). Soil moisture content was not affected in the warmed plots because the high precipitation at this location usually reset any decrease in soil moisture (Schindlbacher et al., 2012).

### 2.3 Fine roots sampling and processing

#### 2.3.1 Soil cores

We conducted fine root (< 2mm in diameter) sampling in October 2012 and October 2019. Ten soil cores were randomly sampled at 0 – 10 and 10 – 20 cm soil depth from each control and warmed plot using a cylindrical soil corer (5 cm in diameter and 20 cm in length). We sampled

six plots in 2012 (n=3) and all the twelve plots in 2019 (n=6), following the addition of new plots (a total of 120 and 240 samples per occasion, respectively). Samples were stored in cooling boxes and transported to the laboratory in Bayreuth, Germany, where they were washed and sorted into live (reddish, resistant fine roots with several lateral root tips) and dead roots (fine roots dark in color and easily breakable) under a microscope. Dead fine roots were oven-dried at 60°C for three days, and fine root necromass was calculated on a soil area basis (g m<sup>-2</sup>).

According to their branching hierarchy, we separated live roots sampled in October 2019 into three different fractions: first-order, second- to third-order, and bulk fine roots (homogenous sample containing all fine roots < 2 mm). Intact root samples of each plot were placed in a petri dish and carefully examined under the microscope to determine mycorrhizal root colonization, and mycorrhizal tips were excised using scalpels. The percentage of EcM colonization in a root sample was calculated as:

$$EcM \text{ colonization } (\%) = 100 \times \frac{\text{number of EcM root tips}}{\text{total number of root tips}}$$

Care was taken to clean the scalpel between samples to avoid cross-contamination. Following Pregitzer et al. (2002), the most distal unbranched roots were classified as first-order, and the second-order began at the intersection of two first-order roots, and so on. To form homogenous bulk fine root samples, subsamples of the ten replicates per plot and depth were thoroughly mixed. There was no order-based separation, and only the bulk was considered for live roots sampled in October 2012. Samples of first-order, second- to third-order and bulk fine roots were oven-dried at 60 °C for three days.

### **2.3.2 Ingrowth cores**

In October 2019, we inserted five polypropylene mesh tubes per plot (Ø 5 cm, length 20 cm, mesh size 6 mm × 4 mm), hereafter referred to as "ingrowth cores", in the holes created by the soil coring as described above. Mesh tubes were filled with homogenous root-free mineral sieved soil from the same site. Ingrowth cores installed in October 2019 were sampled twice: three ingrowth cores per plot were taken in October 2020 (after one year) and the remaining two in October 2021 (after two years). In 2012, the goal was to determine the radiocarbon signatures of freshly produced fine roots and estimate short-term responses of FRP to soil warming. Ingrowth cores installed in October 2012 were sampled in June 2013 (after 8

months), immediately reinstalled, and then resampled in October 2013 (after 4 months). FRP between October 2012 and October 2013 cannot be extrapolated to annual rates because the disturbance by sampling and re-installation of ingrowth cores in June 2013 interrupted the natural seasonal growth process. Roots grown into ingrowth cores were also hand-washed free from soil. Only fine roots from ingrowth cores sampled in October 2021 were sorted into live and dead roots based on the color, presence or absence of root tips, and root elasticity. Samples were finally oven-dried at 60°C for three days, and FRP was calculated on a soil area basis ( $\text{g m}^{-2} \text{yr}^{-1}$ ).

#### **2.4 Radiocarbon sample preparation and analysis**

Subsamples of live fine roots of first-order, second- to third-order (from October 2019), bulk fine roots (from October 2012 and October 2019), and root ingrowth cores (from October 2013, October 2020 and October 2021) were weighed into 16 ml glass tubes and pre-treated with an Acid-Base-Acid (ABA) treatment to remove any easily hydrolyzable C that may potentially post-date fine root formation (Gaudinski et al., 2001). The protocol used was adapted from internal technical reports of the Keck-CCAMS Facility at the University of California, Irvine, USA (<https://www.ess.uci.edu/~ams/Protocols.htm>; last accessed on August 17, 2022) and further described in the supplementary information.

We converted the C contained in fine root samples into graphite using the sealed-tube zinc reduction method (X. Xu et al., 2007). Fine root samples representing 2 – 3 mg C were combusted with copper oxide (CuO, 0.65 × 3 mm, Merck KGaA, 64271 Darmstadt, Germany) and silver wire (1.0 mm, ThermoFisher GmbH, 76870 Kandel, Germany) in sealed 6 mm O.D quartz tube (pre-baked) at 900°C for 3 hours. After combustion, the CO<sub>2</sub> contained in the tube was cryogenically extracted and purified using the vacuum line at the Soil Ecology Laboratory, University of Bayreuth, Germany. The vacuum line was composed of a turbopump (TSU 261, Pfeiffer vacuum GmbH, 35614 Asslar, Germany), water, and CO<sub>2</sub> traps. The combusted quartz tube is cracked in the tube cracker, and a dewar filled with dry ice and ethanol (- 78° C) freeze-out water in the first trap. In the second trap, a dewar filled with liquid nitrogen (- 196° C) is used to freeze-out CO<sub>2</sub>, and other by-products of combustion like oxides of nitrogen (NO<sub>x</sub>), volatile organic compounds (VOCs), sulfur oxides (SO<sub>x</sub>), carbon monoxide (CO) are just pumped away. Approximately 0.7 – 0.9 mg C as CO<sub>2</sub> was transferred into pre-baked reaction tubes, then torch-sealed and baked at 550°C for 7.5 hours. Each reaction tube comprises a 9 mm O.D, 150 mm long Duran glass tube, and a 6 mm O.D, 50 mm long culture tube. In the 9

mm O.D tube, approximately 30 – 35 mg zinc powder (Zn, Sigma Aldrich Chemie GmbH, 89555 Steinheim, Germany) and 10 – 15 mg titanium hydride (TiH<sub>2</sub>, Johnson Matthey GmbH & Co.KG, 76185 Karlsruhe, Germany) were weighed and used as reagents; and in the 6 mm O.D tube, 3 – 5 mg of iron (Fe) was weighed and used as catalyst, and this is where the graphite forms at the end of the reaction. To control the quality of samples extracted with our vacuum line, we processed samples along with blanks and standard reference materials provided by the US National Institute of Standards and Technology (NIST) and the International Atomic Energy Agency (IAEA). We used secondary standards like OX II (oxalic acid; SRM 4990c, NIST), C7 (oxalic acid, IAEA-C7), ANU (sucrose, IAEA-C6); and a blank like acetanilide (Merck KGaA, 64271 Darmstadt, Germany). The graphites obtained were pressed into aluminum targets and sent for analysis to the Keck-CCAMS Facility at the University of California, Irvine, USA, where the radiocarbon signatures of fine roots were measured using accelerator mass spectrometry (AMS, 0.5MV 1.5SDH-2 Pelletron, National Electrostatics Corporation, Middleton, Wisconsin, USA). Radiocarbon results in this study are expressed as  $\Delta^{14}\text{C}$  (in ‰, or parts per thousand), including a correction of sample  $\delta^{13}\text{C}$  value of – 25‰. This correction removes the effects of mass-dependent isotopic fractionation caused by photosynthetic isotope discrimination (Stuiver & Polach, 1977). The  $^{14}\text{C}$  enrichment of a sample is measured as a fraction of the  $^{14}\text{C}$  activity relative to a modern standard of fixed isotopic composition.

## **2.5 Fine root turnover time modeling approach**

### ***2.5.1 Atmospheric $^{14}\text{C}$ forcing data***

A time series of atmospheric  $^{14}\text{C}$  was constructed by performing a linear interpolation of the  $^{14}\text{C}$  record of atmospheric CO<sub>2</sub> measured at the Hohenpeißenberg (2015 - 2020) (Kubistin et al., 2021) and the Schauinsland stations (1986 - 2016) located in the South of Germany (Hammer & Levin, 2017). The result was bound to the Intcal13 dataset, containing Northern hemisphere atmospheric  $\Delta^{14}\text{C}$  for years before 1986 (Reimer et al., 2013). The Schauinsland (47°55'N; 7°54'E) and the Hohenpeißenberg (47°80'11"N; 11°02'46"E) datasets were best suited because of their proximity to the Achenkirch site.

### ***2.5.2 Model structure***

We first tried a *serial-three-pool* model where recent photosynthates pass through a storage C pool where C is drawn to grow a pool of first-order roots, which either die or become suberized and enter the second- to third-order root pool. The latter follows the same path and enters the bulk root pool. However, it was difficult to consistently fit the 2012 and 2019 data with this *serial-three-pool* model. Therefore, the mean age of first-order, second- to third-order, and bulk fine roots was estimated using a *one-pool* model with a storage pool (Figure 1). This model assumes that the probability of death is the same for all fine roots, regardless of their ages. Because old C reserves can also be used to produce new fine roots (Gaudinski et al., 2001), we used  $^{14}\text{C}$  of fine roots from ingrowth cores sampled in October 2013 and October 2020, respectively, to constrain the turnover time of C in the storage pool. Therefore, fine root turnover times reported in this study are unbiased estimates because they account for storage C and represent the time C spent in fine roots after their formation.

The dynamics of  $^{14}\text{C}$  in the storage and the fine root pools can be modeled with the following equations:

$$\frac{d^{14}C_S(t)}{dt} = I_{14c}(t) - \frac{^{14}C_S(t)}{\tau_S} - \lambda \times ^{14}C_S(t) \quad (1)$$

$$\frac{d^{14}C_R(t)}{dt} = \frac{^{14}C_S(t)}{\tau_S} - \frac{^{14}C_R(t)}{\tau_R} - \lambda \times ^{14}C_R(t) \quad (2)$$

with  $^{14}\text{C}$  in the storage pool ( $C_S$ ) being described by the photosynthetic fixation of atmospheric  $^{14}\text{C}$ ,  $I_{14c}(t)$ , and the storage turnover time  $\tau_S$  (Equation 1).  $I_{14c}(t)$  is a time-dependent column vector describing the atmospheric  $^{14}\text{C}$  at time  $t$  (in years). Similarly, the dynamic of  $^{14}\text{C}$  in the fine root pool ( $C_R$ ) is represented by equation (2) with fine root turnover time,  $\tau_R$  (Figure 1). Measured radiocarbon signatures of fine roots from ingrowth cores and fine roots sampled from soil cores at time  $t$  are represented by  $^{14}C_S(t)$  and  $^{14}C_R(t)$ , respectively. The radioactive decay of  $^{14}\text{C}$  in both compartments is represented by  $\lambda$ , the radioactive decay constant ( $1/8267 \text{ yr}^{-1}$ ).

### 2.5.3 Initial conditions, model calibration, and performance

The parameters  $\tau_S$  and  $\tau_R$  were estimated using the Nelder-Mead method (max. iterations = 3000). The model fit relies on minimizing residuals between modeled and measured  $\Delta^{14}\text{C}$  signatures for all years in the modeled time window (Figure S2). The goodness of fit was assessed by examining the sum of squared residuals (SSR) and convergence. We only report

results where calibrations had  $SSR < 2$ . The calibration did not work well in two control plots (plots n° 4 and 6), and a satisfactory fit between modeled and measured  $\Delta^{14}C$  signatures could not be achieved. As a result, they were excluded from subsequent analyses. In the calibration, initial parameter values of the model, i.e., the turnover time of the storage ( $\tau_S$ ) and the fine root pools ( $\tau_R$ ) were both set to equal one year. We defined their lower and upper bounds turnover times (Table S1), and their initial conditions were all set to start from 0. The model was fitted for the entire 1900 – 2020 time window and run for each subplot, treatment, and soil depth.

## 2.6 Estimates of fine root C inputs into soils

Assuming a C fraction of 49% and 47% of fine root dry matter in control and warmed plots, respectively (Kwato Kengdo et al., 2022), we calculated FRT using two approaches. The first approach calculated fine root C input by multiplying FRP from ingrowth cores by C concentrations in fine roots. In the second approach, FRT was calculated as bulk FRB measured in October 2012 and October 2019 at 0 – 10 cm and 10 – 20 cm soil depth, multiplied by fine root turnover times derived from the *one-pool* model.

## 2.7 Statistical analysis

All statistical analyses and graphs were conducted using R version 4.0.3 (R Core Team, 2022). We used the R packages *ggplot2* (Wickham, 2016) for data visualization. Outliers in our data were tested using the Rosner's test with the package *EnvStats* (Millard, 2013). The normality of the data was checked using the Shapiro-Wilk test. Data were square-root transformed before analysis to meet the normality assumption when needed. Differences in FRB, FRP, and FRT between control and warmed plots were examined using paired *t*-tests ( $\alpha = 0.05$ ). Because  $\tau_R$  and  $\tau_S$  were overall highly variable and did not conform to our model assumptions in some plots, differences in storage C and fine root turnover time between control and warmed plots were tested with the Wilcoxon signed-rank test ( $\alpha = 0.05$ ). We examined the overall effect of soil warming on FRT by calculating the effect size (log response ratio, LRR), which quantify the magnitude and direction of the warming treatment. This numerical index is suitable because it is not influenced by any arbitrary aspects of the experimental design like the method, sampling seasons or years (Pustejovsky, 2018). As such, we combined estimates of FRT calculated from ingrowth cores and soil coring (and modeled fine root turnover times) independently of the depth and years of sampling. The LRR was calculated as the natural logarithm of the ratio of FRT in the warming plot over the value found in the control. We expressed this relationship to

the percentage of change as  $\% \text{ Change} = 100 \times (e^{LRR} - 1)$  (Pustejovsky, 2018). We tested whether the response of FRT calculated from ingrowth cores and soil coring differed from zero and we used the package *ggplot2* to illustrate the effect size in a forest plot.

### **3. Results**

#### **3.1 Fine root biomass from soil coring**

Soil warming increased bulk FRB by 13% in 2012 (from 514 to 582 g m<sup>-2</sup>) and by 17% in 2019 (from 355 to 414 g m<sup>-2</sup>) (Table 1). Bulk fine root necromass decreased with soil warming in 2019 (from 85 to 74 g m<sup>-2</sup>). Irrespective of treatment and soil depth, the proportion of fine roots of first-order and second- to third-order relative to bulk fine roots in 2019 were 10% and 39%, respectively (Table 1). The proportion of first-order and second- to third-order fine roots in control and warmed plots was not significantly different. Fine roots of first-order, second- to third-order represented on average ca. 10% and 40% of the total fine root biomass, respectively, in October 2019. The percentage of ectomycorrhizal colonization on first-order roots was 22% in control and 26% in warmed plots.

**Table 1:** Mean  $\pm$  SE of fine root biomass of bulk (in 2012 and 2019), first-order, second- to third-order; fine root necromass and the percentage of EcM colonization of root tips at 0 – 10 and 10 – 20 cm soil depth in control and warmed plots in October 2019. Letters indicate significant differences between control and warming treatments, tested separately for each soil depth ( $p < 0.05$ ).

Treatment	Soil depth	Fine root biomass ( $\text{g m}^{-2}$ )			Fine root necromass ( $\text{g m}^{-2}$ )		EcM root tip colonization (%)
		Bulk_2012	Bulk_2019	1 <sup>st</sup> order	2 <sup>nd</sup> – 3 <sup>rd</sup> order	2019	
Control	0 – 10 cm	397 $\pm$ 34 <sup>a</sup>	270.2 $\pm$ 31 <sup>a</sup>	26.8 $\pm$ 15.9 <sup>a</sup>	73.0 $\pm$ 28.1 <sup>a</sup>	67 $\pm$ 12 <sup>a</sup>	24 $\pm$ 6 <sup>a</sup>
	10 – 20 cm	128 $\pm$ 24 <sup>a</sup>	85.1 $\pm$ 19.8 <sup>a</sup>	13.4 $\pm$ 8.7 <sup>a</sup>	50.8 $\pm$ 16.3 <sup>a</sup>	18 $\pm$ 4 <sup>a</sup>	21 $\pm$ 5 <sup>a</sup>
	Total	513 $\pm$ 66 <sup>a</sup>	355.3 $\pm$ 44.9 <sup>a</sup>	40.2 $\pm$ 10.2 <sup>a</sup>	123.9 $\pm$ 19.5 <sup>a</sup>	85 $\pm$ 16 <sup>a</sup>	22 $\pm$ 4 <sup>a</sup>
Warming	0 – 10 cm	403 $\pm$ 39 <sup>a</sup>	302.1 $\pm$ 28.6 <sup>a</sup>	23.0 $\pm$ 9.6 <sup>a</sup>	91.3 $\pm$ 30.0 <sup>a</sup>	45 $\pm$ 6 <sup>b</sup>	28 $\pm$ 8 <sup>a</sup>
	10 – 20 cm	176 $\pm$ 30 <sup>a</sup>	113.8 $\pm$ 41.8 <sup>a</sup>	8.8 $\pm$ 5.6 <sup>a</sup>	45.8 $\pm$ 18.5 <sup>a</sup>	29 $\pm$ 7 <sup>b</sup>	25 $\pm$ 9 <sup>a</sup>
	Total	582 $\pm$ 95 <sup>a</sup>	414.2 $\pm$ 65.1 <sup>b</sup>	31.8 $\pm$ 6.3 <sup>a</sup>	137.1 $\pm$ 24.4 <sup>a</sup>	74 $\pm$ 9 <sup>b</sup>	26 $\pm$ 6 <sup>a</sup>

### 3.2 Fine root production from ingrowth cores

Soil warming increased FRP in ingrowth cores by 128% ( $p= 0.011$ ) from October 2019 to October 2020 (99 to 225  $\text{g m}^{-2} \text{yr}^{-1}$ ) (Figure 2). The difference between the treatments was 35% and no longer significant ( $p= 0.07$ ) after two years of root ingrowth, where FRP was 138 and 187  $\text{g m}^{-2} \text{yr}^{-1}$  in control and warmed plots, respectively. When considering the second year alone (October 2020 – October 2021), our results showed that FRP was similar in control and warmed plots (177 to 148  $\text{g m}^{-2} \text{yr}^{-1}$ ). Fine root biomass production repeatedly measured on different occasions within a year, from October 2012 to June 2013 and from June 2013 to October 2013, was also variable and increased by 80% and 105% in warmed plots, respectively (Figure S3). The production of new fine roots was low (8 to 14  $\text{g m}^{-2}$ ) between October 2012 and June 2013, indicating slow fine root growth in the springtime. Low FRP (31 to 63  $\text{g m}^{-2}$ ) also occurred between June and October 2012 because of the previous ingrowth cores sampling (Figure S3).

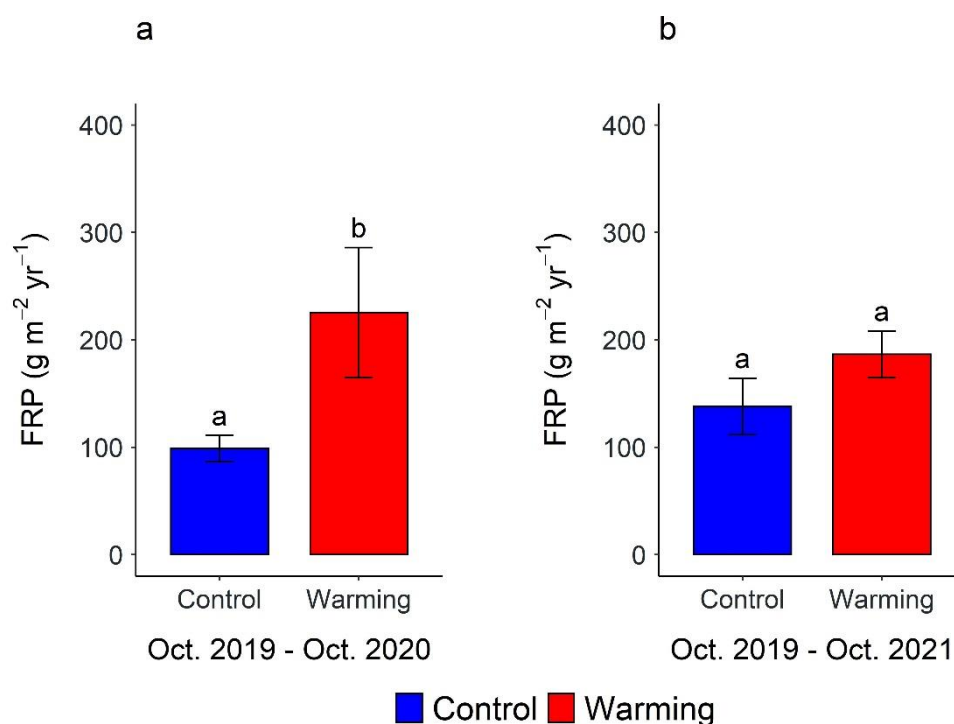


**Figure 2:** Mean  $\pm$  SE of fine root biomass production from ingrowth cores in control and warmed plots in (a) October 2020 (after one year) and (b) October 2021 (after two years) ( $n = 6$ ). Different letters indicate significant differences between control and warmed plots ( $p < 0.05$ ).

### 3.3 $\Delta^{14}\text{C}$ signatures of fine roots from undisturbed soil

The  $\Delta^{14}\text{C}$  signatures of first-order, second- to third-order and bulk fine roots were variable and non-significant between treatments (Table 2). For all sampling occasions, measured  $\Delta^{14}\text{C}$  values of bulk fine roots were above the atmospheric  $\Delta^{14}\text{C}$  signatures of the years of sampling (29.7‰ and  $-2.8$ ‰ in 2012 and 2019, respectively). Except in 2019 at 0 – 10 cm soil depth,  $\Delta^{14}\text{C}$  signatures of bulk fine roots tended to be higher in control than in warmed plots at both sampling occasions and tended to increase with increasing soil depth (Table 2). The  $\Delta^{14}\text{C}$  signatures of first-order and second- to third-order fine roots were also above the  $\Delta^{14}\text{C}$  signature of the atmosphere in 2019. The  $\Delta^{14}\text{C}$  signatures of those root fractions tended to be higher in control plots, but their increases with soil depth were not as strong as for bulk fine root samples.

**Table 2:** Mean  $\pm$  SE of  $\Delta^{14}\text{C}$  signatures (‰) of first-order, second- to third-order, and bulk fine roots sampled in October 2012 ( $n=3$ ) and October 2019 ( $n=6$ ) at 0 – 10 and 10 – 20 cm soil depth in control and warmed plots. In 2012, only radiocarbon signatures of bulk fine roots were analyzed. There was no significant difference between control and warming treatments, tested separately for each sampling occasion.

Root fraction	Soil depth	2012		2019	
		Control	Warming	Control	Warming
1 <sup>st</sup> order	0 – 10 cm	-	-	16.7 $\pm$ 2.8	12.6 $\pm$ 1.0
	10 – 20 cm	-	-	27.5 $\pm$ 5.7	13.0 $\pm$ 5.5
2 <sup>nd</sup> – 3 <sup>rd</sup> order	0 – 10 cm	-	-	16.7 $\pm$ 2.4	17.1 $\pm$ 2.6
	10 – 20 cm	-	-	20.1 $\pm$ 6.0	16.6 $\pm$ 6.2
Bulk	0 – 10 cm	51.4 $\pm$ 3.9	44.7 $\pm$ 4.0	25.3 $\pm$ 6.5	29.1 $\pm$ 5.4
	10 – 20 cm	70.8 $\pm$ 12.7	66.1 $\pm$ 7.7	30.3 $\pm$ 12.1	29.9 $\pm$ 7.1

### 3.4 $\Delta^{14}\text{C}$ signatures of fine roots from ingrowth cores

The  $\Delta^{14}\text{C}$  signatures of fine roots sampled from ingrowth cores were not significantly different across treatments (Table 3). The  $\Delta^{14}\text{C}$  signatures of fine roots from ingrowth cores in October 2013 were 26‰ and 28‰ in control and warmed plots, respectively (Table 3). Fine roots from ingrowth cores retrieved after one year in October 2020 had more negative  $\Delta^{14}\text{C}$  values in control than warmed plots (mean  $\Delta^{14}\text{C}$  of  $-3.9\text{‰}$  and  $2.3\text{‰}$ , respectively). After two years, those ingrowth cores had almost similar  $\Delta^{14}\text{C}$  values in both treatments ( $1.9\text{‰}$  and  $1.2\text{‰}$ , in control and warmed plots, respectively). Compared to the two-year ingrowth cores, fine roots from ingrowth cores sampled in October 2013 and October 2020 had a higher  $\Delta\Delta^{14}\text{C}$  (difference between the  $\Delta^{14}\text{C}$  of fine roots and the  $\Delta^{14}\text{C}$  of the atmosphere in the year of sampling) in warmed ( $6.8$  to  $8.2\text{‰}$ ) than in control plots ( $3.1$  to  $5.8\text{‰}$ ) (Table 3).

**Table 3:** Mean  $\pm$  SE of  $\Delta^{14}\text{C}$  signatures (‰) of fine roots from ingrowth cores and  $\Delta\Delta^{14}\text{C}$  ( $\Delta^{14}\text{C}$  of fine roots  $- \Delta^{14}\text{C}$  of atmospheric  $\text{CO}_2$  in the corresponding year). Mean annual  $\Delta^{14}\text{C}$  of atmospheric  $\text{CO}_2$  was  $19.7\text{‰}$  in 2013 at Schauinsland (Hammer & Levin, 2017) and  $-4.5\text{‰}$  in 2020, and  $-7.2\text{‰}$  in 2021 at Hohenpeißenberg (Kubistin et al., 2021). They were no significant difference between control and warming treatments, tested separately for each sampling occasion.

Treatment	$\Delta^{14}\text{C}$ signature (‰)		
	2013	2020	2021
Control	$25.5 \pm 2.8$	$-1.4 \pm 1.5$	$1.9 \pm 1.6$
Warming	$27.9 \pm 2.2$	$2.3 \pm 1.8$	$1.8 \pm 0.9$
$\Delta\Delta^{14}\text{C}$ Control	$5.8 \pm 2.1$	$3.1 \pm 0.8$	$9.1 \pm 0.9$
$\Delta\Delta^{14}\text{C}$ Warming	$8.2 \pm 1.5$	$6.8 \pm 1.1$	$9.0 \pm 0.2$

### 3.5 Turnover times of storage C and fine roots from undisturbed soil cores

Storage C turnover times constrained from fine roots sampled in ingrowth cores at 0 – 20 cm soil depth tended to increase in warmed plots (Figure 3). When considering fine roots grown

within a year, between October 2012 – June 2013 and October 2019 – October 2020, mean storage C turnover times tended to increase from 1.1 to 1.5 years and 1.1 to 2.0 years in control and warmed plots, respectively. Considering the two-year ingrowth cores (October 2019 – October 2021), storage C turnover times were similar, 2.0 and 2.1 years in control and warmed plots, respectively (Figure 3).

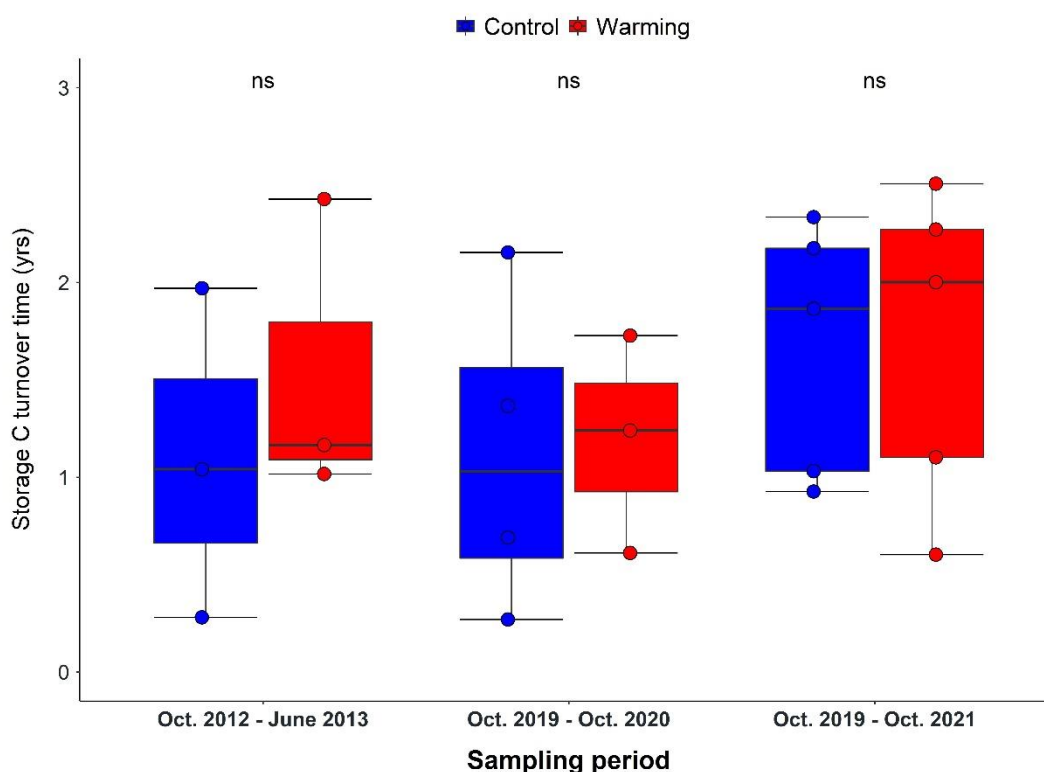


**Figure 3:** Storage C turnover times constrained from fine roots sampled in ingrowth cores in control and warmed plots at 0 – 20 cm soil depth at different sampling occasions. In the boxplots, the line represents the median, the box denotes the interquartile range.

Our results showed that fine root turnover times tended to decrease with warming (Figure 4). Bulk fine roots measured at 0 – 20 cm soil depth in control and warmed plots had turnover times of 6 years and 5 years in 2012, 8 years and 5 years in 2019, respectively. Turnover times of first-order roots generally showed the same trend at 0 – 10 cm and 10 – 20 cm soil depth. However, second- to third-order roots showed an increase, and a decrease in turnover times at 0 – 10 cm and 10 – 20 cm soil depth, respectively (Figure 4). Although soil depth did not show

significant effects, fine root turnover times of first-order, second- to third-order, and bulk fine roots tended to increase with increasing soil depth.

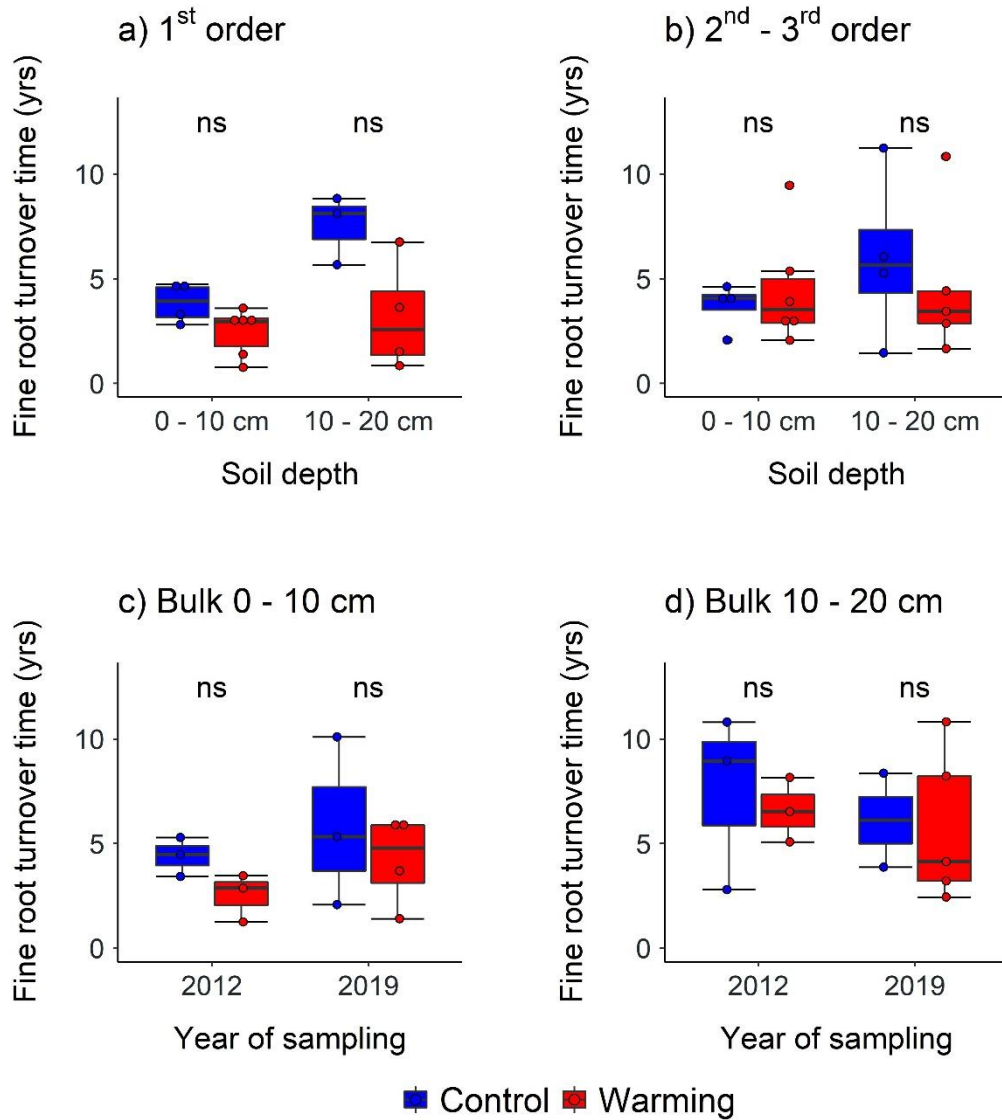


**Figure 4:** Fine root turnover times of (a) 1<sup>st</sup> order, (b) 2<sup>nd</sup> – 3<sup>rd</sup> order, and the bulk fine roots in control and warmed plots at (c) 0 – 10 cm and (d) 10 – 20 cm soil depth at different sampling occasions. In the boxplots, the line represents the median, the box denotes the interquartile range; ns indicate non-significant differences between control and warmed plots.

### 3.6 Belowground C input by fine root turnover

FRT estimated from the two separate approaches (ingrowth cores and soil coring) are presented in Table 4. FRT estimated from ingrowth cores at 0 – 20 cm soil depth for all sampling occasions ranged from 48 – 70 g C m<sup>-2</sup> yr<sup>-1</sup> in control and 94 – 106 g C m<sup>-2</sup> yr<sup>-1</sup> in warmed plots, respectively (Table 4). Our FRT estimates using modeled fine root turnover times and soil coring data ranged from 37 – 63 g C m<sup>-2</sup> yr<sup>-1</sup> in control, and 51 – 100 g C m<sup>-2</sup> yr<sup>-1</sup> in warmed plots, respectively. FRT estimated using soil coring data tended to be higher at 0 – 10 cm than at 10 – 20 cm soil depth. Figure 5 shows the effects of soil warming on FRT estimated from ingrowth cores, soil coring, and the overall effect. Compared with the control, soil warming increased FRT estimated from ingrowth cores by 211% (82.6 – 340.0%,  $p = 0.003$ ,  $n = 29$ , Figure 5), and from soil coring by 109% (10.0 – 209.1%,  $p = 0.02$ ,  $n = 18$ , Figure 5). The overall increase of FRT with warming for both methods combined was 172% (83.8 – 260%,  $p < 0.001$ ,  $n = 47$ , Figure 5), i.e., an increase in FRT from 50 to 106 g C m<sup>-2</sup> yr<sup>-1</sup>.

**Table 4:** Fine root turnover  $\pm$  SE ( $\text{g C m}^{-2} \text{yr}^{-1}$ ) estimated from ingrowth cores and soil coring methods in control and warmed plot at 0 – 10 cm and 10 – 20 cm soil depth at the different sampling occasions.

Soil depth (cm)	FRT _ingrowth cores ( $\text{g C m}^{-2} \text{yr}^{-1}$ )				FRT _soil coring ( $\text{g C m}^{-2} \text{yr}^{-1}$ )			
	2020		2021		2012		2019	
	Control	Warming	Control	Warming	Control	Warming	Control	Warming
0 – 10	-	-	-	-	$50.3 \pm 4$	$86.7 \pm 35$	$31.6 \pm 18$	$44.1 \pm 19$
10 – 20	-	-	-	-	$12.8 \pm 6$	$13.6 \pm 7$	$5.8 \pm 1$	$6.6 \pm 1$
Total	$48.4 \pm 6$	$105.9 \pm 28$	$70.8 \pm 14$	$94.0 \pm 9$	$63.0 \pm 9$	$100.1 \pm 23$	$37.4 \pm 13$	$50.6 \pm 10$

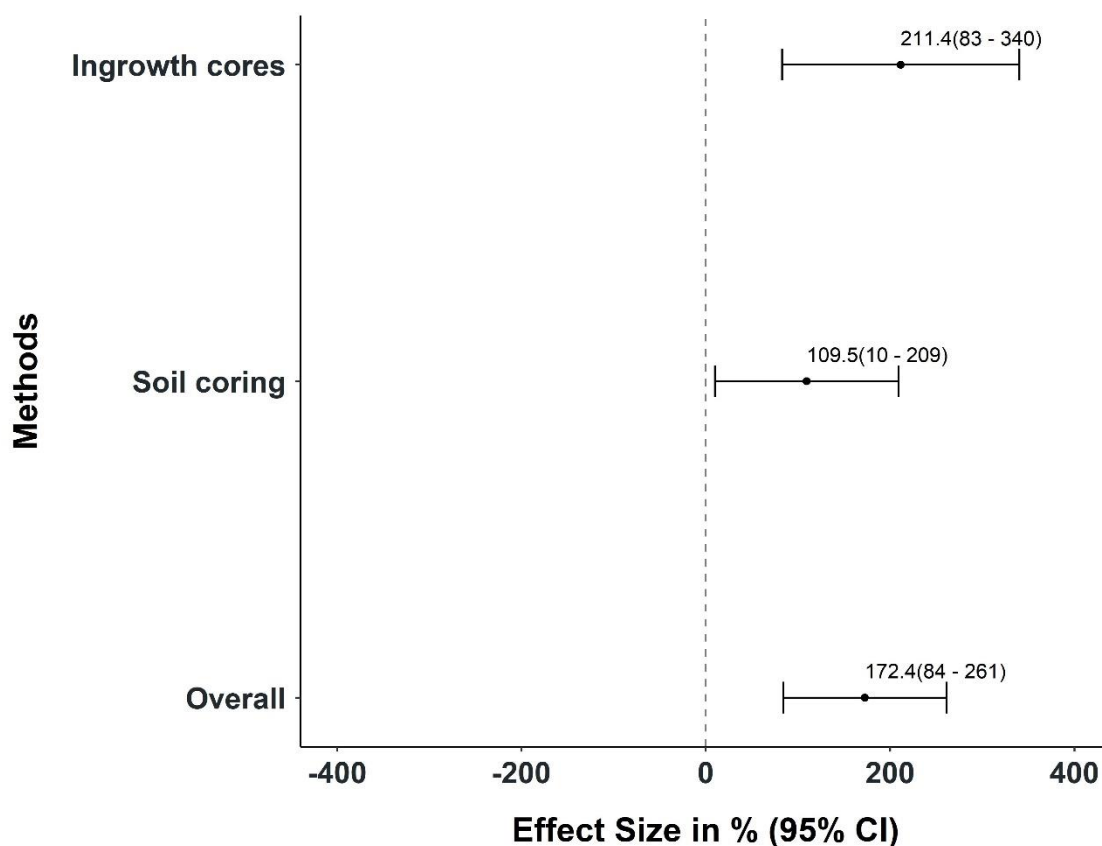


**Figure 5:** Effect of soil warming on FRT ( $\text{g C m}^{-2} \text{ yr}^{-1}$ ) estimated from ingrowth cores ( $n=29$ ), soil coring (and modeled fine root turnover times) ( $n=18$ ), and the overall effect of all methods combined. Coefficients are mean and their 95% confidence intervals, and illustrate the strength of the soil warming effect on FRT compared to the control. Significant warming effects do not overlap with the null effect line (horizontal dashed line).

#### 4. Discussion

This study examined the effects of long-term soil warming on FRP and FRT in a temperate forest. Using ingrowth cores and  $^{14}\text{C}$  signatures of fine roots, we estimated FRP, fine root turnover times, and inputs of C into soils through FRT in control and warmed plots. Our results showed that FRP measured with ingrowth cores substantially increased in warmed plots. Furthermore, soil warming tended to decrease the turnover times of first-order, second- to third-order, and bulk fine roots, and likely more storage C was used by trees for FRP in the warmed

plots. Soil warming also increased FRT by 172% overall. However, the enhanced C input by fine root litter is relatively small compared to the increase in soil CO<sub>2</sub> efflux.

#### 4.1 Soil warming increases fine root production

In agreement with our first hypothesis, soil warming strongly increased annual FRP by 128% in 2019/20 (from 99 to 225 g m<sup>-2</sup> yr<sup>-1</sup>). On the second sampling occasion (October 2019-2021), the increase of 35% in FRP was no longer significant. This suggests that warming accelerated the exploitation of the unrooted soil in ingrowth cores by increasing FRP. During the first year of installation of ingrowth cores (from October 2019 to October 2020), FRP was likely overestimated in the warmed soil because fine roots may grow faster in the absence of competition with other roots (Lukac, 2012). Our study also has the advantage of presenting fine root biomass in ingrowth cores retrieved after two years, and lower FRP (138 g m<sup>-2</sup> yr<sup>-1</sup> versus 187 g m<sup>-2</sup> yr<sup>-1</sup>) suggests that FRB may have reached an equilibrium in the warmed soil in the second year. This is supported by the fact that in warmed plots, FRB in ingrowth cores after two years (400 g m<sup>-2</sup>) was very close to FRB measured by the soil coring method (414 g m<sup>-2</sup>) in October 2019 (Table 1). However, FRP in control plots showed slower equilibration after two years of ingrowth cores placement, and a third-year is likely required for FRP to reach the level of FRB measured with soil coring.

From the ingrowth cores in 2012/2013 we found that FRP was consistently higher in the spring and summer/early autumn. Acceleration of fine root growth in the spring of 2013, starting after snowmelt in late April, is in line with a general shift in the growing season by global warming in recent decades (Rumpf et al., 2022). From the samplings in June and October 2013, it was clear that the installation of ingrowth cores caused a disturbance of the surrounding fine root system and a reduction in fine root growth. Hence, the sum of FRP from both sampling occasions in 2013 was much smaller than the annual FRP in 2019/2020 or 2020/2021.

Another artifact may overcompensate the initial reduction in FRP after installation of ingrowth cores and result in an overestimation of FRP in the later season or the following year as fine roots can expand faster in the ‘root-free’ soil as compared to the undisturbed rooted soil. Thus, we assume an overestimation of FRP in warmed plots in 2019/2020 and more reasonable and realistic estimates in 2021. The increase in FRP with warming has also been observed in a global meta-analysis suggesting an increase in FRP by 30% across various ecosystems (J. Wang et al., 2021). Our estimates of FRP in control and warmed plots in the second sampling

(138 and 186 g m<sup>-2</sup> yr<sup>-1</sup>) are much lower than the global average of 337 g m<sup>-2</sup> yr<sup>-1</sup> for temperate forests but very close to the value of 165 g m<sup>-2</sup> yr<sup>-1</sup> estimated with ingrowth cores by Finér et al. (2011). Taken together, we postulate that estimates of FRP by single-year ingrowth cores are critical due to initial disturbance and the rapid exploitation of unrooted soil in the subsequent growth phase.

#### 4.2 Fine root turnover time

Storage turnover times of bulk fine roots tended to be slower in warmed plots, suggesting that trees used more old C for FRP in the warmed plots, especially during the first year of FRP (Figure 3). Fine roots may be constructed from recent photosynthates during the year of their production, meaning that their  $\Delta^{14}\text{C}$  signatures should equal that of atmospheric CO<sub>2</sub> ( $\Delta\Delta^{14}\text{C} = 0$ ). However, in our study, the  $\Delta^{14}\text{C}$  signatures of ingrowth cores did not support this assumption ( $\Delta\Delta^{14}\text{C} \neq 0$ ), with a high  $\Delta\Delta^{14}\text{C}$  in warmed plots in 2013 and 2020, further pointing towards the use of C up to two years old for FRP in warmed plots (Table 3). We postulate that the use of old C stores for FRP results from increased fine root metabolic activity in warmed plots because high root activity requires more C that cannot be fully covered from fresh photosynthates to sustain FRP and fine root functions. Several hypotheses about the origin of old C in fine roots were presented before (Gaudinski et al., 2001; Trumbore & Gaudinski, 2003), but the redistribution of non-structural carbohydrates stored in the whole tree (mainly in stems and coarse roots) remains the most plausible explanation. Our estimates of  $\leq 2$  years storage turnover times agree with those published by Gaudinski et al. (2009). Evidence of old C in fine roots was suggested by Tierney and Fahey (2002) and observed in boreal and temperate forests (Helmisaari et al., 2015; Hikino et al., 2022; Sah et al., 2011; Solly et al., 2018) and in a tropical forest (Vargas et al., 2009). However, this has never been highlighted in the context of soil warming before.

We do not have strong evidence to support our second hypothesis, though our results showed that fine root turnover times tended to decrease in warmed plots, suggesting greater root litter inputs into warmed soils. Considering FRB from soil cores in 2019 and FRP between October 2020 and October 2021, we calculated a fine root turnover time of 2.8 years in warmed plots. Further, our ingrowth core data showed that it is only after 2 – 3 years that root ingrowth reaches FRB levels found in undisturbed soil cores in warmed plots. The *one-pool* model provided turnover times up to 1 and 4 years older (at 0 – 10 and 10 – 20 cm, respectively) than ingrowth core estimates in the warmed plots, which might be linked to the fact that *one-pool*

models provide a good estimate of fine root age, but not of fine root turnover times (Ahrens et al., 2014). Faster fine root turnover times with warming were also suggested in a few studies in boreal forests (Leppälammı-Kujansuu et al., 2014; Majdi & öhrvik, 2004). Fine root turnover times estimated in this study are much faster than estimates from other temperate and boreal forests using the radiocarbon approach (Gaudinski et al., 2001; Helmisaari et al., 2015; Solly et al., 2018). The reason might be due to the fact that those studies did not account for the use of storage C for FRP. For example, by considering storage C, Gaudinski et al. (2009) estimated that the fine root turnover times they presented before (Gaudinski et al., 2001) were overestimated by up to 2 years.

We also observed a tendency towards slower fine root turnover times with increasing soil depth, irrespective of the treatment, except for bulk fine roots at 10 – 20 cm soil depth. The decrease in fine root turnover times with increasing soil depth has been observed in other studies in temperate (Baddeley & Watson, 2005; Gaudinski et al., 2001; Gaul et al., 2009; Joslin et al., 2006) and boreal (Sah et al., 2013) forests. We postulate that the increase of fine root turnover times with increasing soil depth might be linked to differences in root functions and metabolic activity between 0 – 10 cm and 10 – 20 cm soil depths, being faster in the more nutrient-rich topsoil.

### **4.3 Implications for forest carbon dynamics**

Our findings show that warming responses of tree fine roots could have strong implications for C dynamics in temperate forests. Aboveground litter is a major input of plant C in temperate forests (Bowden et al., 2014; Wunderlich et al., 2012). Aboveground litter at the Achenkirch site in 2020 was about 170 g C m<sup>-2</sup> yr<sup>-1</sup> (Schindlbacher; unpublished data), which is within the range of litter input reported in similar temperate forests. However, fine root litter input in our study is smaller than aboveground litter input, representing 28 – 42 % and 55 – 62 % of aboveground litter in control and warmed plots, respectively, when estimated from ingrowth cores data. These proportions decrease to 22 – 37 % and 30 – 59% when estimated from fine root turnover times and 2019's soil coring data. This suggests that the increase in fine root litter input by warming may only partly explain the increase in soil respiration (Schindlbacher et al., 2012). In addition to the decomposition of aboveground litter, the remaining part might be explained by increased root and microbial respiration, litter input by EcM mycelia, and the exudation of labile C by fine roots, which is quite poorly quantified in most ecosystems (Pausch & Kuzyakov, 2018).

Certainly, our study comes with some limitations. The *one-pool* model we applied in this study has the merit of modeling fine root  $\Delta^{14}\text{C}$  for each plot and depth separately while considering storage C used to grow new fine roots. However, it does not consider the coexistence of fast cycling fine roots, i.e., most fine roots that die soon after growth. As a result, we cannot exclude faster fine root turnover times if a non-steady-state model was used in the modeling framework. For example, Ahrens et al. (2014) and Ahrens and Reichstein (2014) compared the performance of different survival functions in reconciling bomb-radiocarbon and minirhizotron data. They concluded that, compared to the *one-pool* model, *two-pool* models (slow- and fast- cycling pool) were better suited to model fine root dynamics. This implies that our fine root turnover times from the *one-pool* model may have been overestimated, and consequently, we underestimated root litter inputs into soils (Table 4). As mentioned earlier, the reason is due to the fact that *one-pool* models give correct estimates of fine root age but overestimate fine root turnover times. The *serial-three-pool* model we tried could not provide reasonable estimates because of the large variation in the  $^{14}\text{C}$  signatures of fine roots, likely resulting from different amounts and ages of storage C in the individual fine roots. The high variability in our data, which is very common in fine root dynamics studies, might be why, rather than statistical significance, we could only explore tendencies in fine root turnover times at the plot level. Because we separated first-order, second- to third-order, and bulk fine roots, we could at least isolate fine root dynamics for different fine root functional pools. Further, our *one-pool* model assumed that recent photosynthates pass first through the storage pool, where C is drawn for FRP. However, we must acknowledge that different model assumptions were also previously presented. For example, in the *Radix* model, Gaudinski et al. (2010) assumed that the C used to grow fine roots may come from a storage pool, from recent photosynthates, or from both. Yiqi Luo et al. (2004) assumed that C used for FRP is a mixture of recent and stored non-structural C, while Matamala et al. (2003) assumed no storage C pool at all.

## 5. Conclusions

In conclusion, soil warming increased FRB and FRP, and fine roots in warmed plots tended to turn over faster than in control plots. Independently of the method, soil warming increased the C input into the soil from 50 to 106 g C m<sup>-2</sup> yr<sup>-1</sup> through enhanced FRT. However, this root C input accounted for up to 30% and 62% of the aboveground litter input in control and warmed plots, respectively. Schindlbacher et al. (2009) showed that soil warming persistently increased soil respiration by up to 40% compared to control plots, and this tendency still persists, even

after 15 years of soil warming at the Achenkirch site (Schindlbacher, unpublished data). Taken together, the increase in soil respiration can only be explained to a small extent by increased mineralization of fine root litter. The quantification of all C inputs represents a prerequisite to understanding the changes in soil organic C stock and forest C cycling caused by global warming.

## **Acknowledgments**

The authors thank Renate Krauss, Uwe Hell and Karin Söllner for technical assistance. We acknowledge the contribution of Alena Hubach and Inken Krüger during sample preparation and radiocarbon analysis in 2012 and 2013. We gratefully thank Xiaomei Xu and John Southon for valuable assistance during  $^{14}\text{C}$  samples preparation and radiocarbon analysis at the Keck Carbon Cycle AMS Laboratory, University of California, Irvine.

## **Funding Sources**

This research was supported by the German Research Foundation (DFG, BO 1741/13-1) and the Austrian Science Fund (FWF) through the D-A-Ch project I 3745.

## **Author Contributions**

**Steve Kwatcho Kengdo:** Investigation, Formal analysis, Software, Writing - Original Draft, Writing - Review & Editing, Visualization. **Bernhard Ahrens:** Formal analysis, Software, Writing - Review & Editing. **Ye Tian:** Investigation, Writing - Review & Editing. **Jakob Heinze:** Investigation, Writing - Review & Editing. **Wolfgang Wanek:** Conceptualization, Methodology, Funding acquisition, Writing - Review & Editing. **Andreas Schindlbacher:** Conceptualization, Methodology, Funding acquisition, Writing - Review & Editing, Project administration, Resources. **Werner Borken:** Conceptualization, Methodology, Funding acquisition, Writing - Review & Editing, Supervision, Project administration, Resources.

## **Declaration of competing interest**

The authors declare that they have no conflict of interest.

## **Data Availability**

The data that support the findings of this study are openly available on Zenodo at <https://doi.org/10.5281/zenodo.7002808>.

## References

- Ahrens, B., Hansson, K., Solly, E. F., & Schrumpf, M. (2014). Reconcilable differences: A joint calibration of fine-root turnover times with radiocarbon and minirhizotrons. *The New Phytologist*, *204*(4), 932–942. <https://doi.org/10.1111/nph.12979>
- Ahrens, B., & Reichstein, M. (2014). Reconciling  $^{14}\text{C}$  and minirhizotron-based estimates of fine-root turnover with survival functions. *Journal of Plant Nutrition and Soil Science*, *177*(2), 287–296. <https://doi.org/10.1002/jpln.201300110>
- Baddeley, J. A., & Watson, C. A. (2005). Influences of root diameter, tree age, soil depth and season on fine root survivorship in *Prunus avium*. *Plant and Soil*, *276*(1-2), 15–22. <https://doi.org/10.1007/s11104-005-0263-6>
- Bowden, R. D., Deem, L., Plante, A. F., Peltre, C., Nadelhoffer, K., & Lajtha, K. (2014). Litter Input Controls on Soil Carbon in a Temperate Deciduous Forest. *Soil Science Society of America Journal*, *78*(S1). <https://doi.org/10.2136/sssaj2013.09.0413nafsc>
- Brunner, I., Bakker, M. R., Björk, R. G., Hirano, Y., Lukac, M., Aranda, X., Børja, I., Eldhuset, T. D., Helmisaari, H. S., Jourdan, C., Konôpka, B., López, B. C., Miguel Pérez, C., Persson, H., & Ostonen, I. (2013). Fine-root turnover rates of European forests revisited: an analysis of data from sequential coring and ingrowth cores. *Plant and Soil*, *362*(1-2), 357–372. <https://doi.org/10.1007/s11104-012-1313-5>
- Eissenstat, D. M., Wells, C. E., Yanai, R. D., & Whitbeck, J. L. (2000). Building roots in a changing environment: implications for root longevity. *New Phytologist*, *147*(1), 33–42. <https://doi.org/10.1046/j.1469-8137.2000.00686.x>
- Eissenstat, D. M., & Yanai, R. D. (1997). The Ecology of Root Lifespan. In *Advances in Ecological Research*. *Advances in Ecological Research Volume 27* (Vol. 27, pp. 1–60). Elsevier. [https://doi.org/10.1016/S0065-2504\(08\)60005-7](https://doi.org/10.1016/S0065-2504(08)60005-7)
- Finér, L., Ohashi, M., Noguchi, K., & Hirano, Y. (2011). Fine root production and turnover in forest ecosystems in relation to stand and environmental characteristics. *Forest Ecology and Management*, *262*(11), 2008–2023. <https://doi.org/10.1016/j.foreco.2011.08.042>
- Gaudinski, J., Trumbore, S., Davidson, E., Cook, A., Markewitz, D., & Richter, D. (2001). The age of fine-root carbon in three forests of the eastern United States measured by radiocarbon. *Oecologia*, *129*(3), 420–429. <https://doi.org/10.1007/s004420100746>
- Gaudinski, J., Torn, M. S., Riley, W. J., Swanston, C., Trumbore, S. E., Joslin, J. D., Majdi, H., Dawson, T. E., & Hanson, P. J. (2009). Use of stored carbon reserves in growth of temperate tree roots and leaf buds: analyses using radiocarbon measurements and modeling. *Global Change Biology*, *15*(4), 992–1014. <https://doi.org/10.1111/j.1365-2486.2008.01736.x>
- Gaudinski, J., Torn, M. S., Riley, W. J., Dawson, T. E., Joslin, J. d., & Majdi, H. (2010). Measuring and modeling the spectrum of fine-root turnover times in three forests using isotopes, minirhizotrons, and the Radix model. *Global Biogeochemical Cycles*, *24*(3). <https://doi.org/10.1029/2009GB003649>
- Gaul, D., Hertel, D., Borken, W., Matzner, E., & Leuschner, C. (2008). Effects of experimental drought on the fine root system of mature Norway spruce. *Forest Ecology and Management*, *256*(5), 1151–1159. <https://doi.org/10.1016/j.foreco.2008.06.016>

- Gaul, D., Hertel, D., & Leuschner, C. (2009). Estimating fine root longevity in a temperate Norway spruce forest using three independent methods. *Functional Plant Biology : FPB*, 36(1), 11–19. <https://doi.org/10.1071/FP08195>
- Gill, R. A., & Jackson, R. B. (2000). Global patterns of root turnover for terrestrial ecosystems. *New Phytologist*, 147(1), 13–31. <https://doi.org/10.1046/j.1469-8137.2000.00681.x>
- Guo, D. L., Mitchell, R. J., & Hendricks, J. J. (2004). Fine root branch orders respond differentially to carbon source-sink manipulations in a longleaf pine forest. *Oecologia*, 140(3), 450–457. <https://doi.org/10.1007/s00442-004-1596-1>
- Guo, D. L., Li, H., Mitchell, R. J., Han, W., Hendricks, J. J., Fahey, T. J., & Hendrick, R. L. (2008). Fine root heterogeneity by branch order: Exploring the discrepancy in root turnover estimates between minirhizotron and carbon isotopic methods. *New Phytologist*, 177(2), 443–456. <https://doi.org/10.1111/j.1469-8137.2007.02242.x>
- Hammer, S., & Levin, I. (2017). *Monthly mean atmospheric D14CO2 at Jungfraujoch and Schauinsland from 1986 to 2016*. <https://doi.org/10.11588/data/10100>
- Helmisaari, H.-S., Leppälammil-Kujansuu, J., Sah, S., Bryant, C., & Kleja, D. B. (2015). Old carbon in young fine roots in boreal forests. *Biogeochemistry*, 125(1), 37–46. <https://doi.org/10.1007/s10533-015-0110-7>
- Hikino, Kyohsuke; Danzberger, Jasmin; Riedel, Vincent P.; Hesse, Benjamin D.; Hafner, Benjamin D.; Gebhardt, Timo et al. (2022): Dynamics of initial C allocation after drought release in mature Norway spruce - Increased belowground allocation of current photoassimilates covers only half of the C used for fine-root growth. In *Global Change Biol*, Article gcb.16388. DOI: 10.1111/gcb.16388.
- IPCC, 2021: Climate Change 2021: The Physical Science Basis. Contribution of Working Group I to the Sixth Assessment Report of the Intergovernmental Panel on Climate Change [Masson-Delmotte, V., P. Zhai, A. Pirani, S.L. Connors, C. Péan, S. Berger, N. Caud, Y. Chen, L. Goldfarb, M.I. Gomis, M. Huang, K. Leitzell, E. Lonnoy, J.B.R. Matthews, T.K. Maycock, T. Waterfield, O. Yelekçi, R. Yu, and B. Zhou (eds.)]. Cambridge University Press, Cambridge, United Kingdom and New York, NY, USA, In press, doi:10.1017/9781009157896.
- Jackson, R. B., Mooney, H. A., & Schulze, E. D. (1997). A global budget for fine root biomass, surface area, and nutrient contents. *Proceedings of the National Academy of Sciences of the United States of America*, 94(14), 7362–7366. <https://doi.org/10.1073/pnas.94.14.7362>
- Joslin, J. d., Gaudinski, J. B., Torn, M. S., Riley, W. J., & Hanson, P. J. (2006). Fine-root turnover patterns and their relationship to root diameter and soil depth in a <sup>14</sup>C-labeled hardwood forest. *New Phytologist*, 172(3), 523–535. <https://doi.org/10.1111/j.1469-8137.2006.01847.x>
- Kubistin, D., Plaß-Dülmer, C., Arnold, S., Lindauer, M., Müller-Williams, J., & Schumacher, M. (2021). *ICOS ATC/CAL 14C Release, Hohenpeissenberg (131.0 m), 2015-09-24–2020-02-19*. Atmosphere Thematic Centre. <https://hdl.handle.net/11676/sx-gduDzKEjkF3VCer06oWIV>
- Kwatocho Kengdo, S., Peršoh, D., Schindlbacher, A., Heinzle, J., Tian, Y., Wanek, W., & Borken, W. (2022). Long-term soil warming alters fine root dynamics and morphology,

- and their ectomycorrhizal fungal community in a temperate forest soil. *Global Change Biology*, 28(10), 3441–3458. <https://doi.org/10.1111/gcb.16155>
- Leppälammil-Kujansuu, J., Salemaa, M., Kleja, D. B., Linder, S., & Helmisaari, H.-S. (2014). Fine root turnover and litter production of Norway spruce in a long-term temperature and nutrient manipulation experiment. *Plant and Soil*, 374(1-2), 73–88. <https://doi.org/10.1007/s11104-013-1853-3>
- Lu, M., Zhou, X., Yang, Q., Li, H., Luo, Y., Fang, C., Chen, J., Yang, X., & Li, B. (2013). Responses of ecosystem carbon cycle to experimental warming: A meta-analysis. *Ecology*, 94(3), 726–738. <https://doi.org/10.1890/12-0279.1>
- Lukac, M. (2012). Fine Root Turnover. In S. Mancuso (Ed.), *Measuring Roots* (pp. 363–373). Springer Berlin Heidelberg. [https://doi.org/10.1007/978-3-642-22067-8\\_18](https://doi.org/10.1007/978-3-642-22067-8_18)
- Luo, Y. (2003). Uncertainties in interpretation of isotope signals for estimation of fine root longevity: theoretical considerations. *Global Change Biology*, 9(7), 1118–1129. <https://doi.org/10.1046/j.1365-2486.2003.00642.x>
- Luo, Y., White, L., & Hui, D. (2004). Comment on "Impacts of fine root turnover on forest NPP and soil C sequestration potential". *Science*, 304(5678), 1745. <https://doi.org/10.1126/science.1098080>
- Lützow, M., Kögel-Knabner, I., Ekschmitt, K., Matzner, E., Guggenberger, G., & Marschner, B. and Flessa, H. (2006). Stabilization of organic matter in temperate soils: mechanisms and their relevance under different soil conditions – a review. *European Journal of Soil Science*, 54, 426–445. <https://doi.org/10.1111/j.1365-2389.2006.00809.x>
- Lynch, D. J., Matamala, R., Iversen, C. M., Norby, R. J., & Gonzalez-Meler, M. A. (2013). Stored carbon partly fuels fine-root respiration but is not used for production of new fine roots. *New Phytologist*, 199(2), 420–430. <https://doi.org/10.1111/nph.12290>
- Majdi, H., & öhrvik, J. (2004). Interactive effects of soil warming and fertilization on root production, mortality, and longevity in a Norway spruce stand in Northern Sweden. *Global Change Biology*, 10(2), 182–188. <https://doi.org/10.1111/j.1365-2486.2004.00733.x>
- Majdi, H., Pregitzer, K., Morén, A.-S., Nylund, J.-E., & Ågren, G. I. (2005). Measuring Fine Root Turnover in Forest Ecosystems. *Plant and Soil*, 276(1-2), 1–8. <https://doi.org/10.1007/s11104-005-3104-8>
- Matamala, R., González-Meler, M. A., Jastrow, J. D., Norby, R. J., & Schlesinger, W. H. (2003). Impacts of fine root turnover on forest NPP and soil C sequestration potential. *Science (New York, N.Y.)*, 302(5649), 1385–1387. <https://doi.org/10.1126/science.1089543>
- McCormack, M. L., Dickie, I. A., Eissenstat, D. M., Fahey, T. J., Fernandez, C. W., Guo, D., Helmisaari, H.-S., Hobbie, E. A., Iversen, C. M., Jackson, R. B., Leppälammil-Kujansuu, J., Norby, R. J., Phillips, R. P., Pregitzer, K. S., Pritchard, S. G., Rewald, B., & Zadworny, M. (2015). Redefining fine roots improves understanding of below-ground contributions to terrestrial biosphere processes. *The New Phytologist*, 207(3), 505–518. <https://doi.org/10.1111/nph.13363>
- McCormack, M. L., & Guo, D. (2014). Impacts of environmental factors on fine root lifespan. *Frontiers in Plant Science*, 5, 205. <https://doi.org/10.3389/fpls.2014.00205>

- Melillo, J. M., Butler, S., Johnson, J., Mohan, J., Steudler, P., Lux, H., Burrows, E., Bowles, F., Smith, R., Scott, L., Vario, C., Hill, T., Burton, A., Zhou, Y.-M., & Tang, J. (2011). Soil warming, carbon-nitrogen interactions, and forest carbon budgets. *Proceedings of the National Academy of Sciences of the United States of America*, *108*(23), 9508–9512. <https://doi.org/10.1073/pnas.1018189108>
- Melillo, J. M., Steudler, P. A., Aber, J. D., Newkirk, K., Lux, H., Bowles, F. P., Catricala, C., Magill, A., Ahrens, T., & Morrisseau, S. (2002). Soil warming and carbon-cycle feedbacks to the climate system. *Science (New York, N.Y.)*, *298*(5601), 2173–2176. <https://doi.org/10.1126/science.1074153>
- Millard, S. P. (2013). *EnvStats: An R Package for Environmental Statistics*. Springer. <https://www.springer.com>
- Ostonen, I., Lohmus, K., Pajuste, K. (2005) Fine root biomass, production and its proportion of NPP in a fertile middle-aged Norway spruce forest: comparison of soil core and ingrowth core methods. *Forest Ecology and Management* *212* (1-3), 264–277
- Pausch, J., & Kuzyakov, Y. (2018). Carbon input by roots into the soil: Quantification of rhizodeposition from root to ecosystem scale. *Global Change Biology*, *24*(1), 1–12. <https://doi.org/10.1111/gcb.13850>
- Pregitzer, K. S., DeForest, J. L., Burton, A. J., Allen, M. F., Ruess, R. W., & Hendrick, R. L. (2002). Fine root architecture of nine North American trees. *Ecological Monographs*, *72*(2), 293. <https://doi.org/10.2307/3100029>
- Pregitzer, K. S., King, J. S., Burton, A. J., & Brown, S. E. (2000). Responses of tree fine roots to temperature. *New Phytologist*, *147*(1), 105–115. <https://doi.org/10.1046/j.1469-8137.2000.00689.x>
- Pregitzer, K. S., Zak, D. R., Loya, W. M., Karberg, N. J., King, J. S., & Burton, A. J. (2007). The Contribution of Root – Rhizosphere Interactions to Biogeochemical Cycles in a Changing World. In *The Rhizosphere* (pp. 155–178). Elsevier. <https://doi.org/10.1016/B978-012088775-0/50009-4>
- Pustejovsky, J. E. (2018). Using response ratios for meta-analyzing single-case designs with behavioral outcomes. *Journal of School Psychology*, *68*, 99–112. <https://doi.org/10.1016/j.jsp.2018.02.003>
- R Core Team. (2020). *R: A Language and Environment for Statistical Computing*. <https://www.R-project.org/>
- Rasse, D. P., Rumpel, C., & Dignac, M.-F. (2005). Is soil carbon mostly root carbon? Mechanisms for a specific stabilisation. *Plant and Soil*, *269*(1-2), 341–356. <https://doi.org/10.1007/s11104-004-0907-y>
- Reimer, P. J., Bard, E., Bayliss, A., Beck, J. W., Blackwell, P. G., Ramsey, C. B., Buck, C. E., Cheng, H., Edwards, R. L., Friedrich, M., Grootes, P. M., Guilderson, T. P., Hafliðason, H., Hajdas, I., Hatté, C., Heaton, T. J., Hoffmann, D. L., Hogg, A. G., Hughen, K. A., . . . van der Plicht, J. (2013). IntCal13 and Marine13 Radiocarbon Age Calibration Curves 0–50,000 Years cal BP. *Radiocarbon*, *55*(4), 1869–1887. [https://doi.org/10.2458/azu\\_js\\_rc.55.16947](https://doi.org/10.2458/azu_js_rc.55.16947)
- Riley, W. J., Gaudinski, J. B., Torn, M. S., Joslin, J. d., & Hanson, P. J. (2009). Fine-root mortality rates in a temperate forest: Estimates using radiocarbon data and numerical

- modeling. *New Phytologist*, 184(2), 387–398. <https://doi.org/10.1111/j.1469-8137.2009.02980.x>
- Rumpf, S., Gravey, M., Brönnimann, O., Luoto, M., Cianfrani, C., Mariethoz, G., & Guisan, A. (2022). From white to green: Snow cover loss and increased vegetation productivity in the European Alps. *Science*, 376(6597), 1119–1122. <https://doi.org/10.1126/science.abn6697>
- Sah, S. P., Bryant, C. L., Leppälampi-Kujansuu, J., Löhmus, K., Ostonen, I., & Helmisaari, H.-S. (2013). Variation of carbon age of fine roots in boreal forests determined from  $^{14}\text{C}$  measurements. *Plant and Soil*, 363(1-2), 77–86. <https://doi.org/10.1007/s11104-012-1294-4>
- Sah, S. P., Jungner, H., Oinonen, M., Kukkola, M., & Helmisaari, H.-S. (2011). Does the age of fine root carbon indicate the age of fine roots in boreal forests? *Biogeochemistry*, 104(1-3), 91–102. <https://doi.org/10.1007/s10533-010-9485-7>
- Schindlbacher, A., Zechmeister-Boltenstern, S., Glatzel, G., & Jandl, R. (2007). Winter soil respiration from an Austrian mountain forest. *Agricultural and Forest Meteorology*, 146(3-4), 205–215. <https://doi.org/10.1016/j.agrformet.2007.06.001>
- Schindlbacher, A., Zechmeister-Boltenstern, S., & Jandl, R. (2009). Carbon losses due to soil warming: Do autotrophic and heterotrophic soil respiration respond equally? *Global Change Biology*, 15(4), 901–913. <https://doi.org/10.1111/j.1365-2486.2008.01757.x>
- Schindlbacher, A., Rodler, A., Kuffner, M., Kitzler, B., Sessitsch, A., Zechmeister-Boltenstern, S., 2011. Experimental warming effects on the microbial community of a temperate mountain forest soil. *Soil Biol. Biochem.* 43 (7), 1417–1425. <https://doi.org/10.1016/j.soilbio.2011.03.005>
- Schindlbacher, A., Wunderlich, S., Borken, W., Kitzler, B., Zechmeister-Boltenstern, S., & Jandl, R. (2012). Soil respiration under climate change: prolonged summer drought offsets soil warming effects. *Global Change Biology*, 18(7), 2270–2279.
- Schuur, E. A., Druffel, E., & Trumbore, S. E. (2016). *Radiocarbon and Climate Change*. Springer International Publishing. <https://doi.org/10.1007/978-3-319-25643-6>
- Solly, E. F., Brunner, I., Helmisaari, H.-S., Herzog, C., Leppälampi-Kujansuu, J., Schöning, I., Schrupf, M., Schweingruber, F. H., Trumbore, S. E., & Hagedorn, F. (2018). Unravelling the age of fine roots of temperate and boreal forests. *Nature Communications*, 9(1), 3006. <https://doi.org/10.1038/s41467-018-05460-6>
- Stuiver, M., & Polach, H. A. (1977). Discussion Reporting of  $^{14}\text{C}$  Data. *Radiocarbon*, 19(3), 355–363. <https://doi.org/10.1017/S0033822200003672>
- Tierney, G. L., & Fahey, T. J. (2002). Fine root turnover in a northern hardwood forest: a direct comparison of the radiocarbon and minirhizotron methods. *Canadian Journal of Forest Research*, 32(9), 1692–1697. <https://doi.org/10.1139/x02-123>
- Trumbore, S. E., & Gaudinski, J. B. (2003). Atmospheric science. The secret lives of roots. *Science*, 302(5649), 1344–1345. <https://doi.org/10.1126/science.1091841>
- Vargas, R., Trumbore, S. E., & Allen, M. F. (2009). Evidence of old carbon used to grow new fine roots in a tropical forest. *New Phytologist*, 182(3), 710–718.
- Wang, J., Defrenne, C., McCormack, M. L., Yang, L., Tian, D., Luo, Y., Hou, E., Yan, T., Li, Z., Bu, W., Chen, Y., & Niu, S. (2021). Fine-root functional trait responses to

- experimental warming: A global meta-analysis. *The New Phytologist*, 230(5), 1856–1867. <https://doi.org/10.1111/nph.17279>
- Wickham, H. (2016). *ggplot2: Elegant Graphics for Data Analysis*. Springer-Verlag New York. <https://ggplot2.tidyverse.org>
- Wunderlich, S., Schulz, C., Grimmeisen, W., & Borken, W. (2012). Carbon fluxes in coniferous and deciduous forest soils. *Plant and Soil*, 357(1-2), 355–368. <https://doi.org/10.1007/s11104-012-1158-y>
- Xia, M., Guo, D., & Pregitzer, K. S. (2010). Ephemeral root modules in *Fraxinus mandshurica*. *New Phytologist*, 188(4), 1065–1074. <https://doi.org/10.1111/j.1469-8137.2010.03423.x>
- Xu, X., Trumbore, S. E., Zheng, S., Southon, J. R., McDuffee, K. E., Luttgen, M., & Liu, J. C. (2007). Modifying a sealed tube zinc reduction method for preparation of AMS graphite targets: Reducing background and attaining high precision. *Nuclear Instruments and Methods in Physics Research Section B: Beam Interactions with Materials and Atoms*, 259(1), 320–329. <https://doi.org/10.1016/j.nimb.2007.01.17>

**Supplementary Information****Table S1:** Parameter and initial conditions values used to simulate the *one-pool* model

<b>Parameter</b>	<b>Initial condition</b>	<b>Lower bound</b>	<b>Upper bound</b>
$\tau_s$	1	$1/(365 \times 24 \times 60 \times 60)$	100
$\tau_R$	1	1/365	100

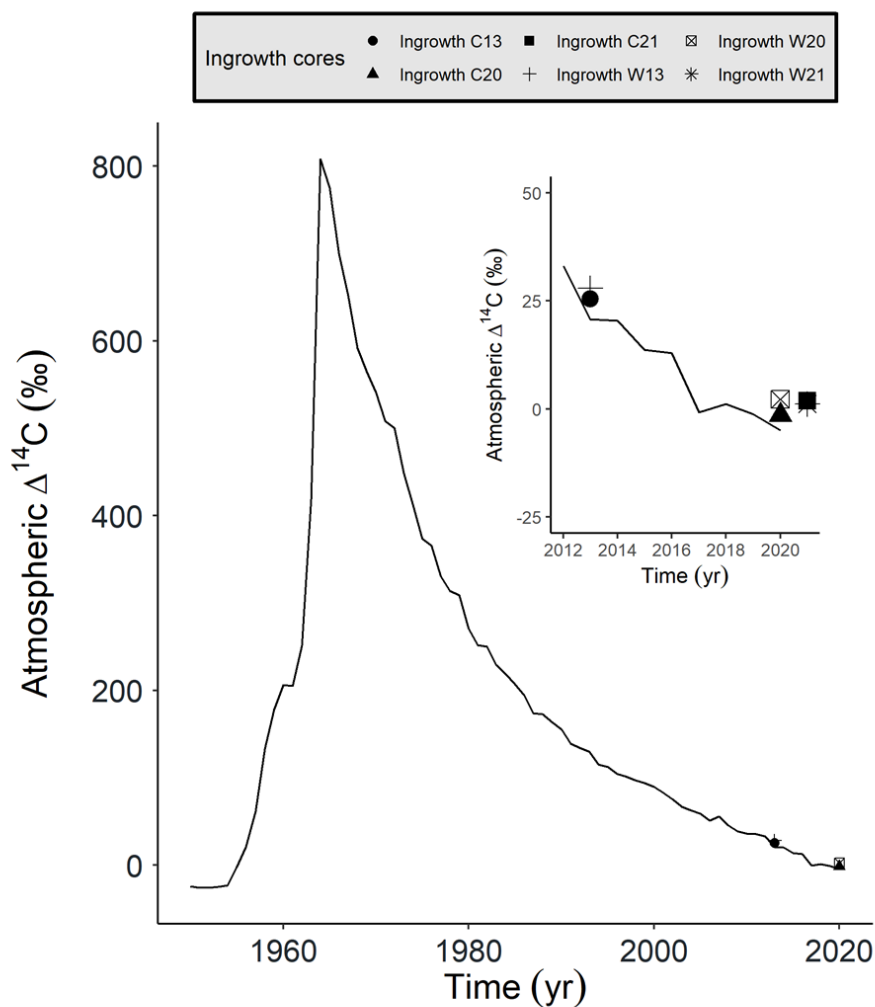


**Figure S1:** The time record of  $\Delta^{14}\text{C}$  in the atmospheric  $\text{CO}_2$  and the mean  $\Delta^{14}\text{C}$  values of fine roots from ingrowth cores sampled in October 2013 (ingrowth 13), October 2020 (ingrowth 20), and October 2021 (ingrowth 21) in control (C) and warmed plots (W). The  $\Delta^{14}\text{C}$  timeseries was constructed from the  $\Delta^{14}\text{C}$  record of atmospheric  $\text{CO}_2$  at Hohenpeissenberg (2015 - 2020), Schauinsland stations (1986 - 2016), and the Intcal13 dataset (for years before 1986). Note that the  $\Delta^{14}\text{C}$  values in ingrowth cores are greater than the atmospheric  $\Delta^{14}\text{CO}_2$ .

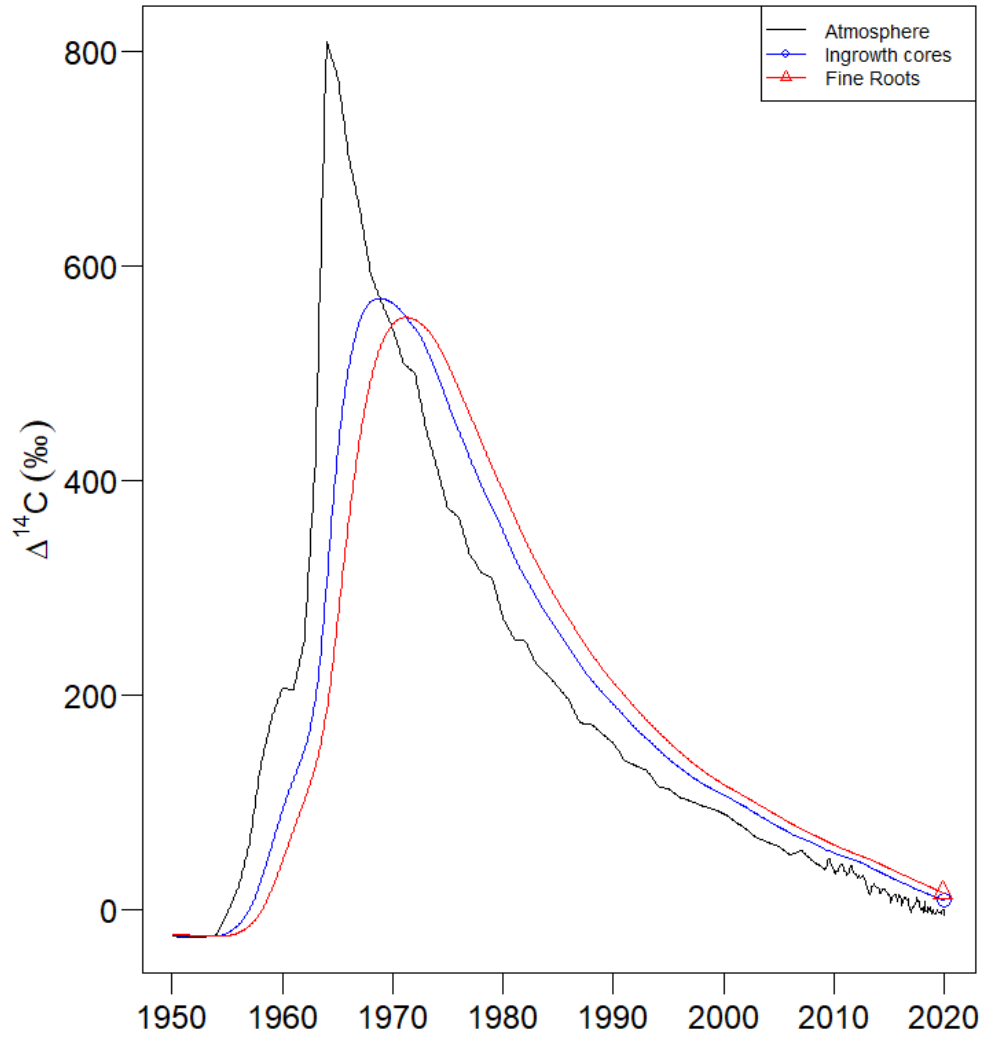


**Figure S2:** Example of modeled and measured  $\Delta^{14}\text{C}$  signatures of fine roots (red line and red triangle) and fine roots measured in ingrowth cores (blue line and blue circle). The black line represents the atmospheric  $\Delta^{14}\text{C}$  signature.

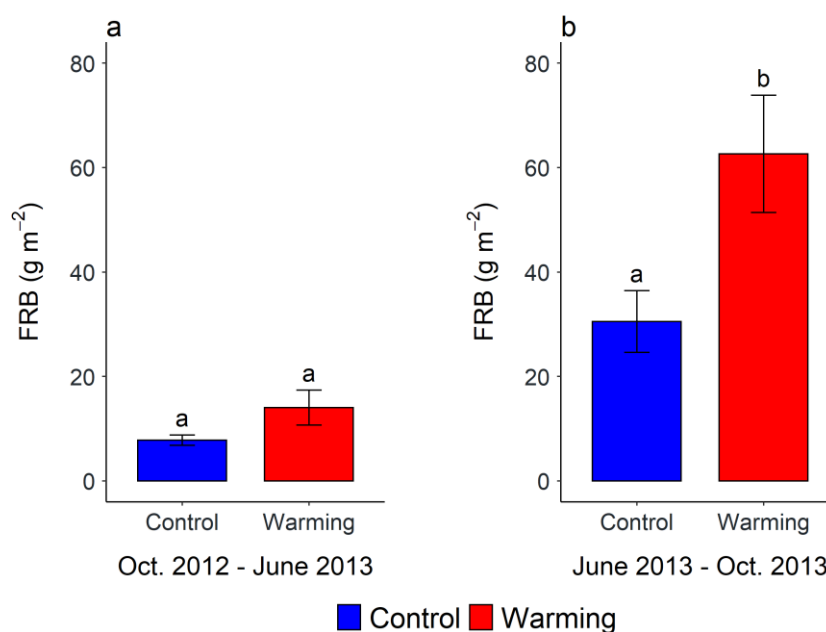


**Figure S3:** Mean  $\pm$  SE of fine root biomass production from ingrowth cores in control and warmed plots in (a) June 2013 (after 8 months), (b) October 2013 (after 4 months) ( $n = 3$ ). Different letters indicate significant differences between control and warmed plots ( $p < 0.05$ ).

**Supplementary Method 1:** Description of the ABA treatment for radiocarbon analyses.

Approximately 100 mg of dry roots were weighted into glass tubes and washed with an acid solution first. Each glass tube was filled about 2/3 with 1 M HCl, capped, and put on a heating block at 70 °C for 30 minutes. After the first acid wash, samples were repeatedly washed with a base solution (1M NaOH) at 70 °C for 30 minutes to remove soil humic substances until the solution remained clear (usually three to four washes). A final dilute acid wash was performed to remove any atmospheric  $\text{CO}_2$  absorbed during the alkali washes. After that, samples were washed two to three times with Milli-Q water at 70°C for 10 minutes to neutralize the pH and remove chloride that could potentially corrode the quartz tubes during sample combustion. Individual disposable pipettes were used to discard the ABA solution throughout the treatment to avoid cross-contamination. At the end of the pre-treatment, samples were oven-dried at 60 °C for three days.

### **Study III**

#### **Long-term warming increased CO<sub>2</sub> efflux but not the transit time of soil carbon in a temperate forest**

Steve Kwatcho Kengdo, Andreas Schindlbacher, Carlos A. Sierra, Jakob Heinzle, Bernhard Ahrens, Ye Tian, Wolfgang Wanek, Werner Borken

In preparation

**Abstract**

The increasing global temperature may accelerate soil organic carbon (SOC) cycling, thereby altering the carbon dioxide (CO<sub>2</sub>) efflux from soils to the atmosphere and SOC stocks. Understanding and predicting the fate of SOC with warming is essential to forecast future changes. We studied the effect of 15 years of soil warming (+4°C) on radiocarbon signature bulk soil, the transit time of carbon, and soil CO<sub>2</sub> efflux in a temperate mountain forest in the Austrian limestone Alps. Radiocarbon signatures of bulk soil from 0 – 10 cm and 10 – 20 cm soil depth, C inputs by aboveground and belowground litter were used to model the transit time of SOC in control and warming plots under the assumption of constant C inputs and SOC stocks over the model window. Our results showed no evidence that soil warming affected the radiocarbon signature of SOC. Although the transit time of carbon in control and warming treatments were similar, measured CO<sub>2</sub> efflux was 41% higher with warming, representing an additional annual C release of 2.6 t C ha<sup>-1</sup> from the warming treatment. Similar SOC stocks and transit times of C suggest that the warming-induced increase in soil CO<sub>2</sub> efflux can be assigned mainly to the increase in rhizosphere respiration. Our results indicate that soil respiration at the Achenkirch site has not yet acclimated to soil warming and that the potential for SOC losses by global warming is relatively small in this forest ecosystem.

**Keywords:** carbon dioxide efflux; soil organic carbon; global warming; radiocarbon signatures; transit time; rhizosphere respiration; acclimation.

## Introduction

Temperate mountain forests in the Alpine region of Europe store large amounts of soil organic carbon (SOC) because, due to their location, cool-moist climate conditions limit soil microbial activity and decomposition of organic matter (Jandl et al., 2021). As a result, mineral topsoils with very high SOC concentrations of up to 10 – 15% have developed under these climatic conditions (D. Liu et al., 2017; Schnecker et al., 2016). However, increasing global temperatures by up to 4.4° C above preindustrial levels (IPCC, 2021) or even stronger above-global average increase in temperature as predicted by regional climatic simulations (Gobiet et al., 2014; Warscher et al., 2019) could lead to significant losses of SOC stocks from those soils.

When water or substrate availability is not limiting, increasing temperature has been found to accelerate soil carbon (C) cycling by increasing soil microbial activity, which in turn increases the mineralization of soil organic matter (SOM), leading to SOC losses and enhanced soil respiration ( $R_s$ , the release of CO<sub>2</sub> produced by biological activity to the atmosphere) (Bardgett et al., 2008; Davidson & Janssens, 2006). In many studies,  $R_s$ , which integrates autotrophic (plant roots and mycorrhizae respiration) and heterotrophic (microbial respiration) components, had been found to strongly increase during the first years following the start of the warming treatment (Melillo et al., 2002; Schindlbacher et al., 2009). This first phase is characterized by the increase in enzymatic activity and the decomposition of labile C, which lead to significant loss of C from the soil (Fanin et al., 2022; Y. Luo et al., 2001). Following substrate depletion, the decline of microbial biomass, and the physiological adaptation of microbes, a second phase may occur and is characterized by the reduction in SOC loss and  $R_s$  returns to the level observed in the control treatment (Fanin et al., 2022). In this second phase, the decline in the temperature sensitivity of  $R_s$ , termed *acclimation* of  $R_s$  (Carey et al., 2016; Y. Luo et al., 2001), is hypothesized to last some years or a few decades and may weaken the positive feedback between SOC and temperature (Fanin et al., 2022; Melillo et al., 2017). However, one crucial question remains whether  $R_s$  will acclimate to future climate warming. Soils may respond differently because SOC stabilization mechanisms are also different (Lützow et al., 2006).

Radiocarbon modeling may provide insight into how SOC cycles under climate warming (Trumbore, 2009; Y. Wang & Hsieh, 2002). Because the radiocarbon signature ( $\Delta^{14}\text{C}$ ) of SOM integrates both the inputs and outputs of C, it can be used as a powerful tracer for temporal changes in C cycling (Schoor et al., 2016). The labeling of the atmosphere by bomb carbon

from the 1950s until the mid-1960s makes the use of  $^{14}\text{C}$  modeling a suitable way to study the dynamics of C in terrestrial ecosystems (Trumbore, 2009). Until recently,  $^{14}\text{C}$  modeling of SOC mainly focused on using single or multiple pool models to estimate the turnover of SOC (Ahrens et al., 2014; Barrett, 2002; Gaudinski et al., 2000). However, studying the age and transit time of C as well as the  $^{14}\text{C}$  distribution in SOC (Chanca et al., 2022; Sierra et al., 2017) with warming might further complement the knowledge of  $R_s$ . For example, the transit time of C representing the age of the output flux or the age of C when leaving the soil may further inform about C storage and flow in the soil (Sierra et al., 2017). Because it can also be interpreted as the time it takes for C to transit the soil system, the transit time of C may therefore inform about the proportional contribution of younger or older C in the release flux from SOM decomposition. At the same time, the  $^{14}\text{C}$  distribution may tell about the shape of the entire radiocarbon distribution in SOC (rather than focusing on mean values) and the proportional distribution of young or old carbon (Chanca et al., 2022).

We aimed to investigate the effects of soil warming on the transit time of C in the soil and soil  $\text{CO}_2$  efflux at the long-term forest soil warming experiment at Achenkirch, Tyrol, Austria. The increase in soil temperature in the warming treatment by  $+4^\circ\text{C}$  (compared to control) over the past 15 years at this site provide an excellent field to study the impact of long-term soil warming on SOC dynamics. We were motivated by the following questions: (i) How does soil warming alter the  $^{14}\text{C}$  distribution of SOC in two soil depths? (ii) Are the transit time of C and the modeled C release from mineralization of litter and SOC (heterotrophic respiration) different between control and warming treatments? (iii) Does  $R_s$  acclimate after 15 years of soil warming? To address these questions, we used inputs of aboveground and belowground litter, the SOC stocks, and the radiocarbon signatures of litter and SOC from two sampling years (2012 and 2019). The radiocarbon model implemented in the environment of the R package *SoilR* was used to assess the transit time of C, the radiocarbon distribution of SOC, and the C release by heterotrophic respiration in the two soil depths of shallow calcareous forest soil.

## Materials and methods

### Site description

The long-term soil warming experiment was located in a temperate forest at Achenkirch, Tyrol, in the Austrian Limestone Alps (47°34'50" N; 11°38'21" E) at 910 m a.s.l (Schindlbacher et al., 2007). This 140-year-old forest was dominated by Norway spruce (*Picea abies* L. H. Karst.), interspersed by European beech (*Fagus sylvatica* L.) and silver fir (*Abies alba* Mill.). The mean annual air temperature and precipitation measured between 1988 to 2017 were 7.0 °C and 1493 mm, respectively. Soils are characterized as a mosaic of shallow Chromic Cambisols and Rendzic Leptosols. They consisted of a mineral A-horizon with an average thickness of about 15 – 20 cm and a C-horizon derived from dolomite. The A-horizon had a C:N ratio between 15 and 18, a near-neutral pH, and stored approximately 104 t C ha<sup>-1</sup>. The L/F- horizons stored approximately 10 t C ha<sup>-1</sup> (Schindlbacher et al., 2011).

### Soil warming experimental setup

The soil warming experiment is composed of six blocks of 2 × 2 m paired plots (each pair consisted of one control and one warmed plot), established in 2004 (n = 3) and 2007 (n = 3). Six plots were warmed (hereafter termed warming treatment) using heating cables (Etherma, Salzburg, Austria) installed at 3 cm soil depth, with a spacing of 7.5 cm. In the remaining six plots (hereafter termed control treatment), heating cables were installed but not heated to account for the disturbance created by their installation. The heating system was fully controlled by a service unit that automatically kept a +4 °C difference between the treatments throughout the snow-free period between April and December. A further description of the experimental setup is provided by Schindlbacher et al. (2007; 2009).

### Soil CO<sub>2</sub> efflux measurements

Soil CO<sub>2</sub> efflux ( $F_{soil}$ ) was measured fortnightly during the snow-free seasons and every third week during snow cover. During the snow-free season,  $F_{soil}$  was measured from permanently installed chambers (20 cm diameter, 10 cm height). Three chambers were randomly distributed at each plot and inserted 1 cm into the mineral soil to establish an airtight seal. Chambers were closed with a stainless steel lid for 300 sec. CO<sub>2</sub> concentrations were measured every 30 seconds using an EGM4 infrared gas analyzer (PP-Systems, Amesbury, USA). The CO<sub>2</sub> concentration increase in the chamber headspace during the last 120 sec was used to calculate the flux (linear fit). CO<sub>2</sub> fluxes were calculated as follows:

$$F_{soil} = \frac{\Delta C}{\Delta t} \times \frac{273.15}{T_{air} + 273.15} \times \frac{p}{1000} \times \frac{M}{M_v} \times \frac{V}{A} \quad Eq. 1$$

where  $F_{soil}$  is the hourly CO<sub>2</sub> flux (mg C m<sup>-2</sup> h<sup>-1</sup>),  $\frac{\Delta C}{\Delta t}$  is the concentration change (ppmv) over time (h),  $T_{air}$  is the air temperature in the chamber headspace (°C),  $p$  is the atmospheric pressure (mbar),  $M$  is the molecular weight of C (g mol<sup>-1</sup>),  $M_v$  is the molar volume of an ideal gas at standard temperature and pressure (22.41 L mol<sup>-1</sup>),  $V$  is the chamber volume (m<sup>3</sup>), and  $A$  is the chamber area (m<sup>2</sup>). During snow cover,  $F_{soil}$  was estimated according to Schindlbacher et al. (2007). Annual cumulative CO<sub>2</sub> efflux (t C ha<sup>-1</sup> yr<sup>-1</sup>) was calculated by linear interpolation between flux measurement dates of the corresponding year.

### **Above-ground litter**

Aboveground litterfall has been monitored at the Achenkirch site since 2007 using litter traps with an area of 0.5 m<sup>2</sup> each, systematically distributed to cover the entire site variability. All litter traps were placed 1.5 m above the forest floor. In addition, leaf and needle litter were directly sampled from the Oi horizon of the forest floors in both treatments in 2012. The litter within the traps was collected every second month, except during the snow season from December to March. Samples from each sampler were sorted into leaves, needles, and other fragments (small branches, cones, bark, twigs, seeds). Aboveground litter samples were oven-dried at 60°C and weighed. Samples were stored until radiocarbon analyses (see below), and aboveground C input by litterfall was calculated assuming a constant C fraction of 50% of dry matter.

### **Bulk soil sampling**

Bulk soils were sampled on two occasions in October 2012 and October 2019. On each occasion, ten soil cores were randomly taken at 0 – 10 cm and 10 – 20 cm soil depth from each control and warmed plot using a cylindrical soil corer (5 cm in diameter and 20 cm in length). We sampled six plots in 2012 (n = 3 per treatment) and twelve in 2019 (n = 6 per treatment), giving a total of 120 and 240 samples per occasion, respectively. Around 30 g of each soil sample were field-sieved (2 mm) and homogenized per plot and soil depth. Aliquots (a total of 12 and 24 soil subsamples in 2012 and 2019, respectively) were immediately taken and stored in cooling boxes filled with ice packs and transported to the laboratory in Bayreuth, where they were held in the freezer at – 24°C until processing.

### **Fine roots sampling**

After taking aliquots of soils as described above, the remaining bulk soils containing fine roots were transferred in plastic bags, stored in cooling boxes, and transported to the laboratory where fine roots (< 2 mm in diameter) were processed as described by Kwatcho Kengdo et al. (2022). After processing, dried subsamples of the ten replicates per plot and soil depth were thoroughly mixed to form homogenous fine root samples (12 and 24 samples in 2012 and 2019, respectively).

### **Radiocarbon sample preparation**

#### ***Bulk soil pre-treatment***

Approximately 5 g of frozen sieved soil of each sample was weighed into 50 ml glass beakers and oven-dried at 105°C for three days. An aliquot of 1 g of each sample was weighed in a petri dish and carefully examined under the binocular microscope. Using tweezers, dolomites (stones), plant residues, and fine roots were removed. When necessary, a mortar and pestle were used for crushing soil aggregates into small pieces. After this physical examination, samples were milled and equally decarbonated with 2 M HCl at 25°C in an oven for a few weeks. After the pre-treatment, samples were dried at 105°C without centrifugation to avoid loss of C and stored until radiocarbon analyses.

#### ***Fine roots and aboveground litter pre-treatment***

Fine roots were treated with an acid-base-acid treatment to remove non-structural carbohydrates and organic contaminants that may post-date fine root formation (Gaudinski et al., 2001). For this purpose, we used and adapted a protocol of the Keck-CCAMS Facility at the University of California, Irvine, USA (<https://www.ess.uci.edu/~ams/Protocols.htm>; last accessed on January 26, 2022). More details of the fine roots pre-treatment procedure are given by Kwatcho Kengdo et al. (2023). Regarding aboveground litter, beech leaves and spruce needles mixture directly sampled at the surface of the plots in 2012 were considered, while in 2019, we treated leaves and needles from the litter collector separately. We used the same acid-base-acid pre-treatment approach, except that alkali washes were reduced significantly for beech leaves because of their soft structure. Pre-treated fine root and aboveground litter samples were oven-dried at 60 °C for three days and stored in glass tubes until radiocarbon analyses.

***Samples conversion into graphite***

The C contained in soil, fine root, and aboveground litter samples was cryogenically extracted, purified, and converted into graphite using the sealed-tube zinc reduction method described by X. Xu et al. (2007). The graphite obtained was pressed into aluminum targets and sent for analysis to the Keck-CCAMS Facility at the University of California, Irvine, USA, where the radiocarbon content of all samples was measured using accelerator mass spectrometry (AMS, NEC 0.5MV 1.5SDH-2 Pelletron, National Electrostatics Corporation, Middleton, Wisconsin, USA) (Southon et al., 2004). Radiocarbon results were expressed as  $\Delta^{14}\text{C}$  (in ‰, or parts per thousand), including a correction of sample  $\delta^{13}\text{C}$  value of  $-25\text{‰}$ . The correction removes the effects of mass-dependent isotopic fractionation (Stuiver & Polach, 1977). The  $^{14}\text{C}$  enrichment of a sample is measured as a fraction of the  $^{14}\text{C}$  activity relative to a modern standard of fixed isotopic composition. More details on the graphitization procedure are given by Kwatcho Kengdo et al. (2023).

**Radiocarbon modeling*****Input data***

A radiocarbon curve integrating the pre- and post-bomb period was constructed by interpolating the Intcal13 dataset (Northern hemisphere atmospheric  $\Delta^{14}\text{C}$  for years  $< 1986$ ) (Reimer et al., 2013) and  $^{14}\text{C}$  records of atmospheric  $\text{CO}_2$  measured at the Hohenpeißenberg (2015 - 2020) (Kubistin et al., 2021) and the Schauinsland stations (1986 - 2016) located in the South of Germany (Hammer & Levin, 2017).

Radiocarbon contents of fine roots (Kwatcho Kengdo et al., 2023) and bulk soil measured at the two sampling occasions (2012 and 2019) were aggregated into mean and standard deviation for each treatment (control and warming) and soil depth (0 – 10 cm and 10 – 20 cm). For aboveground litter, the mean  $\Delta^{14}\text{C}$  and standard deviation were calculated based on values measured on the leaves-needles mixture sampled in each plot in 2012, while the  $\Delta^{14}\text{C}$  of aboveground litter in 2019 corresponds to the weight-average  $\Delta^{14}\text{C}$  of beech and needles that were measured separately. We thus assumed the same  $\Delta^{14}\text{C}$  signature for aboveground litter in both control and warming treatment in 2019 but a faster decay rate of C in the aboveground litter pool in the warming treatment (Aerts, 1997; Freschet et al., 2013; Song et al., 2021).

The mean aboveground litter input was  $1.7 \pm 0.08 \text{ t C ha}^{-1}$  at the study site between 2008 – 2019 (Schindlbacher, unpublished data). This estimate was used to represent the C input from

aboveground litter in both control and warming treatments at 0 – 10 cm soil depth. Fine roots C inputs were estimated by Kwatcho Kengdo et al. (2023) at 0 – 10 cm and 10 – 20 cm soil depths for the two sampling occasions. Fine roots C input for each treatment and soil depth was calculated as the mean for the two sampling occasions. SOC stocks were calculated by multiplying the C concentration (Tian et al. 2023) measured in each plot and soil depth in 2019 by the respective bulk density (Schindlbacher, unpublished data). SOC stocks were also aggregated into mean and standard deviation according to treatment and soil depth.

### ***Model structure***

We used a radiocarbon model to estimate the age and transit time of C in control and warming treatments. This model considered a soil system composed of 0 – 10 cm and 10 – 20 cm soil depths (Figure 1). At 0 – 10 cm, the system comprises three compartments: aboveground litter, fine roots, and bulk soil, while there are only two compartments (fine roots and bulk soil) at 10 – 20 cm soil depth. C compartments were modeled separately for two soil depths, assuming no solid or solute C transfer between them. In the upper soil layer (0 – 10 cm), C enters the system as aboveground litter (compartment 1) and fine roots (compartment 2). The C in those two compartments is subject to exponential decay, with decay rates  $k_1$  and  $k_2$ , respectively. Following that decay, a fraction of the decomposed litter in both compartments is lost (output fluxes, Figure 1a), the remaining is transferred to the bulk soil, and the transfer coefficients  $a_{3,1}$  and  $a_{3,2}$  describe the rate of this flux, respectively. The C in bulk soil is also subject to decay, represented by  $k_3$ . A fraction of that C is also lost, and the remaining accumulates as SOC (Figure 1a). Dissolved organic carbon (DOC) input by throughfall was not considered in the model because the flux is relatively small ( $0.13 \text{ t C ha}^{-1} \text{ yr}^{-1}$ , unpublished data). Throughfall DOC is assumed to be rapidly mineralized by soil microbes (Bradford et al., 2008; Davidson & Janssens, 2006; Lützow & Kögel-Knabner, 2009). Carbon fluxes from living roots to the soil by exudation, mucilage, or transfer to ectomycorrhizal hyphae were also not considered in the model.

For 10 – 20 cm soil depth, we assumed minor input of aboveground litter by soil-dwelling macrofauna and was thus not considered in the model. Carbon enters this soil depth only as fine root litter (compartment 1). The decay rate of C in that compartment is represented by  $k_1$ , and the rate of outflux between the fine root and bulk soil is represented by  $a_{2,1}$ . The decay rate in the bulk soil will be  $k_2$  (Figure 1b).

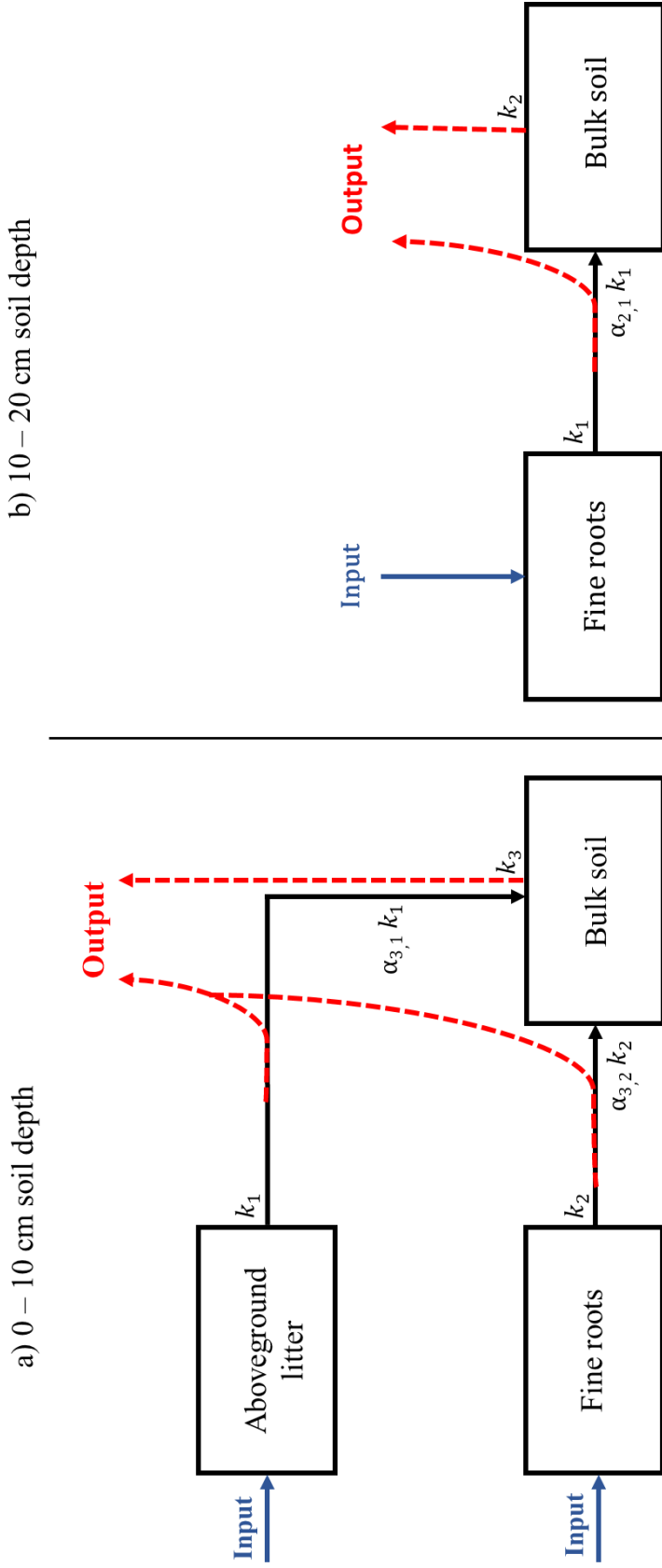


**Figure 1:** Structure of the model used to estimate radiocarbon distributions at (a) 0 – 10 cm and (b) 10 – 20 cm soil depths. At 0 – 10 cm,  $k_1$ ,  $k_2$  and  $k_3$  are the decay rates in the aboveground litter, fine roots, and bulk SOM, respectively.  $\alpha_{3,1}$  and  $\alpha_{3,2}$  describe the proportion of C transferred from aboveground litter to bulk soil and from fine roots to bulk soil, respectively. At 10 – 20 cm,  $k_1$  and  $k_2$  are decay rates in fine roots and bulk soil, respectively, and  $\alpha_{2,1}$  describes the proportion of C from fine roots to bulk soil. Each model structure can be viewed as a system, considered as a set of compartments or pools and mass transfer among them (Sierra et al. 2017).

**Model implementation and fitting**

We considered a steady-state compartment model using the *SoilR* package, version 1.2.105 (Sierra et al., 2012, 2014). The model is described with the following equation (Eq.2):

$$\frac{dC(t)}{dt} = I + B(t) C(t) \quad \text{Eq. 2}$$

Where  $I$  is a constant vector that describes the inputs of C to each compartment  $n$  in the system at a time  $t$ ;  $B(t)$  is a  $n \times n$  square matrix of decomposition and transfer rates within the soil system, and  $C(t)$  is a  $n \times 1$  vector of C stocks in each compartment. Following this general formulation, we can represent the model at 0 – 10 cm and 10 – 20 cm soil depth with Eq.3 and Eq.4, respectively:

$$\begin{pmatrix} dC_1/dt \\ dC_2/dt \\ dC_2/dt \end{pmatrix} = \begin{pmatrix} I_1 \\ I_2 \\ 0 \end{pmatrix} + \begin{pmatrix} -k_1 & 0 & 0 \\ 0 & -k_2 & 0 \\ \alpha_{3,1}k_1 & \alpha_{3,2}k_2 & -k_3 \end{pmatrix} \begin{pmatrix} C_1 \\ C_2 \\ C_3 \end{pmatrix} \quad \text{Eq. 3}$$

$$\begin{pmatrix} dC_1/dt \\ dC_2/dt \end{pmatrix} = \begin{pmatrix} I_1 \\ 0 \end{pmatrix} + \begin{pmatrix} -k_1 & 0 \\ \alpha_{2,1}k_1 & -k_2 \end{pmatrix} \begin{pmatrix} C_1 \\ C_2 \end{pmatrix} \quad \text{Eq. 4}$$

and with initial conditions as follows:

$$\begin{pmatrix} C_{1i} \\ C_{2i} \\ C_{3i} \end{pmatrix} = C_i \begin{pmatrix} y_1 \\ y_2 \\ y_3 \end{pmatrix} \quad \text{Eq. 5}$$

where  $I_i$  represents the input of C to each compartment. Decomposition rates in each compartment  $i$  are represented by  $k_i$ , and transfer rates from a compartment  $j$  to a compartment  $i$  are represented by  $\alpha_{i,j}$ .  $y_i$  represents the proportion of C in each pool.

In the package *SoilR*, the model was built with the function *Model\_14* and fitted for the period 1900 – 2022. This function considered the time vector  $t$ , which contains the point where the solution is sought, a vector containing the initial amounts of C in each compartment, and an object describing the atmospheric  $\Delta^{14}\text{C}$  and the decay rate of  $^{14}\text{C}$ . The model was fitted to the observed data using the Levenberg-Marquart method (Moré, 1978), which estimates the best parameter values by minimizing the difference between model predictions and observed data.

2012 and 2019 radiocarbon data were fitted together as a time series to better integrate the dynamics of  $\Delta^{14}\text{C}$  in each compartment in relation to the atmosphere (Baisden et al., 2013). The  $\Delta^{14}\text{C}$  signatures, the C contents, and the amount of C release for each compartment as a function of time were calculated by the functions *getF14C*, *getC*, and *getReleaseFlux*, respectively. The model was run assuming that the initial SOC stock equaled the measured stocks in 2019 (Table S1).

### ***Age and transit time***

We calculated the system's age and transit time distribution and the age distribution of specific compartments using the approach developed by Metzler and Sierra (2018), which considers the vector of input ***I*** and the matrix ***B*** containing the best parameters values of decay and transfer rates for each compartment (Table S2).

### ***Radiocarbon distribution in soil organic carbon***

Using the age distributions of carbon estimated above, we computed the  $\Delta^{14}\text{C}$  distribution in bulk soil in both control and warming treatments using the algorithm introduced by Chanca et al. (2022). These  $\Delta^{14}\text{C}$  distributions show the proportional mass distribution of SOC for different  $\Delta^{14}\text{C}$  values or classes for a specific year of sampling and thus inform whether the  $\Delta^{14}\text{C}$  distribution differs between control and warming treatments. First, the algorithm normalizes the time variable of the atmospheric  $\Delta^{14}\text{C}$  and the age distribution curves obtained previously. In the second step, both curves are divided into discrete intervals, and the final step combines the mass distribution of discrete age classes with the  $\Delta^{14}\text{C}$  atmospheric curve (Chanca et al., 2022).

### ***Statistics and data repository***

All data analyses were conducted in R version 4.2.1 (R Core Team, 2022). The R packages *ggplot2* (Wickham, 2016), *patchwork* (Pedersen, 2022), and *gridExtra* (Auguie, 2017) (Auguie, 2017) were used for data visualization. Annual cumulative CO<sub>2</sub> fluxes were checked for normality using the Shapiro–Wilk test and, when needed, were square-root transformed before paired t-tests ( $\alpha = 0.05$ ). The differences in  $\Delta^{14}\text{C}$  signatures between control and warmed plots were tested with the Wilcoxon signed-rank test ( $\alpha = 0.05$ ). The R code and data used in this article will be made available on the repository Zenodo.

## Results

### Radiocarbon signatures of aboveground litter, fine roots, and bulk SOM

Except for bulk soil sampled in 2012 at 10 – 20 cm soil depth, the mean  $\Delta^{14}\text{C}$  signatures of aboveground litter, fine roots, and bulk soil across all sampling occasions were all positive, indicating that they contained a high proportion of bomb radiocarbon (Table 1). The mean  $\Delta^{14}\text{C}$  of aboveground litter measured in 2012 in both treatments were 46‰ and 42‰ in control and warming, respectively, and exceeded the contemporary atmospheric mean by 16‰ and 12‰, respectively. As we assumed for both treatments, the same  $\Delta^{14}\text{C}$  for the aboveground litter in 2019 (9.5‰), the difference to the contemporary mean was 12‰. Mean fine root  $\Delta^{14}\text{C}$  values at both sampling occasions were overall variable (as indicated by the spread of their standard deviations) and tended to decrease with soil warming and to increase with increasing soil depth except at 0 – 10 cm in 2019 (Table 1). The mean  $\Delta^{14}\text{C}$  of bulk soil was also variable and showed contrasting patterns on the two sampling occasions. For most samples,  $\Delta^{14}\text{C}$  increased with soil warming and decreased with soil depth in 2012, while they decreased with warming and soil depth in 2019.

### Model parameters

We fitted the data consistently for all treatments and soil depths, except for the control treatment at 10 – 20 cm, where a good fit between modeled and observed  $\Delta^{14}\text{C}$  values was difficult to achieve (Figure S1). Mean parameter values that provide the best fit between model predictions and observations are reported in Table S2. Decay rates for aboveground litter ranged from 0.329 to 0.600  $\text{yr}^{-1}$ . The decay rate of fine roots increased from 0.170 to 0.270  $\text{yr}^{-1}$  with warming at 0 – 10 cm soil depth but did not change at 10 – 20 cm (0.128 to 0.127  $\text{yr}^{-1}$ ). The decay rate of bulk soil was 0.007  $\text{yr}^{-1}$  in both treatments at 0 – 10 cm and 0.001 to 0.002  $\text{yr}^{-1}$  at 10 – 20 cm soil depth. The model also predicted that the proportion of C transferred from aboveground litter to bulk SOC was ca. 17 to 19% in both treatments, while C transferred from fine roots to bulk SOC was ca. 20% and 47% in both treatments at 0 – 10 cm and 10 – 20 cm soil depth.

### The transit time of carbon in control and warming treatment

The median transit time, which characterizes the age of the output flux, was 3.4 yr and 2.0 yr in control and warming at 0 – 10 cm soil depth and around 20 yr in both treatments at 10 – 20 cm soil depth (Figure 2).

**Table 1:** Mean (and standard deviation) radiocarbon signatures (%) in aboveground litter, fine roots, and bulk soil organic matter in control and warming. n = 3 and n = 6 in 2012 and 2019, respectively.

Treatment	Soil depth (cm)	2012				2019			
		Aboveground litter	Fine roots	Bulk SOM		Aboveground litter	Fine roots	Bulk SOM	
Control	0 – 10	46.07 (0.58)	51.36 (6.80)	49.81 (20.01)	9.50 (0.13)	35.26 (27.62)	63.70 (12.97)		
	10 - 20	-	70.79 (22.04)	-11.11 (16.82)	-	30.26 (24.17)	30.21 (20.16)		
Warming	0 – 10	42.25 (1.99)	44.72 (6.99)	57.65 (10.02)	9.50 (0.13)	29.11 (14.14)	58.77 (13.60)		
	10 - 20	-	66.08 (13.41)	13.50 (14.03)	-	35.48 (19.65)	17.49 (24.53)		

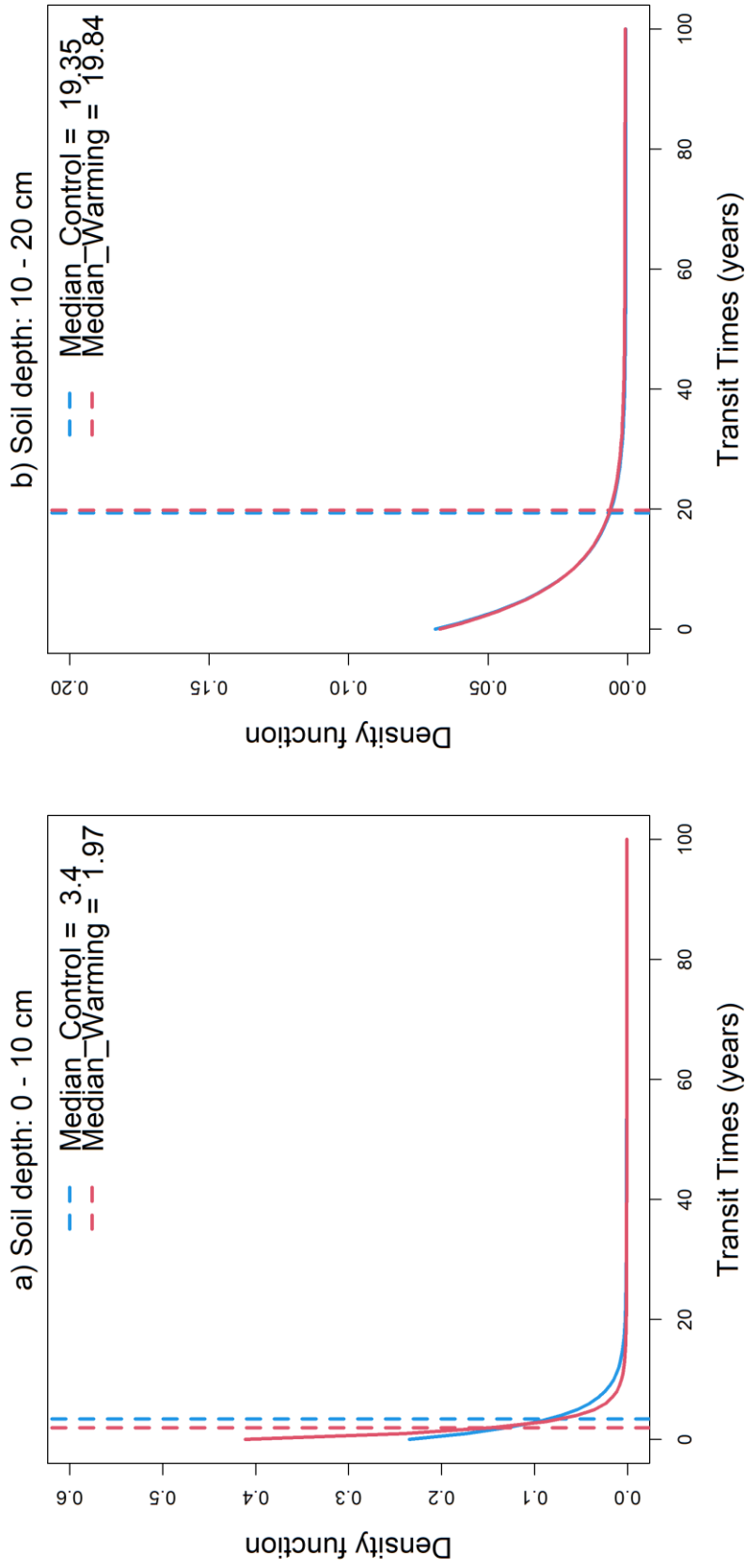


**Figure 2:** Transit of C in control and warming treatments at (a) 0 – 10 cm and (b) 10 – 20 cm soil depth.

**Radiocarbon distribution in SOC after 15 years of soil warming**

The radiocarbon distribution of C from the mineral soil computed for 2019, assuming that initial SOC equals measured values in 2019 overall, showed the same pattern in control and warming treatments for both soil depths (Figure 3). Irrespective of treatment or soil depth, the  $\Delta^{14}\text{C}$  distributions showed a wide range and were highly right-skewed with long tails. At 0 – 10 cm soil depth, the model predicted that around 42% of the total SOC mass in control and warming treatments was pre-bomb (27 and 28 t C ha<sup>-1</sup>, respectively). The remaining is distributed in a relatively recent C class with  $\Delta^{14}\text{C} < 46\%$  accounting for 31% of the total mass (19 t C ha<sup>-1</sup> and 21 t C ha<sup>-1</sup> in control and warming, respectively) and a wide range of older modern C accounting for approximately 18t C ha<sup>-1</sup> in both treatments. A similar mass distribution was observed at 10 – 20 cm soil depth, although the proportion of C was lower compared to the upper soil depth. About 27 and 30% of the total SOC stock was pre-bomb C in control and warming treatments. The remaining SOC at this depth was made of a high proportion of relatively recent C with  $\Delta^{14}\text{C} < 46\%$  (64 % and 59 % in control and warming, respectively). The remaining 10 % in both treatments was older modern C distributed in a wide range of  $\Delta^{14}\text{C}$  values.

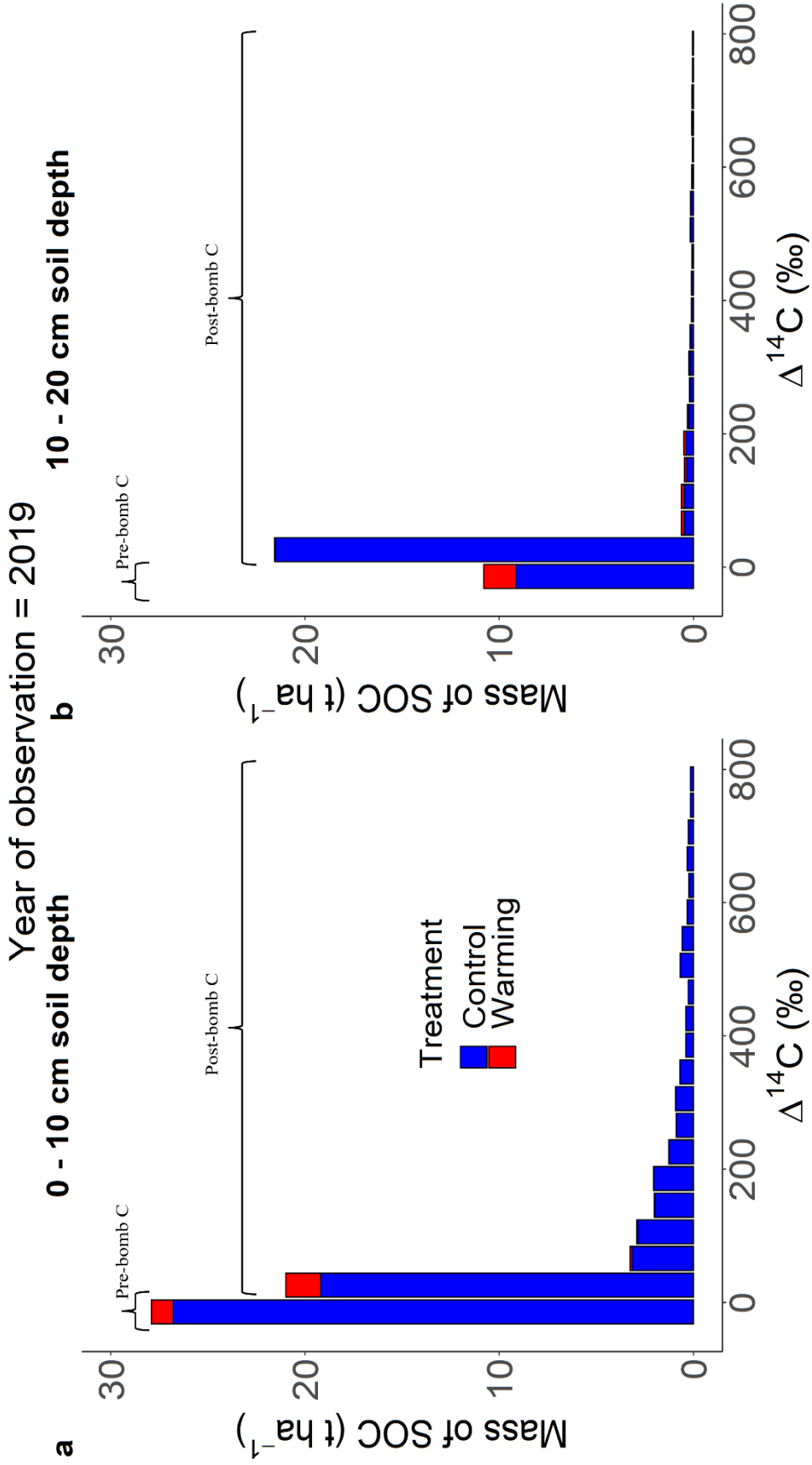


**Figure 3:** Modeled distributions of SOC stocks by radiocarbon signature at (a) 0 – 10 cm and (b) 10 – 20 cm soil depth in control and warming for the year 2019 (after 15 years of soil warming treatment). The distribution at both soil depths was computed over 1000 years and discretized by 0.1 yr.

### Soil CO<sub>2</sub> efflux

Annual soil CO<sub>2</sub> efflux increased in both treatments from 5.5 – 7.5 t C ha<sup>-1</sup> to 7.8 – 10.9 t C ha<sup>-1</sup> over the investigated period (Figure 4). In 2006, soil CO<sub>2</sub> efflux was higher in the warming treatment, but the difference was not significantly different with n=3 plots. Following the addition of new plots in each treatment, CO<sub>2</sub> efflux significantly increased by 37% in 2010 ( $p = 0.002$ ), 39% in 2015 ( $p = 0.005$ ), and 47% in 2019 ( $p = 0.002$ ).

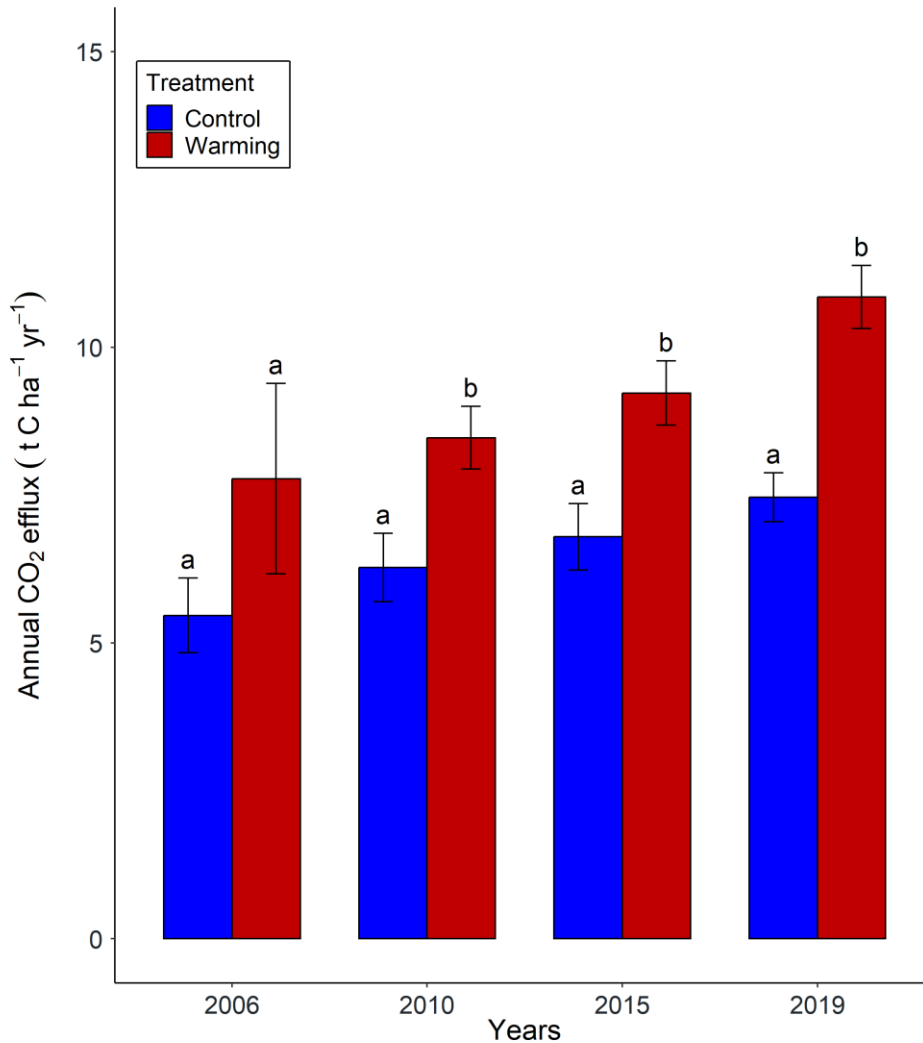


**Figure 4:** Annual cumulative CO<sub>2</sub> efflux ( $\pm$  SE) in control and warming treatment in 2006, 2010, 2015, and 2019. Different letters indicate a significant difference between treatments.

### Modeled carbon release in control and warming treatment

For the period 2004 – 2022, the model predicts that the aboveground litter pool is the pool with high C release on average, with 1.38 and 1.41 t C ha<sup>-1</sup> yr<sup>-1</sup> in control and warming, respectively (Figure 5). Carbon loss from the fine root pool at 0 – 20 cm soil depth slightly increased from 0.53 to 0.71 t C ha<sup>-1</sup> yr<sup>-1</sup> on average with warming, while losses from the SOC pool were 0.48 and 0.52 t C ha<sup>-1</sup> yr<sup>-1</sup> in control and warming, respectively. The total C release predicted by the model was 2.40 and 2.63 t C ha<sup>-1</sup> yr<sup>-1</sup> in control and warming treatments, respectively.

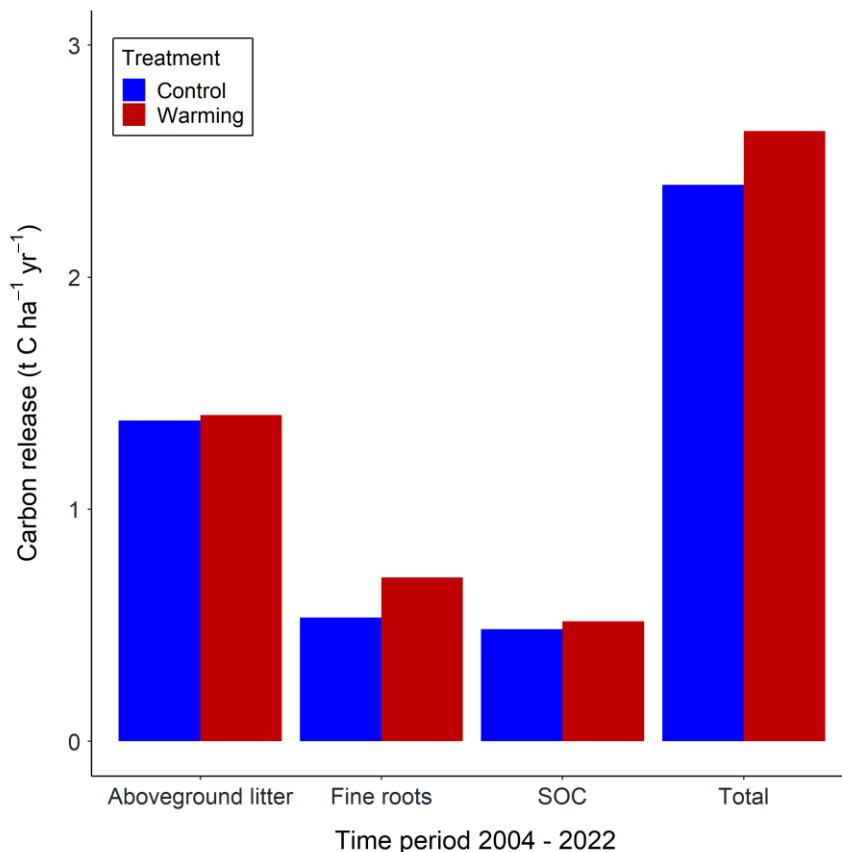


**Figure 5:** Modeled C released from aboveground litter, fine roots, and SOC in control and warming, as well as the means for both treatments at 0 – 20 cm soil depth for the period 2004 – 2022.

### Discussion

After 15 years of soil warming, radiocarbon signatures of SOC, transit times of C, and the C release from aboveground litter, fine root, and SOC pools were barely affected by elevated soil temperature in this temperate mountain forest. Almost similar SOC stocks in control and

warming treatments in 2019 suggest that the SOC pools exhibit a high resilience against long-term soil warming despite relatively short transient times of C. We further explored how soil warming impacts soil CO<sub>2</sub> efflux in different years of the experiment. We found a relatively consistent increase in soil CO<sub>2</sub> efflux by 41% in the warming treatment compared to the control. This increase is likely due to higher rhizosphere respiration enabled by increased belowground C allocation of the trees. This study provides evidence that the root system of trees may have a crucial role in maintaining SOC stocks under future climate warming.

### **Effects of soil warming on the radiocarbon signature of bulk soil**

Our analysis showed that warming did not affect the mean  $\Delta^{14}\text{C}$  signatures of bulk soil in 2012 and 2019, respectively (Table 1; Figure S2). This agrees with Schnecker et al. (2016), who also found that soil warming had no effect on the  $\Delta^{14}\text{C}$  signatures of different SOM fractions on the same site. Our result also agrees with Z. Shi et al. (2020), who found that temperature only influences the spatial distribution of  $\Delta^{14}\text{C}$ . Our finding contradicts the assumption that increasing soil temperature would lead to more recent soil  $\Delta^{14}\text{C}$  signatures (compared to contemporary atmospheric  $\Delta^{14}\text{C}$ ) in the warming treatment due to faster decomposition of plant-derived C and input of young C. This assumption would imply a more rapid exchange between soil C and atmospheric CO<sub>2</sub> (Trumbore et al., 1996; Trumbore, 1997) or an increased loss of more stable SOC (Hopkins et al., 2012). Looking at the means of  $\Delta^{14}\text{C}$  signatures will lead us to conclude that bulk soil in control and warming treatments are similar. However, the distribution of  $\Delta^{14}\text{C}$  in soil (Figure 3), which informs about the proportional distribution of  $\Delta^{14}\text{C}$ , showed slight differences in the proportion of pre-bomb and recent-bomb  $^{14}\text{C}$ . The  $\Delta^{14}\text{C}$  distribution at 0 – 10 and 10 – 20 cm soil depth showed a relatively high proportion of pre-bomb C (negative values) in the warming treatment. This suggests that 15 years of soil warming proportionally did not lead to rapid decay and loss of old C (pre-bomb), as indicated in some climate warming studies (Hopkins et al., 2012). On the other hand, we observed at 0 – 10 cm soil depth a slight increase in the proportion of more recent post-bomb C, likely suggesting a substantial incorporation of fresh C resulting from plant litter decomposition. Because the distribution of  $\Delta^{14}\text{C}$  only informs about proportional distribution, we are not able at this time to make strong conclusions about the changes mentioned above. Mean radiocarbon signatures obtained in this study, regardless of the treatment effect, are in accordance with observations in other temperate forests (Gaudinski et al., 2000; Trumbore, 2000), which also indicate a significant amount of bomb  $^{14}\text{C}$ , therefore suggesting that a substantial proportion of SOM is exchanging C through photosynthetic fixation of atmospheric CO<sub>2</sub>.

**Effects of soil warming on the transit time of carbon and soil CO<sub>2</sub> efflux**

Although we saw a slight decrease in the median transit time of C from 3 to 2 years at 0 – 10 cm soil depth (Figure 2a), our results suggest that soil warming did not significantly affect the transit time of C overall (Figure 2). The similar transit time of C in control and warming treatments suggests that soil warming likely similarly affected labile and recalcitrant SOC fractions (Schnecker et al., 2016). At 0 – 10 cm soil depth, our results overall indicate a very fast transit time of C in both treatments. This suggests that most C inputs exit the soil system relatively quickly and may only barely contribute to SOC sequestration in the forest studied. This agrees with the observation that modeled C release was mainly dominated by aboveground litter in both treatments (Figure 5). The C transfer from aboveground litter and fine roots to SOC of less than 20% overall also suggests this (Table S2). At 10 – 20 cm soil depth, the transit time of C increased to ca. 20 years but is still lower than the mean transit time of 54 years for soil at 0 – 20 cm soil depth globally (Xiao et al., 2022). This suggests that the release of C from decomposition is dominated by relatively younger C in this forest. Our finding that soil warming did not significantly affect the transit time of C sounds intriguing because climate models predict rapid transit time of C as the result of the increased mineralization of the fast-cycling SOC pool (X. Lu et al., 2018). The transit time of C also integrates the age of C atoms, i.e., the weighted mean age of C leaving different SOC pools in relation to the C released from each and to the overall C released from the system (Sierra et al., 2017). We postulate the reason why we don't see a difference in transit time of C between treatments is maybe due to the fact that the increase in fine root C inputs (Kwatocho Kengdo et al., 2023) is relatively small compared to SOC stocks and the age of C which were also less affected by the treatment.

Concerning CO<sub>2</sub> efflux, our results showed that soil C release measured with static chambers in the field was, on average, 41% higher in the warming treatment for the four years considered in this study. This result indicates that  $R_s$  has not yet acclimated to increasing soil temperature and contrasts the results of other soil warming studies (Y. Luo et al., 2001; Melillo et al., 2017), where  $R_s$  in warmed plots decreased after ca. 10 years to the level observed in control. The reduction of microbial biomass, the adaptation of microbial communities, and the reduction of labile C have been considered to drive the acclimation of  $R_s$  (Bradford et al., 2008; Frey et al., 2008). Schindlbacher et al. (2015) found no indication of microbial adaptation to warming at the Achenkirch site, while preliminary results showed no effect on SOC by soil warming. This may suggest that the depletion of the labile substrate did not yet occur, presumably due to increased root litter input (Kwatocho Kengdo et al., 2023), root exudation (Heinzle et al., 2023),

and EcM necromass (Klink et al., 2022). Modeled C released from the decomposition of SOM also showed a slight increase of 8% with soil warming (Figure 5). Taken together, our findings suggest that the persistent increase in CO<sub>2</sub> efflux in the warming treatment at the Achenkirch site primarily originates from rhizosphere respiration. This is further supported by the fact that at the Harvard forest where acclimation of  $R_s$  was first observed, soil warming significantly decreased fine root biomass by 62% (Melillo et al., 2011; Zhou et al., 2011). The consistent increase in fine root biomass and fine root production, coupled with the changes in fine root morphology towards short-lived fine roots in the warming treatment (Kwatocho Kengdo et al., 2022), suggest that rhizosphere respiration might be more important in explaining the sustained increase in soil CO<sub>2</sub> efflux released at the Achenkirch site.

The modeled C release by mineralization of litter and SOM suggests a contribution of rhizosphere respiration by 63 - 71% to the soil CO<sub>2</sub> efflux. Other studies have also reported such a high proportion, but on average, root contributions < 50% are expected for temperate forests (Bond-Lamberty et al., 2004; Hanson et al., 2000). In-situ measurement of autotrophic respiration in forests is hardly possible without disturbances or artifacts (Kuzyakov, 2006). Partitioning soil respiration by trenching the root system revealed an autotrophic contribution of 50% for the Achenkirch warming experiment (Schindlbacher et al., 2009). Trenching, however, can overestimate the heterotrophic component as cut roots represent an artificial input of litter and a source of CO<sub>2</sub>. On the other hand, we cannot exclude that the radiocarbon approach underestimated the input by fine root necromass (Kwatocho Kengdo et al., 2023). Nevertheless, the rhizosphere seems to contribute more to soil CO<sub>2</sub> efflux at this site than in other temperate forests. Ectomycorrhizal roots seem particularly important for respiration as they may represent the strongest sink for photosynthates in trees (Högberg et al., 2008).

In addition to the general limitations coming from the experimental warming setup (e.g., only soil was warmed during the growing period only), our study mainly suffered from our critical assumption concerning initial C stocks in the model, as well as the assumption of no C transfer between 0 – 10 cm and 10 – 20 cm soil depth. In addition, the radiocarbon model we used tried to fit relatively complex curves with only a few data points. The latter is a common pitfall in radiocarbon modeling (Gaudinski et al., 2000). Climate warming is also expected to increase aboveground plant productivity (Rumpf et al., 2022), leading to more C plant inputs to the soil. Therefore, we assume that this site might have a relatively small risk of SOC losses with warming.

## Conclusions

In conclusion, our results showed no evidence that soil warming changed the distribution of  $\Delta^{14}\text{C}$  in soil nor the transit of C. However, on average, soil  $\text{CO}_2$  efflux was 41% higher in the warming treatment. Even after 15 years of soil warming, there was no indication of decreased  $\text{CO}_2$  efflux, suggesting that the soil C cycle did not yet acclimate at the Achenkirch site. Based on C stocks measured in 2019, it appears that the SOC stocks are resilient against warming. More research on belowground C allocation and C flow in the soil is needed to complement the present findings.

## Acknowledgements

This research was funded by the German Research Foundation (DFG, BO 1741/13-1) and the Austrian Science Fund (FWF) through the D-A-Ch project I 3745. The authors thank Renate Krauss, Uwe Hell, and Karin Söllner for technical assistance. We acknowledge the contribution of Alena Hubach and Inken Krüger during sample preparation and radiocarbon analysis in 2012. We thank Xiaomei Xu and John Southon for their valuable assistance during  $^{14}\text{C}$  samples preparation and radiocarbon analysis at the Keck Carbon Cycle AMS Laboratory, University of California, Irvine.

## References

- Aerts, R. (1997). Climate, Leaf Litter Chemistry and Leaf Litter Decomposition in Terrestrial Ecosystems: A Triangular Relationship. *Oikos*, 79(3), 439–449. <https://doi.org/10.2307/3546886>
- Ahrens, B., Reichstein, M., Borken, W., Muhr, J., Trumbore, S. E., & Wutzler, T. (2014). Bayesian calibration of a soil organic carbon model using  $\Delta^{14}\text{C}$  measurements of soil organic carbon and heterotrophic respiration as joint constraints. *Biogeosciences*, 11(8), 2147–2168. <https://doi.org/10.5194/bg-11-2147-2014>
- Auguie, B. (2017). gridExtra: Miscellaneous Functions for "Grid" Graphics. <https://CRAN.R-project.org/package=gridExtra>
- Baisden, W. T., Parfitt, R. L., Ross, C., Schipper, L. A., & Canessa, S. (2013). Evaluating 50 years of time-series soil radiocarbon data: towards routine calculation of robust C residence times. *Biogeochemistry*, 112(1-3), 129–137. <https://doi.org/10.1007/s10533-011-9675-y>
- Bardgett, R. D., Freeman, C., & Ostle, N. J. (2008). Microbial contributions to climate change through carbon cycle feedbacks. *The ISME Journal*, 2(8), 805–814. <https://doi.org/10.1038/ismej.2008.58>
- Barrett, D. J. (2002). Steady state turnover time of carbon in the Australian terrestrial biosphere. *Global Biogeochemical Cycles*, 16(4), 55-1-55-21. <https://doi.org/10.1029/2002GB001860>
- Bond-Lamberty, Ben; Wang, Chuankuan; Gower, Stith T. (2004): A global relationship between the heterotrophic and autotrophic components of soil respiration? In *Global Change Biol* 10 (10), pp. 1756–1766. DOI: 10.1111/j.1365-2486.2004.00816.x.
- Bradford, M. A., Davies, C. A., Frey, S. D., Maddox, T. R., Melillo, J. M., Mohan, J. E., Reynolds, J. F., Treseder, K. K., & Wallenstein, M. D. (2008). Thermal adaptation of soil microbial respiration to elevated temperature. *Ecology Letters*, 11(12), 1316–1327. <https://doi.org/10.1111/j.1461-0248.2008.01251.x>
- Carey, J. C., Tang, J., Templer, P. H., Kroeger, K. D., Crowther, T. W., Burton, A. J., Dukes, J. S., Emmett, B., Frey, S. D., Heskell, M. A., Jiang, L., Machmuller, M. B., Mohan, J., Panetta, A. M., Reich, P. B., Reinsch, S., Wang, X., Allison, S. D., Bamminger, C., . . . Tietema, A. (2016). Temperature response of soil respiration largely unaltered with experimental warming. *Proceedings of the National Academy of Sciences of the United States of America*, 113(48), 13797–13802. <https://doi.org/10.1073/pnas.1605365113>
- Chanca, I., Trumbore, S., Macario, K., & Sierra, C. A. (2022). Probability Distributions of Radiocarbon in Open Linear Compartmental Systems at Steady-State. *Journal of Geophysical Research: Biogeosciences*, 127(3). <https://doi.org/10.1029/2021JG006673>
- Davidson, E. A., & Janssens, I. A. (2006). Temperature sensitivity of soil carbon decomposition and feedbacks to climate change. *Nature*, 440(7081), 165–173. <https://doi.org/10.1038/nature04514>
- Fanin, N., Mooshammer, M., Sauvadet, M., Meng, C., Alvarez, G., Bernard, L., Bertrand, I., Blagodatskaya, E., Bon, L., Fontaine, S., Niu, S., Lashermes, G., Maxwell, T. L., Weintraub, M. N., Wingate, L., Moorhead, D., & Nottingham, A. T. (2022). Soil enzymes in response

- to climate warming: Mechanisms and feedbacks. *Functional Ecology*, Article 1365-2435.14027. Advance online publication. <https://doi.org/10.1111/1365-2435.14027>
- Freschet, G. T., Cornwell, W. K., Wardle, D. A., Elumeeva, T. G., Liu, W., Jackson, B. G., Onipchenko, V. G., Soudzilovskaia, N. A., Tao, J., & Cornelissen, J. H. (2013). Linking litter decomposition of above- and below-ground organs to plant-soil feedbacks worldwide. *Journal of Ecology*, 101(4), 943–952. <https://doi.org/10.1111/1365-2745.12092>
- Frey, S. D., Drijber, R., Smith, H., & Melillo, J. (2008). Microbial biomass, functional capacity, and community structure after 12 years of soil warming. *Soil Biology and Biochemistry*, 40(11), 2904–2907. <https://doi.org/10.1016/j.soilbio.2008.07.020>
- Gaudinski, J. B., Trumbore, S., Davidson, E., Cook, A., Markewitz, D., & Richter, D. (2001). The age of fine-root carbon in three forests of the eastern United States measured by radiocarbon. *Oecologia*, 129(3), 420–429. <https://doi.org/10.1007/s004420100746>
- Gaudinski, J. B., Trumbore, S. E., Davidson, E. A., & Zheng, S. (2000). Soil carbon cycling in a temperate forest: Soil carbon cycling in a temperate forest: radiocarbon-based estimates of residence times, sequestration rates and partitioning of fluxes. *Biogeochemistry*, 51(1), 33–69. <https://doi.org/10.1023/A:1006301010014>
- Gobiet, A., Kotlarski, S., Beniston, M., Heinrich, G., Rajczak, J., & Stoffel, M. (2014). 21st century climate change in the European Alps—a review. *The Science of the Total Environment*, 493, 1138–1151. <https://doi.org/10.1016/j.scitotenv.2013.07.050>
- Hammer, S., & Levin, I. (2017). Monthly mean atmospheric D14CO<sub>2</sub> at Jungfraujoch and Schauinsland from 1986 to 2016. <https://doi.org/10.11588/data/10100>
- Hanson, P. J.; Edwards, N. T.; Garten, C. T.; Andrews, J. A. (2000): Separating root and soil microbial contributions to soil respiration: A review of methods and observations. In *Biogeochemistry* 48 (1), pp. 115–146. DOI: 10.1023/A:1006244819642
- Heinze, J., Liu, X., Tian, Y., Kwatcho Kengdo, S., Heinze, B., Nirschi, A., Borken, W., Inselsbacher, E., Wanek, W., & Schindlbacher, A. (2023). Increase in fine root biomass enhances root exudation by long-term soil warming in a temperate forest. In *Front. For. Glob. Change*, 6, Article 1152142. <https://doi.org/10.3389/ffgc.2023.1152142>.
- Högberg, P.; Högberg, M. N.; Göttlicher, S. G.; Betson, N. R.; Keel, S. G.; Metcalfe, D. B.; Campbell, C.; Schindlbacher, A.; Hurry, V.; Lundmark, T.; Linder, S.; and Näsholm, T. (2008): High temporal resolution tracing of photosynthate carbon from the tree canopy to forest soil microorganisms. In *New Phytol* 177 (1), pp. 220–228. DOI: 10.1111/j.1469-8137.2007.02238.x
- Hopkins, F. M., Torn, M. S., & Trumbore, S. E. (2012). Warming accelerates decomposition of decades-old carbon in forest soils. *Proceedings of the National Academy of Sciences of the United States of America*, 109(26), E1753-61. <https://doi.org/10.1073/pnas.1120603109>
- IPCC, 2021: Climate Change 2021: The Physical Science Basis. Contribution of Working Group I to the Sixth Assessment Report of the Intergovernmental Panel on Climate Change [Masson-Delmotte, V., P. Zhai, A. Pirani, S.L. Connors, C. Péan, S. Berger, N. Caud, Y. Chen, L. Goldfarb, M.I. Gomis, M. Huang, K. Leitzell, E. Lonnoy, J.B.R. Matthews, T.K. Maycock, T. Waterfield, O. Yelekçi, R. Yu, and B. Zhou (eds.)]. Cambridge

- University Press, Cambridge, United Kingdom and New York, NY, USA, In press, doi:10.1017/9781009157896
- Jandl, R., Ledermann, T., Kindermann, G., & Weiss, P. (2021). Soil Organic Carbon Stocks in Mixed-Deciduous and Coniferous Forests in Austria. *Frontiers in Forests and Global Change*, 4, Article 688851. <https://doi.org/10.3389/ffgc.2021.688851>
- Janssens, I. A., Kowalski, A. S., Longdoz, B., & Ceulemans, R. (2000). Assessing forest soil CO<sub>2</sub> efflux: An in situ comparison of four techniques. *Tree Physiology*, 20(1), 23–32. <https://doi.org/10.1093/treephys/20.1.23>
- Klink, S., Keller, A. B., Wild, A. J., Baumert, V. L., Gube, M., Lehndorff, E., Meyer, N., Mueller, C. W., Phillips, R. P., & Pausch, J. (2022). Stable isotopes reveal that fungal residues contribute more to mineral-associated organic matter pools than plant residues. *Soil Biology & Biochemistry*, 168, 108634. <https://doi.org/10.1016/j.soilbio.2022.108634>
- Kubistin, D., Plaß-Dülmer, C., Arnold, S., Lindauer, M., Müller-Williams, J., & Schumacher, M. (2021). ICOS ATC/CAL 14C Release, Hohenpeissenberg (131.0 m), 2015-09-24–2020-02-19. *Atmosphere Thematic Centre*. <https://hdl.handle.net/11676/sx-gduDzKEjkF3VCer06oWIV>
- Kuzyakov, Yakov (2006): Sources of CO<sub>2</sub> efflux from soil and review of partitioning methods. In *Soil Biology and Biochemistry* 38 (3), pp. 425–448. DOI: 10.1016/j.soilbio.2005.08.020.
- Kwatocho Kengdo, S., Ahrens, B., Tian, Y., Heinzle, J., Wanek, W., Schindlbacher, A., & Borken, W. (2023). Increase in carbon input by enhanced fine root turnover in a long-term warmed forest soil. *The Science of the Total Environment*, 158800. <https://doi.org/10.1016/j.scitotenv.2022.158800>
- Kwatocho Kengdo, S., Peršoh, D., Schindlbacher, A., Heinzle, J., Tian, Y., Wanek, W., & Borken, W. (2022). Long-term soil warming alters fine root dynamics and morphology, and their ectomycorrhizal fungal community in a temperate forest soil. *Global Change Biology*, 28(10), 3441–3458. <https://doi.org/10.1111/gcb.16155>
- Luo, Y., Wan, S., Hui, D., & Wallace, L. L. (2001). Acclimatization of soil respiration to warming in a tall grass prairie. *Nature*, 413(6856), 622–625. <https://doi.org/10.1038/35098065>
- Liu, D., Keiblinger, K. M., Schindlbacher, A., Wegner, U., Sun, H., Fuchs, S., Lassek, C., Riedel, K., & Zechmeister-Boltenstern, S. (2017). Microbial functionality as affected by experimental warming of a temperate mountain forest soil—A metaproteomics survey. *Applied Soil Ecology*, 117-118, 196–202. <https://doi.org/10.1016/j.apsoil.2017.04.021>
- Lu, X., Wang, Y.-P., Luo, Y., & Jiang, L. (2018). Ecosystem carbon transit versus turnover times in response to climate warming and rising atmospheric CO<sub>2</sub> concentration. *Biogeosciences*, 15(21), 6559–6572. <https://doi.org/10.5194/bg-15-6559-2018>
- Lützwon, M. von, & Kögel-Knabner, I. (2009). Temperature sensitivity of soil organic matter decomposition—what do we know? *Biology and Fertility of Soils*, 46(1), 1–15. <https://doi.org/10.1007/s00374-009-0413-8>
- Lützwon, M. von, Kögel-Knabner, I., Ekschmitt, K., Matzner, E., Guggenberger, G., & Marschner, B. and Flessa, H. (2006). Stabilization of organic matter in temperate soils:

- mechanisms and their relevance under different soil conditions – a review. *European Journal of Soil Science*, 54, 426–445. <https://doi.org/10.1111/j.1365-2389.2006.00809.x>
- Melillo, J. M., Butler, S., Johnson, J., Mohan, J., Steudler, P., Lux, H., Burrows, E., Bowles, F., Smith, R., Scott, L., Vario, C., Hill, T., Burton, A., Zhou, Y.-M., & Tang, J. (2011). Soil warming, carbon-nitrogen interactions, and forest carbon budgets. *Proceedings of the National Academy of Sciences of the United States of America*, 108(23), 9508–9512. <https://doi.org/10.1073/pnas.1018189108>
- Melillo, J. M., Frey, S. D., DeAngelis, K. M., Werner, W. J., Bernard, M. J., Bowles, F. P., Pold, G., Knorr, M. A., & Grandy, A. S. (2017). Long-term pattern and magnitude of soil carbon feedback to the climate system in a warming world. *Science*, 358(6359), 101–105. <https://doi.org/10.1126/science.aan2874>
- Melillo, J. M., Steudler, P. A., Aber, J. D., Newkirk, K., Lux, H., Bowles, F. P., Catricala, C., Magill, A., Ahrens, T., & Morrisseau, S. (2002). Soil warming and carbon-cycle feedbacks to the climate system. *Science*, 298(5601), 2173–2176. <https://doi.org/10.1126/science.1074153>
- Metzler, H., & Sierra, C. A. (2018). Linear Autonomous Compartmental Models as Continuous-Time Markov Chains: Transit-Time and Age Distributions. *Mathematical Geosciences*, 50(1), 1–34. <https://doi.org/10.1007/s11004-017-9690-1>
- Moré, J. J. (1978). The Levenberg-Marquardt algorithm: Implementation and theory. In G. A. Watson (Ed.), *Numerical Analysis* (pp. 105–116). Springer Berlin Heidelberg.
- Pedersen, T. L. (2022). patchwork: The Composer of Plots.
- R Core Team. (2022). R: A Language and Environment for Statistical Computing. <https://www.R-project.org/>
- Reimer, P. J., Bard, E., Bayliss, A., Beck, J. W., Blackwell, P. G., Ramsey, C. B., Buck, C. E., Cheng, H., Edwards, R. L., Friedrich, M., Grootes, P. M., Guilderson, T. P., Haflidason, H., Hajdas, I., Hatté, C., Heaton, T. J., Hoffmann, D. L., Hogg, A. G., Hughen, K. A., . . . van der Plicht, J. (2013). IntCal13 and Marine13 Radiocarbon Age Calibration Curves 0–50,000 Years cal BP. *Radiocarbon*, 55(4), 1869–1887. [https://doi.org/10.2458/azu\\_js\\_rc.55.16947](https://doi.org/10.2458/azu_js_rc.55.16947)
- Rumpf, S., Gravey, M., Brönnimann, O., Luoto, M., Cianfrani, C., Mariethoz, G., & Guisan, A. (2022). From white to green: Snow cover loss and increased vegetation productivity in the European Alps. *Science*, 376(6597), 1119–1122. <https://doi.org/10.1126/science.abn6697>
- Schindlbacher, A., Rodler, A., Kuffner, M., Kitzler, B., Sessitsch, A., & Zechmeister-Boltenstern, S. (2011). Experimental warming effects on the microbial community of a temperate mountain forest soil. *Soil Biology & Biochemistry*, 43(7), 1417–1425. <https://doi.org/10.1016/j.soilbio.2011.03.005>
- Schindlbacher, A., Schnecker, J., Takriti, M., Borken, W., & Wanek, W. (2015). Microbial physiology and soil CO<sub>2</sub> efflux after 9 years of soil warming in a temperate forest - no indications for thermal adaptations. *Global Change Biology*, 21(11), 4265–4277. <https://doi.org/10.1111/gcb.12996>

- Schindlbacher, A., Zechmeister-Boltenstern, S., Glatzel, G., & Jandl, R. (2007). Winter soil respiration from an Austrian mountain forest. *Agricultural and Forest Meteorology*, 146(3-4), 205–215. <https://doi.org/10.1016/j.agrformet.2007.06.001>
- Schindlbacher, A., Zechmeister-Boltenstern, S., & Jandl, R. (2009). Carbon losses due to soil warming: Do autotrophic and heterotrophic soil respiration respond equally? *Global Change Biology*, 15(4), 901–913. <https://doi.org/10.1111/j.1365-2486.2008.01757.x>
- Schnecker, J., Borken, W., Schindlbacher, A., & Wanek, W. (2016). Little effects on soil organic matter chemistry of density fractions after seven years of forest soil warming. *Soil Biology & Biochemistry*, 103, 300–307. <https://doi.org/10.1016/j.soilbio.2016.09.003>
- Schuur, E. A., Druffel, E., & Trumbore, S. E. (2016). Radiocarbon and Climate Change. Springer International Publishing. <https://doi.org/10.1007/978-3-319-25643-6>
- Shi, Z., Allison, S. D., He, Y., Levine, P. A., Hoyt, A. M., Beem-Miller, J., Zhu, Q., Wieder, W. R., Trumbore, S., & Randerson, J. T. (2020). The age distribution of global soil carbon inferred from radiocarbon measurements. *Nature Geoscience*, 13(8), 555–559. <https://doi.org/10.1038/s41561-020-0596-z>
- Sierra, C. A., Müller, M., Metzler, H., Manzoni, S., & Trumbore, S. E. (2017). The muddle of ages, turnover, transit, and residence times in the carbon cycle. *Global Change Biology*, 23(5), 1763–1773. <https://doi.org/10.1111/gcb.13556>
- Sierra, C. A., Müller, M., & Trumbore, S. E. (2012). Models of soil organic matter decomposition: the SoilR package, version 1.0. *Geoscientific Model Development*, 5(4), 1045–1060. <https://doi.org/10.5194/gmd-5-1045-2012>
- Sierra, C. A., Müller, M., & Trumbore, S. E. (2014). Modeling radiocarbon dynamics in soils: SoilR version 1.1. *Geoscientific Model Development*, 7(5), 1919–1931. <https://doi.org/10.5194/gmd-7-1919-2014>
- Song, S., Hu, X., Zhu, J., Zheng, T., Zhang, F., Ji, C., & Zhu, J. (2021). The decomposition rates of leaf litter and fine root and their temperature sensitivities are influenced differently by biotic factors. *Plant and Soil*, 461(1-2), 603–616. <https://doi.org/10.1007/s11104-021-04855-7>
- Southon, J., Santos, G., Druffel-Rodriguez, K., Druffel, E., Trumbore, S., Xu, X., Griffin, S., Ali, S., & Mazon, M. (2004). The Keck Carbon Cycle AMS Laboratory, University of California, Irvine: Initial Operation and a Background Surprise. *Radiocarbon*, 46(1), 41–49. <https://doi.org/10.1017/S0033822200039333>
- Stuiver, M., & Polach, H. A. (1977). Discussion Reporting of 14 C Data. *Radiocarbon*, 19(3), 355–363. <https://doi.org/10.1017/S0033822200003672>
- Tian, Y., Shi, C., Urbina-Malo, C., Kwatcho Kengdo, S., Heinzle, J., Inselsbacher, E., Ottner, F., Borken, W., Michel, K., Schindlbacher, A., and Wanek, W. (2023). Long-term soil warming decreases microbial phosphorus utilization by increasing abiotic phosphorus sorption and phosphorus losses. *Nature Geoscience*. <https://doi.org/10.1038/s41467-023-36527-8>

- Trumbore, S. E. (1997). Potential responses of soil organic carbon to global environmental change. *Proceedings of the National Academy of Sciences of the United States of America*, 94(16), 8284–8291. <https://doi.org/10.1073/pnas.94.16.8284>
- Trumbore, S. E. (2000). Age of soil organic matter and soil respiration: radiocarbon constraints on belowground C dynamics. *Ecological Applications*, 10(2), 399–411. [https://doi.org/10.1890/1051-0761\(2000\)010\[0399:AOSOMA\]2.0.CO;2](https://doi.org/10.1890/1051-0761(2000)010[0399:AOSOMA]2.0.CO;2)
- Trumbore, S. E. (2009). Radiocarbon and Soil Carbon Dynamics. *Annual Review of Earth and Planetary Sciences*, 37(1), 47–66. <https://doi.org/10.1146/annurev.earth.36.031207.124300>
- Trumbore, S. E., Chadwick, O. A., & Amundson, R. (1996). Rapid Exchange Between Soil Carbon and Atmospheric Carbon Dioxide Driven by Temperature Change. *Science*, 272(5260), 393–396. <https://doi.org/10.1126/science.272.5260.393>
- Wang, Y., & Hsieh, Y.-P. (2002). Uncertainties and novel prospects in the study of the soil carbon dynamics. *Chemosphere*, 49(8), 791–804. [https://doi.org/10.1016/S0045-6535\(02\)00381-8](https://doi.org/10.1016/S0045-6535(02)00381-8)
- Warscher, M., Wagner, S., Marke, T., Laux, P., Smiatek, G., Strasser, U., & Kunstmann, H. (2019). A 5 km Resolution Regional Climate Simulation for Central Europe: Performance in High Mountain Areas and Seasonal, Regional and Elevation-Dependent Variations. *Atmosphere*, 10(11), 682. <https://doi.org/10.3390/atmos10110682>
- Wickham, H. (2016). *ggplot2: Elegant Graphics for Data Analysis*. Springer-Verlag New York. <https://ggplot2.tidyverse.org>
- Xiao, L., Wang, G., Wang, M., Zhang, S., Sierra, C. A., Guo, X., Chang, J., Shi, Z., & Luo, Z. (2022). Younger carbon dominates global soil carbon efflux. *Global Change Biology*, 28(18), 5587–5599. <https://doi.org/10.1111/gcb.16311>
- Xu, X., Trumbore, S. E., Zheng, S., Southon, J. R., McDuffee, K. E., Luttgen, M., & Liu, J. C. (2007). Modifying a sealed tube zinc reduction method for preparation of AMS graphite targets: Reducing background and attaining high precision. *Nuclear Instruments and Methods in Physics Research Section B: Beam Interactions with Materials and Atoms*, 259(1), 320–329. <https://doi.org/10.1016/j.nimb.2007.01.175>
- Zhou, Y., Tang, J., Melillo, J. M., Butler, S., & Mohan, J. E. (2011). Root standing crop and chemistry after six years of soil warming in a temperate forest. *Tree Physiology*, 31(7), 707–717. <https://doi.org/10.1093/treephys/tpr066>

**Supporting information****Table S1:** Measured SOC stocks in control and warming treatment in 2019, and initial carbon stocks used in the model.

		SOC stocks
Treatment	Soil Depth (cm)	2019
Control	0 – 10	62.52 (11.13)
	10 - 20	41.20 (12.43)
Warming	0 – 10	66.22 (15.95)
	10 - 20	38.83 (4.33)

**Table S2:** Mean parameter values following the Levenberg-Marquardt method. The unit is yr<sup>-1</sup> for decay rate, and dimensionless for transfer coefficients.

Treatment	Soil depth (cm)	Parameter	Mean value
Control	0 – 10	$k_1$	0.329
		$k_2$	0.170
		$k_3$	0.007
		$a_{3,1}$	0.187
		$a_{3,2}$	0.196
	10 – 20	$k_1$	0.128
		$k_2$	0.001
		$a_{2,1}$	0.464
Warming	0 – 10	$k_1$	0.600
		$k_2$	0.270
		$k_3$	0.007
		$a_{3,1}$	0.173
		$a_{3,2}$	0.193
	10 – 20	$k_1$	0.127
		$k_2$	0.002
		$a_{21}$	0.470

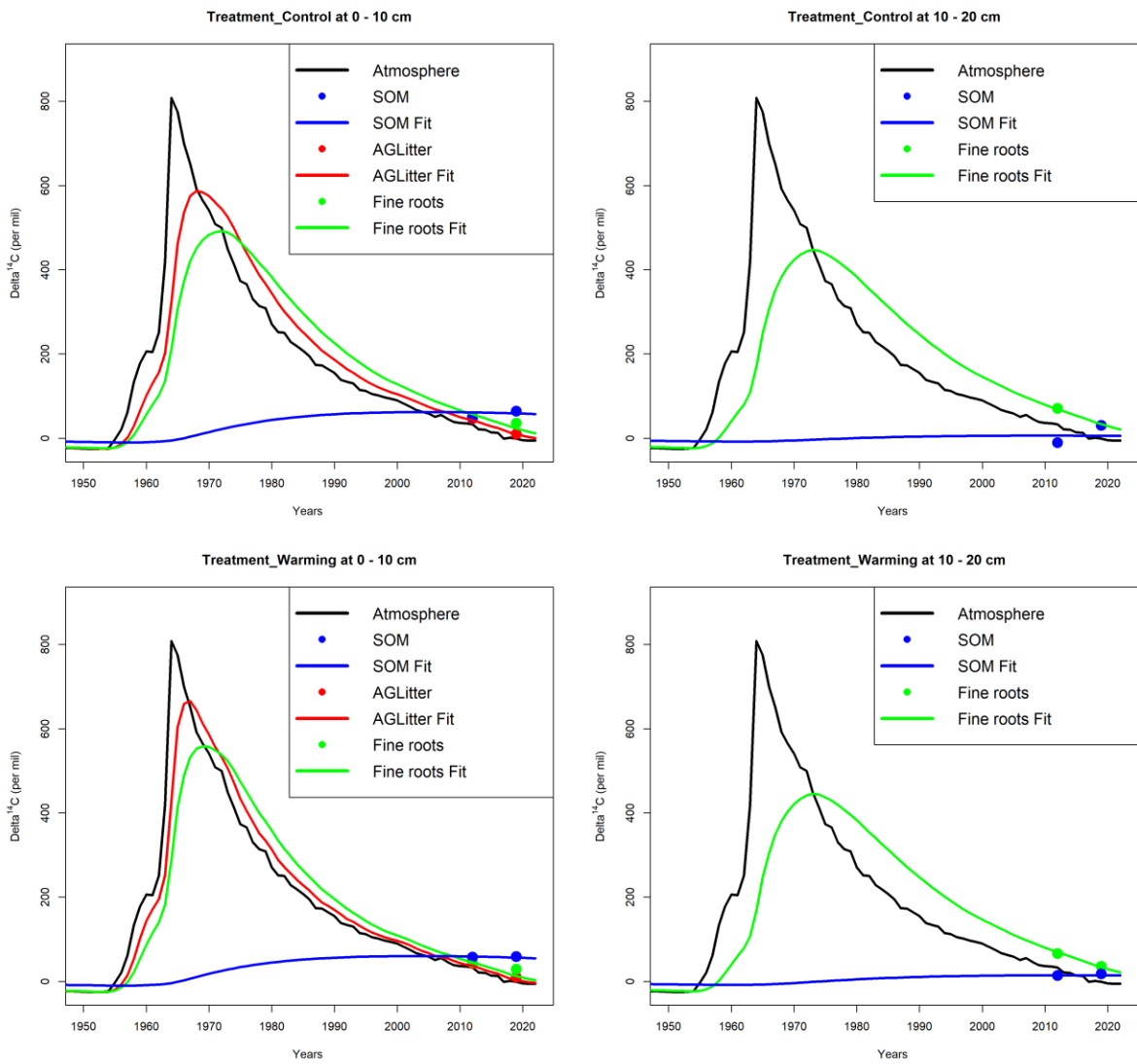


**Figure S1:** Observed and modeled data for each treatment and soil depth.

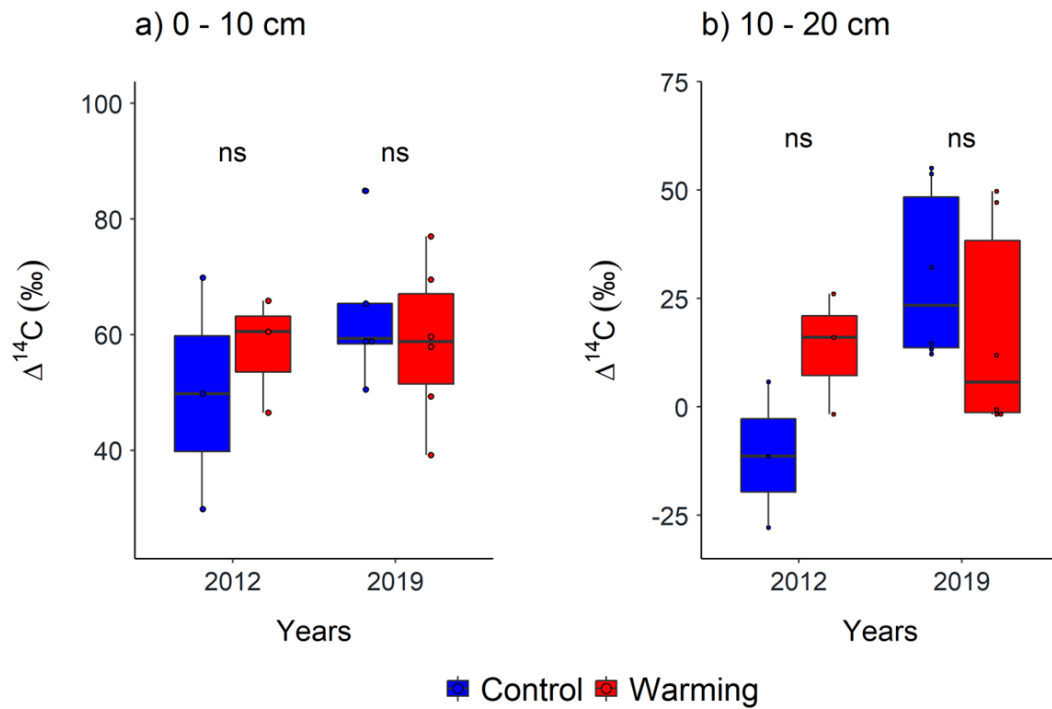


**Figure S2:** Radiocarbon signatures ( $\Delta^{14}\text{C}$ ; ‰) of the bulk soil in control and warmed plots at (a) 0 – 10 cm and (b) 10 – 20 cm soil depth on different sampling occasions. In the boxplots, the line represents the median; the box denotes the interquartile range, and points represent individual measurements.  $\Delta^{14}\text{C}$  values greater than zero contain bomb radiocarbon, while those less than zero indicate that the carbon in the bulk soil has been isolated from the exchange with the atmosphere and significant radioactive decay has occurred (Gaudinski et al., 2000; Trumbore, 2000).

## Contribution to the included manuscripts

The contribution of each author (in %) to the manuscripts included in this thesis are presented as follows and with respect to the following criteria: **a** = Concept and experimental design, **b** = field and laboratory work, **c** = data evolution and statistical analysis, **d** = discussion and interpretation, **e** = manuscript preparation.

Manuscript	Author	a	b	c	d	e	
Long-term soil warming alters fine root dynamics and morphology, and their ectomycorrhizal fungal community in a temperate forest soil. <i>Global Change Biology</i> , 28(10), 3441–3458. <a href="https://doi.org/10.1111/gcb.16155">https://doi.org/10.1111/gcb.16155</a>	Kwatocho Kengdo, S.	10	50	60	40	50	
	Peršoh, D.		20	20	20	10	
	Schindlbacher, A.	30	5		10	5	
	Heinzle, J.		5			5	
	Tian, Y.		5				5
	Wanek, W.	30	5		10	5	
Increase in carbon input by enhanced fine root turnover in a long-term warmed forest soil. <i>The Science of the Total Environment</i> , 158800. <a href="https://doi.org/10.1016/j.scitotenv.2022.158800">https://doi.org/10.1016/j.scitotenv.2022.158800</a>	Borken, W.	30	10	20	30	20	
	Kwatocho Kengdo, S.	10	70	50	50	60	
	Ahrens, B.			30	20	10	
	Tian, Y.		5				
	Heinzle, J.		5				
	Wanek, W.	30	5				
Long-term warming increased CO <sub>2</sub> efflux but not the transit time of soil carbon in a temperate forest.	Schindlbacher, A.	30	5		30	30	
	Borken, W.	30	10	20	30	30	
	Kwatocho Kengdo, S.	10	50	40	50	60	
	Schindlbacher, A.	30	20	20	20	20	
	Sierra, C. A.			15			
	Heinzle, J.		10				
	Ahrens, B.			10			
	Tian, Y.		5				
	Wanek, W.	30	5				
	Borken, W.	30	10	15	30	40	

## ACKNOWLEDGEMENTS

### **Acknowledgments**

Special thanks to my supervisor Prof. Dr. Werner Borcken, for giving me the opportunity to explore this topic under his guidance and work in a very dynamic team. Thank you for your patience, active support, suggestions in many meetings, and manuscript reviews. I appreciated the 1:1 discussions. Your advice and criticism during my work have always been very beneficial.

I would also like to thank all the members of the Achenkrich soil warming experiment. First, I thank Dr. Andreas Schindlbacher, who initiated and maintained the experimental site over the years. Thank you for sharing the long-term data you measured for many years, for the fruitful discussion during meetings, and for the constructive comments. I also thank Prof. Dr. Wolfgang Wanek for his comments, suggestions, and constructive feedback on my work during manuscript reviews and meetings. Thanks to Dr. Erich Inselsbacher for his comments on the manuscripts too. I further thank my colleagues Ye Tian, Jakob Heinzle, Carolina Urbina-Malo, and Chupei Shi for the fruitful collaborations and teamwork in the field and later during data analysis and synthesis. I was so fortunate to be part of this very dynamic team.

I highly appreciate the support of Dr. Derek Peršoh. Thank you for introducing me to DNA extraction in the laboratory and for leading the sequencing and sequence data analysis. I highly appreciated your feedback and suggestions during our meetings. I further thank Dr. Carlos A. Sierra and Dr. Bernhard Ahrens for introducing me to radiocarbon modeling and providing constructive guidance and feedback during data analysis. I thank Dr. Xiaomei Xu and Dr. John Southon for analyzing our graphite samples and providing feedback on data quality over time. I further thank Dr. Sonwa for his continuous support.

I acknowledge the Department of Soil Ecology and all its members. In particular, I would like to thank Prof. Dr. Eva Lehndorff for allocating me an office space to work. Thank you, Karin Söllner, for your laboratory support and guidance and for introducing me to the preparation of radiocarbon samples. I further thank Renate Krauss for her support during laboratory analysis and fine root processing, Uwe Hell for his support with all technical issues, and Ingeborg Vogler for all administrative support. I also thank all my colleagues here at the Department: Ulrike Schwerdtner, Nele Meyer, Ryan Bartnick, Bettina Haas, Christina Gross, and Jacqueline Kaldun. Many thanks, Andreas Scheibe, for providing feedback on my draft. I don't forget student helpers during fine root processing. Thank you Humay Rahimova, Isabell Zeißig, and

## ACKNOWLEDGEMENTS

Grethe-Johanna Ploompou. I acknowledge Alena Hubach and Inken Krüger for sample preparation and radiocarbon analysis in 2012.

Finally, I am deeply grateful to my mother and late father for their support and sacrifices. I also thank my siblings Romaric, Arsene, Ghislain, and Emeline for their support. Thank you, Diana, for your constant support.

I am very grateful to the German Research Foundation (DFG, BO 1741/13-1) and the Austrian Science Fund (FWF) through the D-A-Ch project I 3745, who funded this research.

## Scientific contributions

### Peer-reviewed publications included in this thesis

- [1] **Kwatocho Kengdo, S.**, Peršoh, D., Schindlbacher, A., Heinzle, J., Tian, Y., Wanek, W., & Borken, W. (2022). Long-term soil warming alters fine root dynamics and morphology, and their ectomycorrhizal fungal community in a temperate forest soil. *Global Change Biology*, 28(10), 3441–3458. <https://doi.org/10.1111/gcb.16155>
- [2] **Kwatocho Kengdo, S.**, Ahrens, B., Tian, Y., Heinzle, J., Wanek, W., Schindlbacher, A., & Borken, W. (2023). Increase in carbon input by enhanced fine root turnover in a long-term warmed forest soil. *The Science of the Total Environment*, 158800. <https://doi.org/10.1016/j.scitotenv.2022.158800>
- [3] **Kwatocho Kengdo, S.**, Schindlbacher, A., Sierra, C. A., Heinzle, J., Ahrens, B., Tian, Y., Wanek, W., Borken, W. (2023). Long-term warming increased CO<sub>2</sub> efflux but not the transit time of soil carbon in a temperate forest. *In preparation*

### Further publications

- [1] Tian, Y., Shi, C., Urbina-Malo, C., **Kwatocho Kengdo, S.**, Heinzle, J., Inselsbacher, E., Ottner, F., Borken, W., Michel, K., Schindlbacher, A., and Wanek, W. (2023). Long-term soil warming decreases microbial phosphorus utilization by increasing abiotic phosphorus sorption and phosphorus losses. *Nat Commun* 14, 864. <https://doi.org/10.1038/s41467-023-36527-8>.
- [2] Shi, C., Urbina-Malo, C., Tian, Y., Heinzle, J., **Kwatocho Kengdo, S.**, Inselsbacher, E., Borken, W., Schindlbacher, A., Wanek, W. (2023). Does long-term soil warming affect microbial element limitation? A test by short-term assays of microbial growth responses to labile C, N and P additions. *Global Change Biology*. <https://doi.org/10.1111/gcb.16591>.
- [3] Heinzle, J., Kitzler, B., Zechmeister-Boltenstern, S., Tian, Y., **Kwatocho Kengdo, S.**, Wanek, W., Borken, W., Schindlbacher, A. (2023). Soil CH<sub>4</sub> and N<sub>2</sub>O response diminishes during decadal soil warming in a temperate mountain forest. *Agricultural and Forest Meteorology*, 329, 109287. <https://doi.org/10.1016/j.agrformet.2022.109287>
- [4] Heinzle, J., Wanek, W., Tian, Y., **Kwatocho Kengdo, S.**, Borken, W., Schindlbacher, A., & Inselsbacher, E. (2021). No effect of long-term soil warming on diffusive soil

## SCIENTIFIC CONTRIBUTIONS

- inorganic and organic nitrogen fluxes in a temperate forest soil. *Soil Biology and Biochemistry*, 158, 108261. <https://doi.org/10.1016/j.soilbio.2021.108261>
- [5] Verchot, L. V., Dannenmann, M., **Kwatocho Kengdo, S.**, Njine-Bememba, C. B., Rufino, M. C., Sonwa, D. J., & Tejedor, J. (2020). Land-use change and Biogeochemical controls of soil CO<sub>2</sub>, N<sub>2</sub>O and CH<sub>4</sub> fluxes in Cameroonian forest landscapes. *Journal of Integrative Environmental Sciences*, 1–23. <https://doi.org/10.1080/1943815X.2020.1779092>
- [6] Zistl-Schlingmann, M., **Kwatocho Kengdo, S.**, Kiese, R., & Dannenmann, M. (2020). Management Intensity Controls Nitrogen-Use-Efficiency and Flows in Grasslands—A <sup>15</sup>N Tracing Experiment. *Agronomy*, 10(4), 606. <https://doi.org/10.3390/agronomy10040606>

### Further scientific contributions

#### Oral Presentations

- [1] **Kwatocho Kengdo S.**; Derek Peršoh; Andreas Schindlbacher; Jakob Heinzle; Ye Tian; Wolfgang Wanek; Werner Borken. Long-term soil warming alters fine root dynamics and morphology, and their ectomycorrhizal fungal community in a temperate forest soil. EGU General Assembly 2022, Vienna, Austria, 23–27 May 2022, EGU22-4427. <https://doi.org/10.5194/egusphere-egu22-4427>
- [2] **Kwatocho Kengdo, S.**, Peršoh, D., Schindlbacher, A., Heinzle, J., Tian, Y., Wanek, W., & Borken, W. (2022). Long-term soil warming alters fine root dynamics and morphology, and their ectomycorrhizal fungal community in a temperate forest soil. The 13<sup>th</sup> BayCEER Workshop, University of Bayreuth, Germany, October 14, 2021.

#### Poster presentation

- [1] **Kwatocho Kengdo, S.**, Heinzle, J., Tian, Y., Urbina-Malo, C., Chupei, S., Schindlbacher, A., Wanek, W., & Borken, W. (2020). Warming effects on fine root biomass, morphology, and decomposition in a mountainous forest soil. The 12<sup>th</sup> BayCEER Workshop (Virtual workshop edition), University of Bayreuth (Germany), October 29, 2020.

## SCIENTIFIC CONTRIBUTIONS

### **Awards**

- 12/2022 Outstanding Student and PhD candidate Presentation (OSPP) Award at the European Geosciences Union conference (EGU 2022). Vienna, Austria.
- 10/2019 Poster Award at the 12<sup>th</sup> BayCEER Workshop (Virtual workshop edition), University of Bayreuth (Germany). 2<sup>nd</sup> Prize

# DECLARATION

## **Declaration**

### **(Eidesstattliche) Versicherungen und Erklärungen**

(§ 8 Satz 2 Nr. 3 PromO Fakultät)

*Hiermit versichere ich eidesstattlich, dass ich die Arbeit selbstständig verfasst und keine anderen als die von mir angegebenen Quellen und Hilfsmittel benutzt habe (vgl. Art. 64 Abs. 1 Satz 6 BayHSchG).*

(§ 8 Satz 2 Nr. 3 PromO Fakultät)

*Hiermit erkläre ich, dass ich die Dissertation nicht bereits zur Erlangung eines akademischen Grades eingereicht habe und dass ich nicht bereits diese oder eine gleichartige Doktorprüfung endgültig nicht bestanden habe.*

(§ 8 Satz 2 Nr. 4 PromO Fakultät)

*Hiermit erkläre ich, dass ich Hilfe von gewerblichen Promotionsberatern bzw. –vermittlern oder ähnlichen Dienstleistern weder bisher in Anspruch genommen habe noch künftig in Anspruch nehmen werde.*

(§ 8 Satz 2 Nr. 7 PromO Fakultät)

*Hiermit erkläre ich mein Einverständnis, dass die elektronische Fassung der Dissertation unter Wahrung meiner Urheberrechte und des Datenschutzes einer gesonderten Überprüfung unterzogen werden kann.*

(§ 8 Satz 2 Nr. 8 PromO Fakultät)

*Hiermit erkläre ich mein Einverständnis, dass bei Verdacht wissenschaftlichen Fehlverhaltens Ermittlungen durch universitätsinterne Organe der wissenschaftlichen Selbstkontrolle stattfinden können.*

.....  
Ort, Datum, Unterschrift